Optimization of Microfluidic Parameters for Efficient Production of Liposomes and LNPs

A thesis presented for the degree of

Doctor of Philosophy

from the Institute of Pharmacy and Biomedical Science

at the University of Strathclyde

by

Sarah Victoria Lindsay

Declaration of Authenticity

'This thesis is the result of the author's original research. It has been composed by the author and has not been previously submitted for examination which has led to the award of a degree.'

Signed: Sarah Victoria Lindsay

Date: 28/04/2024

Acknowledgments

I would like to thank my supervisor Professor Yvonne Perrie for her support and guidance throughout this PhD. I am grateful for the opportunity to work in her laboratory and for the opportunities that this has allowed me to have, including attending both national and international conferences. I would also like to thank the team at Janssen, including Dr Sanket Shah and Professor René Holms, for their input and feedback and the statisticians, Olympia Tumolva and Tatsiana Khamiakova, for their help and perseverance with setting up and analysing the DOE study. This project (HBC.2019.2923) was supported by VLAIO (Flemish government funding agency 'Flanders Innovation & Entrepreneurship')

To everyone I have met in the laboratory, I would like to thank you for your constant support and for making this a fun experience and for keeping me motivated when it was getting hard. I would like to thank Jade for all her help, especially on the late nights and helping me with my *in vivo* study. Only a real friend would be willing to help me with all those organs.

I would also like to thank my family for all their encouragement throughout this process. Without you I wouldn't have been able to do this. Thank you for always being there when I needed you and for always pushing me to do my best. I cannot thank you enough.

Abstract

The application of liposomes and lipid nanoparticles as drug delivery vehicles has increased in recent years since the development of the first liposomal drug, Doxil®, to, more recently, the SARS-CoV2 mRNA-LNP vaccines. Liposomes provide a novel and versatile approach to drug delivery with limited off target side effects and increased delivery to the target site. The development of microfluidics has facilitated the simplification and accelerated translation of nanoparticles, including liposomes and lipid nanoparticles, from bench to bedside. Microfluidics as a production method allows for in-process, fine-tuning control of particle physicochemical properties through the altering of the total flow rate (TFR) and flow rate ratio (FRR). Therefore, the aim of this work was to investigate the impact of the parameters on liposome and lipid nanoparticle characteristics and their application in a biological systems to consider the impact of manufacturing and formulation on potency.

To achieve this, microfluidic process parameters and analytical tools were initially developed to support the knowledge space used to underpin subsequent studies. Design of experiments was then used to identify the complex interactions involved in liposome formation and build a predictive model for liposomal critical quality attributes manufactured by microfluidics. From these studies, it was shown flow rate ratio (FRR), lipid concentration and production temperature are critical for the determination of particle size, with higher order interactions present for other factors involved in microfluidic production, such as total flow rate (TFR) and solvent. To further investigate application of microfluidics for the production of liposomes, *in vitro* and *in vivo* studies of these liposomal formulations were conducted. These studies demonstrated that the choice of solvent used within microfluidic manufacturing impacted on both *in vitro* release and *in vivo* biodistribution. Finally, microfluidic manufacturing was applied to the manufacture of LNPs. These studies showed that a range of LNPs could be produced via microfluidics and that the choice of ionisable lipid impacted on their efficacy *in vitro* and *in vivo*; however, these studies demonstrated minimal correlation between *in vitro* and *in vivo* data.

Overall, the work presented in this thesis demonstrates the versatility of microfluidic production for the manufacturing of lipid-based nanoparticles such that their attributes can be in-process controlled, thereby reducing the processing steps required. When manufacturing these systems, it is important to consider all factors involved in lipid composition and production processes, as both are critical for the final product critical quality attributes.

Contents

List of Tables

List Of Figures

Abbreviations

ALC-0315	4-hydroxybutyl)azanediyl]di(hexane-6,1-diyl) bis(2-hexyldecanoa
API	Active pharamaceutical ingredient
C12-200	1,1'-[[2-[4-[2-[[2-[*bis*(2-hydroxydodecyl)amino]ethyl](2-hydroxydodecyl)amino]ethyl]-1-piperazinyl]ethyl]imino]*bis*-2-dodecanol
Chol	Cholesterol
CQA	Critical Quality Attributes
D/L	Drug:Lipid Ratio
DIR	(1,1'-Dioctadecyl-3,3,3',3'-Tetramethylindotricarbocyanine Iodide)
D-Lin-MC3-DMA	(6Z,9Z,28Z,31Z)-Heptatriaconta-6,9,28,31-tetraen-19-yl 4-(dimethylamino)butanoate
DLS	Dynamic Light Scattering
DMG-PEG2000	1,2-dimyristoylrac-glycero-3-methoxypolyethylene glycol-2000
DMPC	1,2-dimyristoyl-sn-glycero-3-phosphocholine
DMPE-PEG2000	1,2-dimyristoyl-sn-glycero-3-phosphoethanolamine-N-[methoxy(polyethylene glycol)-2000]
DODMA	1,2-Dioleyloxy-3-dimethylaminopropane
DOE	Design of Experiments
DOPC	1,2-Dioleoyl-sn-glycero-3-phosphocholine
DPPC	2-DiPalmitoyl-sn-glycero-3-PhosphoCholine
DPPC	Dipalmitoylphosphatidylcholine
DSPC	1,2-dioctadecanoyl-*sn*-glycero-3-phosphocholine
DSPE-PEG2000	1,2-distearoyl-sn-glycero-3-phosphoethanolamine-N-[methoxy(polyethylene glycol)-2000]
EMA	European Medicines Agency
EPR	Enhanced Permeation and Retention
FDA	Food and Drug Administration
Fluc-mRNA	firefly luciferase mRNA
FRR	Flow rate ratio
HFF	hydrodynamic flow focusing

HSPC	hydrogenated soy L-α-phosphatidylcholine
IPA	Isopropanol
LC-MS	Light Chromatography - Mass Spectrometry
LNP	Lipid Nanoparticle
LUV	Large unilamellar vesicle
MHC	Major Histocompatibility Complex
MHRA	Medicines & Healthcare Products Regulatory Agency
MLV	Multilamellar vesicle
mPES	Modified polyethersulfone
MPS	Mononuclear Phagocyte System
MSPC	monostearyl lysophosphatidylcholine
OVA	ovalbumin
PBS	Phosphate Buffered Saline
PC	phosphatidylcholine
PDI	Polydispersity Index
PEG	Polyethylene glycol
PMA	phorbol 12-myristate 13-acetate
PolyA	polyadenylic acid
POPC	1-palmitoyl-2-oleoyl-glycero-3-phosphocholine
PPE	palmar-plantar erythrodysesthesia
QD	Quantum Dot
SHM	Staggered Herringbon Micromixer
SM-102	Heptadecan-9-yl 8-((2-hydroxyethyl)[6-oxo-6-(undecyloxy)hexyl]amino)octanoate
SUV	Small unilamellar vesicle
TFF	Tangential Flow Filtration
TFR	Total flow rate
TM	Toroidal Mixer
Tris	tris(hydroxymethyl)aminomethane

Chapter 1 - Introduction

1.1 Liposomes

Liposomes are one of the first nanocarrier drug delivery systems with the potential to enhance therapeutic efficacy and reduce off target toxicities exhibited by conventional medicines (2). Liposomes were first described in 1965 by Alec Bangham and colleagues, where artificial lipid vesicles composed of lecithin where found to closely resemble biological membranes, allowing for the development of model membranes (3). This work provided the framework for Gregory Gregoriadis and colleagues, who were the first to establish the concept that liposomes could be used as a drug delivery system (4). Since then, liposomes have become the most well-established lipid-based nanomedicines, with the first liposomal drug being approved by the FDA in 1995 (5).

Liposomes are defined as spherical vesicles composed of phospholipid molecules, along with various sterols, such as cholesterol, arranged in one or more concentric lipid bilayers enclosing an aqueous core. The organisation of these amphiphilic phospholipids (such as phosphatidylcholines) into vesicles is driven by the polar interactions between the hydrophilic head groups and the hydrophobic acyl chains in the tails, such that the head groups are in contact with the exterior and interior aqueous environment with the hydrophobic tails in between thereby minimising unfavourable interactions between the hydrophobic acyl chains and the external aqueous environment (6). This organisation makes liposomes ideal drug carriers for not only hydrophilic molecules, which can be encapsulated within the aqueous core (Figure 1.1B) but also lipophilic drugs, which may be entrapped within the lipid bilayer (Figure 1.1A). Through this process, the bioavailability of the otherwise poorly soluble active pharmaceutical ingredients (APIs) can be increased (Figure 1.1) (7). The properties of these liposomes differ considerably depending on lipid composition, surface charge, size and the method of

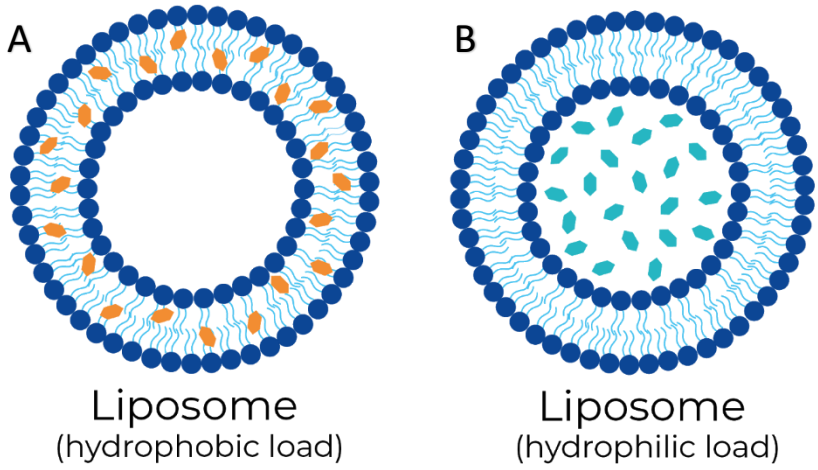

Figure 1.1: The encapsulation of both A) Hydrophobic compounds within the lipid bilayer and B) Hydrophilic compounds within the aqueous core.

Taken from https://www.pharmaexcipients.com/news/cannabinoid-liposome-formulations/

preparation (7). The resulting liposomes can then be further classified based on the number of lamellae into either multilamellar or unilamellar, which can then be separated into either small or large unilamellar vesicles (SUV or LUVs, respectively) (6). The versatility of the liposomes produced allows for the encapsulation and application of a wide variety of drugs with different biopharmaceutical properties.

1.2 Liposomes for Drug Delivery

Currently, there are four types of liposome delivery systems (Fig 1.2): conventional liposomes, sterically stabilised liposomes, ligand-targeted liposomes, and a combination of all the above (1). Conventional liposomes were the first generation of liposomes and are composed of cationic, anionic, or neutral lipids along with cholesterol, which is important for stability. These liposomes were found to reduce *in vivo* toxicity; however, they were rapidly cleared by the liver and spleen. Therefore, these are now generally used to research entrapment and release profiles of compounds (1, 8). In order to increase the stability of the liposomes and reduce macrophage uptake, lipids can be conjugated to polymers of polyethylene glycol (PEG), which acts to increase circulation half-life via preventing uptake and degradation by the mononuclear phagocyte system (MPS)(7). In addition to this, liposomes can be conjugated to specific ligands that aid in targeted delivery of the drugs to specific organs, therefore limiting exposure to other sensitive tissues (9, 10).

As a drug delivery system, liposomes offer several advantages compared with conventional medicines. These lipid-based nanomedicines have been developed due to their ability to 1) protect drugs from *in vivo* degradation, 2) control drug release, 3) modify distribution, 4) enhance solubility and bioavailability and 5) target drug delivery to the site of disease. The majority of these drugs are delivered parenterally, allowing them to bypass first-pass metabolism, increase bioavailability to the target site and reduce gastrointestinal side effects (11).

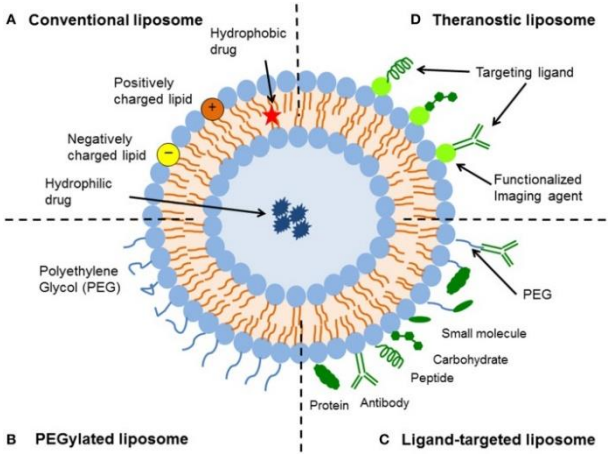

Figure 1.2: Different types of liposomal drug delivery systems. The liposome consists of a lipid bilayer that can be modified depending on the drug to be loaded and delivered. A) represents a conventional liposome that closely represents those found endogenously within the body. B) Liposomes has been modified and conjugated to polyethylene glycol (PEG) on the surface to increase stability and circulation time. C) Ligand-targeted liposome that can be used for the targeting of drugs to specific organs via the addition of specific antibodies and peptides. D) Theranostic liposome that consists of a ligand for specific targeting as well as an imaging agent for in vivo and in vitro analysis.

Taken from (1)

In addition to being used as a drug delivery system, lipid nanoparticles can also be used diagnostically and are called theranostic liposomes. These include iron oxide, quantum dots and gold nanoparticles that can be used for both diagnostic and therapeutic treatment (12). Quantum dots (QD) are semiconducting nanocrystals that have been shown to have higher fluorescent signals compared with traditional organic dyes and can be used as a potential imaging agent for diagnostic testing. The main limitation of these quantum dots is their low hydrophilicity, which limits their *in vivo* effectiveness. One way to overcome this limitation is to encapsulate these QD within the lipid bilayer of liposomes (13).

1.3.3 Drug Encapsulation

In general, drugs can be encapsulated within liposomes using either passive or active loading methods. The incorporation of the drug into the liposomes can be carried out either passively (i.e. during liposome formation) or actively (i.e. after liposome formation) and is dependent on the drug properties (7). Hydrophobic and lipophilic drugs are added to the organic solvent during lipid dissolution, whereas hydrophilic drugs are dissolved in the aqueous buffer. Passive loading involves the addition of the active compound to the aqueous phase and, therefore, can only be used for water-soluble drugs which often results in low encapsulation efficiency (14).

Active loading, on the other hand, is more efficient (14). This method allows for the loading of the API into the aqueous core along a transmembrane pH gradient (15). The remote loading process is dependent on two factors: the transition temperature of the lipid and the strength of the ion/pH gradient between the internal aqueous core of the liposomes and the external environment. For the

active loading process to be effective, the lipid bilayer needs to be in a more fluid phase to allow the selected molecule to diffuse across the membrane. This property is dependent on the transition temperature of the main lipid component of the bilayer. The transition temperature is the temperature at which the lipids transition from a gel phase to a more fluid, crystalline phase and is dependent on the hydrocarbon tail length and degree of saturation. With this pH gradient method, the external pH allows for the drug to exist in the unionised form allowing it to migrate across the lipid bilayer. Once inside the liposomes, the drug can then become ionised/protonated due to the change in pH, thereby trapping it and preventing the compound from diffusing back across the lipid bilayer (14). This method is dependent on the molecule being loaded and is often employed for the encapsulation of weak acids (and weak bases) (14, 15).

Doxorubicin has been shown to be successfully loaded in this way using an ammonium sulfate gradient (16). Small hydrophilic molecules, such as doxorubicin, are widely used for the treatment of many diseases, including cancer and infections. However, their therapeutic effect is limited due to their rapid clearance and biodistribution in the human body (17).

Liposomes, similar to biological membranes, have low permeability to hydrophilic drugs and high permeability to hydrophobic drugs, making the retention of hydrophobic drugs, such as paclitaxel, very difficult (15). Although liposomes are predominantly used for the encapsulation of hydrophilic compounds, they are also good carriers for hydrophobic/lipophilic compounds. Many lipophilic drugs can only be used therapeutically when used alongside toxic solubilising agents, thus preventing their clinical development. Therefore, encapsulating them into lipid vesicles may be an approach to assess whether these issues may be resolved (18).

Liposomes have also been further developed with the introduction of ionisable cationic lipids to increase the efficiency of encapsulation and delivery of siRNA, with Onpattro being the first approved LNP treatment for polyneuropathy in individuals diagnosed with hereditary transthyretin-mediated amyloidosis. In contrast to the production of Doxil, Onpattro is produced using microfluidic manufacturing processes (19).

1.2.1 Liposomal Products approved for human use

The most successful liposomal drug is Doxil®/Caelyx, which contains the anticancer drug doxorubicin and was approved by the FDA in 1995. Doxil® is an example of a 'stealth' or PEGylated liposomal formulation that is actively loaded with doxorubicin using an ammonium sulfate gradient (20). To promote tumour uptake, avoiding clearance via the liver and enhanced circulation times is a key aspect for liposomes. Indeed, studies have shown that liposomes extravasate into the tumour's extracellular fluid through small holes in the tumour's leaky vasculature (21) and this results in a

process known as the enhanced permeation and retention effect (EPR effect). In tumours, the permeability of capillary endothelium is enhanced, and the lymphatic system is underdeveloped (22) allowing for liposomes with a diameter of 100 nm or less to pass into the tissue (22). Overall this process is very slow, and, therefore, long-circulating liposomes possess the advantage due to their repeated passage through the tumour microvasculature (20). Since its initial formulation, various pharmaceutical companies have developed generic products which differ in their composition and manufacturing methods, and this was accelerated due to a shortage of Doxil® in 2011.

Since the approval of Doxil®, there have been multiple other liposomal drugs approved for clinical use, and these aren't limited to just anticancer compounds (Table 1.1). DepoDur™ is a liposomal extended-release formulation of morphine that is shown to provide postoperative analgesia for up to 48 hours (23). Another example is Exparel, which is a liposomal formulation of the analgesic bupivacaine. This formulation has been shown to provide up to 72 hours of pain relief, allowing for reduced opioid administration (24). Both formulations use a liposomal delivery technology called DepoFoam® (discussed in section 1.6.2).

Table 1.1: Clinically approved liposomal drug formulations.

Clinical Product	API	Lipid	Size	Year Approved
Doxil/Caelyx	Doxorubicin Hydrochloride	HSPC, Cholesterol, DSPE-MPEG	100 nm	1995 (US), 1996 (EU)
DaunoXome	Daunorubicin	DSPC, Cholesterol	45-80 nm	1996 (US)
AmBisome	Amphotericin B (AmpB)	HSPC, Cholesterol, DSPG	50-100 nm	1997 (US)
DepoCyte	Cytarabine	DOPC, DPPG, Cholesterol, Triolein	20 µm	1999 (US), 2001 (EU)
Myocet	Doxorubicin Hydrochloride	EPC, Cholesterol	80-90 nm	2000 (EU)
Visudyne	Verteporfin	EPC, DMPC	<100 nm	2000 (US, EU)
DepoDur	Morphine	DOPC, DPPG, Cholesterol, Triolein, Tricaprylin	17-23 µm	2004 (US)
Mepact	muramyl tripeptide phosphatidyl ethanolamine (MTP-PE)	POPC, OOPS	2.0-3.5 µm	2009 (EU)
Exparel	Bupivicaine	DEPC, DPPG, Cholesterol, Tricaprylin	24-31 µm	2011 (US), 2020 (EU)
Marqibo	Vincristine Sulfate	Sphingomyelin (SM), Cholesterol	130-150 nm	2012 (US)

Onivyde	Irinotecan hydrochloride trihydrate	DSPC, Cholesterol, MPEG2000-DSPE	110 nm	2015 (US), 2016 (EU)
Vyxeos	Daunorubicin, cytarabine	DSPC,DSPG, Cholesterol	110 nm	2017 (US), 2018 (EU)
Shingrix	Recombinant varicella-zoster virus glycoprotein E	DOPC, Cholesterol	50-100 nm	2018 (EU)
Arikayce	Amikacin sulfate	DPPC, Cholesterol	200-300 nm	2018 (US), 2020 (EU)

1.3 Lipid Nanoparticles (LNPs)

Similar to liposomes, lipid nanoparticles (LNPs) are lipid-based nanoparticle structures composed primarily of cationic or ionisable lipids and are especially geared towards the encapsulation and delivery of nucleic acids (25). LNPs are becoming increasingly used for gene therapy, protein replacement therapy, with the most notable application being the delivery of mRNA vaccines against both cancer and infectious diseases (26).

In particular, mRNA-LNP vaccines have become prominent as effective delivery systems due to their decreased immunogenicity, simple production and scalability (27). The challenge when trying to deliver mRNA is that naked mRNA is rapidly degraded by endogenous RNases and the hydrophilic nature and negative charge make it very difficult for any undegraded mRNA to enter the target cell due to the electrostatic repulsion by the cell membrane (28). Therefore, the mRNA requires a protective delivery system that can aid in trafficking the mRNA into the cells where it can be translated. Therefore, encapsulating the mRNA within LNPs provides a protective coating that can bind with cell membranes, effectively delivering the payload to the target cells. The advantages of LNP vaccines are that they can combine the advantages of subunit vaccines and live-attenuated vaccines without the associated risks. Unlike DNA therapeutics, mRNA vaccines are not required to cross the nuclear membrane, making them easier to deliver. Onpattro was the first approved LNP drug and is used for the treatment of hereditary transthyretin-mediated amyloidosis. More recently LNP technology has been used to develop vaccines against SARS-CoV-2 (Comirnaty® and Spikevax vaccines) (25). The use of LNP vaccines during the COVID-19 pandemic highlighted their application as an effective strategy for mRNA-based treatments (27).

Unlike liposomes, the internal structure of LNPs is more complex (Figure 1.3). LNPs, are composed of 4 lipids, i) ionisable or cationic lipid, which is required for mRNA encapsulation, ii) helper lipids, such as phosphatidylcholine (e.g. DSPC), which act as the main structural component, iii) cholesterol, which provides stability, and iv) a PEGylated lipid, to improve storage stability and prevent immune

recognition (27). The cationic or ionisable lipid is the key component of LNPs allowing for the encapsulation of nucleic acids due to their electrostatic interactions. The first LNPs developed were composed of cationic lipids that had a permanent positive charge. However, due to high toxicity and low *in vivo* efficacy, they have been replaced with ionisable lipids. These ionisable lipids are pH-sensitive and tend to have a pKa of between 6-6.7 (29), and are designed to have a neutral charge at physiological pH and become positively charged in acidic environments, such as in the endosome (28). In general, these lipids account for 30 - 50% of the overall lipid composition (28).

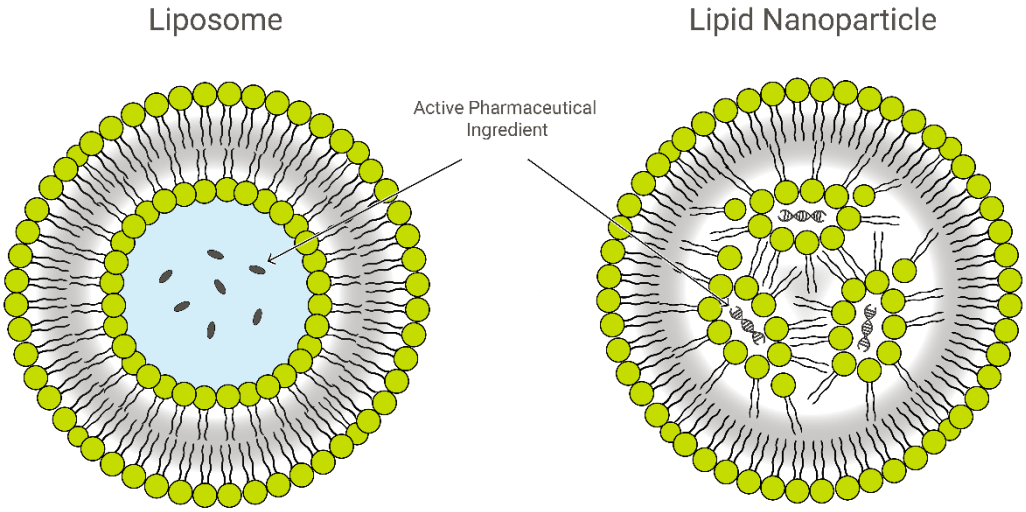

Figure 1.3:Difference in structures of liposomes and LNPs. Liposomes are composed of a lipid bilayer surrounding a large aqueous core, whereas LNPs contain ionisable lipids that for electrostatic interactions with the nucleic acid payload within the interior of the lipid bilayer.

Taken from: Liposomes and Lipid Nanoparticles as Delivery Vehicles for Personalized Medicine (exeleadbiopharma.com)

The key factors that determine LNP biodistribution and efficacy are the particle size, biodistribution and the membrane properties. The exact mechanism by which LNPs efficiently deliver mRNA to the cytoplasm is not fully understood. However, it is thought that LNPs are taken up into the target cell via endocytosis, through electrostatic attachment and fusion with the cell membrane. Once inside the cell, the LNP is directed to the lysosome, where the LNP is degraded (30). It is estimated that <2% of the LNPs escape this degradation and reach the cytosol (31) where the resulting mRNA is transcribed, and the encoded antigen is then degraded into smaller peptides that are presented on major histocompatibility complex (MHC) class I molecules on the cell surface (32). In addition to being easier to deliver, synthesis and purification of mRNA is fast, easy and lower cost compared with other vaccines (32). However, the main challenge faced by mRNA vaccines for clinical approval is their intracellular delivery. mRNA is unstable under physiological conditions and is sensitive to ribonuclease degradation therefore, several strategies have been developed to overcome this, including LNPs (32).

1.4 Liposomes and LNP Manufacturing

Despite being widely researched since their discovery in the 1960s, very few liposomal drug formulations have made it to clinical application due to the cost of manufacturing and limited industrial-scale production techniques. The production of liposomes is a multi-batch process that produces limited batch sizes and relies on the uncontrolled self-assembly of lipids, resulting in the production of non-uniform liposomes, in terms of polydispersity, size and lamellarity, therefore requiring further processing which subsequently increases costs, limits production and hinders development (11, 19, 33). In addition to production costs, liposomes are relatively unstable and have a very short shelf-life. Phospholipids can be sensitive to changes in temperature and have to be stored in relatively cool conditions (2-8 °C), making them difficult to transport (11). Liposomes also tend to fuse together or leak out the encapsulated drug, altering drug loading and therapeutic efficacy. This has been overcome via freeze-drying the final liposome products, which are then rehydrated upon administration. However, this adds another parameter to production and additional costs. Similar to liposomes, LNPs can be prepared by a range of methods, but microfluidics is the preferred method of manufacturing due to the high reproducibility and scalability of the processes (28).

1.4.1 Conventional Production Methods

The manufacturing of nanoparticles, in general, can be separated into two categories: bottom-up and top-down. The top-down approach involves the production of large vesicles that then undergo size reduction techniques to produce homogenous, unilamellar vesicles. Whereas bottom-up involves the manufacturing of vesicles from individual monomers, therefore negating the need for size-reduction techniques (34).

Currently, there are a wide variety of production methods, with thin-film hydration, ethanol injection and reverse-phase evaporation being the preferred methods for laboratory-scale production, with lipid-film hydration and ethanol injection being implemented in commercial-scale production. All these techniques follow the same general process, involving the dissolution of the lipids in a solvent, which is then removed, resulting in the spontaneous self-assembly of the phospholipids into vesicles. Different techniques are used depending on the type of liposomes to be produced, for example, lipid film hydration is used for the production of multilamellar vesicles and ethanol injection tends to produce larger unilamellar vesicles (7). These initial vesicles are heterogenous and, therefore, require further modifications in order to reduce particle size and minimise polydispersity (35). The most common method of reducing particle size is the extrusion of the liposomes through a polycarbonate filter of defined pore size (7, 35).

Thin-Film Hydration: The thin-film hydration method is the most commonly used traditional method for the product of liposomes and is an example of a top-down manufacturing approach. This technique is most suited for the loading of lipophilic molecules, which can be incorporated into the organic phase (36). This method involves the evaporation of the solvent containing the lipids under vacuum to create a thin film. This film is then dissolved in the aqueous buffer, resulting in the formation of MLVs. The particle size of these liposomes can then be further reduced via extrusion (36).

Reverse-Phase Evaporation: Reverse-phase evaporation is based on the production of inverse micelles that are produced upon sonication of the aqueous buffer, containing the molecule to be encapsulated, and the organic solvent containing the lipids. The solvent is then removed using rotary evaporation, resulting in the formation of a gel that, in turn, collapses to form liposomes suspended in the aqueous buffer, resulting in the formation of LUVs with high encapsulation (7). However, there are a couple of drawbacks to this method, the first is that the liposomes would then need to undergo further downsizing processes, and the second is that the molecule to be encapsulated will have brief contact with the organic solvent and undergo short periods of sonication which could result in damage and degradation of the molecule (7).

Ethanol Injection: In this technique the lipids are dissolved in an organic solvent and then injected into a large volume of aqueous buffer, resulting in the spontaneous formation of SUVs. As the particles produced in this method are small in size (80-100 nm) no downstream size reduction processes are required (36). One of the disadvantages of this method is that the resultant liposome solution is very dilute (7). This method has since been modified and is used in microfluidic devices.

There are several critical quality attributes that have to be monitored throughout the liposome production process including particle size, stability, polydispersity, drug loading and release. Monitoring of these parameters therefore adds additional control points and unit operations that further increase the complexity and time required for production (11).

1.4.2 Size-Reduction Methods

Particle size and polydispersity are critical attributes for the safety and efficiency of liposomal delivery systems, as these can influence drug loading, biodistribution, clearance and therapeutic efficiency (37). Liposomes produced by the conventional techniques above often rely on subsequent particle size reduction to produce small, heterogeneous, unilamellar vesicles. The earliest method for size reduction was sonication, either using a bath or probe sonicator. In this method, liposomes are exposed to ultrasonic energy that results in the destabilisation of the membrane, causing the membrane to break apart and reform into smaller vesicles. Both bath and probe sonication have their own advantages and disadvantages. Bath sonication is a non-contact method, therefore limiting the

risk of contamination and allowing for the size reduction of multiple samples at the same time. However, it is limited by the ability to produce enough energy to cause the membrane to break apart. Probe sonication, on the other hand, is simple and well-researched, however, the use of a probe means that there is an increased risk of contamination as well as the risk of lipid degradation due to the generation of heat by the probe (34). The most common method for size reduction is extrusion. In this method, the liposomes are passed across multiple, layered membranes of defined pore size multiple times. The resultant characteristics of the liposomes are dependent on the pore size of the membrane, the pressure applied during the extrusion process, and the number of times the particles are passed through the various membranes (38). For this method to work efficiently it is required to carry out the extrusion process above the transition temperature of the helper lipid. The disadvantages of this method is that similar to probe sonication is the risk of contamination, as this is a contact method, and also there is a risk of lipid loss and degradation due to oxidation and overheating (34).

1.5 Microfluidics for Scale-Up Production of Liposomes

Microfluidics is an example of a bottom-up manufacturing approach. Microfluidic mixing involves the rapid and controlled mixing of an organic lipid phase with an aqueous buffer under controlled conditions. Microfluidic devices have been applied in many fields, including drug development and biomedical diagnostics, as well as the food and chemical industries (39, 40). However, microfluidics has increased in popularity as one of the most recent manufacturing techniques to produce liposomes and LNPs. This technology provides many advantages, such as the use of smaller sample volumes and higher control over the physical properties of the product. The ability to precisely control and manipulate fluids at the micrometre scale makes microfluidics an attractive technique for the production of liposomes and LNPs (41). The manufacturing of nanoparticles requires precise control of both the kinetic and thermodynamic reactions, allowing for the production of nanoparticles with varying sizes, shapes, and internal structures (42).

The aim of microfluidic mixing is to enhance the mixing efficiency and, therefore, increase the production of small homogenous particles (39). There are 2 types of mixers that can be used during microfluidics: passive mixers and active mixers. Passive mixers do not apply any external forces to the sample and instead rely on the microchannel geometry to increase the contact area/time to enhance the diffusive mixing of the aqueous and organic phases. Active mixers on the other hand, incorporate external mechanical forces within the microfluidic device to increase the mixing efficiency (39, 43, 44).

During passive microfluidic manufacturing laminar flow is used to mix both the aqueous and the organic phase within the microfluidic mixer. As the organic phase dilutes and diffuses into the aqueous

phase the lipids begin to form liposomes which become more stable as the mixture reaches equilibrium (33). The formation of these liposomes within a confined microenvironment and controlled fluid flow rate allows for precise control of liposome size and reduces processing into a single step, thereby reducing costs and increasing production. As previously mentioned, Patisiran (Onpattro) is produced using microfluidics, with production being described in five main steps compared with conventional techniques, which can involve a minimum of 9 and up to 18 unit operations, in the case of Doxil® production (11).

In order to understand and characterise these mixing systems, there are a couple of process parameters which need to be described; these include microflows and dimensionless numbers. The fluid flow in these microfluidic systems can be characterised by two dimensionless numbers, the Reynolds number and the Peclet number. The Reynolds number is defined as the ratio between inertial forces and viscous forces and determines the type of flow within the microfluidic device (Equation 1) (45). The value of the Reynolds number increases with flow velocity and channel dimensions, and decreases with viscosity (46). The value of the Reynolds number is an indicator of the type of flow that will occur in the microfluidic device. At Reynolds number below 2000 the flow is considered to be laminar and anything above this value will be considered to be turbulent flow. In general, microfluidic devices have low Reynolds number and therefore are considered a laminar flow mixer (45, 46).

Equation 1.1: Reynolds number equation

$$Re = \frac{(\rho * D * V)}{\mu}$$

Where: Re = Reynolds Number

P = Density

D = Diameter

V= Velocity (flow speed)

μ = Viscosity

The Peclet number is a measure of the molecular diffusion between convective and advective diffusion processes and is crucial for optimisation of passive mixing devices (45). The diffusion between fluids within microchannels occurs at the interface of where these two fluid streams meet and can often be a slow process, therefore requiring increased channel lengths to allow for sufficient diffusion and mixing. The Peclet number can, therefore, be used to determine the optimal channel length for

effective mixing (Equation 1.2), with a larger number indicating a shorter mixing length is needed due to the increased convective processes (45).

Equation 1.2: Peclet number equation

$$Pe = \frac{VL}{D}$$

Where: Pe = Peclet number

V = Velocity (Flow speed)

L = Length

D = Diffusion Coefficient

The structure of these microfluidic devices is an important determinant for nanoparticle synthesis and resultant properties. Even slight differences in the geometry of these devices can result in large differences in mixing and subsequent nanoparticle characteristics and properties. There are a number of different microfluidic mixer designs available, such as the T-junction, Y-junction, flow focussing, and staggered herringbone mixers, which are some of the most popular (47).

T- and Y-junction: The T-junction mixer is one of the simplest microfluidic designs. There are two proposed designs for this mixer (Figure 1.4). Figure A shows a T-mixer where the inlet channels are located facing each, allowing for the two liquid phases to meet in the middle and be mixed down the length of the mixer. The second proposed design (Figure 1.4B) in this design the organic phase inlet is located perpendicular to the aqueous stream, creating droplet formation at the point where the two phases bisect each other (47, 48). The Y-junction micromixer is similar to the T-junction design. In this mixer the two inlets are at an angle.

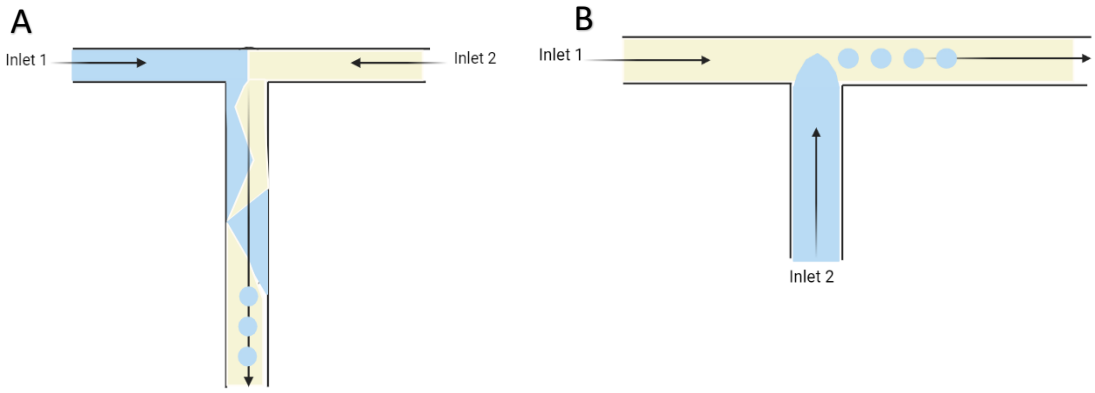

Figure 1.4: Two different T-mixer configurations. A) Two inlet streams facing each other and B) Two inlet streams sit perpendicular to each other. Created with BioRender.com

Flow Focussing: In the flow-focussing mixer, there are 3 inlets, rather than just the two that are commonly observed in the majority of micromixers. In this method of mixing, the 2 side channels contain the aqueous phase, and the central stream contains the organic lipid phase (Figure 1.5). The resultant liposome size is controlled by adjusting the flow rates of the aqueous phase (coming from the side inlets) and the ratio between the two phases. The higher the difference in flow rate between the aqueous and organic phases, the thinner the central stream and the shorter the mixing time, resulting in smaller nanoparticles.

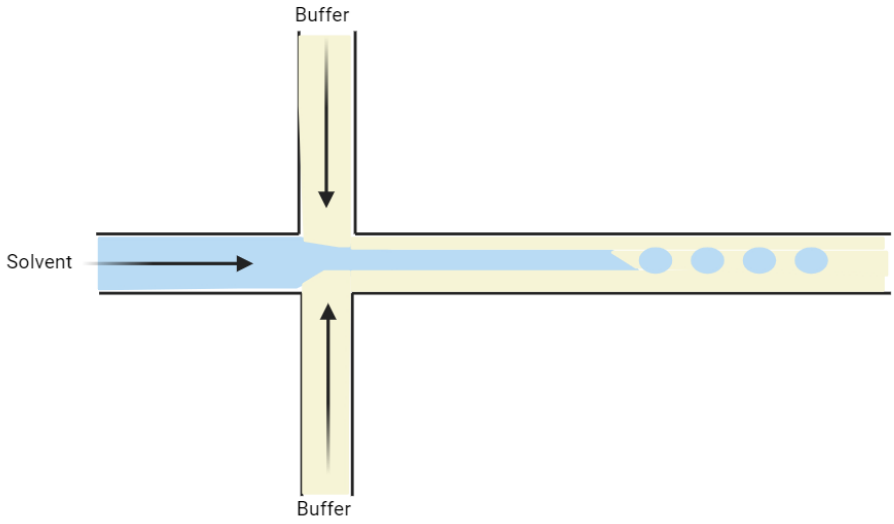

Figure 1.5: Schematic of a flow focusing mixer. Created with BioRender.com

Staggered Herringbone: The staggered herringbone micromixer (SHM) is one of the newer micromixer designs that has attracted a lot of attention due to its simple design and ease of manufacturing (49)The design of this mixer includes the application of raised, herringbone groves within the microchannels (Figure 1.6). These groves cause the formation of counter-rotating vortices, which alter the flow pattern along the length of the mixing channel. This results in the uniform mixing and dispersion of the organic and aqueous phases, which produces small, homogenous dispersions.

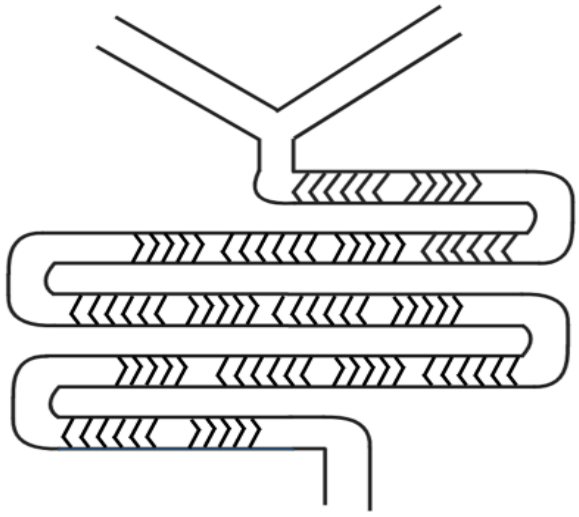

Figure 1.6: Schematic of a staggered herringbone micromixer

1.6 Factors affecting Liposome and LNP Properties

There are a number of parameters that can be manipulated in order to produce liposomes and LNPs of the desired size and lamellarity; these include manufacturing parameters, such as flow rate ratio and total flow rate, as well as formulation parameters, such as lipid composition and solvent selection. Of these process parameters, flow rate ratio (FRR) is considered to be one of the most important for both liposome and LNP manufacturing (50). FRR is the ratio between the aqueous and organic phases and determines particle size and biodistribution, with a higher FRR resulting in the production of smaller liposomes and LNPs (16, 50). The formation of nanoparticles is driven by the self-assembly of the lipids in an aqueous environment. Altering the FRR changes the volume of the aqueous environment, leading to changes in the diffusion rate of the organic phase in the aqueous buffer (i.e. at lower FRR there is a larger volume of both the organic and aqueous phases meaning that the diffusion of the organic phase into the aqueous and subsequently the spontaneous formation of the lipid bilayer takes longer than when there is a larger aqueous volume and smaller organic volume at higher FRR). The total flow rate (TFR) has been shown to have minimal impact on the final nanoparticle properties, allowing for increased production rates and scalable manufacturing.

The accumulation of liposomes into target tissues is thought to be dependent on a number of factors including the circulation time in the bloodstream, the diffusion of liposomes from the bloodstream into the tissue, the retention time within the tissue and the efflux of the liposomes back into the blood (22).

1.6.1 Particle size

Prolonged circulation in the bloodstream is critical for increased liposome uptake and accumulation within the target tissue. Liposome size is a key factor for circulation time in the bloodstream and is also attributed to their uptake into tissues as well as by the mononuclear phagocytic system (MPS). As with any foreign material that enters the body, nanoparticles can be detected as foreign, resulting in the initiation of a biological response. Upon administration and contact with biological matrices, these nanoparticles can be coated by proteins, leading to the formation of a protein corona surrounding the nanoparticle. This corona can be made up of a variety of different cellular components that determine the fate of the nanoparticle (51). The smaller the liposomes, the less likely they are to be recognised by compliments in the blood, and therefore, they will have a more prolonged circulation time and subsequently increased accumulation within the target tissue (20, 22).

Choosing the optimal particle size for the nanoparticle formulation will also depend on the route of administration. Research has shown that smaller siRNA LNPs (45 nm) were most potent when delivered subcutaneously, whereas larger particles (80 nm) showed increased efficacy when delivered intravenously (28).

1.6.2 Lipid composition and structure

The lipid composition is a key factor in determining the biodistribution of both liposomes and LNPs. Changing the lipid composition can result in changes to the structure, particle size, membrane stability and, subsequently, circulation time and biodistribution profile of the nanoparticle formulation. Naturally occurring phospholipids, such as 1-palmitoyl-2-oleoyl-glycero-3-phosphocholine (POPC) and 1,2-Dioleoyl-sn-glycero-3-phosphocholine (DOPC) have higher affinity and likelihood of binding to membrane bound proteins which can help facilitate uptake and transport across cellular membranes (38). It has been shown that the inclusion of saturated phospholipids, such as HSPC and DSPC, and cholesterol increases membrane rigidity and subsequently the circulation time whereas anionic lipids tend to decrease circulation time (22). The hydrophobicity of the nanoparticles is also another important factor that influences protein binding and subsequently uptake and clearance of the nanoparticle from the circulation. Hydrophilic nanoparticles are opsonised more quickly and are therefore cleared from the circulation quicker. Not only does hydrophilicity influence the amount of opsonisation but also determines the types of proteins that will bind the nanoparticles (51). The

binding of these proteins alters the size and surface charge and therefore influence the internalisation processes and biodistribution of the nanoparticle. Binding of IgG and complement factors are said to promote phagocytosis by cells of the MPS which then migrate to the spleen and liver where the nanoparticles are cleared from the circulation, whereas binding of albumin to the nanoparticle surface has been shown to promote prolonged circulation (51).

Since the development and approval of Doxil® there have been several other marketed liposomal doxorubicin formulations that differ in composition and properties. Compared with Doxil®, Myocet is a non-PEGylated version of liposomal doxorubicin. The PEGylated coating on Doxil®, enhances circulation time consequentially resulting in the dose-limiting side effect of this formulation which is the development of palmar-plantar erythrodysesthesia (PPE) which is more commonly known as hand-foot syndrome (52). This is due to the prolonged half-life of the formulation, which has been shown to leak out in the sweat, resulting in accumulation resulting in redness and peeling of the skin on the hands and feet (52, 53). The absence of the PEGylated lipid in Myocet reduces the incidence of hand-foot syndrome whilst showing no loss of efficacy (52).

The development of temperature sensitive liposomes has allowed for more controlled and targeted drug delivery. These liposomes are composed of phospholipids with transition temperature just above physiological temperature such as ,2-DiPalmitoyl-sn-glycero-3-PhosphoCholine (DPPC) which has a transition temperature of 41 °C. The incorporation of lysolipids, such as monostearyl lysophosphatidylcholine (MSPC), has been used lower the transition temperature required for release (54, 55). ThermoDox® was the first temperature-sensitive liposomal formulation to make it to clinical trial however, did not progress past Phase III due to failure to reach its primary endpoint. It is designed to prevent drug leakage at physiological temperature; however, upon exposure to increased temperature (42 °C), it releases its contents into the intended target.

As mentioned briefly in section 1.2.1, DepoDur and Exparel are examples of liposomal formulations that utilise the DepoFoam® technology. These liposomes are classed as multilamellar liposomal formulations however are distinguished from other multilamellar vesicles (MLV) by their structure and composition (56). Compared with other MLV that have concentric bilayers, DepoFoam® have non-concentric lipid bilayers that are arranged to form multiple little “pockets” with in the liposomes that each encapsulated the active compound. It is this internal structure that allows for the slow, sustained release of the encapsulated compound. As the internal membranes burst and the drug is redistributed within the liposomes and it is only when the outermost layer of the liposomes is ruptured that the active compound is released into the external environment (56).

In terms of LNPs, the structure of the ionisable lipid is critical for the encapsulation and transfection potency of the formulation (57). The pKa of the ionisable lipid is one of the most important factors for LNP delivery and transfection as it determines the ionisation behaviour, surface charge, stability and potency of the nanoparticles (58). The structure of the ionisable lipid is also important for endosomal escape. It has been shown that ionisable lipids with branched tails, and therefore more cone-like in shape, show increased endosomal disruption due to the increased cross-section of the hydrocarbon tail of the lipids (59).

1.6.3 Surface Charge

Research has shown that neutrally charged liposomes have a slower opsonisation rate than both anionic and cationic particles. The binding of opsonins to the particle surface creates a molecular signature which is recognised by cells of the immune system and is a key factor in the determination of the internalisation route of the nanoparticles. It has also been shown to enhance uptake by cells of the MPS (51).

As briefly mentioned in section 1.6.2, the pKa of the ionisable lipid can determine the surface charge of the LNP. The surface charge of the LNP affects the uptake and endosomal release, as well as the biodistribution of the LNP formulation (58). LNPs containing ionisable lipids rely on the change in pH for uptake and release of the nucleic acid payload. As mentioned previously in section 1.3, the LNPs rely on the change in pH in the endosome for release of the payload into the endosome for processing and translation. At optimum pKa the LNPs carry a neutral charge, thereby preventing nonspecific binding and toxicity (58).

1.6.4 Solvent selection used during manufacture

Solvent selection has also been shown to impact on liposome physicochemical characteristics with more polar solvents, resulting in an increase in liposome particle size (60). A recent study investigated the effect of different organic solvents, including methanol, ethanol, propanol-2 and Transcutol, on liposome properties produced using a periodic disturbance mixer. The results of this study showed that Transcutol produced liposomes of the smallest size compared with IPA, ethanol and methanol, and this was thought to be due to the different polarities of the solvents. Transcutol has the lowest polarity followed by IPA, ethanol and methanol, and it has been reported that using Transcutol will produce the highest polarity gradient, resulting in a more drastic and faster polarity change, producing smaller liposomes (61). Other studies have shown contradicting results (60) This may suggest that the mixing method plays an important role in the resulting liposome physicochemical characteristics, as this is primarily what is responsible for the change in polarity and, therefore, the resulting liposome size.

1.7 Aims and Objectives

The overall aim of the work within this thesis was to explore the impact on manufacturing conditions of resultant lipid-based nanoparticle (liposomes and LNPs) characteristics and how the manufacturing and formulation conditions affect the encapsulation and subsequent *in vitro* and *in vivo* release of small molecule compounds. The effect of microfluidic manufacturing conditions, such as FRR, TFR and production temperature, as well as the effect of formulation parameters, such as type of lipid and solvent, was tested for liposomes. The produced liposomes were then loaded with a variety of small molecule compounds and the characteristics determined by DLS measurement to determine the particle size, PDI and zeta potential. Selected formulations were tested *in vitro* and *in vivo* to determine whether the manufacturing and formulation parameters have an effect on release and biodistribution of liposomes. LNPs closely resemble liposomes and the application of LNPs in clinical use has increased in recent years due to the importance of these formulations in the COVID-19 pandemic. There are a variety of different LNP formulations in circulation and it is therefore important to determine their *in vitro* and *in vivo* efficacy prior to clinical use. Four approved LNP formulations were therefore tested both *in vitro* and *in vivo* to determine whether there was any correlation and to determine how different LNP formulations behave.

To achieve this aim, the objectives were:

1. Optimisation and assessment of the effect of altering microfluidic parameters (FRR and TFR) on liposome characteristics and active loading of the model compounds, acridine orange and doxorubicin.
2. Carry out a design of experiments (DOE) study to determine the interactions between manufacturing and formulation parameters on resultant liposome physicochemical characteristics.
3. Determine how microfluidic and formulation parameters affect the liposome properties and encapsulation of small molecule compounds loaded across and ammonium sulfate, pH gradient.
4. To determine the effect of manufacturing and formulation conditions on liposome *in vitro* and *in vivo* release profiles and biodistribution of doxorubicin loaded liposomes.
5. Translate the manufacturing of liposomes to LNPs and determine the correlation between *in vitro* and *in vivo* expression profiles.

Chapter 2 - Process Development and Analytical Tools

2.1 Introduction

Since their discovery by Bangham et al. in 1965, nanomedicines, including liposomes and lipid nanoparticles (LNPs), have been extensively researched and used to deliver various compounds for various diseases (5). The structure and composition of these vesicular delivery systems makes them carriers for not only hydrophilic compounds but also hydrophobic compounds as well as nucleic acids (7). There have been a number of methods developed for the production of liposomes; however, most of these methods rely on batch processing that requires further downstream optimisation that can be both expensive and time-consuming (11). Therefore, it is important to develop a new manufacturing method that is more efficient and cost-effective.

As mentioned in Chapter 1, microfluidics is a manufacturing method that involves mixing 2 liquids within micrometre channels (33). During microfluidic manufacturing, the aqueous and organic lipid-containing phases are injected into a microfluidic mixing device. The formation of the liposomes relies on the rate at which the organic phase is diluted in the aqueous phase (60). As the organic phase mixes and is diluted in the aqueous phase, the lipids orientate themselves in such a way that the hydrophilic head group is in contact with the aqueous environment, and the hydrophobic tails are in the middle of the bilayer. This spontaneous arrangement allows the encapsulation of an aqueous core.

Due to the way in which the liposomes are formed during microfluidic mixing, there are a number of factors that can be manipulated to determine the final liposome properties. There are two manufacturing parameters that can be altered during microfluidic production; these include the total flow rate (TFR) and the flow rate ratio (FRR) (16). The TFR is the speed at which the two syringes containing the aqueous and organic phases are injected into the microfluidic chip, whereas the FRR is the ratio of aqueous to organic phase.

Depending on the properties of the drug compound, it can either be loaded into the liposomes in the lipid bilayer or the aqueous core. Hydrophobic drugs are encapsulated within the lipid bilayer, and this is achieved by putting the API in the organic lipid phase. In contrast, hydrophilic compounds can be loaded via two different methods. These are called passive and active loading. Passive loading involves adding the API to the aqueous buffer prior to mixing and liposome formation, whilst active loading involves the addition of the drug after the liposomes have been formed. During this process, the active compound is loaded into the liposomal aqueous core along a transmembrane pH gradient. This process allows for the high encapsulation of various compounds.

Aims and Objectives

This chapter aimed to investigate the effect of microfluidic production on liposome physicochemical characteristics and to characterise and optimise the active loading process. To achieve this, the objectives were:

- Evaluate how altering microfluidic parameters will affect liposome characteristics.
- Investigate the optimal method for liposome purification and removal of unencapsulated compound.
- To establish standard protocols to investigate the active loading of liposomes manufactured by microfluidics.

A range of factors were considered within this chapter using acridine orange as the model API drug as it has been used previously to investigate transmembrane pH gradients (62).

2.2 Methods and Materials

2.2.1 Materials

1,2-dioctadecanoyl-*sn*-glycero-3-phosphocholine (DSPC), 1,2-dioleoyl-sn-glycero-3-phosphocholine (DOPC), hydrogenated soy L-α-phosphatidylcholine (HSPC, > 99%), 1,2-distearoyl-sn-glycero-3-phosphoethanolamine-N-[methoxy(polyethylene glycol)-2000] (sodium salt) (DSPE-PEG2000,>99%) and cholesterol (chol, >99%). Acridine orange hydrochloride hydrate and ammonium sulfate ($[NH_4]^2SO_4$,>99%) were obtained from Sigma-Aldrich Ltd. (Poole, UK). Phosphate buffered saline tablets (10 mM, PBS pH 7.3) were acquired from Oxoid Ltd (Basingstoke, UK). All reagents (ethanol, methanol, isopropyl alcohol) were of analytical grade (HPLC grade,> 99.8%), and Transcutol was of general purpose grade and purchased from commercially available suppliers.

2.2.2 Manufacturing of PEGylated Liposomes Encapsulating Ammonium Sulfate

PEGylated liposomes were prepared using the bench-scale microfluidic system (NanoAssemblr Benchtop) from Precision NanoSystems Inc. (Vancouver, Canada), which uses a staggered herringbone micromixer (SHM). Liposome formulations containing HSPC, cholesterol and DSPE-PEG2000 at a w/w ratio of 3:1:1, respectively, were produced from a 40mg/mL total lipid stock solubilised in ethanol. Lipids were heated for solubilisation but were stable once in solution. The lipids were allowed to reach room temperature before injection into the micromixer. Ammonium sulfate ($[NH_4]_2SO_4$, 250 mM) was used as the aqueous phase. Liposomes were initially produced at a total flow rate (TFR) of 10 mL/min and a flow rate ratio (FRR) of 3:1. The effect of the microfluidic process parameter, total flow rate (TFR), was evaluated. Liposomes produced on the NanoAssemblr Benchtop were then compared with those produced on the updated model, the Ignite from Precision NanoSystems Inc. (Vancouver,

Canada), which uses a disposable toroidal micromixer. These liposomes were produced from the same HSPC:Cholesterol:DSPE-PEG2000 40mg/ml stock (w/w 3:1:1) at a FRR of 3:1 and TFR 10 mL/min encapsulating an aqueous ammonium sulfate ($[NH_4]_2SO_4$, 250 mM) core. The effect of flow rate ratio (FRR) was also investigated. HSPC:Cholesterol:DSPE-PEG2000 liposomes were produced at TFR 10 mL/min encapsulating ammonium sulfate (250 mM), and the flow rate was varied from 1:1 to 10:1.

2.2.3 Buffer Exchange of PEGylated Liposomes using Tangential Flow Filtration

The PEGylated liposomal formulation encapsulating $[NH_4]_2SO_4$, 250 mM was produced, and the solvent was removed whilst simultaneously conducting buffer exchange to establish a pH gradient between the liposome interior and the exterior medium for active-loading of drugs. A tangential flow filtration system (KR2i TFF System, Repligen, Waltham, US) using a Repligen 500 kDa modified polyethersulfone (mPES) column and masterflex tubing 13 was used. The sample was filtered at a 20 mL/min flow rate and 12 diafiltration volumes with PBS (pH 7.3, 10 mM). Samples were diluted 1:5 with ammonium sulfate prior to filtration and recovered to the original volume. This resulted in PEGylated liposomes encapsulating acidic pH ($[NH_4]_2SO4$, pH 5.5) and suspended in PBS (pH 7.3), creating a gradient for the diffusion of drugs with protonisable amine functions. These liposomes were then diluted 1:1 with PBS prior to sizing and active-loading of acridine orange.

2.2.4 Buffer Exchange of PEGylated Liposomes using Dialysis

The PEGylated liposomal formulation encapsulating $[NH_4]_2SO_4$, 250 mM was produced, and the solvent was removed whilst simultaneously conducting buffer exchange to establish a pH gradient between the liposome interior and the exterior medium for active-loading of drugs. Formulations were dialysed (MWCO 12,000–14,000 Da, Sigma-Aldrich, Poole, UK) for 1- 3h under magnetic stirring against 200 mL PBS buffer per 1 mL sample to establish a pH gradient. After remote loading, the liposomes were dialysed against PBS buffer for either 3 h, changing the buffer every 1 h, or overnight to remove free drug.

2.2.5 Active-loading of Acridine Orange into PEGylated Liposomes

Liposomes were produced using microfluidics at a final concentration of 10 mg/mL before being diluted and purified using tangential flow filtration to a final concentration of 5 mg/mL. Acridine orange stock was prepared at 1 mg/mL in PBS. A specific volume was added to the liposomes at a ratio of 0.004 g acridine orange/ g lipid. The effect of incubation time was evaluated. Liposomes were incubated in a water bath at 60°C for different times (20 minutes, 40 minutes, 1 hour and 2 hours), and the percentage of acridine orange loading was calculated. After loading, the liposomes were allowed to cool down to room temperature and non-encapsulated acridine orange was removed using tangential flow filtration again. The quantification of acridine orange loading was measured using a

microplate reader (Bio-rad Laboratories Inc. Hertfordshire, UK), which measured the UV absorbance at 490nm. Liposome samples were mixed with 50% isopropyl alcohol in order to disrupt the liposome membrane and allow quantification of the encapsulated drug. Calibration curves (2 – 40 µg/mL) were performed under the same conditions for each sample.

2.2.6 Determination of the Physicochemical Characteristics of the Produced Liposomes

The physicochemical characteristics of the liposomes, z-average diameter (d.nm), polydispersity index (PDI) and zeta potential were measured using the Malvern Zetasizer from Malvern Panalytical (Worcestershire, UK). Liposome formulations were diluted 2-fold in deionised water in order to get an attenuator position between 6 and 7. The same dilution was used to measure zeta potential. Each sample was measured three times at 25°C. The SOP for the measurement of particle size and PDI was created with the following parameters (Table 2.1). The sensitivity of the zetasizer was assessed using DSPC:Chol:PEG2000 liposomes produced from a 40 mg/mL stock (w/w 3:1:1) at a FRR 3:1 and TFR 10 mL/min with a final lipid concentration of 10 mg/mL. The liposomes were diluted with filtered PBS to varying concentrations, and the size, PDI and attenuator level were measured.

Table 2.1: Protocol used to determine the sensitivity of the Malvern Zetasizer

Material	
Refractive Index	1.45
Absorption	0.001
Dispersant	PBS
Temperature	25 °C
Viscosity	1.0200cP
Refractive Index	1.335
General options	
Equilibrium time	120 s
Cell type	ZEN0040
Measurement	
Angle	173° Backscatter
Number of runs	Automatic
Number of measurements	3
Delay between measurements	10 s
Data Processing	General Purpose (Normal resolution)

2.2.7 Stability Study

Encapsulated and non-encapsulated PEGylated liposome suspensions were stored at 4 ± 3 °C for 48 hours. The stability was evaluated by measuring the physicochemical characteristics as mentioned

above at selected time points (0, 24 and 48 hours). Acridine orange retention was measured at each of these time points as previously.

2.2.8 Statistical Analysis

One-way ANOVA followed by Tukey's multiple comparison test and 2-sample T-test (p-value of less than 0.05) were used for the data analysis. All the experiments were carried out at least in triplicate unless otherwise stated and are shown as the mean of the measurements ± standard deviation plotted as error bars.

2.3 Results

2.3.1 Production and Stability of Liposomes

Liposome stability is essential as any changes to the liposome characteristics, such as changes in size due to aggregation or leakage of the encapsulated compound, can affect the efficiency of the liposomal drug delivery (63).

2.3.1.1 Empty Liposome Stability

Liposomes were produced from a 40 mg/mL stock solution of HSPC:Cholesterol:DSPE-PEG2000 (w/w 3:1:1) solubilised in ethanol. These liposomes encapsulated an aqueous ammonium sulfate (250 mM) core and were produced at a TFR of 10 mL/min and a FRR of 3:1. The liposomes then underwent buffer exchange with PBS via tangential flow filtration (TFF) to remove residual solvent. The liposome physicochemical properties were then measured using a zetasizer at 0 hours and after 24 and 48 hours of storage at 4°C. The results show that generally, over the time period studied, there is no significant difference in the formulation attributes, with the liposome size and PDI remain stable at approximately 83 nm and 0.2, respectively (Fig 2.1A), and the zeta potential remains stable at approximately -12 mV (Fig 2.1B) over the specific time period of the study.

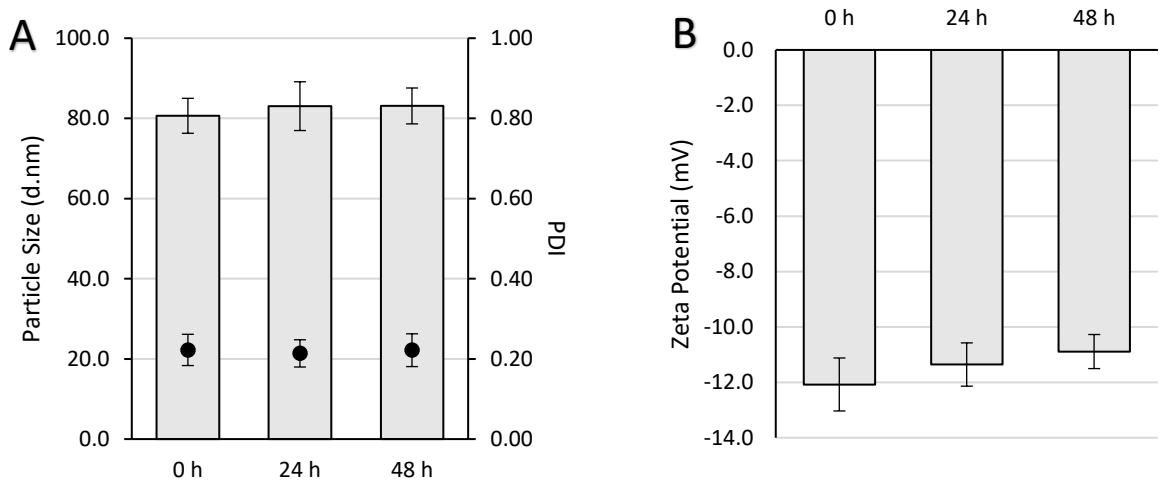

Figure 2.1: Stability of empty HSPC:Chol:DSPE-PEG2000 liposome over 48-hours. Physicochemical characteristics A) particle size (d.nm; represented by the bars) and PDI (represented by the discrete points) and B) zeta potential (mV) were measure for HSPC:Chol:DSPE-PEG2000 liposome that had been stored at 4 ± 3 °C for a period of 48 hours. Results represent mean ± SD, n=3 of independent batches.

2.3.1.2 Loading and Stability of Loaded Liposomes

Liposomes to be loaded with acridine orange were produced using the same parameters as above. Briefly, HSPC:cholesterol:DSPE-PEG2000 liposomes were produced from a 40 mg/mL stock (w/w/ 3:1:1) at a TFR of 10 mL/min and at a FRR of 3:1. These liposomes were diluted 2-fold with ammonium sulfate (250 mM) prior to buffer exchange with PBS via TFF. A small sample of these liposomes was then incubated with a corresponding volume of acridine orange in a water bath at 60°C for 40 minutes. Free drug was removed via TFF, and the physicochemical properties, pre- and post-loading, and acridine orange loading was subsequently measured.

The results in Fig 2.2A show that drug loading significantly increased the liposome size by approximately 10% (from 63 to 70 nm) but did not impact PDI, which remained at 0.2. After acridine orange loading, the particle size and PDI remain relatively stable, with liposomes being approx 70 nm with a PDI of 0.2, with no significant difference across the time points tested (Figure 2.2A). The zeta potential also showed no notable change pre- and post-loading and remained stable at approximately -6 mV over the 48-hour time period (Fig 2.2B). Acridine orange loading was also measured over the 48-hour time period and was found to remain stable at approximately 85% loading (Fig 2.2C).

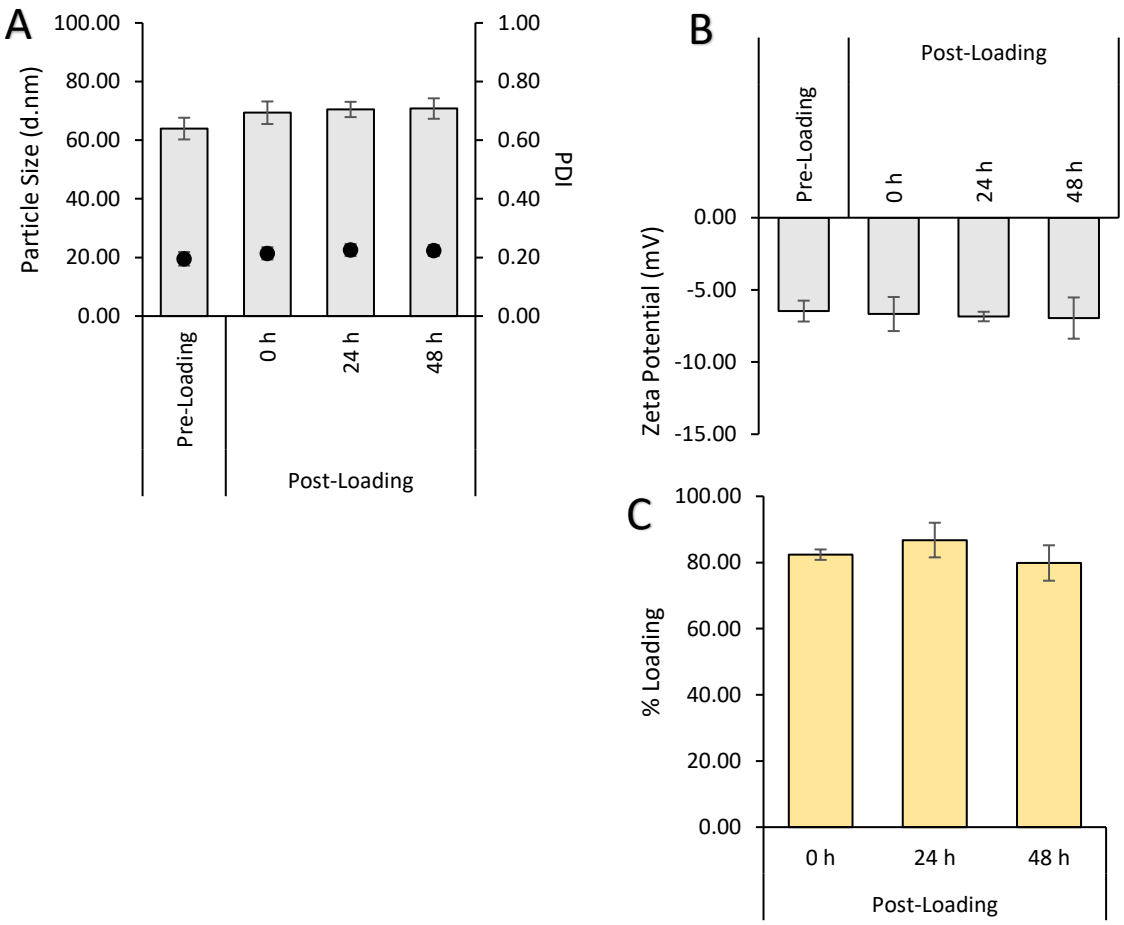

Figure 2.2: Loading and stability of acridine orange loaded HSPC:Cholesterol:DSPE-PEG2000 liposomes monitored over a 48-hour period. Physicochemical characteristics A) particle size (d.nm; represented by the bars) and PDI (represented by the discrete points) and B) zeta potential (mV) were measure for HSPC:Chol:DSPE-PEG2000 liposome that had been stored at 4 ± 3 °C for a period of 48 hours. Acridine orange loading (C) was also measured over the 48-

2.3.2 Active-loading of Acridine Orange

2.3.2.1 Impact of Incubation Time

In order to optimise acridine orange loading, the impact of incubation time was investigated. The liposomes were incubated in a 60°C water bath for either 20 minutes, 40 minutes, 1 hour or 2 hours before removal of free drug and quantification of acridine orange loading and measurement of physicochemical properties pre- and post-loading. Particle size, PDI and zeta potential were similar both pre- and post-loading across all time points (sizes 70 -80 nn, PDI approx. 0.2 and zeta potential -5 to -10 mV; Fig 2.3A & B). There was no notable trend observed for acridine orange loading (Fig 2.3C) suggesting that the incubation time ranges tested had no impact on the encapsulation efficiency of the liposomes.

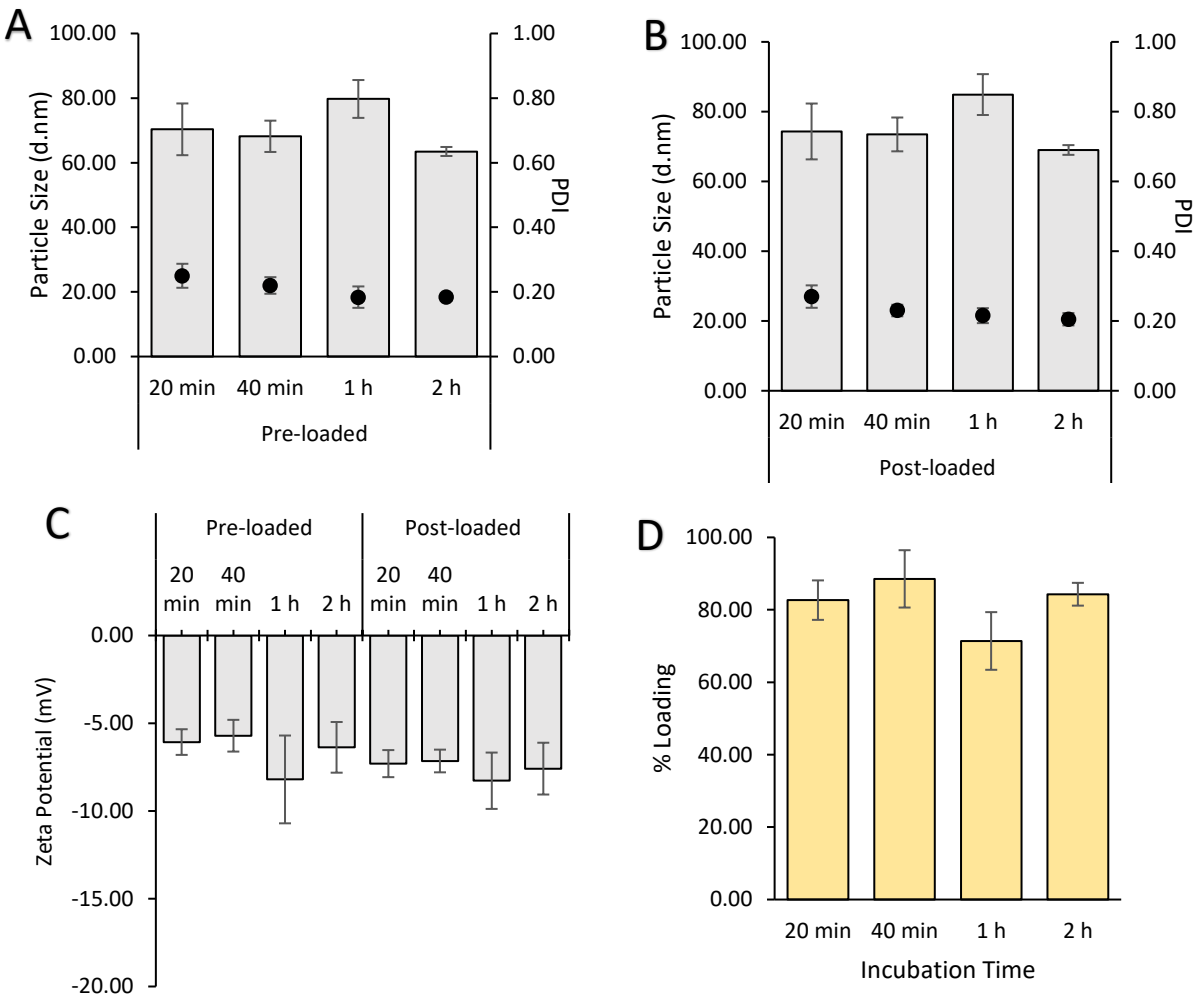

Figure 2.3: Effect of incubation time of percentage acridine orange loading. A) particle size (d.nm; represented by the bars) and PDI (represented by the discrete points) pre-loading with acridine orange, B) particle size (d.nm; represented by the bars) and PDI (represented by the discrete points) post-loading with acridine orange, C)zeta potential (mV) and D) acridine orange loading of the HSPC:Chol:DSPE-PEG2000 liposomes remote loaded with acridine orange and incubated for either 20 mins, 40 mins, 1 hr or 2 hrs. Results represent mean ± SD, n=3 of independent batches.

2.3.2.2 Acridine Orange Degradation

To further investigate the effect of time on drug loading, it was also important to determine whether acridine orange absorbance was being degraded in the water bath during incubation. Acridine orange was diluted in PBS to the same concentration used in our experiments and incubated in the water bath at 60°C for 20 min, 40 min, 1 h and 2 h as previously carried out in section 3.2.2. The results from this show that acridine orange absorbance is not affected by incubation at 60°C over 2 h (Figure 2.4), and therefore, any differences in encapsulation efficiency were not due to degradation at high temperatures.

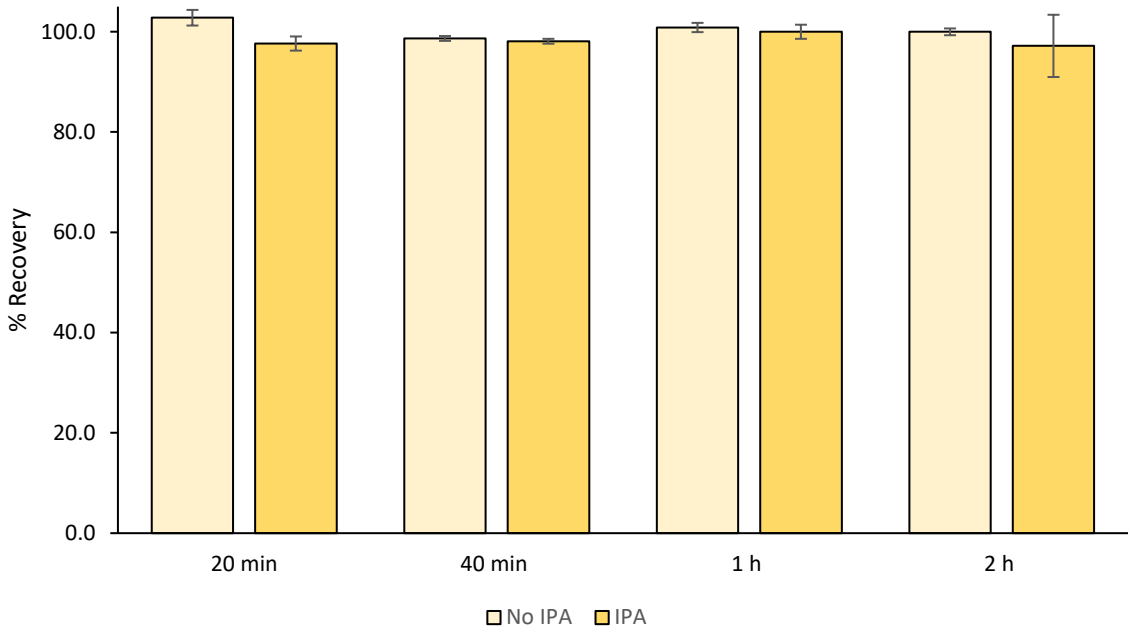

Figure 2.4: Percentage recovery of acridine orange, based on outlined analytical method, in the presence and absence of 50% v/v IPA after incubation at 60°C for 20 min, 40 min, 1 h and 2 h. n=2 of independent batches

2.3.2.3 Comparison between microfluidic mixers

To consider the impact of microfluidic mixers, two different mixers were tested – a staggered herringbone and a toroidal mixer. HSPC:Chol:PEG2000 liposomes were produced from the same stock solution on the Ignite. The Ignite uses a disposable toroidal micromixer compared with the reusable staggered herringbone micromixer of the Benchtop. HSPC:Chol:PEG2000 liposomes encapsulating an aqueous ammonium sulfate core were produced at the same process parameters, FRR 3:1 and TFR 10 mL/min, on both the Ignite and the Benchtop and loaded with acridine orange for 40 minutes at 60°C.

The results show that the liposomes produced on a toroidal mixer were a slightly smaller particle size compared to the staggered herringbone mixer (59 ± 4 nm vs 68 ± 5 nm pre-loading, & 64 ± 2 nm vs 73 ± 4 nm post-loading, respectively; Figure 5A) and the PDI was significantly lower ($p<0.05$) for the liposomes produced using a toroidal mixer (0.17 vs 0.22; Figure 2.5A). However, the zeta potential

(Figure 2.5B) and remote loading of acridine orange (Figure 2.5C) were not significantly different between liposomes produced using the two different mixers. Whilst these sizes are significantly different, they may not be clinically relevant and are most likely a result of the SHM mixer being a reusable cartridge compared to the toroidal mixer being a single use system.

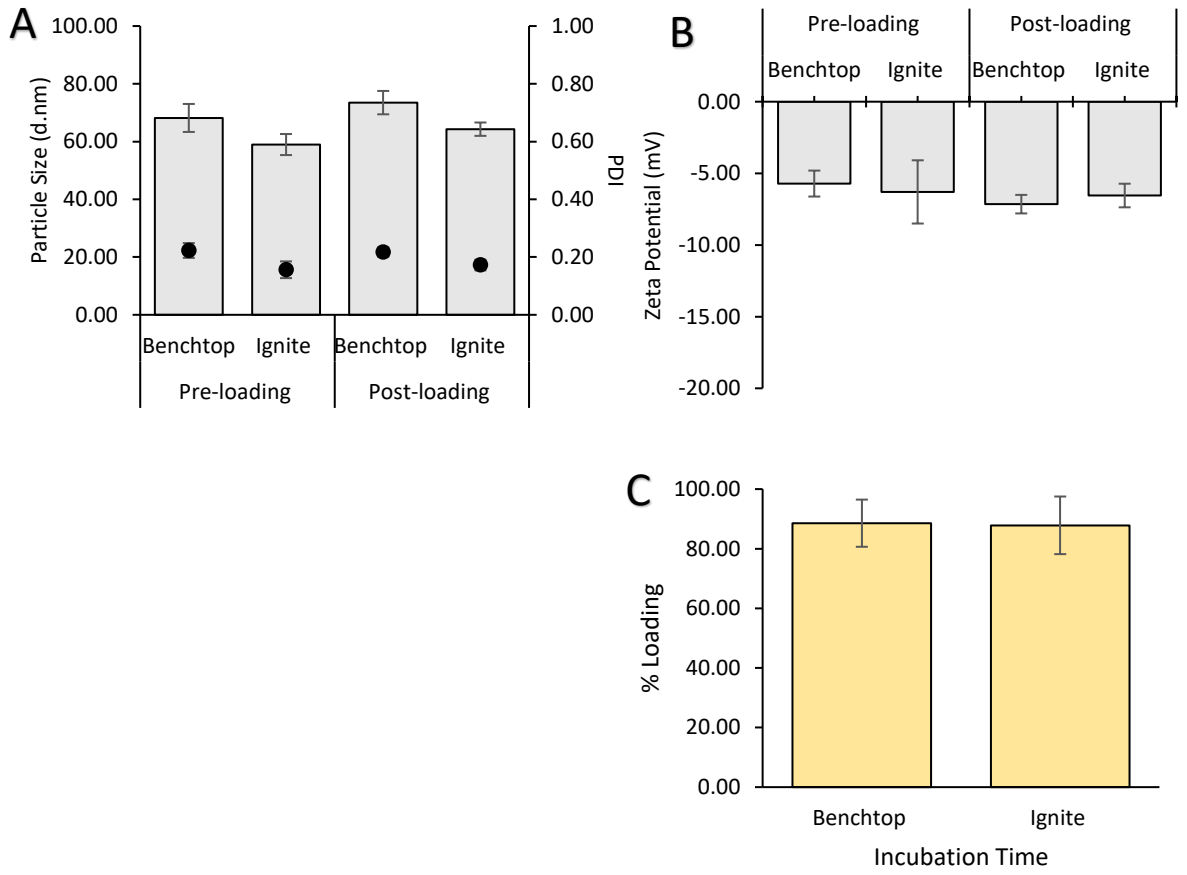

Figure 2.5: Comparison between Ignite and Benchtop. A) particle size (d.nm; represented by the bars) and PDI (represented by the discrete points) pre- and post-loading with acridine orange, B)zeta potential (mV) and C) acridine orange loading of the HSPC:Chol:DSPE-PEG2000 liposomes remote loaded with acridine orange and incubated for 40 mins, at 60°C. Results represent mean ± SD, n=3 of independent batches.

2.3.2.4 Impact of Total Flow Rate (TFR) on Liposome Physicochemical Properties

The total flow rate is a key (TFR) parameter that controls the production speed of the liposome formulations and, therefore, may be critical for increasing production and scale-up of manufacturing. Increasing the TFR from 10 mL/min to 20 mL/min resulted in a significant ($p<0.05$) decrease in particle size (Fig 2.6A) (from 60 ± 1 nm to 52 ± 1 nm pre-loading and from 66 ± 1 nm to 57 ± 1 nm post-loading at 10 and 20 mL/min respectively). The PDI remained low (<0.25) (Fig 2.6A), and zeta potential remained similar (-6 mV) at both TFRs (Fig 2.6B), and acridine orange loading was unaffected (Fig 2.6C) (from 82 ± 3 % to 81 ± 3%). These results show that the production speed can be increased with minimal impact on resultant liposome properties and the potential for microfluidics for increased industrial production.

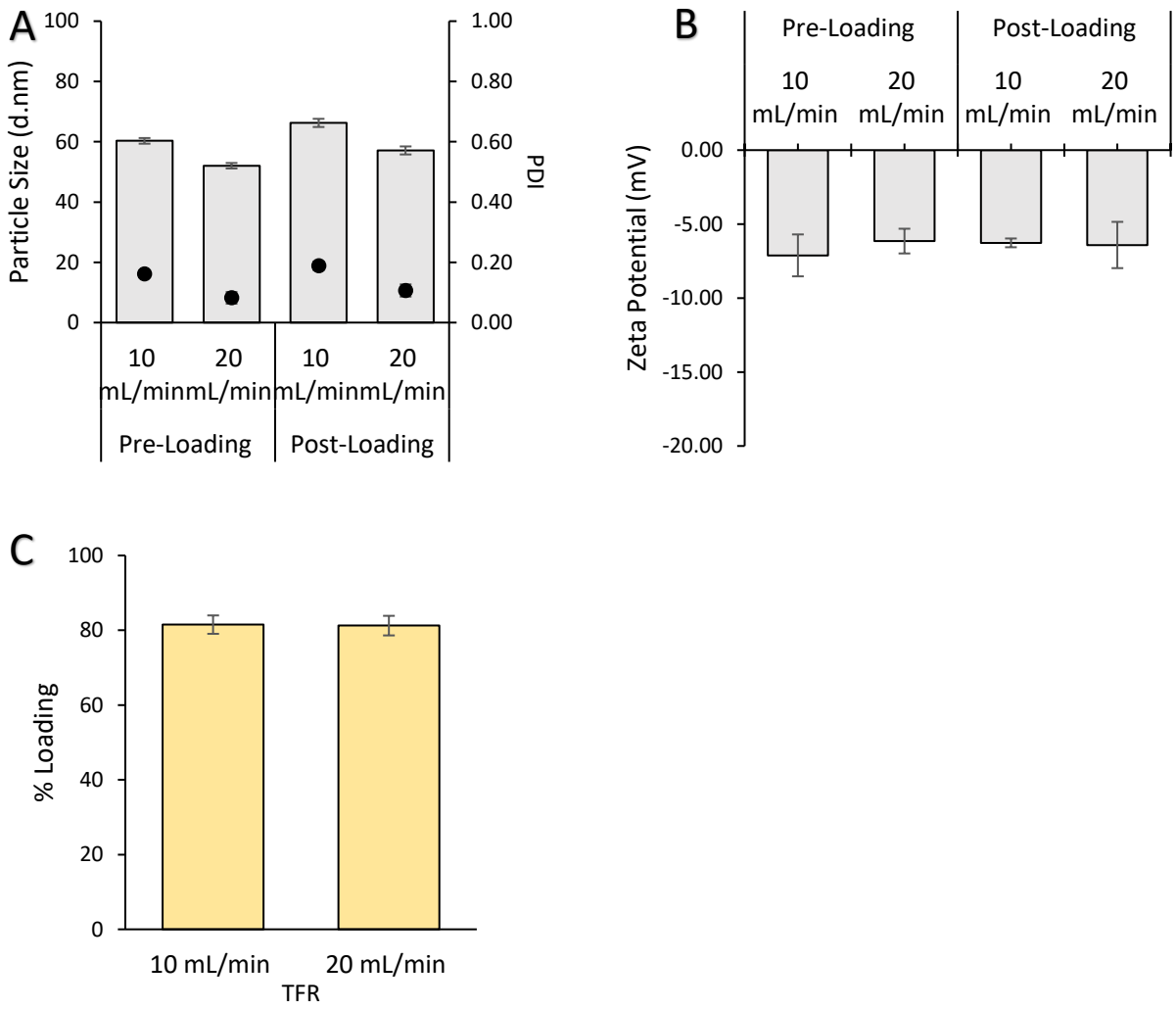

Figure 2.6: Effect of total flow rate (TFR) on acridine orange loading of HSPC:Cholesterol:DSPE-PEG2000 liposomes. A) particle size (d.nm; represented by the bars) and PDI (represented by the discrete points), B) zeta potential (mV) and C) acridine orange loading of the HSPC:Chol:DSPE-PEG2000 liposomes produced at a TFR of either 10 mL/min or 20 mL/min and remote loaded with acridine orange. Results represent mean ± SD, n=3 of independent batches.

2.3.2.5 Impact of Flow Rate Ratio (FRR) on acridine orange loading

Further studies were carried out investigating the impact of changing the FRR on liposome physicochemical characteristics and remote loading of acridine orange. HSPC:Chol:DSPE-PEG2000 liposomes were produced at a final lipid concentration of 2 mg/mL at a TFR 10 mL/min, and a FRR of either 1:1 or 10:1. TFF was used to establish a pH gradient for the active loading of acridine orange at a drug: lipid ratio of 0.004 g drug/g lipid at 60°C for 40 minutes. The results show that the liposomes produced at the higher FRR (10:1) were significantly smaller ($p<0.05$) in size pre- and post-loading (65 ± 4 nm vs 108 ± 5 nm & 72 ± 4 nm vs 112 ± 4 nm, respectively) (Figure 2.7A). PDI (Figure 2.7A), zeta potential (Figure 2.7B) and acridine orange loading (Figure 2.7C) were similar at both flow rate ratios. These results demonstrate the ability of microfluidics to produce a variety of particle sizes with minimal impact on the drug-loading capacity of the resultant liposomal formulation.

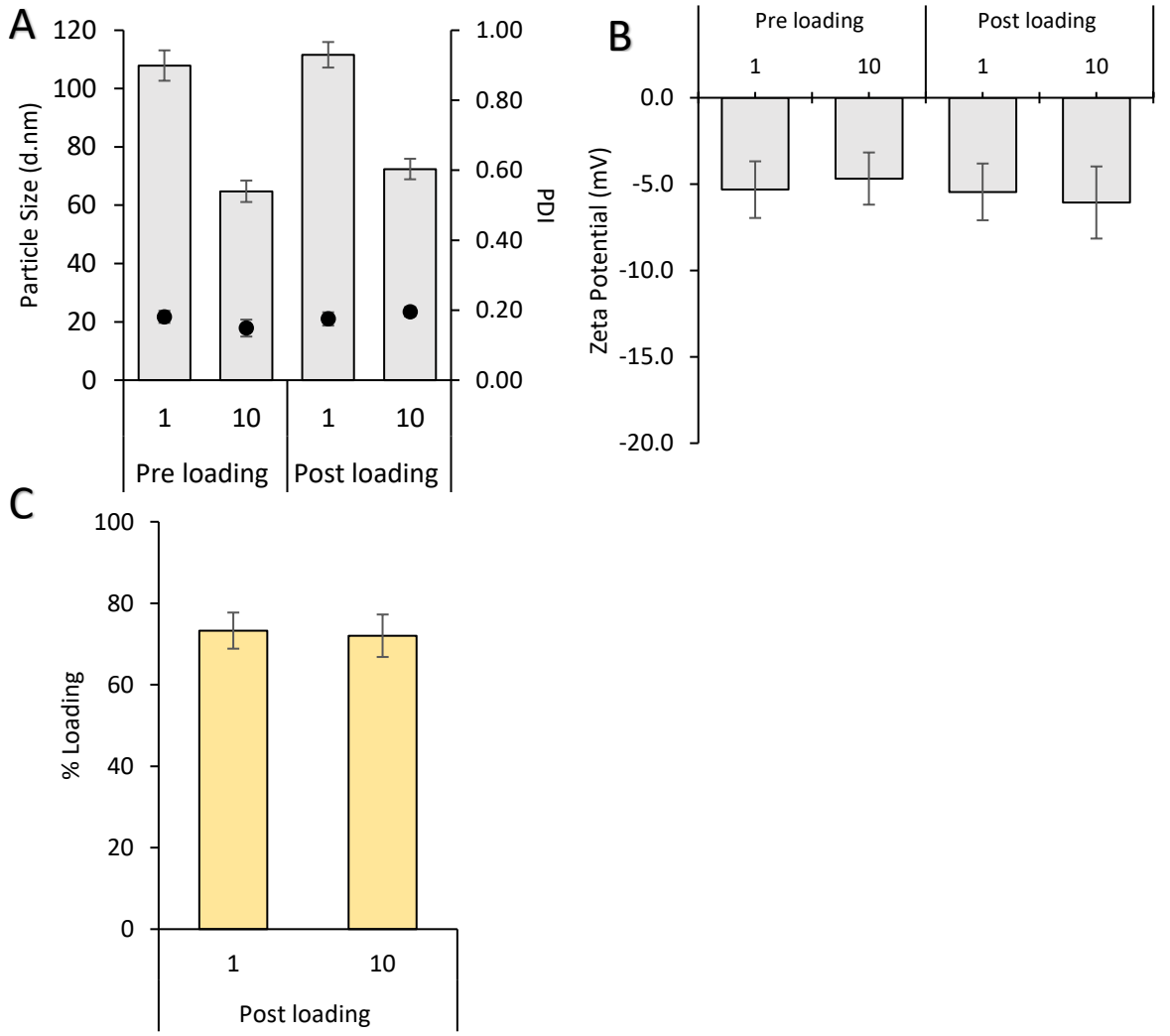

Figure 2.7: Effect of FRR on liposome physicochemical characteristics and acridine orange loading. A) particle size (d.nm; represented by the bars) and PDI (represented by the discrete points) pre- and post-loading with acridine orange B) zeta potential (mV) and C) acridine orange loading of the HSPC:Chol:DSPE-PEG2000 liposomes produced at FRR 1:1 (1) and 10:1 (10), remote loaded with acridine orange and incubated for 40 mins, at 60°C. Results represent mean ± SD, n=3 of independent batches.

2.3.2.6 Effect of Drug: Lipid Ratio on Remote Loading

We have shown how the microfluidic manufacturing parameters (TFR and FRR) can affect the liposome characteristics and loading of acridine orange into these liposomes. It was also important to see if changing the concentration of acridine orange encapsulated within the liposome aqueous core without affecting resultant liposome properties. HSPC:Chol:DSPE-PEG2000 (w/w 3:1:1) liposomes were produced at FRR 3:1 and TFR 10 mL/min and were then loaded with various concentrations of 1 mg/ml acridine orange for 40 minutes at 60°C. Liposomes were loaded with either 2 mg drug/ g lipid, 4 mg drug/ g lipid, or 8 mg drug/ g lipid. The results show no notable difference in particle size pre- and post-loading (Fig 2.8A) or zeta potential (Fig 2.8B). The loading of these liposomes was shown to be significantly lower ($p<0.05$) for those liposomes incubated with 2 mg drug/ g lipid, and there was no significant difference between liposomes incubated with 4 mg drug/ g lipid and 8 mg drug/ g lipid (Fig 2.8C). Whilst significantly different from a biological viewpoint, it is unlikely these changes would have an impact delivery or distribution of the liposomes.

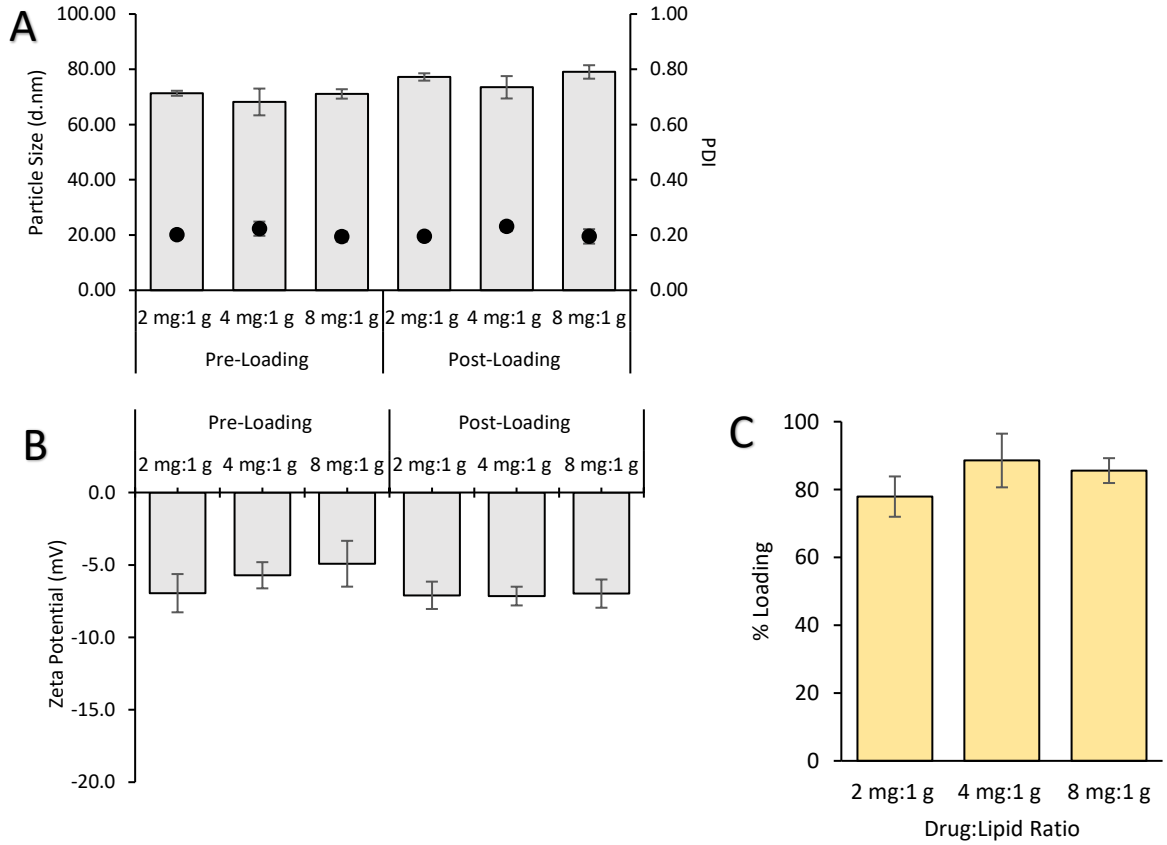

Figure 2.8: Effect of drug:lipid ratio on liposome physicochemical characteristics and acridine orange loading. A) particle size (d.nm; represented by the bars) and PDI (represented by the discrete points) pre- and post-loading with acridine orange B) zeta potential (mV) and C) acridine orange loading of the HSPC:Chol:DSPE-PEG2000 liposomes remote loaded with acridine orange at either 2 mg drug/ g lipid, 4 mg drug/ g lipid or 8 mg drug/g lipid, and incubated for 40 min, at 60°C. Results represent mean ± SD, n=3 of independent batches.

2.3.3 Establishing Dialysis Protocol for Remote Loading of Acridine Orange

Purification of the liposomal formulation is required for the removal of residual solvent as well as any unencapsulated payload. There are a number of methods that can be used for purification, such as dialysis and tangential flow filtration (TFF). TFF is an efficient and scalable purification method for solvent and unencapsulated compound removal; however, it is limited to the purification of a single formulation at a time. Therefore, it would be advantageous to develop a dialysis protocol that could be used for the screening of a large variety of formulations that could then be remotely loaded with various compounds.

Initial experiments were carried out using an HSPC:Cholesterol:DSPE-PEG2000 (w/w 3:1:1) lipid stock and were loaded with acridine orange for 2 h at 60°C. The liposomes produced then either underwent tangential flow filtration or dialysis to establish a pH gradient and remove free drug. The liposomes that underwent dialysis were initially dialysed in 200 mL PBS for 1 h to establish a pH gradient and again for removal of free drug. The results from the TFF and experiments were compared to determine

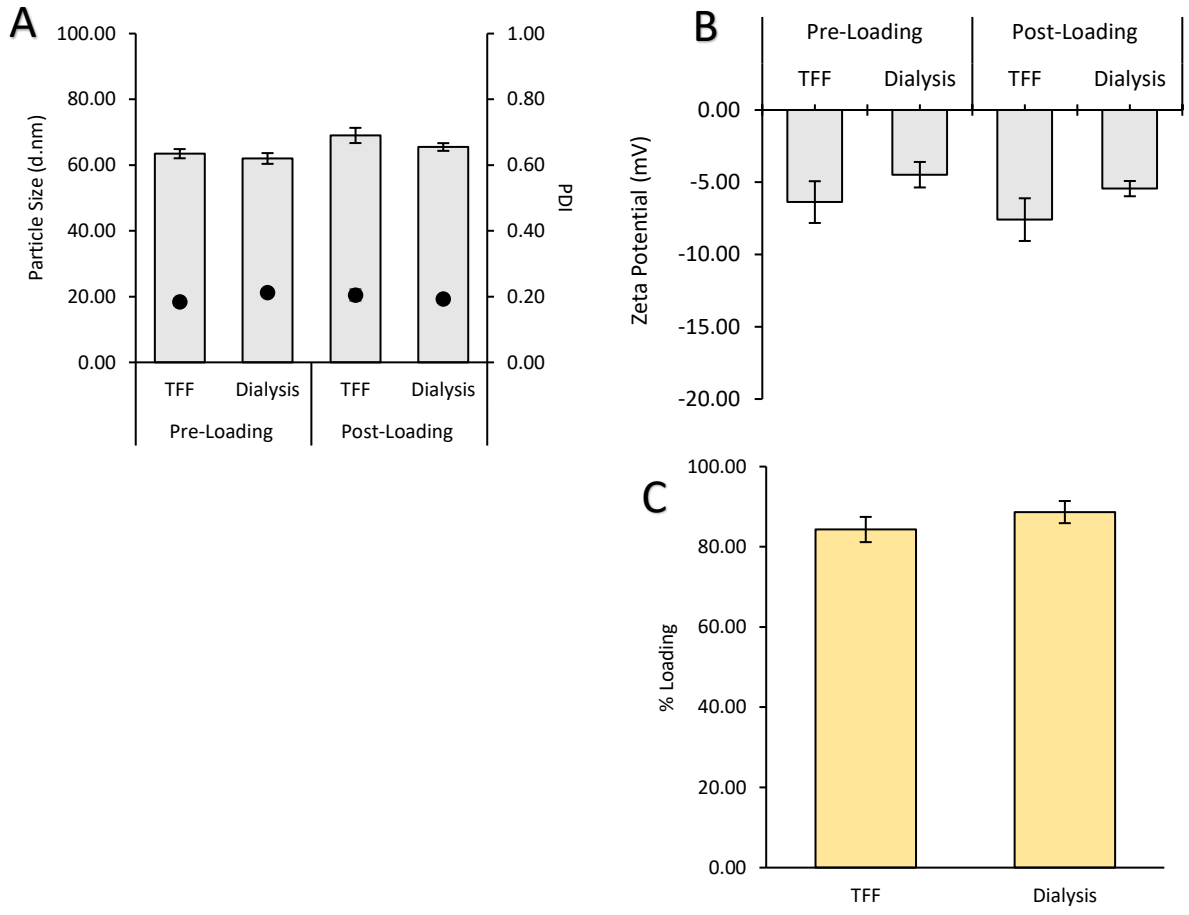

Figure 2.9: Remote loading of HSPC:Cholesterol:DSPE-PEG2000 liposomes purified by either TFF or dialysis. Physicochemical characteristics A) particle size (d.nm; represented by the bars) and PDI (represented by the discrete points), B) zeta potential (mV) were measure for HSPC:Chol:DSPE-PEG2000 liposome pre- and post-loading after purification. Acridine orange loading (C) was also measured. Results represent mean ± SD, n=3 of independent batches.

whether the dialysis protocol was establishing a pH gradient for remote loading and removing all unentrapped drug. The results from these experiments (Figure 2.9) show that the liposomes purified via TFF and those purified using dialysis were of similar size, PDI (Figure 2.9A) and zeta potential (Figure 2.9B) with no significant difference in the remote loading of acridine orange (Figure 2.9C). Therefore, it was concluded that this dialysis protocol produced liposomes comparable to those produced via TFF.

2.3.3.1 pH Gradient confirmation

To confirm 1 h dialysis was sufficient for buffer exchange and to fully establish the pH gradient, HSPC:Cholesterol:DSPE-PEG2000 liposomes were produced on the NanoAssemblr Benchtop and then 1 mL of the liposome sample was dialysed in 200 mL PBS for either 1, 2 or 3 hours, changing the buffer every hour. After dialysis, the sample was collected, and the pH of the external environment was measured using pH indicator sticks, and the liposome physicochemical characteristics were measured.

The results of these experiments show that 3 hours of dialysis was required to fully establish a pH gradient (Figure 2.10A) and that this increase in dialysis time did not affect the result liposome characteristics (Figure 2.10B &C).

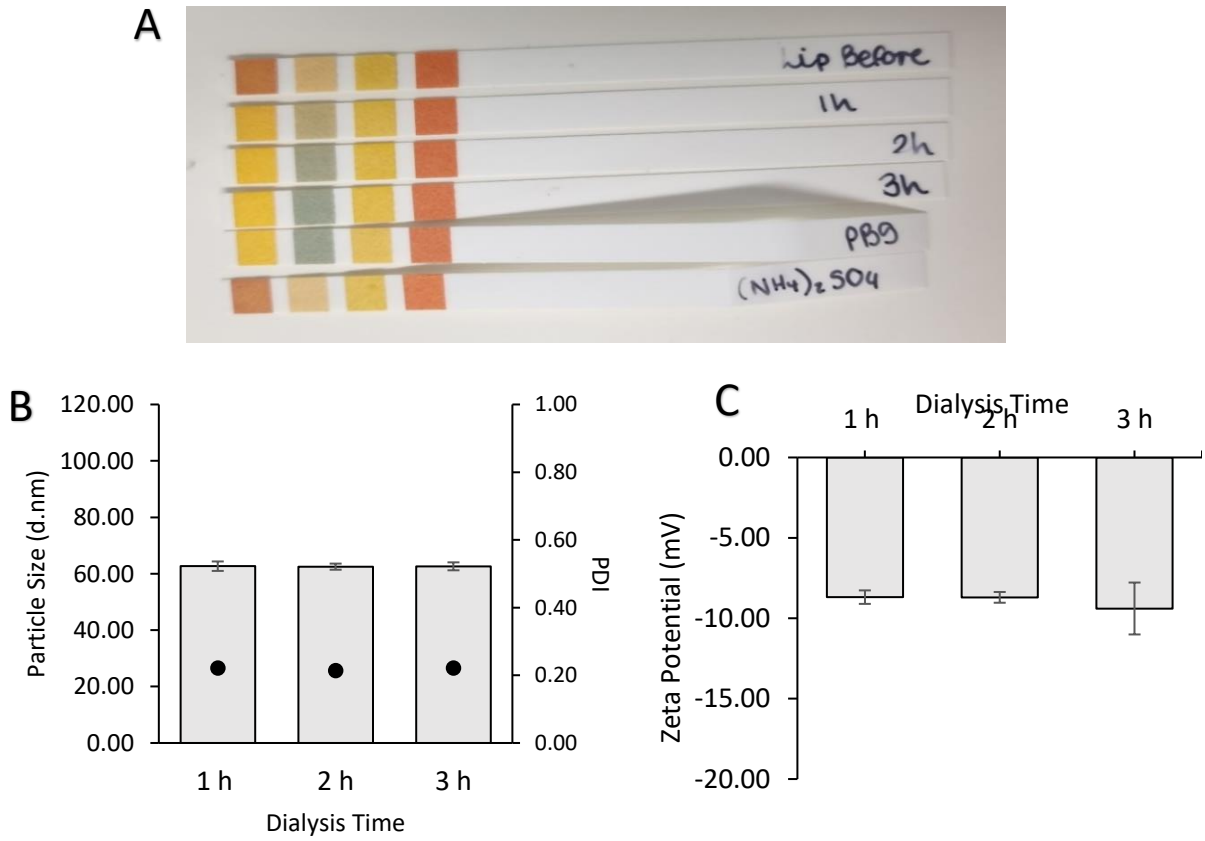

Figure 2.10: Determination of dialysis time required for pH gradient to be established. The pH of the external environment was measured using pH indicator sticks (A) and show that 3 h of dialysis is required to remove ammonium sulfate and replace it with PBS. B) particle size (d.nm; represented by the bars) and PDI (represented by the discrete points) and C)zeta potential (mV) were unaffected by this increase in dialysis time. Results represent mean ± SD, n=1 of independent batches.

2.3.3.2 Free Drug Removal Protocol

The next step was to determine the length of dialysis needed to remove the unentrapped drug from the liposomal suspension. To do this, HSPC:Cholesterol:DSPE-PEG2000 liposomes were dialysed for 3 h in PBS, changing the buffer every 1 h. After loading with acridine orange for 40 minutes at 60°C, the loaded liposomes were split and half dialysed for 3 h as previous, changing the buffer every 1 h, and the other half were dialysed overnight. Both of these samples were then measured for % loading and physicochemical characteristics before undergoing TFF to determine if all free drug had been removed. The results from these experiments show a slight reduction in loading after TFF (Figure 2.11C) with no meaningful impact on liposome properties (Figure 2.11A & B), and therefore, it was determined that a minimum of 3 h dialysis would be adequate for free drug removal.

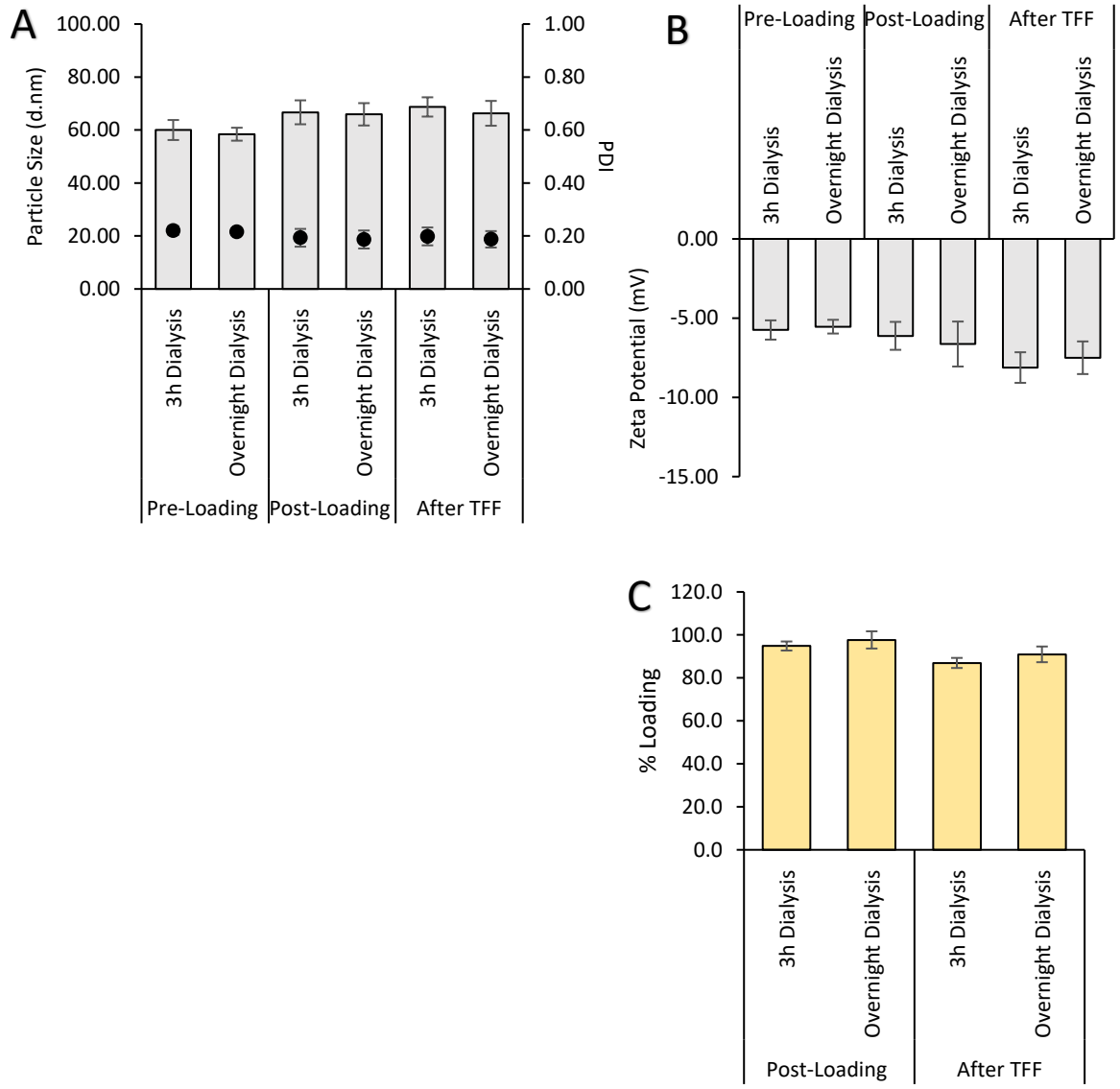

Figure 2.11: Determination of dialysis time for free drug removal. A) particle size (d.nm; represented by the bars) and PDI (represented by the discrete points) pre- and post-loading with acridine orange after dialysis and TFF, B)zeta potential (mV) and C) acridine orange loading of the HSPC:Chol:DSPE-PEG2000 liposomes remote loaded with acridine orange and incubated for 40 mins, at 60°C. Results represent mean ± SD, n=3 of independent batches.

2.3.4 Remote Loading of Acridine Orange at Different Temperatures

2.3.4.1 Dialysis Protocol

The remote loading of compounds into liposomes via a pH gradient requires the liposomes to be heated above the transition temperature of the main lipid in order to change the structure of the liposomes to make it more fluid to allow the compound to pass across the membrane. In the case of DSPC (and HSPC), the transition temperature is 55°C and, therefore, requires heating above this temperature to allow the compounds to pass through. The effect of loading temperature was therefore investigated. DSPC:Cholesterol:DSPE-PEG2000 liposomes were loaded with acridine orange at 20°C and 60°C for 40 minutes using the dialysis protocol above before undergoing further purification via TFF to check for free drug removal. The results show no significant difference in particle size, PDI or Zeta potential between liposomes loaded at 20°C and 60°C after both dialysis and TFF (Figure 2.12A & B). However, it was observed that after the liposomes underwent TFF, the loading of acridine orange dropped significantly (Figure 12C), and therefore, it was concluded that the dialysis protocol had not been successful in establishing the pH gradient or removing the unentrapped drug.

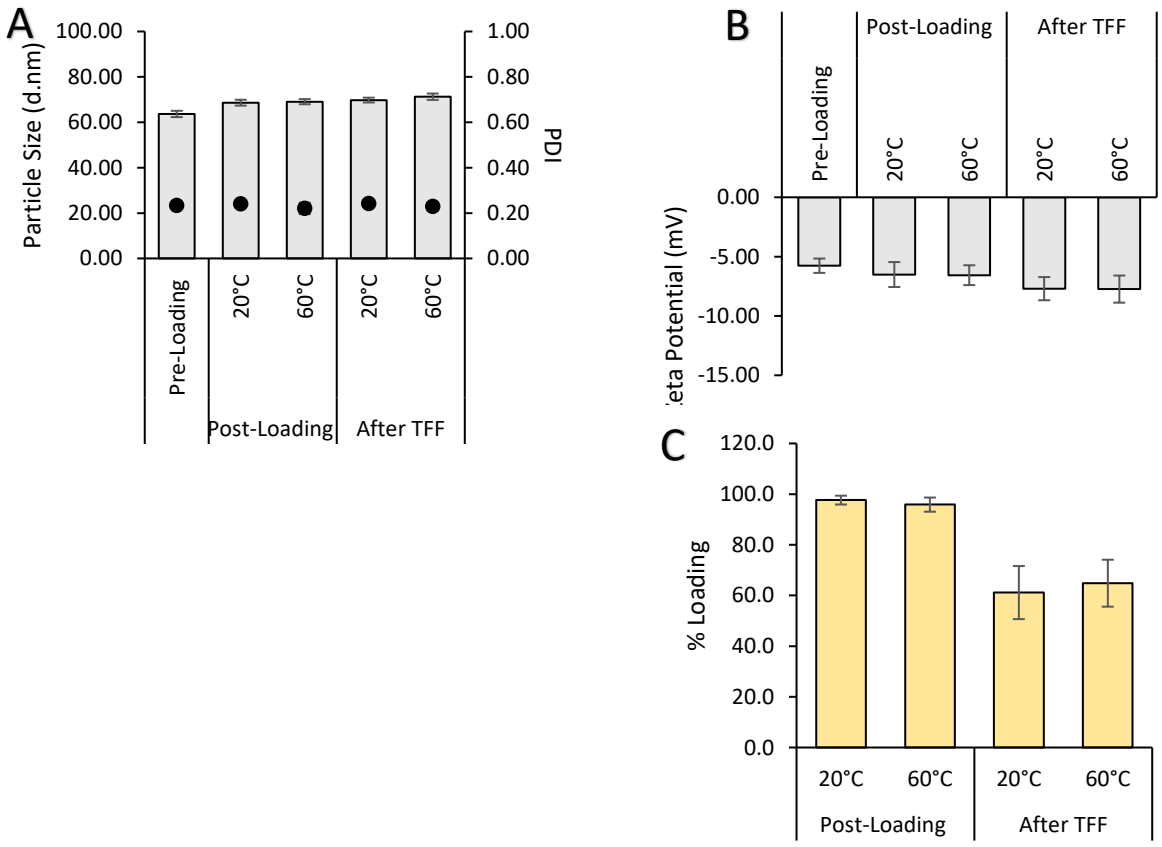

Figure 2.12: Comparison of DSPC:Cholesterol:DSPE-PEG2000 liposomes loaded at 20°C and 60°C after both dialysis and TFF. A) particle size (d.nm; represented by the bars) and PDI (represented by the discrete points) pre- and post-loading with acridine orange after dialysis and TFF, B)zeta potential (mV) and C) acridine orange loading of the DSPC:Chol:DSPE-PEG2000 liposomes remote loaded with acridine orange and incubated for 40 mins, at 60°C and underwent overnight dialysis and TFF for free drug removal. Results represent mean ± SD, n=2 of independent batches.

This may have been due to a larger sample volume being dialysed which may need a longer dialysis duration.

2.3.4.2 TFF protocol

2.3.4.2.1 Loading of Acridine Orange into DSPC & DOPC:Cholesterol:DSPE-PEG2000 Liposomes

Due to this reduction in loading after TFF, it was decided that the dialysis protocol may not be sufficient for free drug removal from the liposomal suspensions, and therefore, TFF would be a more reproducible and reliable method. DOPC was also investigated as it has a significantly lower transition temperature than DSPC (-17°C vs 55°C). DSPC & DOPC:Cholesterol:DSPE-PEG2000 were produced at TFR 10 mL/min and FRR 3:1 and encapsulated ammonium sulfate. The liposomes underwent TFF to establish the pH gradient before being remote loaded with acridine orange. These liposomes were incubated with 4 mg acridine orange/1 g lipid for 40 minutes at either 20°C or 60°C before undergoing TFF again to remove unentrapped drug. The results show that the remote loading of acridine orange into liposomes is not impacted by the incubation temperature or the transition temperature of the

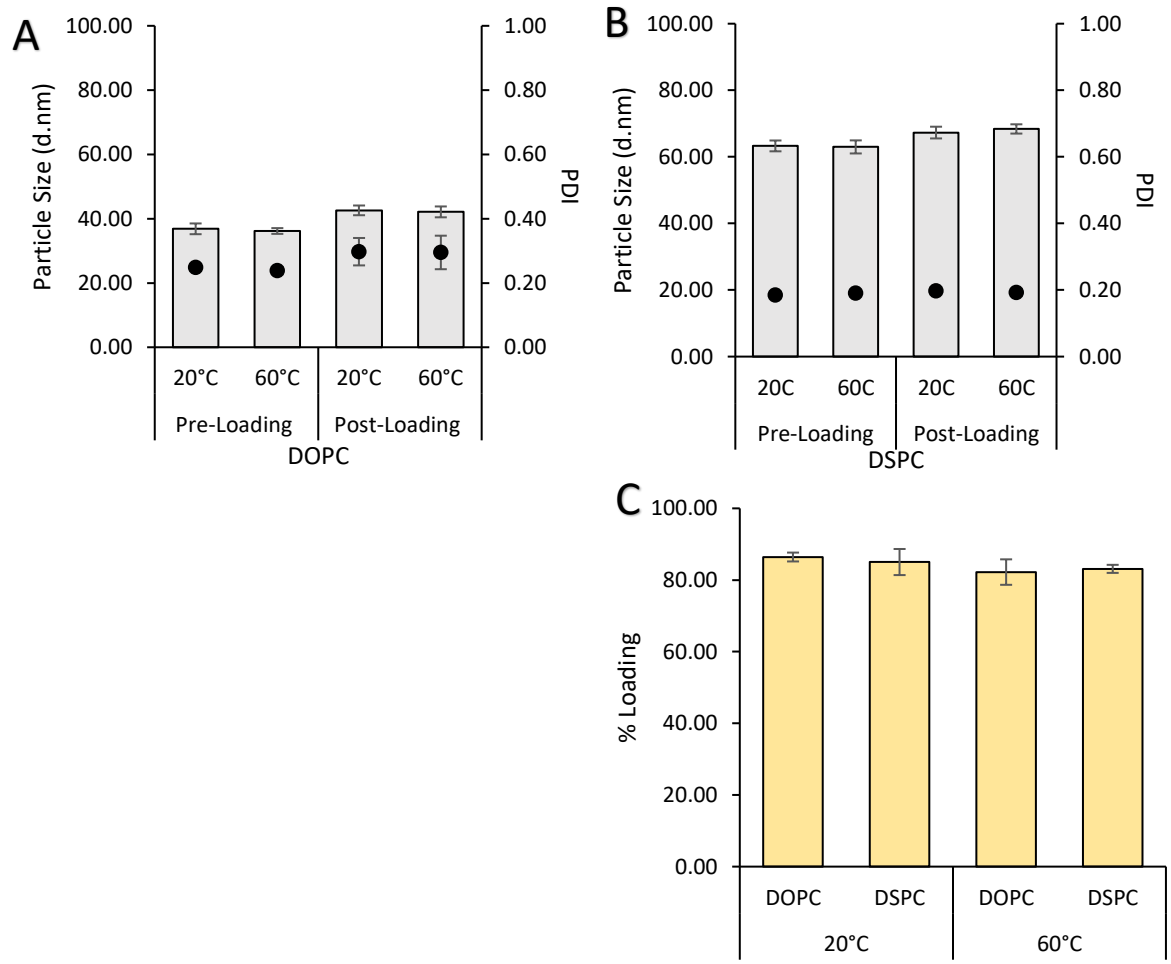

Figure 2.13: Comparison of DSPC & DOPC:Cholesterol:DSPE-PEG2000 liposomes loaded at 20°C and 60°C. A) particle size (d.nm; represented by the bars) and PDI (represented by the discrete points) pre- and post-loading of DOPC liposomes with acridine orange, B) particle size (d.nm; represented by the bars) and PDI (represented by the discrete points) pre- and post-loading of DSPC liposomes with acridine orange and C) acridine orange loading of the DOPC and DSPC liposomes remote loaded with acridine orange and incubated for 40 mins, at 60°C. Results represent mean ± SD, n=3 of independent batches.

lipids as loading was similar when DSPC was used. There is no significant impact ($p>0.05$) on liposome characteristics (Figure 2.13A & B) or remote loading of liposomes incubated at 20°C and 60°C (Figure 2.13C). This would suggest that acridine orange is membrane-permeable and does not require heat to allow for movement across the membrane.

2.3.4.3 Loading Liposomes with No pH Gradient

2.3.4.3.1 Loading of Acridine Orange into DSPC & DOPC:Cholesterol:DSPE-PEG2000 Liposomes

In order to confirm that acridine orange required the pH gradient for remote loading, liposomes were produced with encapsulated PBS and, therefore, did not have a pH gradient. The results show no difference in liposome physicochemical characteristics both pre- and post-loading with acridine

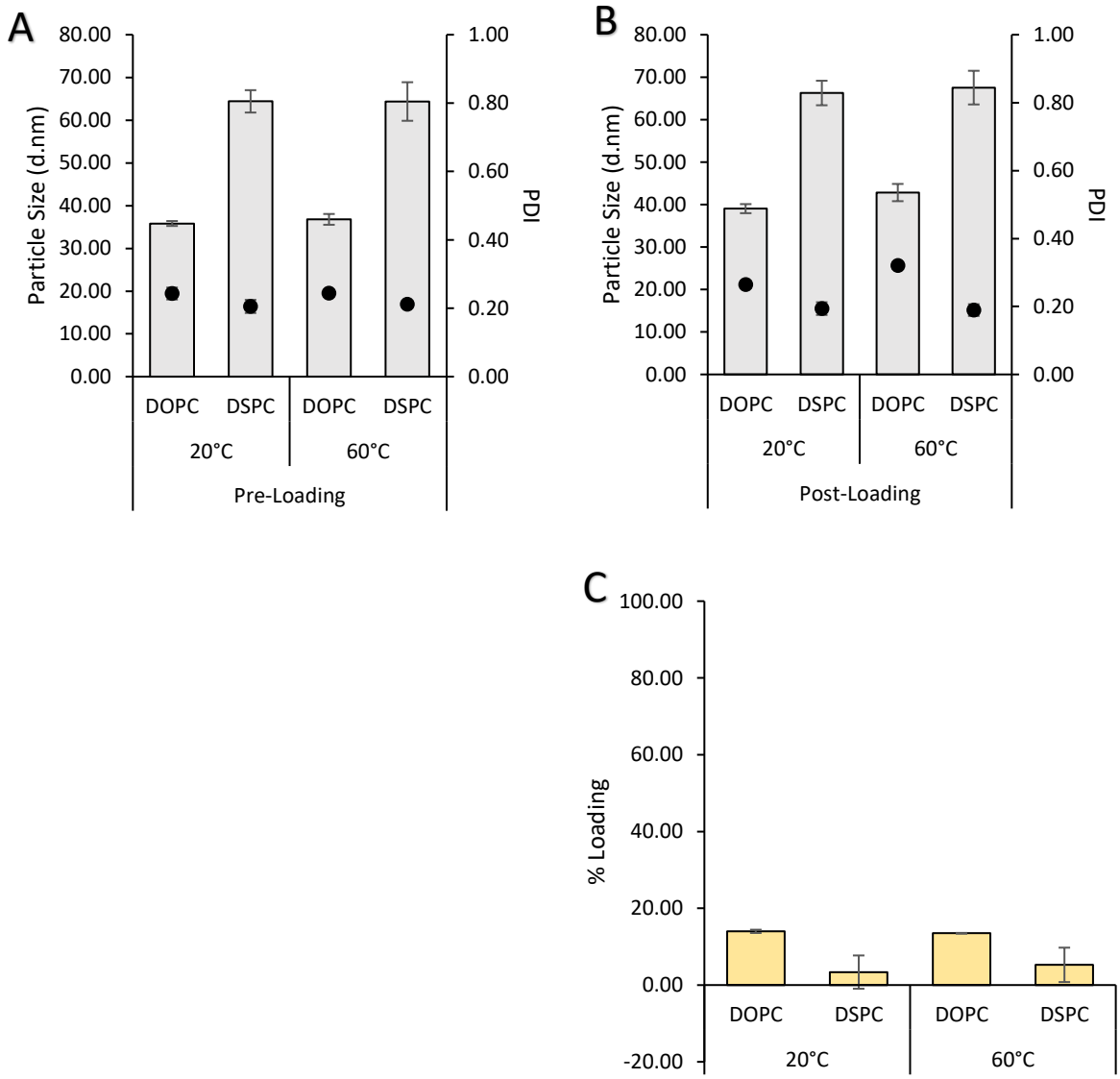

Figure 2.14: Comparison of DSPC & DOPC:Cholesterol:DSPE-PEG2000 liposomes encapsulating PBS and remote loaded at 20°C and 60°C. A) particle size (d.nm; represented by the bars) and PDI (represented by the discrete points) pre-loading with acridine orange, B) particle size (d.nm; represented by the bars) and PDI (represented by the discrete points) post-loading with acridine orange and C) acridine orange loading of the DSPC and DOPC liposomes remote loaded with acridine orange and incubated for 40 mins, at 20°C and 60°C. Results represent mean ± SD, n=1 of independent batches for DOPC and n=3 of independent batches for DSPC.

orange (Figure 2.14A & B), and there was very little encapsulation of acridine orange at both 20°C and 60°C (Figure 2.14C); therefore, confirming that acridine orange requires a pH gradient for active into liposomes.

2.3.5 Testing Acridine Orange Crystallisation

The next step to confirm that acridine orange was membrane permeable was to determine if the acridine orange was crystallising with the PBS or ammonium sulfate outside the liposomes at lower temperatures. Acridine orange was therefore incubated with PBS and with varying concentrations of ammonium sulfate to determine if the unentrapped drug was crystallising and, hence, may not be removed by the TFF. The same concentration of acridine orange as used in previous loading experiments (20 µg/mL) was added to each sample along with PBS or ammonium sulfate. The samples containing ammonium sulfate contained a volume equivalent to either 5 or 50% of the sample volume being made up of the aqueous liposomes' environment. The results (Figure 2.15) show that almost no acridine orange was retained in the buffer after purification via TFF and therefore confirmed that the TFF was removing all unentrapped drug and the high loading at both 20 °C and 60 °C was due to the movement of acridine orange into the liposomes along the pH gradient.

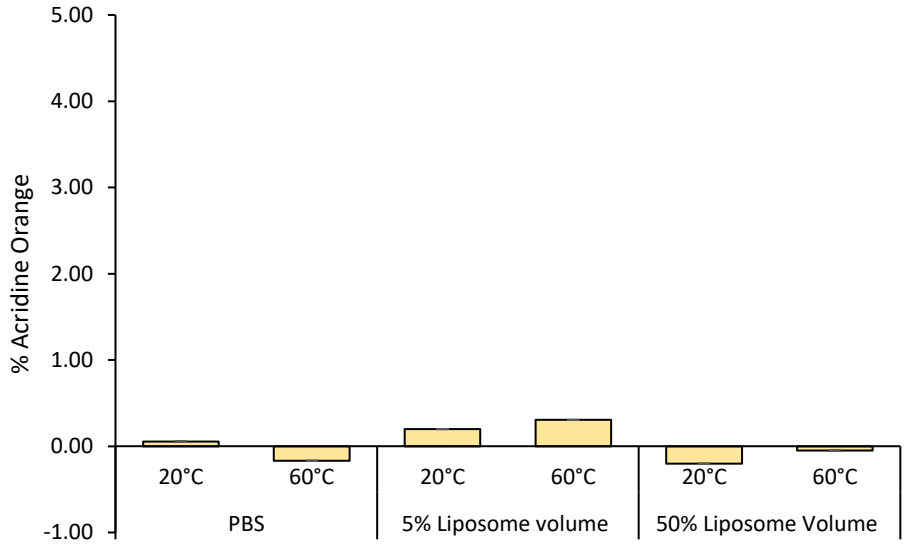

Figure 2.15: Percentage of acridine orange retained in the aqueous buffer after purification via TFF when compared with sample taken before TFF and after incubation. n=1 of independent batches

2.3.6 TFF Purification

A key process in the manufacturing of liposomal delivery vehicles is the purification process. In order to be suitable for clinical application, small molecules, residual solvent, and any unentrapped drug must be removed to allow for prolonged, targeted delivery. This can be carried out via tangential flow

filtration (TFF). The pressure in this system can be controlled by varying the filtration speed but may also be affected by the size and concentration of the liposome sample.

In this study, liposomes were produced from a 40 mg/mL DSPC:Cholesterol:DSPE-PEG2000 (w/w 3:1:1) ethanol stock at a FRR 3:1 and TFR 10 mL/min. The initial TFF was carried out at a constant speed of 16 mL/min to remove any residual solvent and create a pH gradient for the remote loading of acridine orange. The second TFF was carried out to remove any unentrapped drug, and this was carried out at various filtration speeds in order to determine whether increasing the speed resulted in any changes in liposome characteristics and if this subsequently affected the remote loading. The results (Figure 2.16) from this study show that there is no notable impact on the liposome physicochemical characteristics with increasing filtration speeds. Zeta potential (figure 2.16B) and loading (figure 2.16C) remained constant across all speeds tested. There is a slight increase in the particle size and PDI at the higher production speeds (> 30 mL/min) (Figure 2.16A); however, further experiments would need to be carried out in order to determine if this is a significant difference.

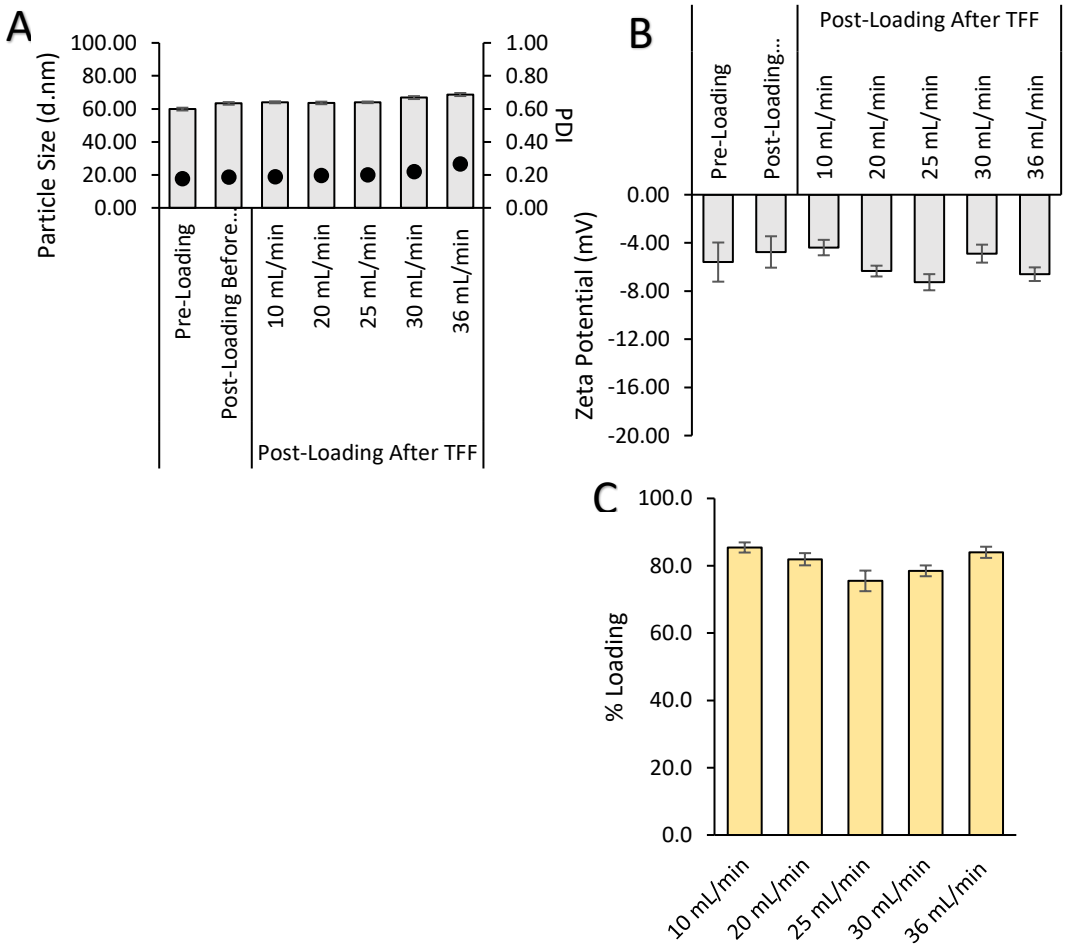

Figure 2.16:Effect of increasing the TFF filtration speed on DSPC:Cholesterol:DSPE-PEG2000 liposome physicochemical characteristics and loading. A) particle size (d.nm; represented by the bars) and PDI (represented by the discrete points) pre- and post-loading with acridine orange, B) zeta potential (mV) and C) acridine orange loading of the liposomes remote loaded with acridine orange and incubated for 40 min at 60°C. Results represent mean ± SD, n=1 independent batches.

2.4 Discussion

The aim of this chapter was to establish protocols to support the testing of liposomes produced via microfluidics for active drug loading. In this process, there are a range of factors that were considered, as shown in Figure 2.17, and these were considered within this chapter using acridine orange as the model API drug (62).

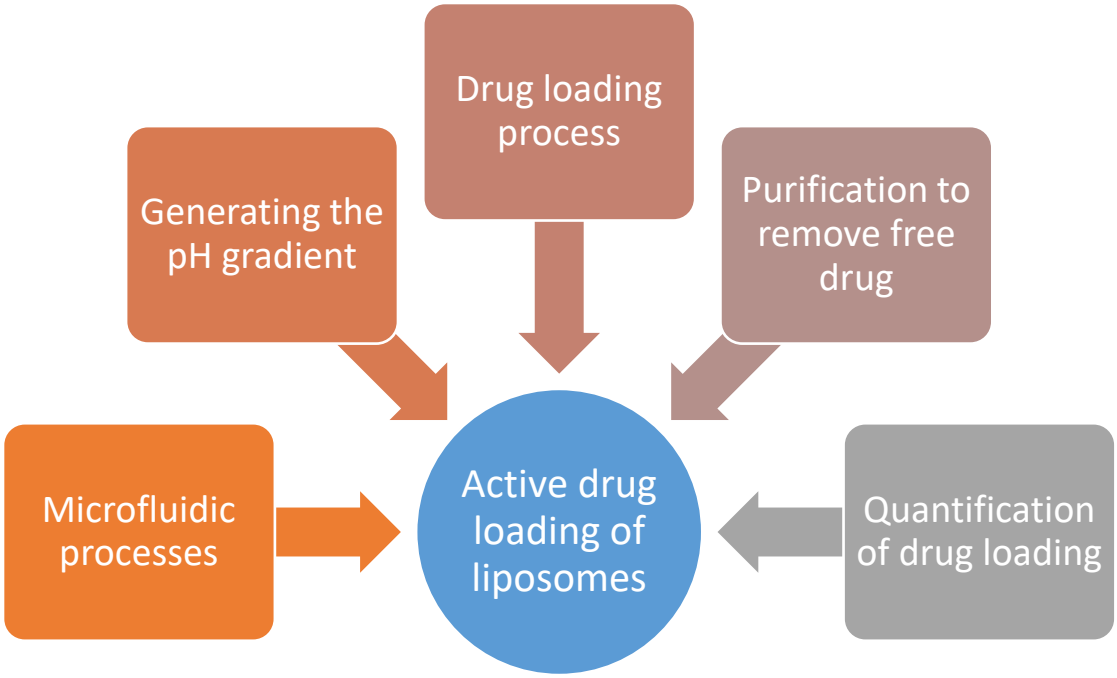

Figure 2.17: Factors impacting the production of liposomes loaded using the pH gradient method.

The key findings from these studies and how this will inform further studies are summarised in Table 2.2.

Table 2.2: Summary of Key Findings

	Factor	Key finding	Conclusions
Microfluidic Process Parameters	Choice of mixer	No notable difference between SHM and TM mixers	The SHM mixer will be adopted for the majority of studies
	Total flow rate	Production speed has no notable effect on liposome properties.	Standard mixing speed between 10 – 20 mL/min can be used with no impact on final properties.
	Flow rate ratio	Increasing the mixing ratio results in decreased particle size.	Given these differences, it merits further investigation
Buffer exchange	Establishing the pH gradient via dialysis	A pH gradient is required for active loading	For small liposome batches 3 h dialysis is sufficient

		For complete buffer exchange (and establishing the pH gradient) 3 h dialysis is required	Larger liposome batches may require longer dialysis
Active loading	Stability of liposomes after buffer exchange prior to drug loading	Liposomes stable for up to 48 h	Liposomes are stable once purified and may be stored for prolonged periods with no impact on the characteristics
	Stability of liposomes after drug loading	Liposomes stable for up to 48 h	Liposomes are stable once purified and may be stored for prolonged periods with no impact on the encapsulation
	Incubation time required to promote drug loading	20 min incubation was shown to give equivalent loading compared to up to 2 h	Prolonged exposure to high temperatures has no impact on the encapsulation and characteristics of the liposomes
	Incubation temperature required to promote drug loading	Incubation temperature has no impact on the loading of membrane permeable compounds	Encapsulation via an ammonium sulfate gradient provides efficient encapsulation
	Drug:Lipid ratio	Increasing the concentration of drug has no notable impact on characteristics of loading efficiency	Liposomes are capable of encapsulating high concentrations of compound with minimal impact on characteristics
	Removal of free drug	Both dialysis and TFF purification is capable of efficient free drug removal TFF purification is capable of increased purification rate with no notable impact on liposome characteristics or loading efficiency	TFF purification will be adopted for all future work due to quicker, efficient purification of large batches of liposomes.

During microfluidic manufacturing, the critical production parameters are the micromixer design, the flow rate ratio (FRR) and the total flow rate (TFR) (64). Micromixer design is critical for the efficient production of homogenous liposomal populations as the way in which the aqueous and organic phases mix is critical for the spontaneous formation of the lipid bilayer. Here, two different mixer designs were compared: the staggered herringbone micromixer (SHM) and the toroidal mixer (TM) (Fig 2.18).

Figure 2.18: Micromixer designs. A) Toroidal mixer that was used on the Ignite vs B) Staggered Herringbone mixer used on the Benchtop. Adapted from https://www.cytivalifesciences.com

Both mixers rely on chaotic advection; however, this is achieved using 2 different internal design structures. With the SHM, the two fluids are passed over a series of asymmetric protruding herringbone structures, thereby creating vortices leading to faster mixing performance and homogenous particle sizes, whereas in the TM, this is achieved through laminar flow whereby the fluid streams are passed through circular structures within the flow path (19). The results here (Fig 2.5) have shown that both micromixers can produce liposomes of similar physicochemical characteristics with no effect on the loading efficiency. FRR has been shown to be the key parameter in determining liposome size independent of the micromixer design. This is due to the FRR affecting the rate at which the organic solvent disperses into the aqueous phase. At lower FRR, there is less aqueous phase to dilute the organic solvent, resulting in slower lipid disc formation and, therefore, increased final particle sizes (60). As the FRR increases there is less organic solvent to be diluted in the aqueous phase, therefore resulting in reduced time required for disc formation and small particle sizes. These results are in agreement with previous research that also demonstrates the importance of FRR on resultant liposome size and polydispersity, with the higher FRR resulting in smaller, more homogenous liposome populations (65-68).

Purification and buffer exchange are required to remove any residual solvent and unentrapped compounds from the liposome sample. This can be carried out by several methods, including centrifugation, tangential flow filtration (TFF) and dialysis. Although dialysis is effective for the purification of small batches, it is not applicable for larger liposome batches that will require increased volumes and potentially increased time for complete purification. Dialysis is also a time-consuming technique that is not always reliable due to leakage of encapsulated drug during the dialysis process (69). The TFF, on the other hand, is a much more scalable option that has been implemented in the industrial production of liposomal medicines.

In general, drug loading into liposomes can be carried out by either passive or active methods. Active or remote loading can result in high encapsulation efficiency, minimal waste and enhanced stability.

During this process there are several factors that can be considered that may affect the resultant encapsulation efficiency. These can include the incubation time and temperature, the drug:lipid (D/L) ratio and how the unencapsulated compound is removed from the sample. During the active loading process, the liposomes are heated to a temperature above the transition temperature of the helper lipid. This then allows the membrane to transition from a solid phase to a gel-like phase, allowing for the compound to pass through the lipid bilayer along the pH gradient and complex with the ions in the acidic aqueous core (70). Data presented in Figures 2.13 & 14 show that heating the lipids is not always required and is dependent on the properties of the compound to be encapsulated. In the case of acridine orange, heating is not required as the drug can freely pass across the lipid bilayer along the pH gradient and, once internalised, forms a complex with the ammonium ions, thereby preventing it from diffusing back across the lipid bilayer. Incubation time is another important factor during the active loading process. Previous research has shown that the encapsulation efficiency is dependent not only on the incubation time but that this is also dependent on the drug properties and the lipid composition of the liposome. Cullis et al. (71) showed that in the case of doxorubicin, incubation at higher temperatures achieved high encapsulation with low incubation times; however, decreasing the incubation temperature required longer incubation time to achieve high encapsulation efficiency. It was also shown that the presence of cholesterol reduced the encapsulation at shorter incubation times. Research has shown that increasing the D/L ratio can result in increased encapsulation until a certain point, after which the encapsulation efficiency decreases. This is thought to be due to insufficient loading capacity within the aqueous core, resulting in drug precipitation and membrane disruption (10, 71). Results presented here (Fig 2.8) show that we can double the acridine orange D/L ratio with no impact on encapsulation efficiency, therefore suggesting that we have not reached the saturation levels for acridine orange and that the concentration could be increased further. Remote loading of acridine orange was found to not be affected by FRR and the subsequent difference in particle size, which may be attributed to there being more smaller liposomes produced at the higher FRR compared with fewer larger liposomes produced at lower FRRs. To confirm that the acridine orange was being taken up by the liposomes and not crystallising in the buffer, liposomes encapsulating PBS and mixtures of PBS and ammonium sulfate were incubated with acridine orange to confirm that the pH gradient was required for remote loading and that the TFF was removing all the unentrapped drug. The results confirmed that the acridine orange was encapsulated within the liposome and that there was no unentrapped drug remaining in the buffer. Therefore, this suggests that acridine orange is membrane permeable, and once encapsulated within the aqueous liposomes core, it complexes with the sulfate ions, thus preventing it from escaping.

It was important for us to cover all the basic aspects of microfluidic production and active loading initially so that we could identify which parameters appear to be important for liposomal formation. From these initial experiments, we have identified a number of factors (Table 2.3) that we wanted to investigate further using a systematic design of experiments (DOE) approach to identify how these factors affect liposome manufacturing both alone and how they may interact to affect the resultant characteristics and subsequent drug loading into these liposomes.

Table 2.3: Factors identified for further screening studies using a DOE approach.

Factors for Investigation	• FRR • TFR • Production Temperature • Solvent selection • Buffer selection • Choice of helper lipid • Initial lipid concentration
Critical Quality Attributes	• Particle size • PDI

2.5 Conclusion

From these experiments, the parameters important for liposome formation and active loading were identified. During the manufacturing process, the FRR appears to be the most important factor for determining final liposome particle size, with the TFR and micromixer design having less impact. When purifying the liposome sample, dialysis and TFF are both capable of efficient purification; however, dialysis is better suited for multiple small batches, such as when screening a lot of formulations. However TFF purification is capable of larger-scale purification and is more applicable to industrial purification methods. Therefore, it was decided that dialysis would be used for initial formulation screening and the selected formulations for active loading and *in vitro* and *in vivo* analysis would then undergo TFF purification. When loading the liposomes with acridine orange, it has been shown that the incubation time and temperature have no effect on the encapsulation efficiency of the liposome formulations and that it is possible to increase the concentration of the drug with no effect on liposome properties. These findings underpin further studies which will identify how the microfluidic manufacturing parameters interact with each other to effect resultant liposome physicochemical characteristics and how these may affect the loading of various APIs into these different liposome formulations.

Chapter 3 - Design of Experiments

3.1 Chapter Declaration

This chapter is written as an article to be submitted by (hence is the structure of this chapter):

Sarah Lindsay, Olympia Tumolva, Tatsiana Khamiakova, Hans Coppenolle, Martin Kovarik, Sanket Shah, René Holm, Yvonne Perrie

The named researchers below contributed to this chapter as follows:

SL devised the concept, performed design of experiments, and wrote the manuscript

OT part of the statistical team that created the design of experiment model and processed the data

TK part of the statistical team that created the design of experiment model and processed the data

HC part of the statistical team that helped process the data

MK part of the statistical team that helped process the data

SS contributed to scientific discussion and corrected the manuscript

RH contributed to scientific discussion and corrected the manuscript

YP develop the concept, supervised the work and corrected the manuscript

3.2 Introduction

Liposomal drug delivery systems have the potential to improve treatments of a variety of diseases through targeted delivery. Since their discovery in 1961, liposomes have become the most extensively researched drug delivery system owing to their unique ability to transport a large variety of drugs (72). Despite their proven ability to improve the delivery and efficacy of drugs, the clinical application of liposomes remains limited due to the cost and complexity of their manufacturing process. Conventional manufacturing methods use a top-down approach which involves the breakdown of initial material to the desired size through a series of processing steps. In order to obtain a uniform and monodisperse population, further downstream processing is required, which is unsuitable for many active pharmaceutical ingredients due to the high-shear forces involved in the manufacturing process (73). Therefore, new manufacturing techniques that are less time-consuming and scale-independent, which might precisely and easily control the manufacturing of liposomal products, are being investigated.

Among the different manufacturing methods that have been investigated for liposome manufacturing, microfluidics offers many advantages including its low cost and flexibility. Microfluidic devices promote self-assembly of the liposomes through rapid mixing of the organic solvent and aqueous phases and hydrodynamic manipulation of the fluids through chaotic advection (74, 75). In contrast to conventional methods, microfluidics uses a bottom-up approach, which addresses some of the limitations associated with the top-down approaches, such as high polydispersity, batched based production and user variability (73). Microfluidic mixers can be made from various materials such as polymers, silicon or glass and can be manufactured in various 'designs' (75). In general, an organic solvent stream containing the lipids is forced through a central channel, where it is then intersected on either side by the aqueous buffer stream. This hydrodynamic flow focusing (HFF) method was first described by Jahn *et al.* in 2004 (76) and has since been modified to produce the staggered herringbone micromixer (SHM) (41). Similar to HFF, the SHM involves the controlled mixing of an organic solvent with an aqueous buffer; however, the design of this micromixer uses rapid mixing through chaotic advection induced by injecting the solvent and aqueous streams into a Y-shaped mixer in which the two fluid streams are passed over a series of protruding herringbone structures within the channel (75). The most notable feature of this microfluidic technique is the ability to control the aqueous:solvent mixing ratio, also known as the flow rate ratio (FRR), as well as the speed at which these two fluid streams mix, known as the total flow rate (TFR). The formation of liposomes by microfluidics is driven by the diffusion of the organic solvent in the aqueous buffer, and therefore liposome characteristics, such as particle size, can be controlled through the manipulation of the FRR and TFR.

Previous studies have investigated the importance of both TFR and FRR, as well as various formulation parameters, such as lipid and solvent, on the resultant liposome properties, e.g. polydispersity and particle size. There have been numerous research papers demonstrating the importance of FRR on liposome particle size, with increasing FRR resulting in smaller liposomes (65-67). TFR has been reported to have minimal impact on resultant liposome characteristics, demonstrating that microfluidics is capable of high throughput production with minimal impact on the resultant liposomes (16, 64, 67). Solvent selection has also been shown to have an important impact on resultant liposome size and PDI (60). Research carried out by Webb *et al.* has shown that increasing the solvent polarity results in smaller particle sizes (60). This was suggested to be due to the rate of polarity change, with an increased rate of change in the polarity during microfluidic mixing, causing smaller lipid disc formation and, therefore, smaller liposomes (60). Recent design of experiment (DoE) studies have been carried out investigating the relationship between FRR, TFR, as well as solvent and lipid composition (64, 77); however, these studies have used limited FRRs, TFRs and lipid concentrations. Therefore, in order to further understand the important parameters for microfluidics in the liposome manufacturing, the aim of the present study was to investigate the use of microfluidic production for liposomes and identify the relationship between not only TFR, FRR and lipid concentration, but also solvent selection, aqueous buffer and production temperature applying a design of experiment (DoE) combined with machine learning, thereby mapping as many formulation and process parameters as possible within one study allowing a deep and unique cross factorial analysis.

3.3 Method

3.3.1 Materials

1,2-dioctadecanoyl-sn-glycero-3-phosphocholine (DSPC), 1,2-dioleoyl-sn-glycero-3-phosphocholine (DOPC) and cholesterol (chol, >99%) were obtained from Sigma-Aldrich Ltd. (Poole, UK). 1,2-distearoyl-sn-glycero-3-phosphoethanolamine-N-[methoxy(polyethylene glycol)-2000] (sodium salt) (DSPE-PEG2000,>99%) was obtained from Lipoid (Ludwigshafen, Germany).. Ammonium sulfate ([NH4]2SO4,>99%) was obtained from Sigma-Aldrich Ltd. (Poole, UK). Phosphate buffered saline tablets (10 mM, PBS pH 7.3) were acquired from Oxoid Ltd (Basingstoke, UK). All reagents (ethanol, methanol, isopropyl alcohol) were of analytical grade (HPLC grade,> 99.8%), and Transcutol was of general-purpose grade and purchased from commercially available suppliers. Dialysis tubing with molecular weight cut-off 12 – 14 kDa was purchased from Sigma-Aldrich Ltd. (Poole, UK).

3.4 Microfluidic production of liposomes

3.4.1 Preparation of liposomes using a bench-scale system

PEGylated liposomes were prepared using the bench-scale microfluidic system (NanoAssemblr Benchtop) from Precision NanoSystems Inc. (Vancouver, Canada) using a staggered herringbone micromixer (SHM). Individual lipid stocks were prepared at concentrations of 2 to 40 mg/mL in either ethanol, methanol, 2-propanol (IPA) or Transcutol and contained either DOPC or DSPC, cholesterol and DSPE-PEG2000 at a w/w ratio of 3:1:1, respectively. Lipids were heated for solubilisation but were stable once in solution. The lipids were heated to either 20°C or 60°C before injection into the micromixer, according to the experimental plan. Ammonium sulfate ($[NH_4]^2SO_4$, 250 mM) or phosphate buffered saline (10 mM) was used as the aqueous phase. Liposomes were produced at a total flow rate (TFR) of 5, 12.5 or 18 mL/min and a flow rate ratio (FRR) of 1:1, 10:1 or 19:1 (aqueous: organic). Formulations were dialysed (MWCO 12,000–14,000 Da, Sigma-Aldrich, Poole, UK) for 1 h under magnetic stirring against 200 mL PBS or ammonium sulfate buffer.

3.4.2 Characterization of particle size and polydispersity using dynamic light scattering

The particle sizes, measured as the hydrodynamic diameters, polydispersity indexes (PDI) and zeta potentials were measured by dynamic light scattering using a Zetasizer Nano ZS (Malvern Instruments Ltd, Worcestershire, UK) equipped with a 633 nm laser and a detection angle of 173°. The samples were measured at 25°C in the buffer mapped to each formulation, and the values of either PBS or ammonium sulfate were used for refractive indexes (1.335 and 1.52, respectively) and viscosity (1.02 cP and 1.338 cP, respectively). Zetasizer Software v.7.11 (Malvern Instruments Ltd) was used for acquisition of data.

Table 3.1: Protocol used to determine the sensitivity of the Malvern Zetasizer

Material	
Refractive Index	1.45
Absorption	0.001
Dispersant	PBS
Temperature	25 °C
Viscosity	1.0200cP
Refractive Index	1.335
General options	
Equilibrium time	120 s
Cell type	ZEN0040

Measurement	
Angle	173° Backscatter
Number of runs	Automatic
Number of measurements	3
Delay between measurements	10 s
Data Processing	General Purpose (Normal resolution)

3.5 Statistical Methodology

3.5.1 DoE

The study design involved setting up an I-Optimal DoE (14) with 135 experimental runs, including control runs, to check the reproducibility of the process and measurement. The DoE has the possibility to estimate several third-order interaction terms and fourth-order interaction terms. Additionally, 18 validation runs were created to check how well the statistical model predicts the PSD and PDI on new combinations of factor settings which were not used in the first DoE.

3.5.2 Statistical Modelling

As the current dataset was obtained via I-Optimal DoE, the multiple linear regression models, as well as regularized linear regression models (such as Elastic Net and Lasso), were considered. The primary linear regression model had very good performance on the training set and high error on the validation set of experiments, the phenomenon known in statistical data analysis as overfitting. To overcome the overfitting, regularized linear models were employed. Application of regularized models allows to avoid overfitting and perform model selection at the same time, as the least relevant model terms would be set to zero. The resulting prediction error of regularized regression using Elastic Net was higher compared to the original multiple linear regression model. However, the prediction error was comparable to the training and validation set, which justifies its use from the prediction perspective. Additional modelling efforts have included machine learning methods, such as Random Forests and XGBoost but their performance in terms of prediction error was not better compared to the Elastic Net models. Full technical details on the modelling are provided in Supplementary Information.

3.5.3 Visualization of modelling results

Due to the complexity of DoE and the final selected models involving higher-order interactions, which were relevant for prediction, contour plots were constructed for ease of interpretation. A typical contour plot would display the average response surface in terms of continuous factors TFR and FRR for different combinations of categorical factors solvent, buffer, lipid and discretized lipid concentrations and temperatures. Contour plots allow us to visualize and put emphasis on the

complex interactions. However, the model uncertainty (i.e. average prediction error) is not considered. In addition, the measured data points from the training and validation sets were added to the contour plots to demonstrate how the final selected model fits measurements from both sets of results.

3.6 Results

3.6.4 DoE Data

To investigate the individual effects of, and the interactions between formulation and process parameters, a DoE was set up with a total of 135 runs (plus an additional nine control runs carried out weekly). The testing parameters are shown in Table 3.2 and the DOE analysis highlighted the simulated key factors based on this workspace.

Table 3.2: Factors Investigated and Range tested in the DoE study

Factor	**Range**
Total Flow Rate (TFR)	5, 10, 12.5, 18 mL/min
Flow Rate Ratio (FRR)	1:1, 3:1, 10:1, 19:1
Lipid Concentration	2 – 40 mg/mL
Lipid	DSPC, DOPC
Solvent	Ethanol, Methanol, IPA, Transcutol
Buffer	Phosphate buffered saline (PBS), Ammonium Sulfate
Temperature	20°C, 60°C

3.6.4.1 Exploration of overall effects of DoE factors

The boxplots were constructed (Figures 3.1 and 3.2) to highlight the overall (marginal) effects of the investigated process and formulation parameters on PDI and PSD. These boxplots show the distribution of particle size or PDI for different levels of a given parameter without considering the levels of other parameters in the study. It must be noted that no clear difference in response values

on the boxplot does not exclude a situation when a parameter in question has a meaningful impact in combination with specific settings of other parameters.

3.6.4.1.1 Process Variables

Initially, the process variables of total flow rate, flow rate ratio and production temperature were considered (Figure 3.1). Based on Boxplots, the TFR and production temperature showed no obvious overall effects on either the size or PDI of the resultant liposomes produced; however, the FRR appeared to affect both the size and PDI (Figure 3.1A and B). These results also showed a wider data distribution at FRR 1:1 for particle size, with FRR 1:1 resulting in an overall larger particle size (Figure 3.1A), whilst the highest FRR gave the widest spread for PDI (Figure 3.1B). These results aligned with previous research showing that FRR had a greater influence over particle size when compared with TFR (Figure 3.1C and D), and that increasing the FRR resulted in smaller particles, but high dilutions can result in more heterogenicity ((64, 77, 78)).

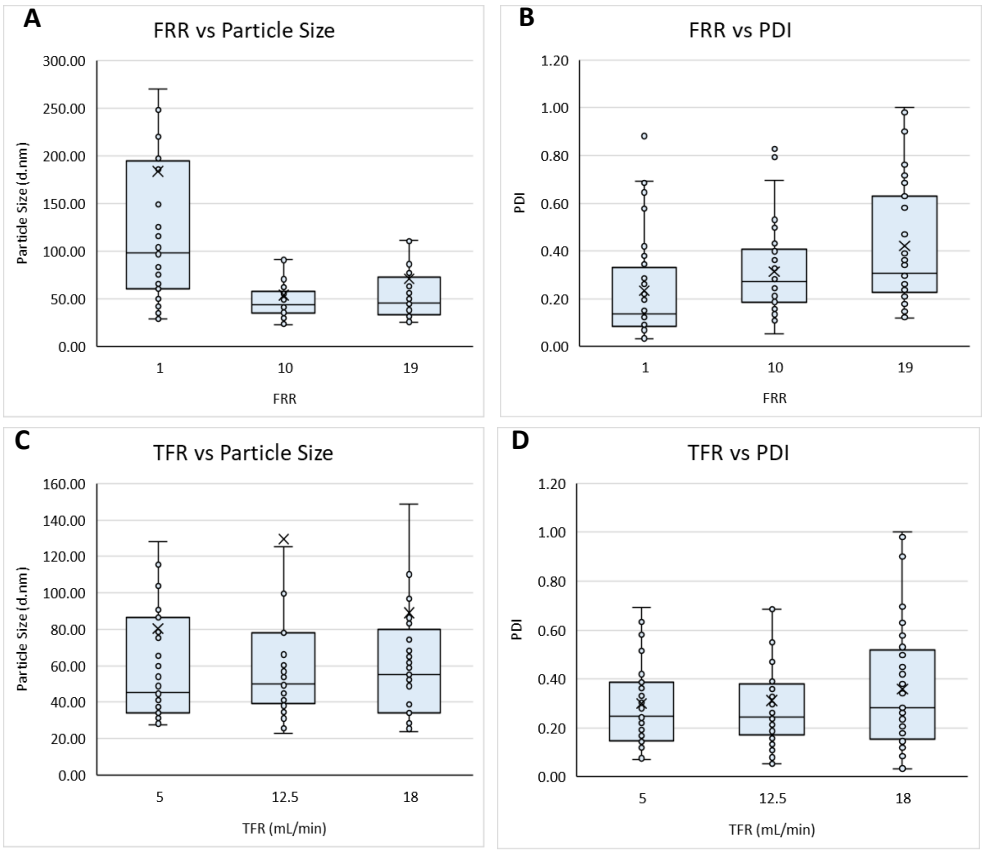

Figure 3.1: Boxplots of Flow Rate Ratio (FRR) against A) Particle size and B) PDI, and Total Flow Rate (TFR) against C) Particle size and D) PDI for liposomes prepared via microfluidics following a DoE. Each point represents a result from an individual run. The outlier points have been removed to get a clearer view of the mean effect of each parameter. Factors tested are shown in Table 3.2.

3.6.4.1.2 Formulation Variables

The lipid composition of liposomes and the buffers used within the formulation can determine the loading efficiency, targeting and circulation time of the resultant product and, therefore, needs to be carefully considered from a manufacturing perspective. Therefore, to study this, we tested different lipid compositions (DSPC vs DOPC; Table 3.2), with different solvents (Transcutol, methanol, ethanol, and IPA) and considered their size and PDI (Figure 3.2).

Overall, the buffer did not impact size nor PDI, whereas the lipid used impacted particle size, with liposomes composed of DSPC (Figure 3.2A) showing an overall larger particle size when compared to liposomes produced with DOPC (B) (Figure 3.2A & B). The organic solvent used also impacted particle size and PDI of the liposomes produced from a Transcutol lipid stock having an overall smaller mean size when compared to the liposomes produced with IPA, which produced the largest mean size. Liposomes produced from methanol, ethanol and Transcutol all had similar average PDI; however, those produced from IPA had an overall larger average PDI. Lopez and coworkers (61) reported that liposomes produced from a Transcutol stock were smaller than those produced from an ethanol stock independent of the production temperature and lipid concentration, in contrast to the data reported in this work.

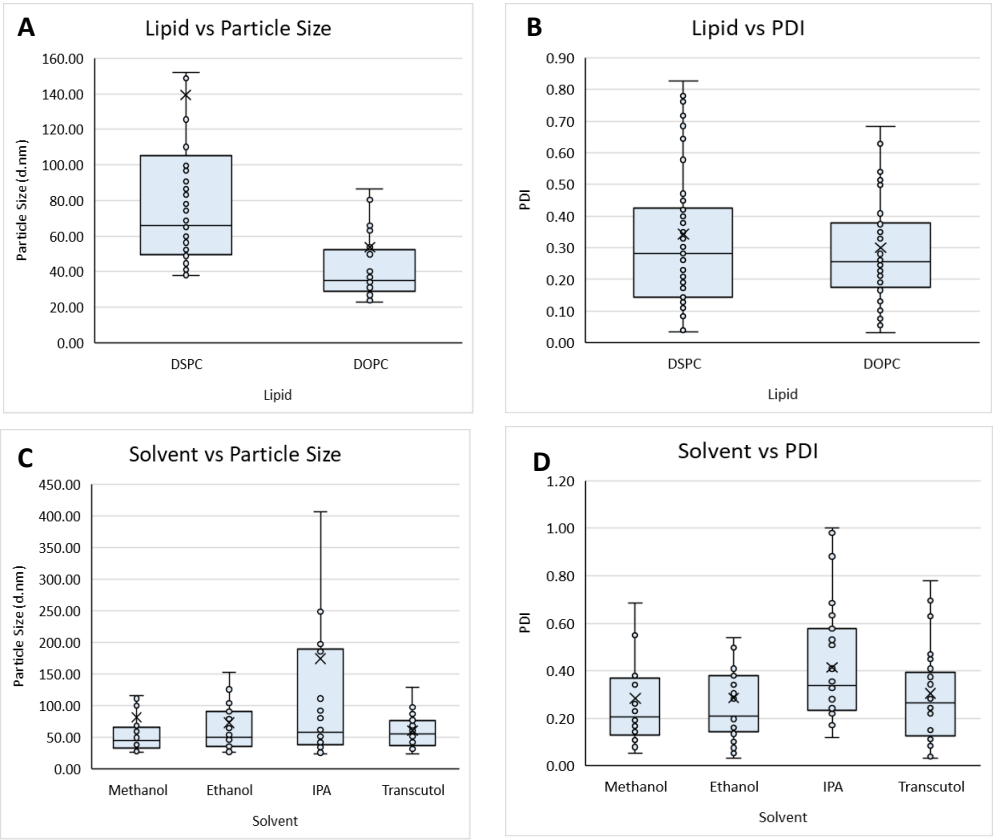

Figure 3.2: Boxplot of helper lipid against A) Particle size and B) PDI, and solvent against C) Particle size and D) PDI for liposomes prepared by microfluidics following the DoE. Each point represents a result from an individual run. The outlier points have been removed to get a clearer view of the mean effect of each parameter. Factors tested are shown in Table 3.2.

When investigating differences in the obtained particle size and PDI as a function of lipid concentration, it was difficult to determine whether there was any effect or not, as the concentration of the lipid stock used depended on the lipid solubility in each solvent and the production temperature. Therefore, the data were separated according to the lipid and solvent used to visualise the effect of lipid concentration on liposomes produced by microfluidics. When ethanol was used, there was no obvious effect on either the particle size or PDI of liposomes composed of DSPC. However, at low concentrations, DOPC liposomes, whilst having similar size, showed a relatively higher PDI. When IPA was used, there was no impact on particle size for DSPC or DOPC; however, again, DOPC liposomes showed a higher PDI at lower lipid concentrations. In the case of methanol, different concentrations of lipids were used depending on the production temperature. When comparing the concentrations at 20 °C, low lipid concentration resulted in smaller PDI and particle size for DSPC liposomes, whereas DOPC showed a slightly higher PDI and particle size at low concentrations. At 60 °C, the lipid concentration showed minimal effect on the particle size and PDI of DSPC liposomes, whereas DOPC liposomes showed a slightly higher particle size and PDI at low

concentrations. Similar to using methanol in the production process, the initial concentration of the DSPC liposomes was determined by the production temperature. At 20°C the lipid concentration did not show any impact on the particle size, but the PDI was higher at the high concentration, whereas at 60 °C, the lipid concentration had no impact on the PDI or particle size. When DOPC was dissolved in Transcutol the lipid concentration had minimal impact on the particle size and no effect on the PDI.

3.6.5 Exploring Interactions by Regression Trees

On top of boxplots, which focus on the overall effects, the regression trees were constructed for both measured outcomes (particle size and PDI) using the data collected to explore the interactions between factors. The regression tree can then be used to visualize how factors influence either particle size (Figure 3.3) or PDI (Figure 3.4), where the first or 'root' node variable is the one that may have more of an impact on response compared with the other factors tested, next splits are indicating, which variables would lead to important interaction effects. If a variable is not present in the tree it means that its explanatory ability is limited in the given dataset for the response of interest. The terminal node on a graph shows the average response in the branch of the data following the split of a regression tree.

In terms of particle size (Figure 3.3), FRR was determined to be a root variable, which follows the observation in the boxplot: the right branch (FRR less than 2) has terminal nodes with larger particle size, with the largest average particle size when the solvent IPA is used. Smaller particle size is observed for FRR less than 2 when methanol and Transcutol are used with Lipid B (DOPC). Looking at the left-hand side of the tree, when FRR is greater than 2, lower particle size was observed for Lipid B compared to Lipid A (DSPC). However, lower particle size (averages between 39 and 61) was observed for temperatures higher or equal to 40 °C. Temperature had a different effect direction for Lipid B (DOPC) in low concentration. Therefore, we cannot exclude the effect of temperature on the particle size fully, despite that we have not observed an overall effect. The complexity of the tree emphasizes that different factor combinations may potentially lead to the formation of liposomes with lower particle size, and some combinations lead to liposomes with large particle sizes.

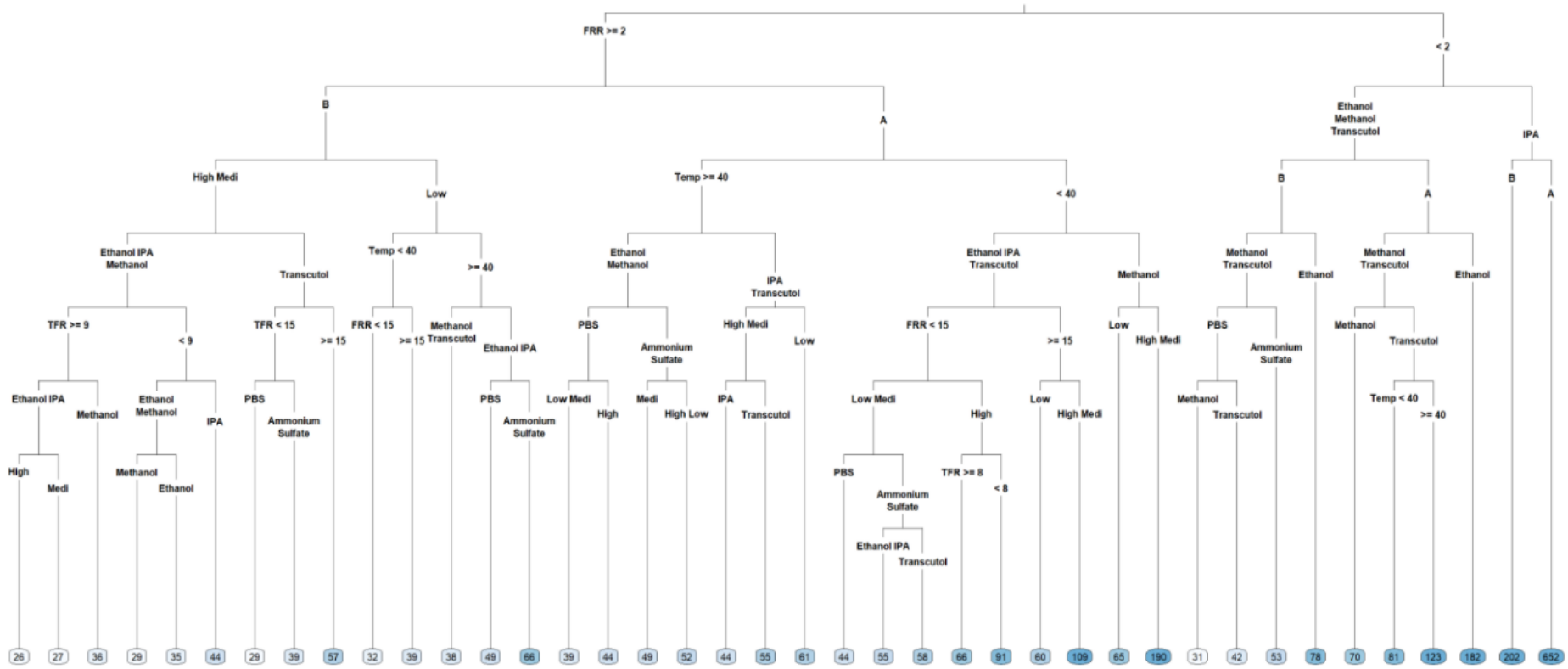

Figure 3.3: Regression tree for particle size of liposomes produced via microfluidics following a DoE. Factors tested are shown in Table 3.2.

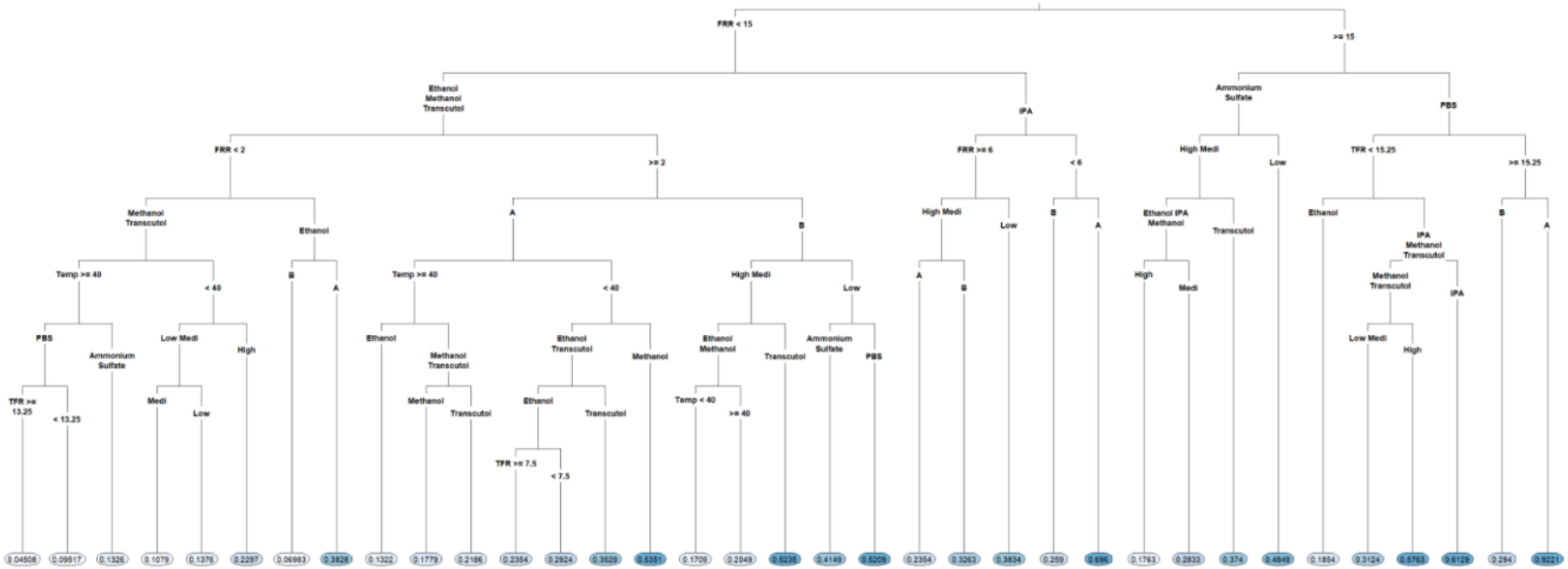

Figure 3.4: Regression tree of polydispersity index (PDI) of liposomes produced via microfluidics following a DoE. **Factors tested are shown in Table 3.2.**

In terms of PDI (Figure 3.4), similar to the particle size, the FRR was determined to be a root variable with the threshold being an FRR 15:1, confirming boxplot visualization for the overall effect of FRR. In the next level, when the FRR was less than 15, the PDI was split according to the solvent used, and when the FRR was greater than or equal to 15, the PDI was split according to the buffer used, pointing out that interactions of FRR with buffer and solvent were important for explaining PDI. Furthermore, liposomes with the lowest PDI were produced at FRR less than 2 from either methanol or Transcutol at temperatures below 40 °C when PBS was used as the buffer, and the TFR was greater than or equal to 13.25 mL/min (Figure 3.4 following the furthest left branches), indicating that higher-order interactions were present in case of PDI.

Both regression trees point out that the statistical model fitting the particle size and PDI results would be complex and contain higher-order interactions and nonlinear (quadratic and even cubic) effects.

3.6.6 Modelling results: Selected Factor Interactions

The model used to design the experiments was fitted using the collected data and had a good prediction performance. However, it was found to be overfitting the collected data, which was not generally observed in the fitted machine learning models (Appendix Table 8.2 & 8.3). Thus, Lasso regression (which was the selected final model) was then used to simulate the particle size and PDI across the experimental ranges defined in Table 3.2 to determine the combination of factors required for optimal liposome production.

In terms of particle size, Lasso regression determined that the mixing ratio (FRR), lipid concentration and production temperature used were important factors in controlling particle size whereas the production speed, lipid, solvent and the buffer used had no notable effect individually (Table 3.3), which confirmed the exploratory analysis provided in Section 3.6.5.

Table 3.3: Selected model terms for particle size of liposomes prepared using microfluidics using Lasso regression

Model term (PSD)
FRR
LipidConc
Temp
TFR2
FRR:LipidConc
FRR:Solvent
FRR:TFR2
LipidConc:Lipid
LipidConc:LipicConc2
Temp:Lipid
Temp:Solvent

Temp:LipidConc2
Lipid:TFR2
Buffer:TFR2
Solvent:TFR2
TFR2:LipidConc2
TFR:Temp:TFR2
TFR:Lipid:TFR2
TFR:Buffer:TFR2
FRR:LipidConc:LipidConc2
FRR:Buffer:Solvent
FRR:Solvent:TFR2
LipidConc:Temp:FRR2
LipidConc:Temp:LipidConc2
Temp:Lipid:Buffer
Temp:Lipid:Sovent
Buffer:TRF2:FRR2
TFR:FRR:LipidConc:LipidConc2
TFR:FRR:Temp:LipidConc2
TFR:LipidConc:Temp:Lipid
TFR:LipidConc:Temp:TFR2
TFR:LipidConc:FRR2:LipidConc2
TFR:Temp:Lipid:Solvent
FRR:LipidConc:Temp:LipidConc2
FRR:LipidConc:Lipid:Buffer
FRR:LipidConc:Lipid:Solvent
FRR:LipidConc:FRR2:LipidConc2
FRR:Temp:Lipid:Solvent
FRR:TFR2:FRR2:LipidConc2
LipidConc:Temp:Lipid:TFR2
LipidConc:Temp:Buffer:TFR2
LipidConc:Temp:TFR2:FRR2
LipidConc:Lipid:TFR2:FRR2
Temp:Lipid:Buffer:Solvent
Temp:Lipid:Buffer:FRR2
Temp:Solvent:FRR2:LipidConc2
Lipid:Buffer:Solvent:LipidConc2
Buffer:Solvent:FRR2:LipidConc2

The mixing ratio (FRR) has been shown to be one of the key determinants of particle size (25, 65, 68) and this data not only demonstrated the factor importance individually but also showed how it could interact with other factors.

The particle size range could be fairly predicted when the interaction between FRR and either production speed (TFR), solvent, or lipid concentration were considered. Solvent has previously been shown to influence particle size with higher polarity solvents resulting in smaller particles formed (60).

Webb *et al* (60) reported that liposomes produced from methanol were significantly smaller than those produced from IPA. The work by Webb and co-workers suggested that this difference in particle size was driven by the rate of change in polarity of the solvents upon mixing with the aqueous buffer (60). Higher polarity solvents have a higher rate of change, which resulted in smaller disc formation, and therefore smaller liposomes (60). In a DoE study carried out by Lopez *et al* (61) where the influence of organic solvent was assessed, specifically methanol, ethanol, IPA and Transcutol, on liposomes produced using a periodic disturbance mixer, Lopez and co-workers reported that Transcutol, the lowest polarity solvent, produced the smallest liposomes when compared with ethanol in contrast to the present study and the data reported by Webb and co-workers (12). These contradicting results may demonstrate that the type of micromixer may affect liposome size as it would subsequently affect the rate of change of the polarity (61).

Lipid concentration was shown to have higher-order interactions with a number of factors, including production speed, mixing ratio, lipid, buffer and temperature. These interactions may be due to the variation in concentrations that were dependent on the lipid, solvent and production temperature. Lipid concentration was shown to have an impact on resultant liposome particle size; however, the type of lipid used was not selected as a model term. This suggested that the lipid concentration had a significant effect on the particle size independent of the lipid used and that the effect of lipid concentration was similar for both lipids used.

Similarly, lipid concentration was shown to affect PDI; however, mixing speed and lipid were also found to impact the PDI of resultant liposomes (Table 3.4). When identifying 2-way interactions, a couple of factors together impacted polydispersity whereas they had no effect individually. These interactions included the interaction between mixing ratio and solvent (FRR:Solvent) and between temperature and solvent (Temp:Solvent).

Table 3.4: Selected model terms for PDI using Lasso regression

Model term
TFR
LipidConc
Lipid
TFR:FRR
FRR:Solvent
LipidConc:LipidConc2
Temp:Solvent
Temp:LipidConc2
Solvent:LipidConc2
Solvent:TFR2
TFR:FRR:Solvent

TFR:LipidConc:Lipid
TFR:LipidConc:TFR2
TFR:Temp:Lipid
TFR:Temp:FRR2
TFR:Lipid:TFR2
TFR:FRR2:LipidConc2
FRR:LipidConc:Temp
FRR:LipidConc:TFR2
FRR:LipidConc:LipidcConc2
FRR:Buffer:Solvent
FRR:Solvent:LipidConc2
LipidConc:Temp:FRR2
LipidConc:Lipid:Solvent
LipidConc:Lipid:TFR2
LipidConc:Lipid:FRR2
Temp:Lipid:Solvent
Lipid:Solvent:TFR2
Buffer:Solvent:TFR2
TFR:FRR:LipidConc:Temp
TFR:FRR:LipidConc:Lipid
TFR:FRR:Temp:LipidConc2
TFR:FRR:Lipid:LipidConc2
TFR:FRR:Solvent:LipidConc2
TFR:Temp:Lipid:Buffer
TFR:Temp:Buffer:TFR2
TFR:Temp:Buffer:FRR2
TFR:Temp:FRR2:LipidConc2
TFR:Lipid:Buffer:TFR2
TFR:Buffer:Solvent:TFR2
FRR:LipidConc:Temp:Lipid
FRR:LipidConc:Temp:Solvent
FRR:LipidConc:Temp:LipidConc2
FRR:LipidConc:FRR2:LipidConc2
FRR:Lipid:Buffer:Solvent
LipidConc:Temp:Buffer:TFR2
LipidConc:Temp:Buffer:FRR2
LipidConc:TFR2:FRR2:LipidConc2
Temp:Lipid:Buffer:Solvent

Overall, when looking at all the model-selected interactions (individual, 2-way, 3-way and 4-way), the factor that occurred the most for both particle size and PDI was the lipid concentration, closely followed by the TFR. This may be due to the varying solubility of the lipids in each solvent, and as previously mentioned, the self-assembly of lipids into liposomes is reliant on the diffusion rate of the solvent in the aqueous buffer, which is determined by the mixing speed. In the following section, we

show the contour plots constructed based on the model simulations for further discussion on factor effects.

3.6.7 Contour Plots

To be delivered to their target site, nanocarriers must be of a small enough size to enter the target site and also evade detection by the mononuclear phagocyte system (MPS). Therefore, nanocarriers are generally designed in the size range of less than 100 nm and low PDI with smaller liposomes having longer circulation times (e.g. (79, 80)) or distributing better into the relevant tissue (66). Contour plots allow us to check the regions where the final product would be within the desired range in terms of PDI and particle size.

Figure 3.5 shows the contour plots of the simulated particle size of liposomes produced at 20°C (Figure 3.5A) and 60°C (Figure 3.5B), where the smaller particles appear green, and the larger particles appear red. In general, smaller liposomes were produced at 60°C compared with 20°C, with IPA showing the largest variability in size across all temperatures, lipid, buffer, and lipid concentrations. Liposomes produced from IPA at low FRR (e.g. 1:1) at all TFR tested showed relatively larger particle sizes compared with the other solvents tested. This may be due to the polarity of this solvent as solvents with lower polarity (e.g. IPA) result in larger liposomes than high polarity solvents (e.g. methanol). This is due to the low polarity solvents having a lower rate of change in polarity when mixed with the aqueous phase, leading to larger lipid disc formation and, therefore, larger liposomes forming (60). As the concentration of the lipid increased, the size of the liposomes increased (at 20°C).

Figure 3.5: Contour plots of particle size produced across all the variables tested. A) Liposomes produced at 20°C from lipid A (DSPC) and lipid B (DOPC) at concentrations of 2 – 40 mg/mL. B) Liposomes produced at 60°C from lipid A (DSPC) and lipid B (DOPC) at concentrations of 2 – 40 mg/mL where smaller liposomes are shown in green and larger liposomes are shown in red.

Figure 3.6 shows the contour plots for the polydispersity index (PDI) of the liposomes produced at both 20°C (Figure 3.6A) and 60°C (Figure 3.6B). When produced at 20°C, liposomes composed of DSPC showed an increase in PDI with increasing lipid concentration when PBS was used as the aqueous buffer. However, this was not observed when ammonium sulfate was used. When ammonium sulfate was used as the aqueous buffer, the PDI of DSPC liposomes decreased with increasing lipid concentration. This trend can be observed across all the solvents tested. Liposomes composed of DOPC showed a similar trend, with liposomes produced using PBS having increased PDI with increased lipid concentration, whereas those produced using ammonium sulfate show decreased PDI with increased lipid concentration. Again, this was observed across all the solvents tested. However, when DSPC and DOPC liposomes were produced at 60°C (Figure 3.6B), the opposite trend was observed. When DOPC was produced in PBS, the PDI decreased as the lipid concentration increased, whereas DSPC did not appear to change as the concentration increased.

A.

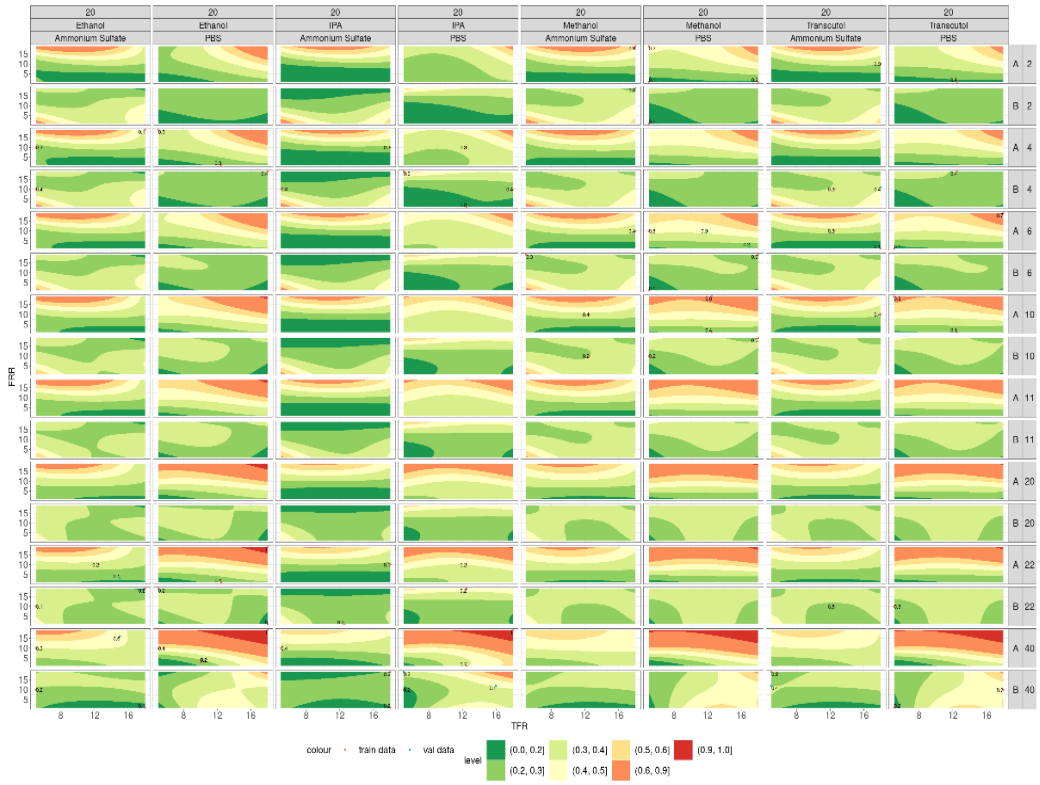

B.

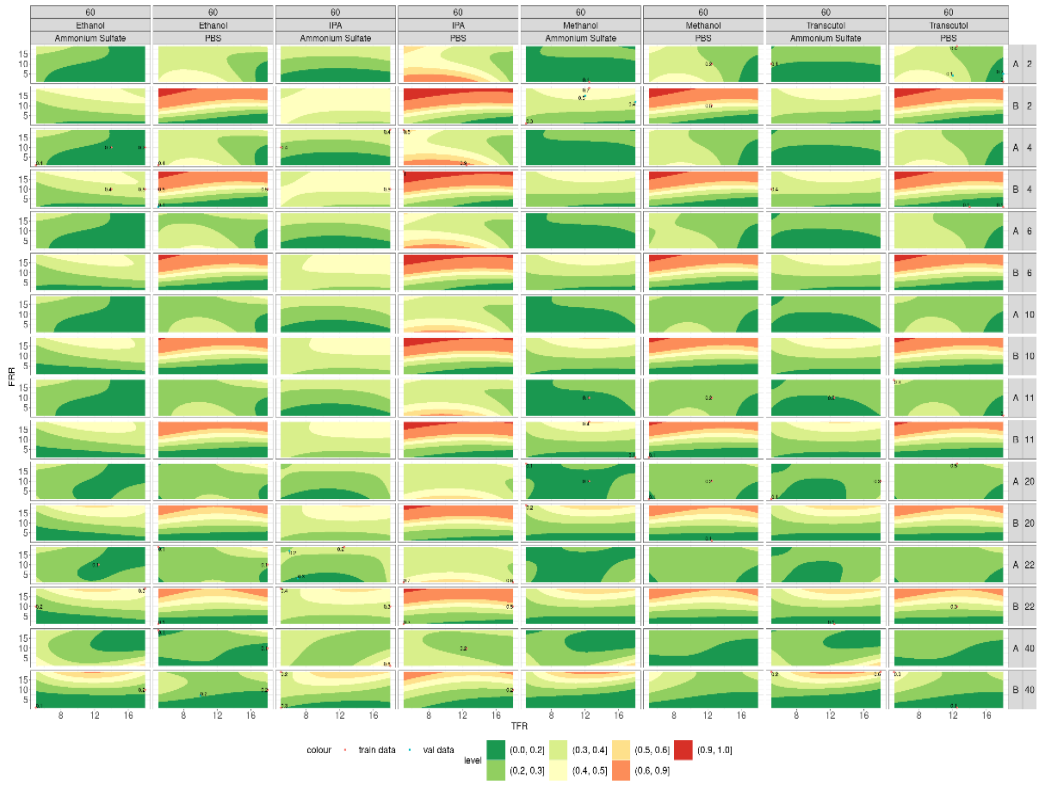

Figure 3.6: Contour plots of polydispersity index of liposomes produced across all the variables tested. A) PDI of liposomes produced at 20°C from lipid A (DSPC) and lipid B (DOPC) at concentrations of 2 – 40 mg/mL. B) PDI of liposomes produced at 60°C from lipid A (DSPC) and lipid B (DOPC) at concentrations of 2 – 40 mg/mL where lower PDI appears green and higher PDI appears red.

3.6.8 Confirmatory Experiments

Verification runs were then carried out to confirm the average simulated outcomes of the initial model using the original data set. Eighteen runs were selected where the average simulated values were ranging from low to high, specifically (23, 273) and (0.097, 0.755) for PSD and PDI, respectively. The results from these experiments showed that the initial model accurately simulated the majority of the particle size and a few of the PDI for some of the runs carried out. However, there were results that deviated from the simulated outcomes based on the model obtained through machine learning (Figure 3.7). These deviations may be due to the low final lipid concentration used when measuring the liposomes and the high complexity of the model. This is supported by some initial investigations performed (see supporting information), where we showed that at lipid concentrations below 1 mg/mL there can be significant deviations in both size and PDI compared with samples of higher concentrations (Figure 8.5).

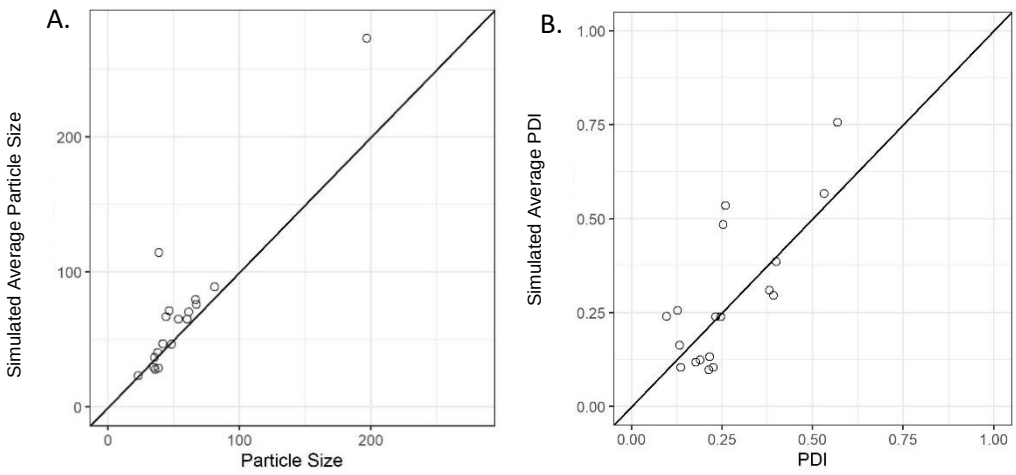

Figure 3.7: Average simulations for the validation runs using the initial model for A) Particle size versus observed, and B) PDI versus observed ,solid dashed line is an identity line.

3.7 Discussion

Microfluidic production of liposomes may provide a cost-effective and scalable approach to the manufacturing of liposomes. Since the first documented application of microfluidics for the production of liposomes by Jahn et al. (76), research has focused on how this technology can be developed and fine-tuned to produce a variety of liposomes for drug delivery.

Extensive research has demonstrated the impact of microfluidic parameters, including the mixing ratio, or flow rate ratio (FRR), and the production speed, or total flow rate (TFR), on the critical quality attributes of the liposomes, such as particle size and particle size distribution. Of these, the most notable parameter affecting liposome size was the mixing ratio, which has been shown to have a

significant impact on the liposome size, independent of the production speed and formulation tested in the present work. Increasing the FRR resulted in larger particle formation, as shown in (Figure 3.1A & B), whereas lower FRR (1:1) resulted in significantly larger particles compared with FRR > 10:1. This difference in size may be due to the dilution rate of the solvent in the aqueous buffer, as also previously suggested by Lopez and coworkers (18). As the aqueous phase and the organic phase mix together the alcohol concentration was diluted into the aqueous buffer. Therefore, increasing the FRR resulted in an increased aqueous volume and increased solvent dilution, thereby promoting faster mixing and resulting in the production of smaller liposomes (81). The formation of liposomes was, therefore, also dependent on the change in the polarity of the solvents (60). During microfluidic production, the lipids were initially dissolved in an organic solvent, which was then mixed with the aqueous buffer to promote self-assembly of the liposomes. As previously mentioned, it was the reduction in polarity and diffusion of the solvent into the aqueous buffer that drove liposome formation. Therefore, these data suggested that reducing the polarity of the solvent will result in increased liposome size. This was demonstrated when comparing liposomes produced from IPA and those produced from Transcutol. As mentioned previously, research carried out by Webb et al (60) showed that liposomes produced from either methanol or ethanol were of similar size, however, there was a noticeable increase in size when IPA was used.

Before selecting the solvent, there are several other factors that must be considered, such as the solubility of the lipid in the selected solvent and aqueous phase. As mentioned above, increasing the solvent polarity results in smaller liposome formation; however, Joshi et al. have also suggested that the sensitivity to this polarity change may be lipid-dependent (81). When changing from methanol to ethanol, there was no notable difference in the size of liposomes composed of PC, DMPC or DPPC; however, those composed of DSPC:Cholesterol showed a significant increase in particle size. The same sensitivity was also shown when switching the buffer from PBS to Tris buffer (81). The initial lipid concentration is another important consideration when preparing liposomes as it has been shown that increasing the initial lipid concentration results in smaller vesicle formation irrespective of the alkyl chain length (78, 81). In order to determine whether this difference in particle size was due to lipid alkyl chain length or the lipid transition temperature, Forbes et al. compared the particle size of DSPC and DOPC:Cholesterol at a constant TFR and FRR and at the same initial lipid concentration. It was shown that DOPC liposomes were significantly larger than DSPC liposomes which is in disagreement with the results presented here, however, it is important to consider that the liposomes produced in this study had the addition of DSPE-PEG2000 in the bilayer. The addition of PEG polymers to the liposome surface reduces opsonisation and clearance by the immune system therefore

extending their circulation in the bloodstream (82). Increasing the concentration of PEG has been shown to result in a decrease in liposome size (83), therefore accounting for the difference in size.

When produced by conventional manufacturing methods, liposomes have to be manufactured at temperatures above the transition temperature of the main lipid. The lipids would initially be dissolved in a solvent and undergo evaporation, before then being rehydrated in the desired aqueous buffer. During the rehydration stage, the lipids are heated to change the structure of the lipid from a crystalline structure to a more fluid gel phase, allowing for the lipid disc to bend and curve to form vesicles. However, microfluidics can produce small, monodisperse liposomes at temperatures below the transition temperature. Supplementary Figure 12 shows that there was no notable difference in particle size of liposomes produced at 20 °C and 60 °C; however, statistical analysis showed that temperature was a significant factor when considered in combination with other production parameters. This may be attributed to the bottom-up manufacturing approach where the liposomes were produced from lipid monomers, which self-assemble into vesicles in the presence of an aqueous buffer. Whereas in conventional top-down approaches, the liposomes are produced and then undergo subsequent size reduction steps in which the liposomes are broken down and reformed (78). To form curved vesicles, these lipids need to be heated to make them more flexible and fluid.

Further analysis of the data presented in the present study has provided insight into how microfluidic and formulation parameters can interact to determine resultant liposome size and polydispersity. Similar DoE studies have been carried out to demonstrate the interaction between various liposome production parameters, including TFR, FRR, and solvent; however, none have previously investigated as many factors or as wide a range as the present DoE (Kastner et al. (64) carried out a microfluidic-based study to assess the impact of FRR and TFR using multivariate analysis. In the study by Kastner and co-workers, cationic liposomes were manufactured at FRR 1:1 – 5:1 and at TFR 0.5-2 mL/min, and it was found that increasing the FRR resulted in decreased particle size, and TFR had no significant effect. These results confirm previous data (65, 68) as well as the data presented in this study. It was also shown that increasing the FRR had a significant impact on PDI. This aligns with the results in this study, as increasing the FRR from 1:1 – 19:1 resulted in a steady increase in PDI (Figure 5).

Transcutol, more commonly known as diethylene glycol monoethyl ether (DEGEE), was originally used as an industrial solvent under the trade name Carbitol and, up until the 1990s, was not suitable for pharmaceutical application due to the high level of impurities, such as ethylene glycol (84). Transcutol is an ethylene oxide derivative with high purity that is used commercially in over-the-counter topical products due to its ability to enhance skin penetration (84, 85). Recent research carried out by Lopez et al. investigated the use of Transcutol for liposome production (61). In these experiments,

DMPC:cholesterol:DHP liposomes were produced using a periodic disturbance mixer using four different solvents: methanol, ethanol, IPA and Transcutol. These liposomes were initially produced at a constant TFR, FRR and initial lipid concentration and it was shown that liposomes produced from IPA had a larger PDI and Transcutol produced the smallest liposomes. These results agree with the results presented here; however, Lopez et al. found that Transcutol and IPA produced smaller liposomes than ethanol and methanol. These contradicting results may be due to the different types of micromixers. The design of the micromixer influences the mixing and subsequent dilution of the organic solvent in the aqueous buffer, and therefore, different designs may result in different mixing efficiencies (61). It was also shown that the production temperature and resultant size of the liposomes may be dependent on the solvent used. Transcutol and ethanol were compared at four different temperatures, and it was shown that with increasing temperature, the size of the liposomes produced from ethanol decreased, whereas the liposomes produced from Transcutol showed no effect. In the present study, it was shown that temperature alone had no overall effect on the resultant liposome physicochemical characteristics. However, further analysis showed that temperature can interact with the lipid concentration, lipid and solvent used to determine both the size and PDI.

Confirmatory experiments were carried out to help validate the model developed in this DoE, and the results from this demonstrated that the model was able to accurately determine the liposome characteristics of 5 out of the 8 runs carried out (approx. 63% accuracy). The error in the simulated output may come from higher-order interactions that we were not able to determine with the current model due to the number and wide range of variables tested in this study.

In line with previous research and design of experiment studies investigating microfluidic production, our study provided further in-depth statistical analysis of not only the process but also formulation parameters and how these influence liposome physicochemical characteristics. Compared with previous research, the present study investigated a larger number of manufacturing factors and a wider range of manufacturing parameters. Through this, we have tested the limits of the NanoAssemblr benchtop system and demonstrated the ability of microfluidics to produce a wide range of liposomes under various production conditions.

3.8 Conclusions

Our studies have demonstrated the versatility and ability of the microfluidic platform to produce liposomes of various compositions and particle sizes. Design of experiments analysis confirmed the statistical significance of both microfluidic process parameters and formulation parameters on the resultant liposome particle size and polydispersity. The complexity of the data generated by the DoE required machine learning to effectively model the results. The model suggests that the resultant

particle size and PDI can be adjusted through the tuning of the formulation, such as the lipid and solvent used, as well as through changing the mixing ratio (FRR) and production speed (TFR). However, it was only possible to simulate directions of particle size and PDI with the generated models, not to accurately simulate the liposome size and PDI. This demonstrates the complexity of liposome formulation and manufacturing and the large connectivity between the factors.

Chapter 4 - The effect of microfluidic production parameters on liposomes loaded via a pH gradient

4.1 Introduction

Lipid-based nanocarriers have been shown to increase drug delivery and bioavailability of various pharmaceutical compounds through encapsulation of these drugs inside either the aqueous core or the lipid bilayer of nanoparticles (86). Doxil®/Caelyx (US/UK) was the first nanomedicine to be approved by the Food and Drug Administration (FDA) in 1995 and is a type of PEGylated (Stealth) liposome formulation (16).

Doxorubicin is an anthracycline drug, and an analogue of the original anthracycline daunorubicin, that is used for the treatment of various cancers such as breast, lung, and ovarian cancer (87, 88). One of the major limitations for the use of doxorubicin is its cumulative and dose-dependent cardiotoxicity (89). Doxorubicin works by inhibiting RNA synthesis through intercalation with DNA, leading to single and double-stranded breaks. These breaks in the DNA are thought to be mediated by the activity of topoisomerase II and through the production of oxidative stress and subsequent free radicals (90). It is these free radicals that lead to cardiotoxicity as a result of mitochondrial disruption (87).

Liposomal doxorubicin (Doxil®) was developed to increase therapeutic efficacy whilst also reducing toxicity to healthy tissues. Doxil® is a PEGylated liposomal formulation composed of HSPC, cholesterol (Chol) and DSPE-PEG2000 encapsulation in an ammonium sulfate aqueous core. Doxil® exhibits enhanced circulation time, improved half-life as well as the ability to target certain tumours through the enhanced permeability and retention (EPR) effect. The EPR effect allows small particles (<100 nm) to pass through and accumulate in tissue with leaky vasculature (e.g. in tumours) (91). Encapsulation of doxorubicin within liposomes prevents accumulation of doxorubicin within tissues containing tight capillary junctions (e.g. the heart muscle) and instead allows for distribution in tissues containing fenestrations/gaps in the vasculature (e.g. liver and spleen) (90). Although liposomal drug delivery helps to increase circulation time, there is a risk of being detected as foreign by phagocytic cells of the mononuclear phagocyte system (MPS). Recognition by these cells is dependent on the size and charge of the liposomes. The PEG-lipid that is conjugated to the surface of the liposomes helps to prevent aggregation of the liposomes following administration, therefore preventing uptake by the MPS and subsequently increasing the circulation time of the liposomes (90).

Doxorubicin is encapsulated within the aqueous core of liposomes, and this can be achieved through both passive and active loading methods, as mentioned in Chapter 1. Active loading relies on creating a pH gradient between the aqueous core of the liposome and the external buffer. This can be achieved through both direct and indirect methods. The direct method involves manufacturing the liposomes in an acidic buffer and then adjusting or changing the external buffer through buffer exchange via dialysis or tangential flow filtration (TFF) (90). As the drug diffuses across the lipid membrane it

becomes protonated and complexes with the salts present in the core of the liposomes. One of the most successful methods of encapsulation is active loading along a sulfate gradient (e.g. ammonium sulfate) (92). As doxorubicin diffuses into the liposomes, it forms a complex with the sulfate ion, resulting in precipitation and self-aggregation to form fibre bundles that form a rod-like structure across the diameter of the liposomes.

Traditionally, production of Doxil® is a multi-step batch process consisting of at least 18 unit operations that can take up to 5 days to produce a batch (16). Microfluidics is, therefore a good alternative manufacturing process that allows for particle size control and high reproducibility (86). Therefore, doxorubicin was selected as the model compound as it is one of the most extensively studied liposomal drugs; however, other compounds that can be actively loaded across an ammonium sulfate gradient were also identified to determine whether these manufacturing parameters will affect all compounds that are loaded via the same route in the same way. These other compounds included daunorubicin, vincristine and ciprofloxacin.

Daunorubicin is the first discovered anthracycline that is used for the treatment of various cancers, including acute myeloid leukaemia and is the building block from which doxorubicin was derived (93). Daunorubicin acts as a topoisomerase II inhibitor, resulting in DNA double-stranded breaks and initiates apoptosis (88). There are two major dose-limiting toxicities with daunorubicin, and these are myelosuppression and cardiotoxicity (88). DaunoXome is a commercially available liposomal daunorubicin that consists of liposome composed of DSPC:Cholesterol at a 2:1 molar ratio (94). Encapsulation of daunorubicin within these liposomes protects the drug from enzymatic degradation and also reduces the conversion of daunorubicin into its metabolite daunorubicinol, which is inactive against cancer cells and can contribute to the cardiotoxicity (94).

Vincristine is a vinca alkaloid that is usually used in combination with other anti-cancer drugs for the treatment of a variety of cancers including leukaemia, lymphomas, and Kaposi's sarcoma. Vinca alkaloids work by disrupting microtubules, resulting in cell cycle arrest at the metaphase (M)-phase and, subsequently, apoptotic cell death (88). As with the majority of anti-cancer compounds, vincristine has dose-limiting side effects. Vincristine causes severe tissue necrosis, neurotoxicity and myelosuppression (88). Encapsulation of vincristine within liposomes improves the efficacy of this compound and has been shown to reduce accumulation of vincristine within healthy tissues reducing overall toxicity. It has also been shown to increase the antitumour potency through increased circulation time and exposure (95).

Ciprofloxacin, on the other hand, is a fluoroquinolone antibiotic used for the treatment of bacterial infections, such as respiratory and urinary tract infections (96). Encapsulation of ciprofloxacin can

provide a sustained, slow release of the antibiotic and can also deliver the drug to macrophages, which can improve the treatment of intracellular infections (97).

In the previous chapter, a DOE was carried out to determine the relationship and interactions between the microfluidic manufacturing and formulation parameters and how these affect the final liposome characteristics. The next step was to identify how changing these parameters will affect the encapsulation efficiency of the resultant formulations. In this chapter, the process parameters were selected from the DOE so as to produce a variety of liposomes of various sizes using different microfluidic manufacturing and formulation variables.

Aim and Objectives

The aim of the studies within this chapter was to determine how microfluidic production parameters can affect liposome characteristics and how these subsequently impact the active loading potential of the liposomes. It was also important to determine whether the same effects were observed when the actively loaded compound was changed or if these effects were compound dependent. To achieve this, the objectives were:

- manufacture liposomes of similar characteristics using different manufacturing parameters,
- manufacture liposomes of different characteristics,
- test a range of CQAs in these liposomal formulations before and after drug loading.

To do this, a series of compounds were tested for their loading into liposomes (Table 4.1).

Table 4.1: Compounds tested for drug loading via the pH gradient into liposomes. Acridine orange structure taken from Scientific Laboratory Supplies, daunorubicin, doxorubicin, vincristine and ciprofloxacin structure taken from Medchem Express.

Compound	Mwt	pKa	LogP	Structure	Application
Acridine Orange	301.81	9.65	4.65	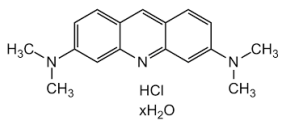	Model compound shown to load via the pH gradient (16)
Daunorubicin	527.52	7.85	1.83	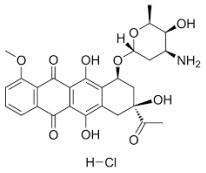	Precursor for doxorubicin and is commercially available as a liposomal

					delivery system (DaunoXome)
Doxorubicin	543.52	8.46	1.27	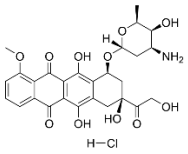	Most extensively studies liposomal drug delivery system and is commercially available (Doxil/Caelyx)
Vincristine	923.04	5	2.82	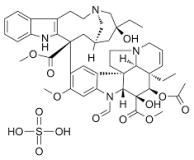	Shown to be loaded via pH gradient (16, 98). Commercially available (Marqibo)
Ciprofloxacin	363.82	6.16	0.28	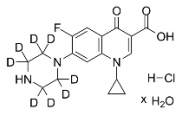	Shown to be loaded via an pH gradient (99).

4.2 Methods and Materials

4.2.1 Materials

1,2-dioctadecanoyl-sn-glycero-3-phosphocholine (DSPC), 1,2-dioleoyl-sn-glycero-3-phosphocholine (DOPC), hydrogenated soy L-α-phosphatidylcholine (HSPC, > 99%), 1,2-distearoyl-sn-glycero-3-phosphoethanolamine-N-[methoxy(polyethylene glycol)-2000] (sodium salt) (DSPE-PEG2000,>99%) and cholesterol (chol, >99%). Acridine orange hydrochloride hydrate and ammonium sulfate ($[NH_4]^2SO_4$,>99%) were obtained from Sigma-Aldrich Ltd. (Poole, UK). Doxorubicin hydrochloride, daunorubicin hydrochloride, vincristine sulfate and ciprofloxacin hydrochloride hydrate were obtained from Fisher Scientific (Loughborough, UK). Phosphate buffered saline tablets (10 mM, PBS pH 7.3) were acquired from Oxoid Ltd (Basingstoke, UK). All reagents (ethanol, methanol, isopropyl alcohol) were of analytical grade (HPLC grade,> 99.8%) and Transcutol was of general-purpose grade and purchased from commercially available suppliers.

4.2.2 Manufacturing of PEGylated Liposomes Encapsulating Ammonium Sulfate

PEGylated liposomes were prepared using the bench-scale microfluidic system (NanoAssemblr Benchtop) from Precision NanoSystems Inc. (Vancouver, Canada) which uses a staggered herringbone micromixer (SHM). Liposome formulations containing HSPC, DSPC or DOPC, cholesterol and DSPE-PEG2000 at a w/w ratio of 3:1:1, respectively, were produced from a 40 or 20 mg/mL total lipid stock solubilised in ethanol, methanol or Transcutol. Liposome formulations containing DSPC:Cholesterol contained varying cholesterol content (w/w 2:1, 3:1, 4:1 or 5:1) and were produced from a 10 mg/mL total lipid stock solubilised in ethanol. Lipids were heated for solubilisation but were stable once in solution. The lipids were allowed to reach room temperature before injection into the micromixer. Ammonium sulfate ($[NH_4]_2SO_4$, 250 mM) or phosphate buffered saline (PBS) was used as the aqueous phase unless otherwise stated. Liposomes were originally produced at a total flow rate (TFR) of 10 mL/min, and a flow rate ratio (FRR) of 3:1. TFR and FRR were altered to produce liposomes of specific sizes.

4.2.3 Buffer Exchange of PEGylated Liposomes using Tangential Flow Filtration

The PEGylated liposomal formulations encapsulating $[NH_4]_2SO_4$, 250mM, were produced, and the solvent was removed whilst simultaneously conducting buffer exchange to establish a pH gradient between the liposome interior and the exterior medium for active-loading of drugs. A tangential flow filtration system (KR2i TFF System, Repligen, Waltham, US) using a Repligen 500 kDa modified polyethersulfone (mPES) column and masterflex tubing 13 was used. The sample was filtered at a 20 mL/min flow rate and 12 diafiltration volumes with PBS (pH 7.3, 10 mM). Samples were diluted 1:5 with ammonium sulfate prior to filtration and recovered to the original volume. This resulted in PEGylated liposomes encapsulating acidic pH ($[NH_4]_2SO_4$, pH 5.5) and suspended in PBS (pH 7.3), creating a gradient for the diffusion of drugs with protonisable amine functions. These liposomes were then diluted with PBS prior to sizing and active-loading of compounds.

4.2.4 Active-Loading of Doxorubicin & Daunorubicin into PEGylated Liposomes

Liposomes produced using microfluidics were purified using tangential flow filtration. Doxorubicin stock was prepared at 10 mg/mL in deionised water. A specific volume was added to the liposomes at ratio of 0.125 g doxorubicin/daunorubicin: 1 g lipid. The effect of incubation temperature was evaluated. Liposomes were incubated in a water bath at either 60°C or 20°C for 40 minutes, and the percentage encapsulation was calculated. After loading, the liposomes were allowed to cool down to room temperature and non-encapsulated doxorubicin and daunorubicin was removed using tangential flow filtration. Quantification of doxorubicin/daunorubicin loading was measured using a microplate reader (Bio-rad Laboratories Inc. Hertfordshire, UK), measuring the UV absorbance at

490nm. Liposome samples were mixed with 50% isopropyl alcohol in order to disrupt the liposome membrane and allow quantification of the encapsulated drug. Calibration curves (0.025 – 0.6 mg/mL) were performed under the same conditions for each sample.

4.2.5 Active-Loading of Vincristine Sulfate into PEGylated Liposomes

Liposomes produced using microfluidics were purified using tangential flow filtration. Vincristine sulfate stock was prepared at 10 mg/mL in deionised water. A specific volume was added to the liposomes at a ratio of 0.071 g vincristine: 1 g lipid. Liposomes were incubated in a water bath at either 60°C or 20°C for 40 minutes, and the percentage encapsulation calculated. After loading, the liposomes were allowed to cool down to room temperature and non-encapsulated vincristine was removed using tangential flow filtration. Quantification of vincristine loading was measured using the PolarStar Omega measuring the UV absorbance at 295 nm. Liposome samples were mixed with 50% isopropyl alcohol in order to disrupt the liposome membrane and allow quantification of the encapsulated drug. Calibration curves (0.01 – 0.5 mg/mL) were prepared under the same conditions for each sample.

4.2.6 Active Loading of Ciprofloxacin Hydrochloride into PEGylated Liposomes

Liposomes produced using microfluidics were purified using tangential flow filtration. Ciprofloxacin hydrochloride stock was prepared at 10 mg/mL in deionised water. A specific volume was added to the liposomes at a ratio of 0.1 mg ciprofloxacin: 1 g lipid. Liposomes were incubated in a water bath at 60°C for 40 minutes, and subsequently, the percentage encapsulation was calculated. After loading, the liposomes were cooled down to room temperature and non-encapsulated ciprofloxacin was removed using tangential flow filtration. Quantification of ciprofloxacin loading was measured using a Polarstar Omega, measuring the UV fluorescence at an excitation-emission wavelength of 355-460 nm and a fluorimeter at an excitation-emission wavelength of 278-455 nm. Liposome samples were mixed with 50% isopropyl alcohol to disrupt the liposome membrane and allow quantification of the encapsulated drug. Calibration curves (0.01 – 0.1 mg/mL) were performed under the same conditions for each sample.

4.2.7 Statistical Analysis

One-way ANOVA followed by Tukey's multiple comparison test was used for the data analysis. All the experiments were carried out at least in triplicate unless otherwise stated and are shown as the mean of the measurements ± standard deviation, which is plotted as error bars.

4.3 Results

4.3.1 Effect of Microfluidic Production on Liposomes for Active Loading

Key in the development of a new manufacturing process for liposomes to be loaded via the pH gradient was to consider how the manufacturing of liposomes can affect the remote loading of a variety of different compounds. Using the DoE model developed within Chapter 3, the manufacturing parameters were selected to have a variety of different-sized liposomes and to manufacture liposomes of the same size using different parameters (such as TFR, FRR and Solvent).

4.3.1.1 Active Loading of Daunorubicin

DSPC:Cholesterol:DSPE-PEG2000 (w/w 3:1:1) liposomes were produced from either methanol, ethanol or Transcutol according to Table 4.1 and loaded with daunorubicin at a drug:lipid ratio of 0.125 g daunorubicin: 1 g lipid for 40 minutes at 60°C. The liposomes produced using methanol and ethanol stocks were manufactured to be of similar size, whereas those produced from Transcutol were selected to be of the largest size possible. The objective of this experiment was to identify whether the manufacturing process can impact the resultant encapsulation of the liposomes (methanol vs ethanol) and if the size of the liposomes is an important factor for encapsulation (ethanol vs Transcutol). Thus, for these studies, size, PDI and drug loading were taken as the CQA to be measured.

Table 4.2: Process parameters for the production of DSPC:Cholesterol:DSPE-PEG2000 (w/w 3:1:1) liposomes of specified size.

Solvent	FRR	TFR (mL/min)	Production Temperature (°C)	Final Lipid (mg/ML)
Methanol	10:1	12.5	60	1.82
Ethanol	3:1	10	20	16
Transcutol	1:1	5	60	16

The results (Figure 4.1) show that the liposomes produced from methanol and ethanol were of similar size and that those produced from Transcutol were significantly ($p<0.05$) larger (approx. 60 nm vs 100 nm; Figure 4.1A). The vesicle sizes were shown to significantly increase ($p<0.05$) post-loading with daunorubicin for both methanol and ethanol formulations (56 nm vs 62 nm and 60 nm vs 74 nm, respectively; Figure 4.1A) with no significant change in particle size for the Transcutol liposomes. The PDI was shown to increase slightly for the methanol and ethanol formulations (0.13 vs 0.19 and 0.18 vs 0.23, respectively; Figure 4.1A). However, all formulations showed a PDI below 0.25 (Figure 4.1A). Size was shown to impact the loading of daunorubicin, with larger liposomes (Transcutol) having higher encapsulation (approximately 90%) than those produced from methanol and ethanol, which showed approximately 50% encapsulation (Figure 4.1B).

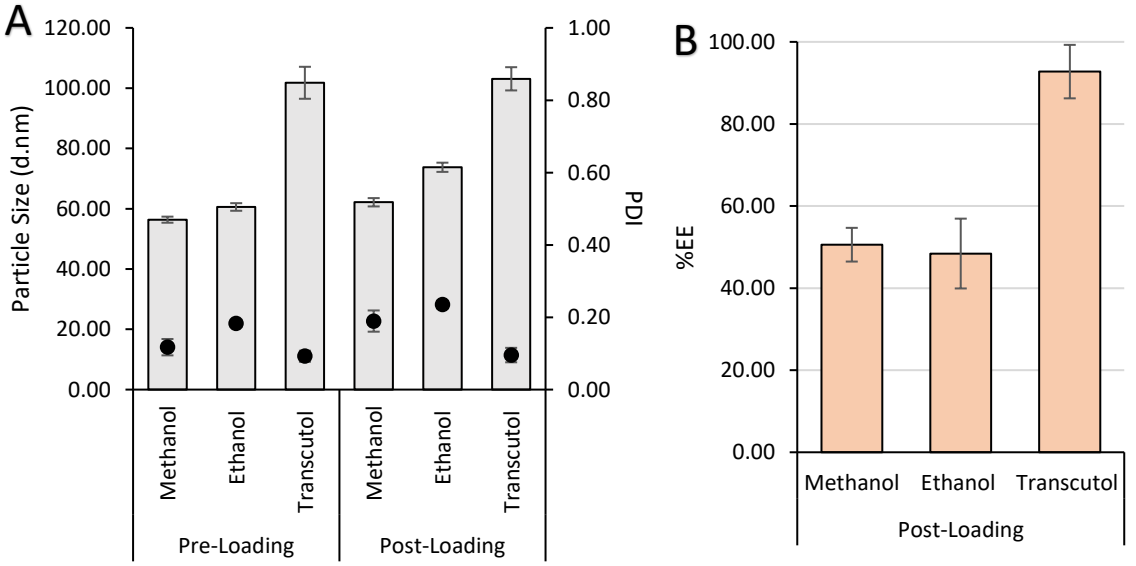

Figure 4.1: Effect of microfluidic production and resultant particle size on loading efficiency of daunorubicin A) particle size (d.nm; represented by the bars) and PDI (represented by the discrete points) of each formulation pre- and post-loading with daunorubicin, and B) daunorubicin loading of the liposomes remote loaded with daunorubicin and incubated for 40 min, at 60°C. Results represent mean ± SD, n=3 independent batches.

To confirm that the solvent was not impacting the resultant characteristics and loading% of the liposomes, DSPC:Cholesterol:DSPE-PEG2000 (w/w 3:1:1) liposomes were produced at the same parameters from each solvent (i.e. 20 mg/mL initial lipid concentration, TFR 12.5 mL/min, FRR 10:1, temperature 60°C) and loaded with the same concentration of daunorubicin as mentioned above. The results show that the liposome size and PDI is the same across all the solvents tested (60 – 65 nm with PDI approx. 0.2; Figure 4.2A) with no effect on the encapsulation efficiency (45-55%; Figure 4.2B) of the liposomes demonstrating that the solvent has no significant effect on the resultant liposome properties measured.

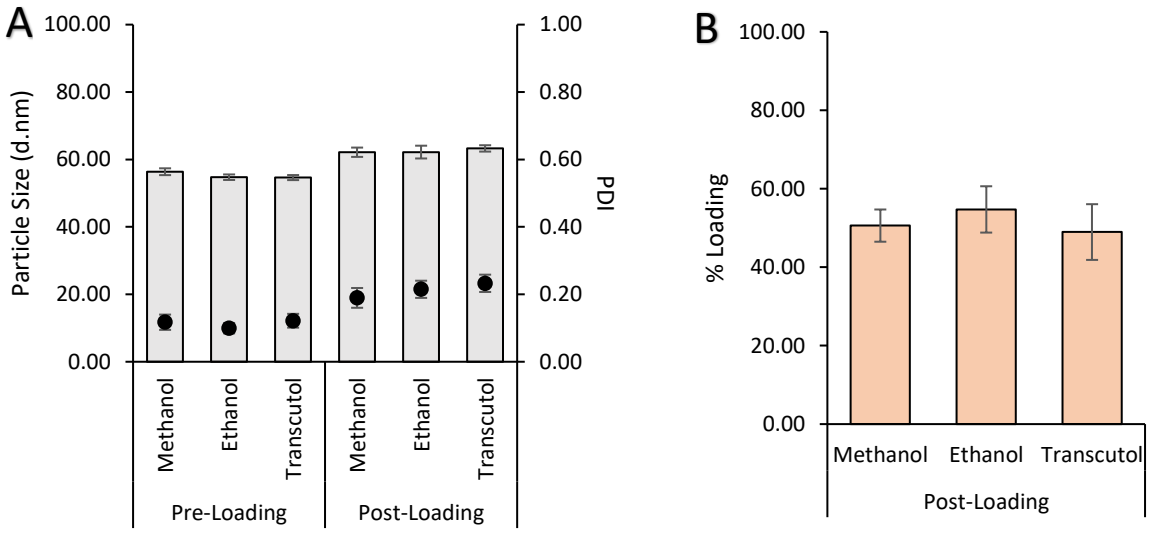

Figure 4.2: Effect of solvent selection on loading efficiency of daunorubicin A) particle size (d.nm; represented by the bars) and PDI (represented by the discrete points) of each formulation pre- and post-loading with daunorubicin, and B) daunorubicin loading of the liposomes remote loaded with daunorubicin and incubated for 40 min, at 60°C. Results represent mean ± SD, n=3 independent batches.

4.3.1.2 Active Loading of Doxorubicin

DSPC:Cholesterol:DSPE-PEG2000 (w/w 3:1:1) liposomes were again produced using the same parameters as detailed in Table 4.3 and loaded with doxorubicin at a ratio of 0.125 g doxorubicin: 1 g lipid for 40 minutes at 60°C. The results show a significant increase ($p<0.05$) in size for both the methanol (Sample 1) and ethanol (Sample 2) formulations post-loading (54 nm vs 84 nm, and 62 nm vs 112 nm, respectively, Table 4.3) with no change in particle size observed for the Transcutol (Sample 3) formulation (Table 4.3). The PDI was also shown to significantly increase ($p<0.05$) for methanol (0.11 vs 0.23, Sample 1) and ethanol (0.19 vs 0.36, Sample 2) post-loading with doxorubicin whereas again, no change was observed for Transcutol (Sample 3, Table 4.3). In terms of doxorubicin loading, the methanol (Sample 1) and Transcutol (Sample 3) formulations showed a similar trend to that observed when daunorubicin was loaded with the smaller methanol liposomes, resulting in reduced loading compared with the larger Transcutol formulation (55% vs 86%., Table 4.3). However, the ethanol (Sample 2) formulation showed higher loading (80%, Table 4.3).

Again, it was important to confirm that solvent does not affect the resultant liposome characteristics and encapsulation of doxorubicin. Therefore, liposomes were all produced using the same method (Initial lipid concentration 20 mg/mL, FRR 10:1 and TFR 12.5 mL/min) and loaded with doxorubicin for 40 minutes at 60°C. The results from this show that solvent has no overall effect on the size of the liposomes or the encapsulation efficiency (Samples 1, 4 & 5, Table 4.3).

Table 4.3: Parameters and CQAs for liposomes loaded with doxorubicin.

Sample	Solvent	TFR (mL/min)	FRR	Final Lipid Concentration (mg/mL)	Particle Size Pre-Loading & Post-Loading (d.nm)	PDI Pre-Loading & Post-Loading (d.nm)	%Loading
1	**Methanol**	12.5	10:1	1.82	54 ± 1.2 84 ± 14	0.11 ± 0.01 0.23 ± 0.05	54 ± 2
2	**Ethanol**	10	3:1	16	62 ± 1.1 112 ± 3.2	0.19 ± 0.01 0.36 ± 0.06	82 ± 2
3	**Transcutol**	5	1:1	16	102 ± 2.8 103 ± 1.6	0.11 ± 0.02 0.10 ± 0.01	86 ± 2
4	**Ethanol**	12.5	10:1	1.82	54 ± 0.9 97 ± 11.0	0.12 ± 0.01 0.33 ± 0.04	53 ± 4
5	**Transcutol**	12.5	10:1	1.82	55 ± 1.6 88 ± 5.0	0.22 ± 0.02 0.43 ± 0.04	52 ± 12

To determine what caused this increase in size and PDI, liposomes were produced from ethanol stocks and either diluted to a final concentration of 1.82 mg/mL or produced at a final concentration of 1.82 mg/mL (Table 4.4) to determine whether it was the manufacturing or the lipid concentration that caused this increase in size and PDI.

Table 4.4: Manufacturing parameters used to prepare the various liposome formulations. The effect of manufacturing parameters was investigated (Control vs Control FRR 10:1) and the effect of final lipid concentration (Control vs Diluted) was tested. The effect of particle size was also investigated when comparing all formulations to the Large formulation.

Formulation	FRR	TFR (mL/min)	Initial Lipid (mg/mL)	Final Lipid (mg/mL)
Control	3:1	10	40	16
Control FRR 10:1	10:1	10	40	16
Diluted	3:1	10	40	1.82
Low Conc	10:1	12.5	20	1.82
Large	1.5:1	10	20	16

The results show that post-loading, the size and PDI of the liposomes increased independent of the lipid concentration and manufacturing parameters tested (Figure 4.3A). However, the loading decreased in the sample produced at the low lipid concentration (Figure 4.3B). Liposomes were then manufactured to be as large as possible from ethanol stocks and again loaded with doxorubicin to determine if increasing the size would prevent an increase in PDI post-loading. The results show that it was possible to produce liposomes using ethanol at a size of approximately 100 nm and that post-

loading with doxorubicin, this size and PDI did not change (Figure 4.3A), and the loading efficiency remained high (Figure 4.3B). These results, taken together, suggest that the initial size of the liposomes is an important factor in determining the loading capacity as well as the final characteristics of the loaded liposomes with larger liposomes capable of loading with higher efficiency and minimal impact on liposome physicochemical characteristics.

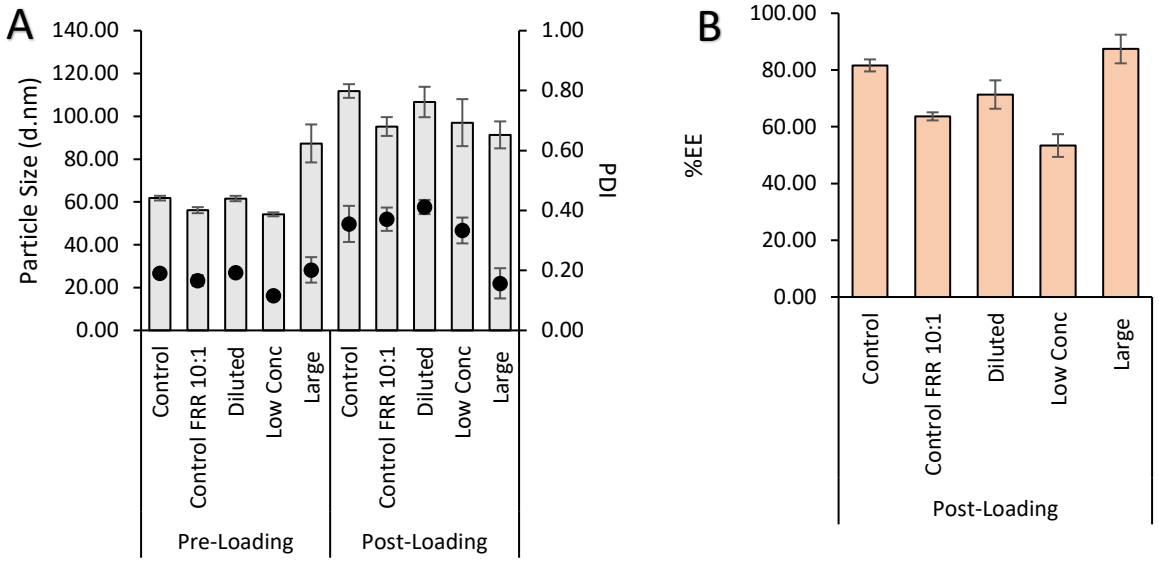

Figure 4.3 Effect of microfluidic production and lipid concentration on loading efficiency of doxorubicin. The effect of manufacturing parameters was investigated (Control vs Control FRR 10:1) and the effect of final lipid concentration (Control vs Diluted) was tested. The effect of particle size was also investigated when comparing all formulations to the Large formulation. A) particle size (d.nm; represented by the bars) and PDI (represented by the discrete points) of each formulation pre- and post-loading with doxorubicin, and B) doxorubicin loading of the liposomes remote loaded with doxorubicin and incubated for 40 min, at 60°C. Results represent mean ± SD, n=3 independent batches.

Due to the differences in encapsulation efficiency, it was thought that maybe the purification methods were causing the loss of encapsulated doxorubicin. Three different purification methods were therefore tested to determine whether the TFF was causing the loss of doxorubicin. Liposomes were produced using the same parameters as the low-concentration and large ethanol samples (Table 4.4). The pH gradient was first established using the TFF system, and the unencapsulated drug was removed by either TFF (Figure 4.4A), centrifugation using spin columns (Figure 4.4B), or via dialysis (Figure 4.4C). The results for the low-concentration sample show that the purification method had no significant effect ($p>0.05$) on the encapsulation efficiency of the liposomes; however, the sample that was purified using the TFF showed a significantly ($p<0.05$) larger particle size than those purified via dialysis or spin column. However, the larger ethanol sample purified using TFF showed no significant ($p>0.05$) difference in particle size with a significant ($p<0.05$) increase in particle size observed for both spin and dialysis. There was significantly ($p<0.05$) lower encapsulation in the sample that was purified via spin column compared with the other two purification methods.

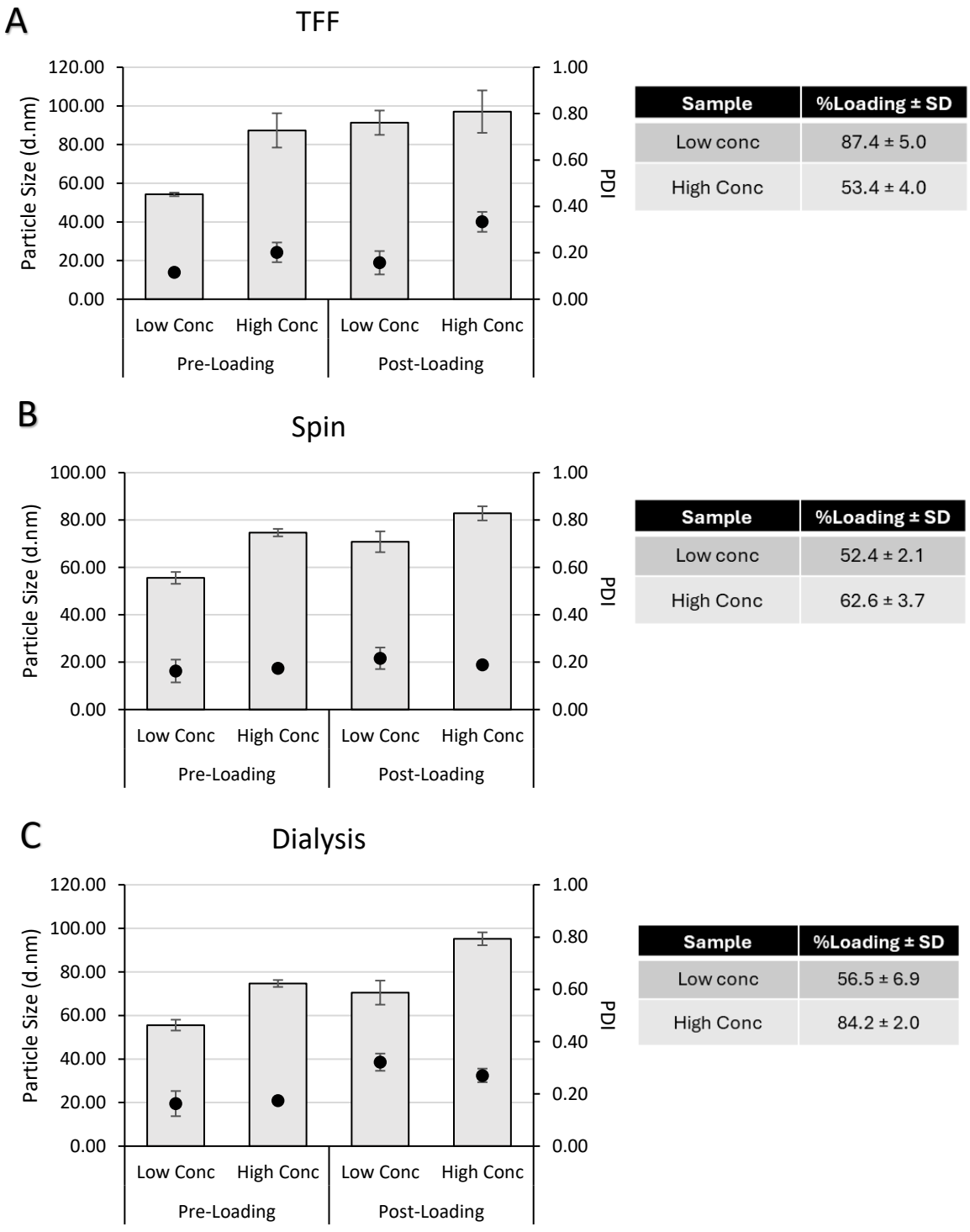

Figure 4.4: Effect of purification method on liposome characteristics and loading efficiency of doxorubicin A) particle size (d.nm; represented by the bars) and PDI (represented by the discrete points) of each low and high concentration formulation pre- and post-loading with doxorubicin and purified using TFF and the corresponding loading of doxorubicin, B) particle size (d.nm; represented by the bars) and PDI (represented by the discrete points) of each low and high concentration formulation pre- and post-loading with doxorubicin and purified using Spin columns and the corresponding loading of doxorubicin, and C) particle size (d.nm; represented by the bars) and PDI (represented by the discrete points) of each low and high concentration formulation pre- and post-loading with doxorubicin and purified using Dialysis and the corresponding loading of doxorubicin. Results represent mean ± SD, n=3 independent batches.

In order to fully determine that liposome size was affecting remote loading of doxorubicin, it was important to determine whether there were any issues with the purification method using the TFF. Liposomes were produced using the same parameters as the low-concentration sample, as this gave the lowest encapsulation efficiency. These liposomes were tagged with DilC to quantify the amount of lipid present in the sample after TFF purification. DilC is a fluorescent dye that is incorporated into the lipid bilayer, where it acts as an indicator of lipid recovery. The results show that the TFF was not affecting the lipid content of the liposomes therefore ruling out lipid loss as a possible factor for the differences in encapsulation (Figure 4.5).

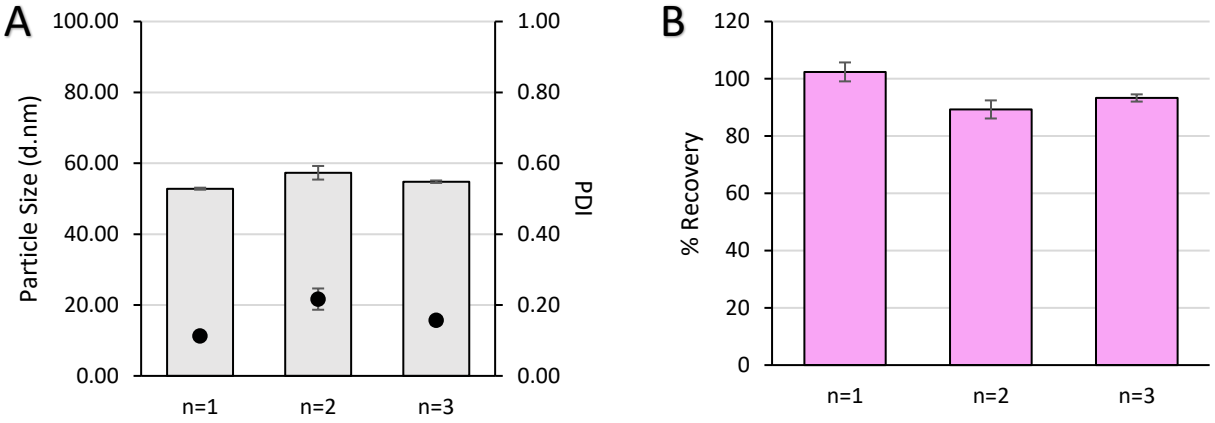

Figure 4.5: Lipid recovery of liposomes tagged with DilC after TFF purification. A) particle size (d.nm; represented by the bars) and PDI (represented by the discrete points) of liposomes after TFF purification. B) Liposome recovery after TFF purification.

4.3.1.3 Active Loading of Vincristine

DSPC:Cholesterol:DSPE-PEG2000 (w/w 3:1:1) liposomes were again produced using the same parameters as Table 4.2, including the large ethanol formulation shown in Figure 4.3. These liposomes were then loaded with vincristine at a ratio of 0.071 g vincristine: 1 g lipid for 40 minutes at 60°C. There was no significant difference ($p>0.05$) in particle size or PDI post-loading (Figure 4.6A), and the results showed an increase in encapsulation with increasing particle size (Figure 4.6B). These results show a similar trend to that observed with daunorubicin, where increasing the size of the liposomes results in increased encapsulation.

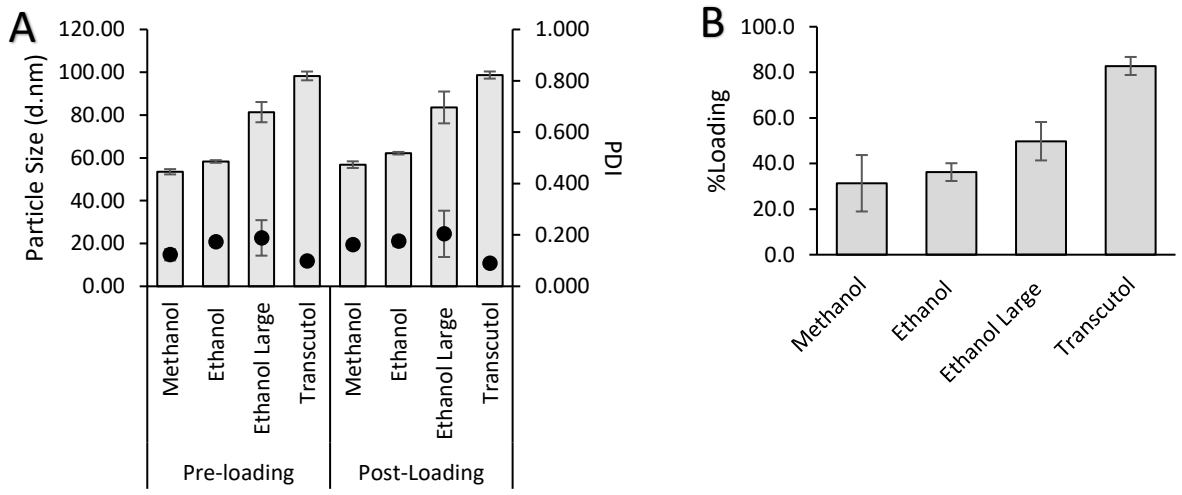

Figure 4.6: Effect of microfluidic production and lipid concentration on loading efficiency of vincristine A) particle size (d.nm; represented by the bars) and PDI (represented by the discrete points) of each formulation pre- and post-loading with vincristine, and B) vincristine loading of the liposomes remote loaded with vincristine and incubated for 40 min, at 60°C. Results represent mean ± SD, n=3 independent batches.

4.3.1.4 Active Loading of Ciprofloxacin Hydrochloride

DSPC:Cholesterol:DSPE-PEG2000 (w/w 3:1:1) liposomes were again produced using the same parameters as Table 4.2, including the large ethanol formulation shown in Figure 4.3. These liposomes were then loaded with ciprofloxacin at a ratio of 0.1 mg ciprofloxacin: 1 mg lipid for 40 minutes at 60°C. The results again show a similar trend, with the smallest liposomes (methanol) showing significantly ($p>0.05$) lower encapsulation (approximately 20%) compared with the largest liposomes (Transcutol), which showed approximately 70% encapsulation (figure 4.7B). The encapsulation in Figure 4.7B was measured using the Polarstar Omega at an excitation-emission wavelength of 355-480nm.

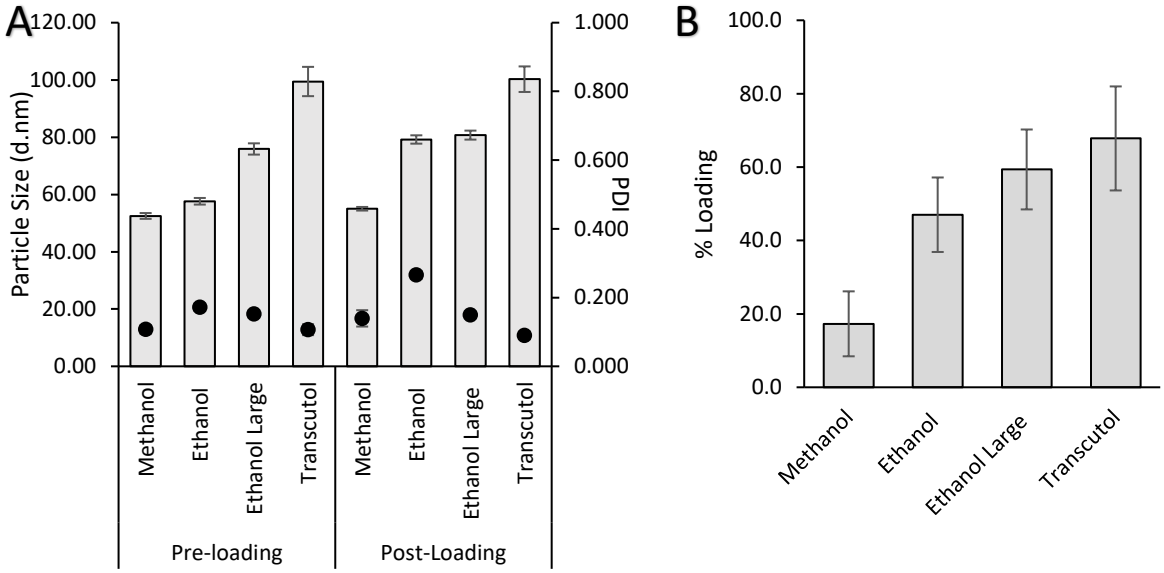

Figure 4.7: Effect of microfluidic production and lipid concentration on loading efficiency of ciprofloxacin A) particle size (d.nm; represented by the bars) and PDI (represented by the discrete points) of each formulation pre- and post-loading with doxorubicin, and B) ciprofloxacin loading of the liposomes remote loaded with ciprofloxacin and incubated for 40 min, at 60°C. Results represent mean ± SD, n=3 independent batches for methanol and ethanol and n=2 for ethanol large and Transcutol.

The excitation-emission wavelength for ciprofloxacin is 278-455 nm, and therefore, the samples were also measured using a fluorimeter at the exact excitation-emission wavelengths. The results show contradicting results to those observed when measured on the Polarstar. Here, the results show that the smallest liposomes had the highest encapsulation of ciprofloxacin, whereas the other formulations showed slightly lower encapsulation (Figure 4.8). This may be due to the difference in lipid

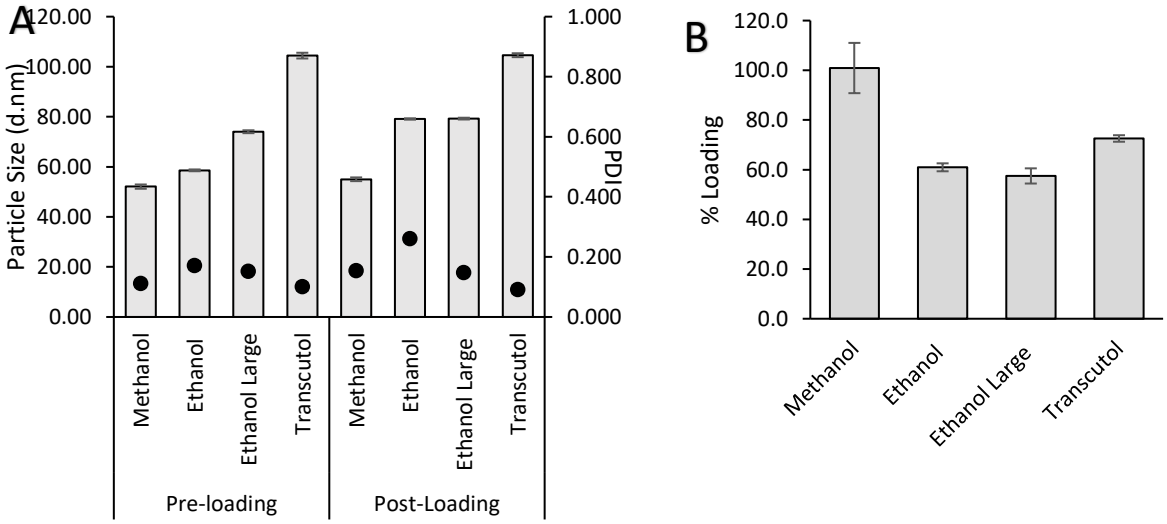

Figure 4.8: Effect of microfluidic production and lipid concentration on loading efficiency of ciprofloxacin A) particle size (d.nm; represented by the bars) and PDI (represented by the discrete points) of each formulation pre- and post-loading with ciprofloxacin, and B) ciprofloxacin loading of the liposomes remote loaded with ciprofloxacin and incubated for 40 min, at 60°C. Results represent mean ± SD, n=2 independent batches for methanol and n=1 for ethanol, ethanol large and transcutol.

concentration between the methanol sample and the ethanol, ethanol large and Transcutol samples, which were all loaded and measured at the same lipid concentration, whereas the lipid concentration of the methanol sample was much lower. Future experiments would need to be carried out to optimise the quantification of this compound.

4.4 Discussion

The aim of this chapter was to determine how microfluidic production parameters as well as liposome formulation parameters, can affect resultant liposome properties and encapsulation efficiencies of small molecule compounds. It is well established how microfluidic parameters, specifically FRR and TFR, affect the physicochemical properties of lipid-based nanocarriers (16, 78, 100), however it is also important to determine how the formulation parameters may also affect resultant liposome properties.

Four compounds were selected for active loading into these different liposomal formulations: daunorubicin, doxorubicin, vincristine, and ciprofloxacin. These compounds were selected as they are capable of active loading using an ammonium sulfate gradient (16, 98, 101). Daunorubicin and doxorubicin were selected as doxorubicin is one of the most extensively studied compounds used in liposomal formulations (i.e. Doxil/Caelyx), and daunorubicin is the precursor to doxorubicin. The main difference between these compounds is their chemical structure, with doxorubicin being the hydroxylated form of daunorubicin and has a different side chain to that of daunorubicin (table 4.1) (102).

Initial experiments were carried out using daunorubicin and involved comparing liposomes of the same particle size and PDI but produced using different methods and comparing liposomes that were produced to be of significantly larger size (Figure 4.1). The results in Figure 4.1 demonstrated that the particle size is a determinant of the encapsulation of daunorubicin. The liposomes showed no notable change in CQAs post-loading. However, the larger liposomes (100 nm) showed significantly higher encapsulation compared with the smaller liposomes (60 nm). When these experiments were repeated with doxorubicin (Table 4.3), the smaller liposomes produced from methanol and ethanol showed an increase in both size and PDI post-loading. However, the larger liposome produced from Transcutol showed no change in CQAs post-loading and showed the highest encapsulation efficiency. These results both demonstrate how particle size is a determining factor for efficient encapsulation of both doxorubicin and daunorubicin but also demonstrate that even when similar compounds are encapsulated within liposomes, they can have different effects on the resultant liposome properties.

When analysing the relationship between particle size and encapsulation, it was important to determine whether the initial particle size was affecting the loading or if the loading was affecting the

particle size. When comparing all the compounds together there was no trend observed in terms of how the initial particle size (Figure 4.9A) or the final particle size affects encapsulation (Figure 4.9B). However, when the compounds were separated there was a strong correlation between both particle size and encapsulation pre- and post-loading for both daunorubicin (R^2 = 0.9594 & R^2 = 0.8829 respectively, Figure 4.9D) and vincristine (R^2 = 0.9223 & R^2 = 0.9148 respectively, Figure 4.9E), but no correlation observed for doxorubicin (R^2 = 0.6881 & R^2 = 0.348 respectively, Figure 4.9C). These results further highlight the importance of particle size for high encapsulation. The linear relationship observed with daunorubicin and vincristine, but not doxorubicin, could be attributed to the way in which these compounds are encapsulated within the aqueous core. The large rod-like crystals found in doxorubicin could cause increases in particle size that are not correlated with increased encapsulation. Whereas daunorubicin and vincristine have no such structures observed within the vesicles and hence would not impact on vesicle size (103).

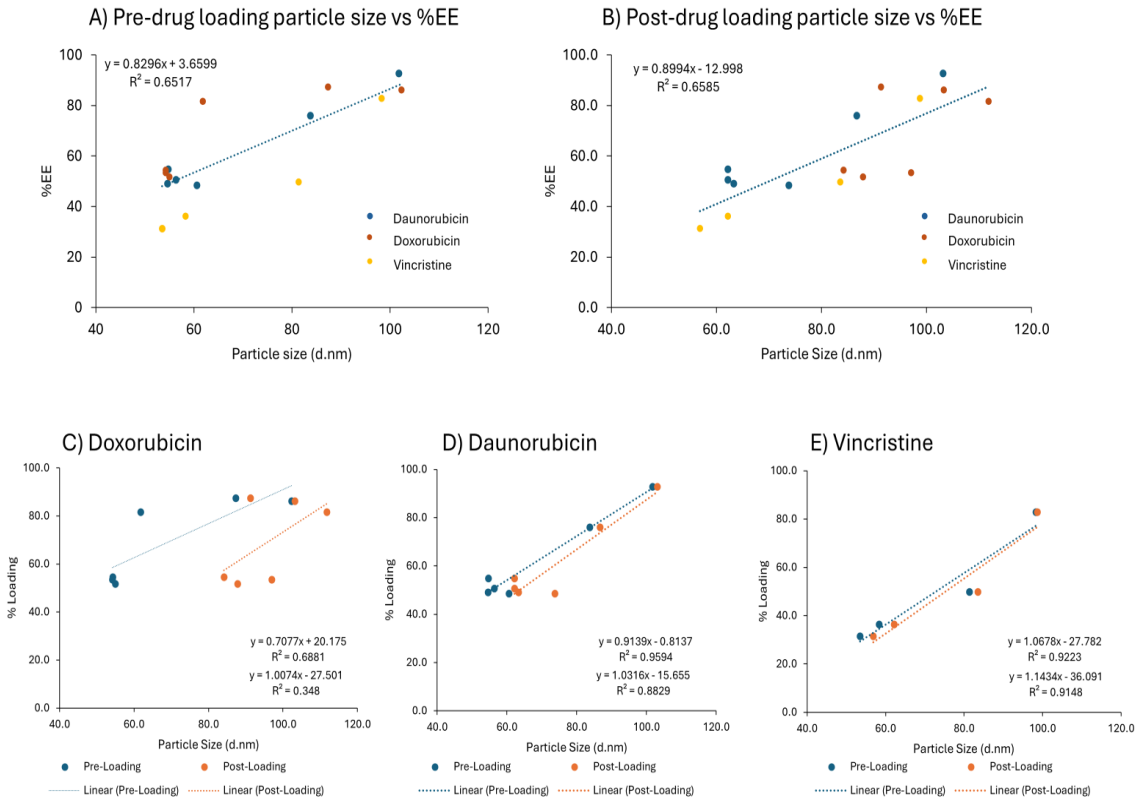

	Drug	Equation	R^2
Pre-drug loading particle size vs %EE	All	y = 0.8296x + 3.6599	R^2 = 0.6517
Post-drug loading particle size vs %EE	All	y = 0.8994x - 12.998	R^2 = 0.6585
Pre-drug loading particle size vs %EE	Doxorubicin	y = 0.7077x + 20.175	R^2 = 0.6881
Post-drug loading particle size vs %EE	Doxorubicin	y = 1.0074x - 27.501	R^2 = 0.348
Pre-drug loading particle size vs %EE	Daunorubicin	y = 0.9139x - 0.8137	R^2 = 0.9594
Post-drug loading particle size vs %EE	Daunorubicin	y = 1.0316x - 15.655	R^2 = 0.8829
Pre-drug loading particle size vs %EE	Vincristine	y = 1.0678x - 27.782	R^2 = 0.9223
Post-drug loading particle size vs %EE	Vincristine	y = 1.1434x - 36.091	R^2 = 0.9148

Figure 4.9: Linear regression analysis of the relationship between particle size and encapsulation of small molecule compounds. A)Scatter plot of particle size pre-loading vs encapsulation of daunorubicin (blue), doxorubicin (orange) and vincristine (yellow), B) Scatter plot of particle size post-loading vs encapsulation of daunorubicin (blue), doxorubicin (orange) and vincristine (yellow), C) Scatter plot of particle size vs encapsulation of doxorubicin, pre-loading (blue) and post-loading (orange), D) Scatter plot of particle size vs encapsulation of daunorubicin, pre-loading (blue) and post-loading (orange), E) Scatter plot of particle size vs encapsulation of vincristine, pre-loading (blue) and post-loading (orange)

As there were multiple variables altered between these formulations (e.g. FRR, TFR, initial lipid concentration and solvent used in the organic phase), it was important to be able to determine what the main contributing factor affecting encapsulation efficiency as well as the resultant CQAs of the liposomes. Liposomes were therefore produced using the same methods, just altering the solvent used and were subsequently loaded with either daunorubicin (Figure 4.2) or doxorubicin (Table 4.3,

Samples 1, 4&5). The results from these showed no differences in the encapsulation of either daunorubicin or doxorubicin demonstrating that solvent had no effect on the encapsulation of these compounds. However, all the liposomes encapsulating doxorubicin showed an increase in both size and PDI post-loading.

The increase in size and PDI observed when doxorubicin (Table 4.3) was loaded but not daunorubicin (Figure 4.2) may be attributed to the way in which these molecules complex within the aqueous core. Doxorubicin has been shown to form rod-like structures across the diameter of the liposome (104) whereas no such structures have been reported for daunorubicin (105). Lasic et al. were the first to report the physical state of doxorubicin within an ammonium sulfate core, and they observed doxorubicin forming an electron opaque band within the liposomes. From this, it was concluded that doxorubicin complexes with the sulfate ions to form one-dimensional rods which do not interact with the lipid bilayer (106, 107). Depending on the ion gradient used for remote loading, doxorubicin can crystallise in different shapes. When loaded along a citrate gradient, the resultant doxorubicin crystals form fibrous bundles, whereas when loaded along a sulfate gradient, doxorubicin has been reported to form curved or cylindrical bundles (108). Yamamoto et al. reported doxorubicin formed folded, undulating, fibrous crystals that varied in thickness and were distorted in shape (108). This formation of crystals causes the liposome morphology to change from a spherical shape to what is described as a coffee-bean shape (Figure 4.10) (109).

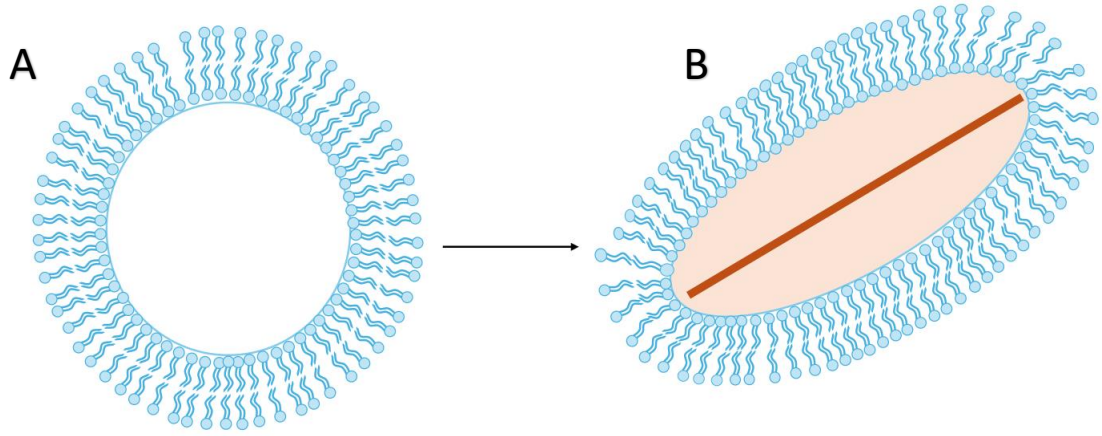

Figure 4.10: Diagram showing the change in morphology of liposomes post-loading with doxorubicin. A) Shows an empty spherical liposomes consisting of a lipid bilayer surrounding an aqueous core and B) shows a liposome post-loading with doxorubicin. Once encapsulated within the internal acidic, aqueous core the doxorubicin complexes with the sulfate ions to form rod-like crystal across the diameter of the liposome, giving the liposome a coffee bean like appearance and distorting the shape from circular to more oval.

Ruiz et al. have also reported that the internal aqueous phase used, as well as the drug:lipid ratio, can affect the crystallisation as well as the in vitro and in vivo properties in temperature-sensitive liposomal formulations (103). In this work, temperature-sensitive liposomes were actively loaded with doxorubicin using either an ammonium sulfate, ammonium-EDTA or a manganese sulfate pH gradient,

and the drug-to-lipid ratio was varied from 1:2 to 1:20. The doxorubicin that was loaded along either the ammonium sulfate or ammonium-EDTA gradients and loaded at a ratio of 1:2, appeared as either rod-shaped or as thin-ring bundles. Cryo-TEM images also showed that at increased drug:lipid ratio, there was a higher proportion of empty vesicles, and at lower ratio (1:20), the morphology of the liposomes showed two separate populations of vesicles, either spherical or elongated (similar to Figure 4.10) with the crystals appearing thicker (than at 1:2). Whereas the liposomes that were loaded with doxorubicin along the manganese sulfate gradient all appeared empty which was attributed to the lower encapsulation efficiency of this method (103).

Particle size is an important factor for the cellular uptake, biodistribution and delivery of liposomes to the intended target. It is also an important measure of quality from a regulatory perspective (110). Therefore, it is important to be able to manufacture liposomes of appropriate size to demonstrate controlled manufacturing processes and to deliver the active compound to the target tissue without being detected and cleared by the immune system. However, these liposomes must be able to encapsulate a high enough concentration of drug so as to be therapeutically advantageous. To address this, more extensive studies were carried out to determine the important factors in determining doxorubicin encapsulation. The impact of production parameters, including the effect of the concentration method and final lipid concentration, was investigated (Figure 4.3). The main finding from these experiments was that all liposomes of 60 nm showed a significant ($p<0.05$) increase in size post-loading, whereas the larger liposomes of 90 nm showed no notable changes post-loading. Fonseca et al. produced liposomes composed of DPPC:DPPG:Chol (10:1:4) with a mean particle size of 70, 100 or 200 nm and showed that all liposomes showed an increase in particle size post-loading with doxorubicin, with the smallest liposomes showing the most dramatic increase in size (111). This change in particle size may be attributed to the lower aqueous volume present in smaller liposomal formulations. It was thought that the unencapsulated doxorubicin caused aggregation of the liposomes, which was most notable for small liposomes with liposomes larger than 100 nm showing only slight changes in particle size. The lower aqueous volume present in smaller liposomes will also limit the amount of space for the formation of these doxorubicin crystals. As all formulations encapsulated the same concentration of ammonium sulfate, they should be capable of encapsulating the same concentration of doxorubicin, with the main limiting factor being the aqueous volume. This would, therefore, contribute to the distortion of the liposome's shape as the rod-like crystals form across the diameter of the liposomes, with larger aqueous volumes capable of accommodating the crystal formation better than smaller aqueous volumes. However, the smaller aqueous volume may also result in lower ionic strength and, therefore, may result in the pH gradient depleting faster than with larger formulations with a larger aqueous core. Wei et al. demonstrated that the formation of

the nanocrystals is dependent on the concentration of ammonium sulfate present in the core. At ammonium sulfate concentrations of 100 mM, there were no obvious crystals identified. However, some liposomes did contain low electron density nanocrystals, suggesting that these crystals had not fully developed (112). Therefore, this demonstrates that the formation of these nanocrystals is concentration-dependent and, therefore, dependent on the ionic strength of the aqueous buffer. In terms of protein and enzymes encapsulation higher encapsulation was observed at lower ionic strength (113, 114). It was thought that this was due to a decrease in the electrostatic interaction between the negatively charged protein and the positively charged liposomes, but also dependent on the amount of protein added.

When vincristine was selected for active loading, the results showed a size dependent encapsulation, with increasing encapsulation with increased particle size (Figure 4.6). Vincristine has been shown to form amorphous, rather than crystalline forms, within the aqueous core in response to loading via a magnesium sulfate gradient (107, 115). This may explain why there was no notable change in particle size post-loading compared to doxorubicin.

4.5 Conclusion

Here, the impact of microfluidic and formulation parameters on the encapsulation of small molecule drugs was evaluated. The results from these studies showed that particle size is critical for the encapsulation of all the compounds tested and that different compounds may be encapsulated within the aqueous core in different crystalline forms. These results highlight the complex interplay between microfluidic and formulation parameters, as well as compound properties, in determining the encapsulation efficiencies and liposomal characteristics. Based on these results, the optimal CQAs for the active loading into liposomes would be to produce liposomes with a particle size between 80 – 100 nm to allow for high encapsulation efficiency with no impact on the characteristics of the liposomes. This particle size will also prevent detection by the immune system, thereby increasing the circulation time and therapeutic potential of these drug delivery systems.

Chapter 5 - The Impact of solvent selection in the microfluidic production of liposomes: Pre-Clinical Biodistribution of Liposomal Doxorubicin

5.1 Introduction

In the previous chapters, the impact of altering both process and formulation parameters on the resultant liposomal physicochemical characteristics has been investigated. Within this chapter, the aim was to determine whether the choice of solvent used within the manufacturing of liposomes affects the resultant release properties both *in vitro* and *in vivo*.

When designing liposomal drug delivery systems, it is important to understand how they will react with biological membranes from their site of administration to the target organ. The biodistribution of liposomes is determined by their interactions with biological fluids and different organs. Following administration into the circulation system, liposomes can interact with plasma proteins and blood cells (116).

In contrast to free drug molecules, liposomal formulations show limited accumulation in healthy tissues and are biased towards sites of inflammation and tumours. This is due to the enhanced permeation and retention (EPR) effect. The accumulation of liposomes in healthy tissue is restricted due to the presence of tight junctions in the endothelial walls. Tumours, on the other hand, have large endothelial fenestrations and porous blood capillaries that facilitate the uptake of liposomes from the circulation into the tissues (116). There are 3 key variables that affect the biological activity and toxicity of liposomal formulations: (i) lipid composition, (ii) the drug properties, and (iii) the interaction between the drug and the lipid vesicle (20). The distribution of the liposomes from the blood into the tissues is determined by the physicochemical properties of the liposomes, including particle size, surface charge and lipid composition. In turn, once administered, there are 3 main clearance pathways that will also affect the pharmacokinetics and biodistribution: (i) uptake by cells of the mononuclear phagocytic system (MPS) in the liver, spleen and bone marrow resulting in metabolism and excretion, (ii) leakage of the drug from the liposomes in the circulation; and (iii) accumulation of liposomal drug formulations in tissues such as solid tumours via the EPR effect (20).

It has been well documented that particle size is a key determinant for cell uptake and circulation time; however, the particle size also determines the endocytic pathway by which the drug delivery vector is internalised (117). Liposomes of size < 100 nm showed reduced detection and internalisation by the MPS system, thereby prolonging their time in circulation, whereas liposomes > 100 nm showed increased uptake and clearance by the immune system (117). The addition of PEGylated lipids to the liposome has also been shown to increase circulation time as these lipids prevent opsonisation and detection by the immune system (20). PEGylation has also been shown to change the mechanism of endocytosis, with PEGylated liposomes showing preferential uptake via non-clathrin-mediated mechanism (117).

Aim and Objectives

This chapter aimed to investigate the effect of liposome production on the *in vitro* and *in vivo* release of doxorubicin. To achieve this, the objectives were:

- Manufacture liposomes of similar physicochemical characteristics using conventional thin film hydration method and microfluidics.
- Determine whether the manufacturing method affects *in vitro* release.
- Determine whether the manufacturing method affects *in vivo* release and biodistribution.

The liposomes produced all contained the same lipid composition and final concentrations of both lipid and drug. Only the manufacturing method or the solvent varied.

5.2 Methods

5.2.1 Materials

1,2-dioctadecanoyl-sn-glycero-3-phosphocholine (DSPC), 1,2-distearoyl-sn-glycero-3-phosphoethanolamine-N-[methoxy(polyethylene glycol)-2000] (sodium salt) (DSPE-PEG2000,>99%) and cholesterol (chol, >99%). Doxorubicin and daunorubicin were purchased from Fisher Scientific (Loughborough, UK), and ammonium sulfate ([NH4]2SO4,>99%) was obtained from Sigma-Aldrich Ltd. (Poole, UK). Phosphate buffered saline tablets (10 mM, PBS pH 7.3) were acquired from Oxoid Ltd (Basingstoke, UK). All reagents (ethanol, methanol) were of analytical grade (HPLC grade,> 99.8%), and Transcutol was of general-purpose grade and purchased from commercially available suppliers.

5.2.2 Manufacturing of PEGylated Liposomes Encapsulating Ammonium Sulfate via Microfluidics

PEGylated liposomes were prepared using the bench-scale microfluidic system (NanoAssemblr Benchtop) from Precision NanoSystems Inc. (Vancouver, Canada), which uses a staggered herringbone micromixer (SHM). Liposome formulations containing DSPC, cholesterol and DSPE-PEG2000 at a w/w ratio of 3:1:1, respectively, were produced from a 20 mg/mL total lipid stock solubilised in ethanol, or Transcutol. Lipids were heated for solubilisation but were stable once in solution. Ammonium sulfate ($[NH_4]_2SO_4$, 250 mM) was used as the aqueous phase unless otherwise stated. Liposomes produced from the ethanol stock were produced at a total flow rate (TFR) of 10 mL/min and a flow rate ratio (FRR) of 1.5:1. Liposomes produced from the Transcutol stock were produced at a TFR of 5 mL/min and at a FRR of 1:1.

5.2.3 Manufacturing of PEGylated Liposomes Encapsulating Ammonium Sulfate Via Rotary Evaporator

PEGylated liposomes were prepared according to the solvent evaporation method. DSPC, cholesterol and DSPE-PEG2000 were dissolved in methanol at a total lipid concentration of 20 mg/mL (w/w 3:1:1, respectively). The lipid stock was transferred to a round bottom flask and the solvent evaporated under vacuum using a rotary evaporator. Once the solvent had evaporated, the thin lipid film was rehydrated in 50 mL of 250 mM ammonium sulfate. The lipid suspension was then heated to 60C and vortexed until the lipids were no longer coating the wall of the flask. Once fully suspended in the ammonium sulfate, the sample underwent extrusion (Liposo-Fast™-50, Avestin Inc., Ottawa, Canada) through polycarbonate filters of decreasing pore sizes (0.8, 0.4, and 0.2 µm) and sonication for 3 cycles (30 sec on, 30 sec off) to produce a final particle size of 90-100 nm.

5.2.3 Buffer Exchange of PEGylated Liposomes using Tangential Flow Filtration

The PEGylated liposomal formulation encapsulating $[NH_4]_2SO_4$, 250 mM was produced, and the solvent was removed whilst simultaneously conducting buffer exchange to establish a pH gradient between the liposome interior and the exterior medium for active-loading of doxorubicin. A tangential flow filtration system (KR2i TFF System, Repligen, Waltham, US) using a Repligen 500 kDa modified polyethersulfone (mPES) column and masterflex tubing 13 was used. The sample was filtered at a 20 mL/min flow rate and 12 diafiltration volumes with PBS (pH 7.3, 10 mM). Samples were diluted 1:5 with ammonium sulfate prior to filtration and concentrated to a final lipid concentration of 20 mg/mL. This resulted in PEGylated liposomes encapsulating acidic pH ($[NH_4]_2SO_4$, pH 5.5) and suspended in PBS (pH 7.3), creating a gradient for the diffusion of drugs with protonisable amine functions. These liposomes were then diluted with PBS prior to sizing and active-loading of doxorubicin.

5.2.4 Active-Loading of Doxorubicin into PEGylated Liposomes

Liposomes produced using microfluidics and rotary evaporation were purified using tangential flow filtration. Doxorubicin stock was prepared at 10 mg/mL in deionised water. A specific volume was added to the liposomes at a ratio of 0.125 g doxorubicin: 1 g lipid. Liposomes were incubated in a water bath at 60°C for 40 minutes, and the percentage encapsulation was calculated. After loading, the liposomes were allowed to cool down to room temperature and non-encapsulated doxorubicin was removed using tangential flow filtration. Quantification of doxorubicin loading was measured using a microplate reader (Bio-rad Laboratories Inc. Hertfordshire, UK), measuring the UV absorbance at 490nm. Liposome samples were mixed with 50% isopropyl alcohol to disrupt the liposome membrane and allow quantification of the encapsulated drug. Calibration curves were performed under the same conditions for each sample.

5.2.7 USP-4 Dissolution Release Study

Doxorubicin release was carried out following the optimised method from Yuan et al (118) using a USP-4 apparatus (SOTAX®) assay in a closed loop at 16 mL/min (118). The release media was freshly prepared and consisted of 100 mM NH_4HCO_3, 75 mM 2-(N-morpholino) ethane sulfonic acid (MES), 5% w/v hydroxypropyl-cyclodextrin (HP-CD) to avoid doxorubicin precipitation, and 5% w/v sucrose. The drug release assay was performed at 45 °C in a closed loop. Aliquots were taken at 0.5, 1, 2, 3, 4, and 6 h. A dialysis membrane with a cut-off 300 kDa (Repligen, Waltham, US) was used. The media volume per cell was 39.2 mL, and the sample volume was 0.8 mL (diluted to a doxorubicin concentration of 1 mg/mL). Free drug (1 mg/mL) was used as a control on each run. The cumulative release was calculated (as described by Yuan et al. (118)) as the percentage of the calculated doxorubicin concentration from the liposomes at each time point, divided by the detected concentration of free doxorubicin from the control at the same time point. A UV plate reader at 490 nm was used for this purpose (300 µL/well).

5.2.8 *In Vivo* Biodistribution Study

Male, Sprague-Dawley rats were divided into 6 groups (3 groups of 9 rats, 3 rats sacrificed at each time point and 3 groups of 6 rats, all sacrificed at the same time point) and were intravenously injected with 1 mL/kg of doxorubicin-loaded liposomes produced by either, thin-film hydration (rotary evaporator), microfluidics with either ethanol or Transcutol. At 4 predetermined time points, rats were anesthetised, and blood together with organs/tissues were collected. Blood was collected by heart puncture, and the plasma was separated by centrifugation for 10 min at 4°C at 1900 g. All specimens were stored at -20°C until analysed.

5.2.9 LC-MS Analysis of Doxorubicin Biodistribution in Plasma and Tissues

Plasma samples were mixed 1:1 with 0.1% formic acid in acetonitrile and centrifuged at 4°C at 15,000 g for 30 min. The supernatant was removed to a clean Eppendorf and filtered through a 0.22 µm filter. All samples were spiked with 800 ng internal standard (daunorubicin) and used for LC-MS assay.

Separation was achieved on a Phenomenex Kinetex C18 (50 x 3 mm, 2.6 µm) column maintained at 30 °C. The mobile phase consisted of 0.1% formic acid (v/v) in water and acetonitrile. The flow rate was set at 0.4 mL/min, and the following gradient of acetonitrile was applied: 5% 0 – 8 min, increasing to 40% 8 – 9 min, and then decreasing to 5% at 9.2 min. The injection volume was 1 µL.

A Nexera-i (LC-2040C) chromatographic system was coupled with an LCMS-8050 mass spectrometer (Shimadzu). The mass spectrometer was equipped with an electrospray ionization source operating in

positive ion mode for analysis of doxorubicin and daunorubicin. The ion pairs were m/z 544.2 -> 397.2 and m/z 528.1 -> 321.1 for doxorubicin and daunorubicin respectively.

Frozen tissue samples of liver and spleen were weighed and homogenised in the mobile phase (4 mL/g). Tissues were homogenized using a Lab GEN 7B homogenizer (Cole Palmer). Tissue homogenate was then mixed 1:1 with 0.1% formic acid in acetonitrile and centrifuges at 4°C at 15,000 g for 30 min. The supernatant was collected and filtered through a 0.22 µm filter. All samples were spiked with 800 ng internal standard (daunorubicin).

5.2.8 Statistical Analysis

One-way ANOVA followed by Tukey's multiple comparison test was used for the data analysis. All the experiments were carried out at least in triplicate unless otherwise stated and are shown as the mean of the measurements ± standard deviation, which is plotted as error bars. For the statistical analysis of the drug release studies from various formulations, the f2 similarity test was followed.

5.3 Results

5.3.1 Microfluidic Production Compared with Traditional Manufacturing Methods

Before the development of microfluidics, liposomal drug delivery systems were produced using traditional methods, including the rotary evaporator. In this method, the lipid phase is evaporated under a vacuum to form a thin lipid film, which is subsequently rehydrated in the aqueous buffer. This process produces a large heterogeneous liposome suspension which requires further downstream process to reduce the particle size and polydispersity. These methods include extrusion and sonication. Extrusion involves passing the sample through multiple membranes of varying pore sizes to produce a homogenous suspension. During probe sonication, the liposome suspension is placed within a water bath and is exposed to ultrasonic waves to ensure the gradual size reduction of the liposome suspension. This is a multistep batch process that is very time-consuming and not very efficient. During the sonication process, the lipids can degrade and breakdown, resulting in the release of encapsulated compound due to the production of heat during the sonication process (119).

From the previous experiments doxorubicin was selected as our model compound to take forward *in vitro* and *in vivo* as it is one of the most extensively studied and the first liposomal formulation approved by the FDA. Ethanol and Transcutol were selected for the microfluidic production of liposomes and rotary evaporation used to produced liposomes that would then be remote loaded with doxorubicin.

5.3.1.1 In Vitro Release of Doxorubicin from Liposome Manufactured Using Microfluidics and Rotary Evaporator

The pharmacokinetics and pharmacodynamics of liposomes are dependent on the vesicle size, drug loading and release. In addition to the critical quality attributes (CQAs) of the liposomes (e.g. particle size, zeta potential and encapsulation efficiency), the drug release/retention profile is an important factor that should be considered. Roces et al. previously published the release profile of doxorubicin from liposomes produced at different FRR, from different lipids and at different incubation temperatures using the USP-4 dissolution apparatus (16)The same method has been used here to measure the release of doxorubicin from liposomes produced by either microfluidics or thin film hydration. The aim of these experiments was to determine how the production method influences liposomal characteristics and release profile and how the solvent selected can impact liposome properties.

Liposomes composed of DSPC:Cholesterol:DSPE-PEG2000 (w/w 3:1:1) were produced from either an Ethanol or Transcutol stock using microfluidics or a Methanol stock using the rotary evaporator. All liposome formulations were purified and concentrated to a final lipid concentration of 16 mg/mL using tangential flow filtration (TFF) and loaded with 0.125 g doxorubicin/1 g lipid at 60°C for 40 minutes. The resultant liposomes were between 80 – 110 nm with a PDI <0.2 pre-loading with doxorubicin (Figure 5.1 A&B). Post-loading the particle size increased by approximately 6-10 nm for the smaller liposomes produced via microfluidics using the Ethanol stock and for the liposomes produced on the rotary evaporator, with no significant change in size observed for liposomes produced using the Transcutol stock via microfluidics (Figure 5.1). These increases in particle size align with previous doxorubicin data (Table 4.3), which showed that the smaller liposomes show a larger increase in size post-loading with doxorubicin compared with liposomes closer to 100 nm in size.

USP-4 apparatus was used to compare the release profiles of liposomal doxorubicin, produced via thin-film hydration and microfluidics, with the release of free (unencapsulated) doxorubicin. Liposomes were all diluted to the same concentration, and the same volume was added to the dialysis tubing. Aliquots of each sample were then taken at 0.5, 1, 2, 3, 4, and 6 h and the concentration of doxorubicin was calculated at each time point. Non-encapsulated doxorubicin as a solution was used as a control. The liposomes produced via the rotary evaporator and those produced via microfluidics with ethanol were of similar sizes pre- and post-loading, whereas those produced via microfluidics using Transcutol were slightly larger at approx. 110 nm (vs 94 nm) (Figure 5.1 A). Zeta potential showed no significant difference between the formulations (Figure 5.1B), and all formulations showed high encapsulation efficiency (> 85%) (Figure 5.1C). The results show that the free doxorubicin was completely released from the dialysis tubing at the first time point measured (0.5 h), as expected, and

that all liposomal formulations showed much longer sustained release profiles with > 20% release at 0.5 h and complete release observed after 6 h (Figure 5.1D). When comparing all liposomal formulations with free doxorubicin, there was a significant difference in release profiles (f_2 < 50). However, when comparing the release profiles of all the liposomal formulations, there were no significant differences (f2 >50), therefore demonstrating that the manufacturing process had no effect on the release profile of the liposomes *in vitro*.

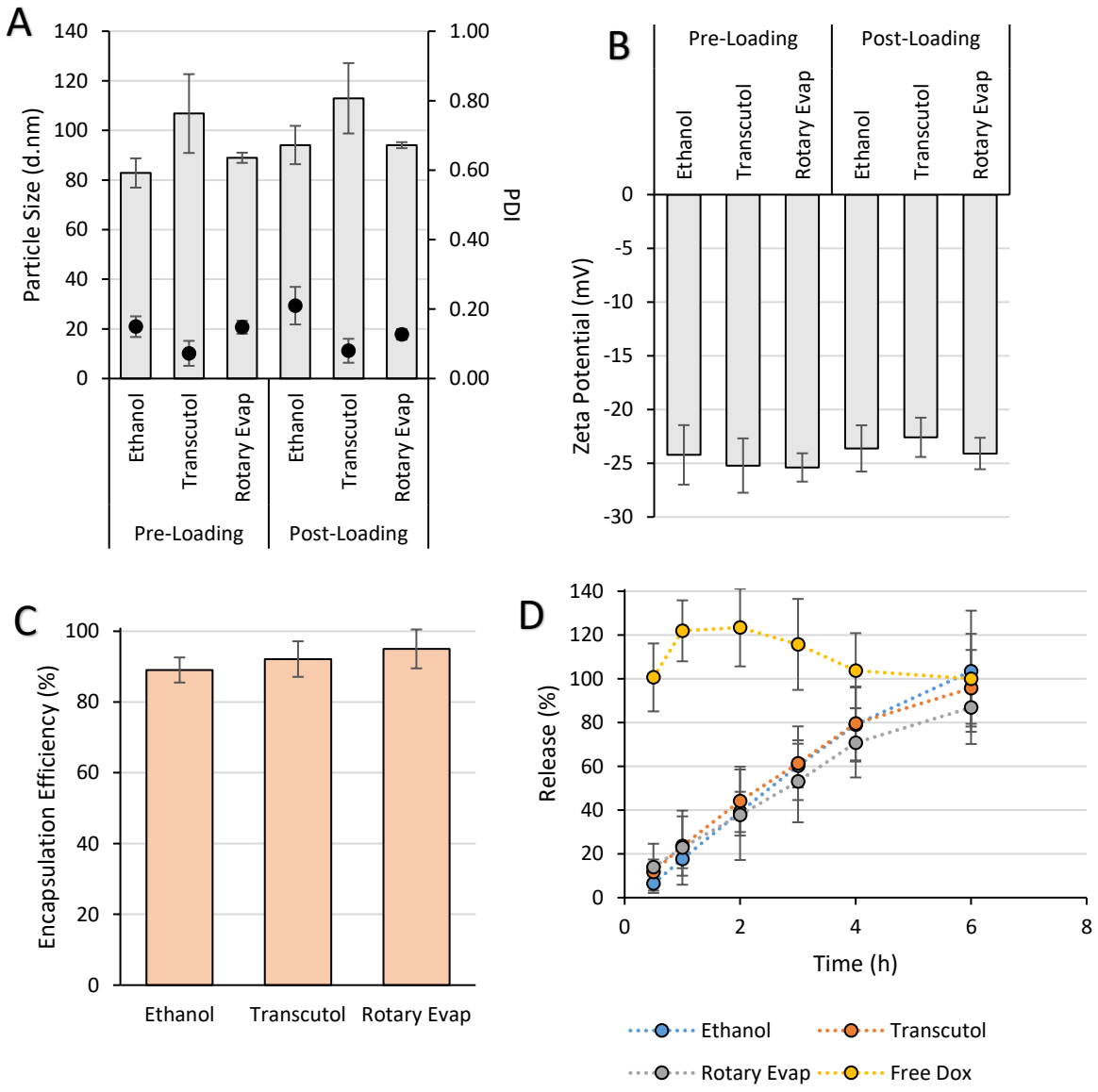

Figure 5.1: Release study using the USP-4 apparatus. A) particle size (d.nm; represented by the bars) and PDI (represented by the discrete points), B) zeta potential of each formulation pre- and post-loading with doxorubicin and, C)doxorubicin loading of the liposomes remote loaded with doxorubicin and incubated for 40 min, at 60°C. D) Release profiles of liposomes produced via microfluidics from either ethanol or Transcutol, liposomes produced using the rotary evaporator or free doxorubicin. Release studies were carried out at 45°C in release media composed of 100 mM NH4HCO3, 75 mM 2-(N-morpholino) ethane sulfonic acid (MES), 5% w/v hydroxypropyl-cyclodextrin (HP-CD) to avoid doxorubicin precipitation, and 5% w/v sucrose. Results represent mean ± SD, n=5 independent batches.

5.3.2 *In Vivo* Biodistribution of PEGylated Liposomal Doxorubicin in Rats Tissues

Liposomes were again produced as described in section 5.3.1, and the physicochemical characteristics are shown in Table 5.1. The liposomes produced from Transcutol via microfluidics were slightly larger (approx. 125 nm; Table 5.1) than those produced via microfluidics using ethanol or produced using the rotary evaporator (approx. 100 nm; Table 5.1), with all formulations having a zeta potential of approx. -20 mV. All liposomal formulations showed high encapsulation of between 90 – 100% with minimal change in particle size post-loading. All formulations were injected into male Sprague-Dawley rats at a concentration of 1 mg/kg.

Table 5.1: Samples for in vivo biodistribution study. Results represent mean ± SD, n=1 independent batches.

		Size (nm)	PDI	Zeta (mV)	%EE
Pre-Loading	Rotary Evap	92.7 ± 0.7	0.17 ± 0.01	-23.4 ± 0.6	
	Transcutol	125.4 ± 0.8	0.04 ± 0.02	-18.6 ± 1.1	
	Ethanol	89.0 ± 1.3	0.14 ± 0.01	-21.4 ± 0.2	
Post-Loading	Rotary Evap	98.2 ± 1.0	0.13 ± 0.01	-20.3 ± 0.7	92.0 ± 1.2
	Transcutol	122.7 ± 1.9	0.06 ± 0.00	-16.2 ± 0.4	101.6 ± 0.7
	Ethanol	99.5 ± 1.1	0.23 ± 0.01	-17.7 ± 0.2	95.6 ± 0.6

Tissue and plasma samples were collected at 1, 9, 24 and 48 hours after IV administration of 1 mg/kg of liposomes produced via rotary evaporator, or microfluidics using either Ethanol or Transcutol, and the concentration-time profiles of doxorubicin in each tissue was determined. The plasma concentration-time curve is presented in Figure 5.2, and the area under the curve (AUC) was calculated for each formulation. The results show that all formulations follow the same trend. However, the liposomes produced from Transcutol via microfluidics had significantly higher concentrations than the rotary evaporator sample at all time points and significantly higher concentrations than the ethanol sample at 1 hour post-injection ($p<0.05$). When comparing the rotary evaporator samples with the microfluidic ethanol samples there was no significant ($p>0.05$) difference at any time point.

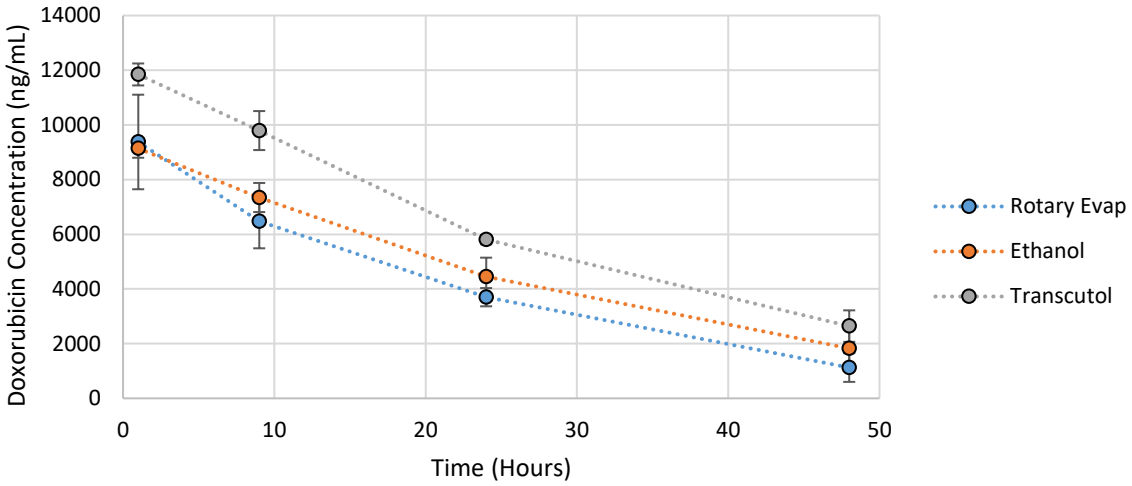

Formulation	AUC ± SD
Rotary Evaporator	197608 ± 16059
Ethanol	229820 ± 16194
Transcutol	304880 ± 10545

Figure 5.2: Plasma concentration – time curve for liposomes produced via either rotary evaporator or microfluidics using either ethanol or Transcutol as the organic solvent. The area under the curve (AUC) was calculated for each formulation. Results represent mean ± SD, n=3 of independent samples, except for 48 h time point where results represent mean ± SD, n=6 of independent samples.

In the liver (Figure 5.3), all formulations showed similar doxorubicin concentrations at 1 hour and 9 hours post-injection; however, the concentration of doxorubicin in the liver of rats treated with the ethanol formulation rapidly decreased after 9 hours post-injection. The doxorubicin concentration in the liver of rats treated with liposomes produced via the rotary evaporator increased at 24 hours before decreasing rapidly to the same concentration as the ethanol formulation 48 hours post-injection. The rats treated with the Transcutol formulation showed a significantly higher concentration of doxorubicin 48 hours post-injection when compared with both the rotary evaporator and the ethanol formulations, suggesting slower clearance from the liver compared with the other 2 formulations.

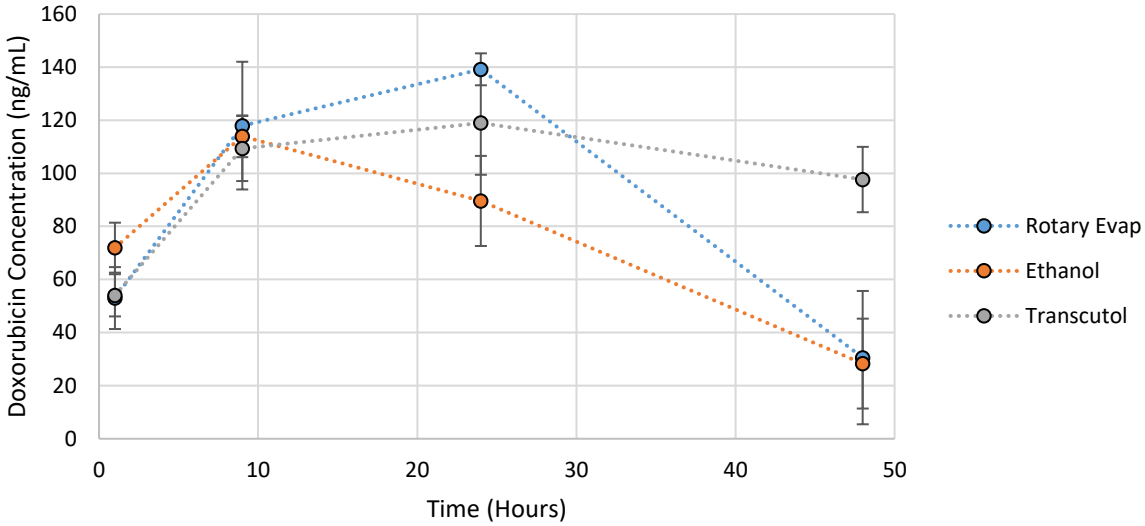

Formulation	AUC ± SD
Rotary Evaporator	4649 ± 386
Ethanol	3685 ± 361
Transcutol	4965 ± 994

Figure 5.3: Liver concentration – time curve for liposomes produced via either rotary evaporator or microfluidics using either ethanol or Transcutol as the organic solvent. The area under the curve (AUC) was calculated for each formulation. Results represent mean ± SD, n=3 of independent samples, except for 48 h time point where results represent mean ± SD, n=6 of independent samples.

In the spleen (Figure 5.4), when comparing the liposomes produced via microfluidics, the concentration of doxorubicin was significantly ($p<0.05$) higher for rats treated with the ethanol formulation compared with the Transcutol formulation from 1 hour to 24 hours post-injection with the doxorubicin concentration in the ethanol samples decreasing rapidly at the 48-hour time point. Whereas there was no significant difference between the rotary evaporator formulation and either ethanol or Transcutol. Both the rotary evaporator and ethanol formulations follow the same trend, with the doxorubicin concentration at 48 hours post-injection decreasing to the same concentration. The Transcutol formulation follows the same trend as the other 2 formulations between 1 and 24 hours post-injection. However, the doxorubicin concentration does not appear to decrease as fast as the rotary evaporator and ethanol formulations, which may suggest that the liposomes produced from Transcutol may be releasing the doxorubicin slower or that the structure of these liposomes is different from the other 2 formulations, thereby preventing breakdown and release of the payload.

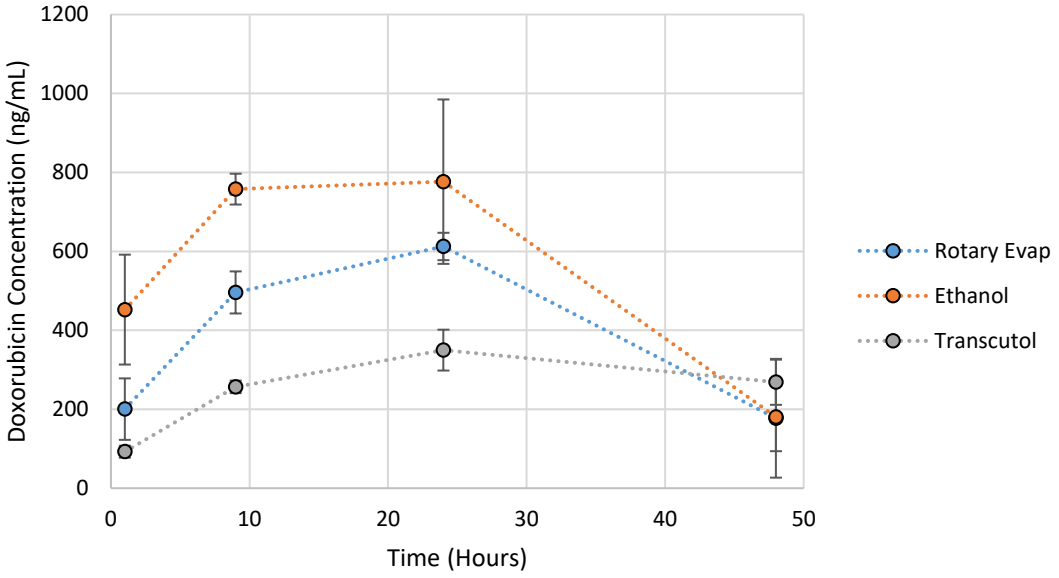

Formulation	AUC ± SD
Rotary Evaporator	20571 ± 1779
Ethanol	27834 ± 3178
Transcutol	13365 ± 994

Figure 5.4: Spleen concentration – time curve for liposomes produced via either rotary evaporator or microfluidics using either ethanol or Transcutol as the organic solvent. The area under the curve (AUC) was calculated for each formulation. Results represent mean ± SD, n=3 of independent samples, except for 48 h time point where results represent mean ± SD, n=6 of independent samples.

When taken together, the rotary evaporator and the ethanol formulations show very similar biodistribution profiles (Figure 5.5 A&B), demonstrating how it is possible to translate the production

of liposomes from more traditional manufacturing methods (i.e. rotary evaporator) to more modern and scalable methods such as microfluidics. The results also demonstrate how the manufacturing parameters may affect resultant liposome properties. Both the ethanol and Transcutol formulations were produced using microfluidics and were of similar particle characteristics post-loading with doxorubicin (Table 5.1). However, despite having similar CQAs, the formulations have slightly different biodistribution profiles (Figure 5.5 B&C). Liposomes produced from Transcutol have prolonged, higher concentrations in the plasma compared with the ethanol formulation and showed reduced accumulation in the spleen and reduced clearance in the liver.

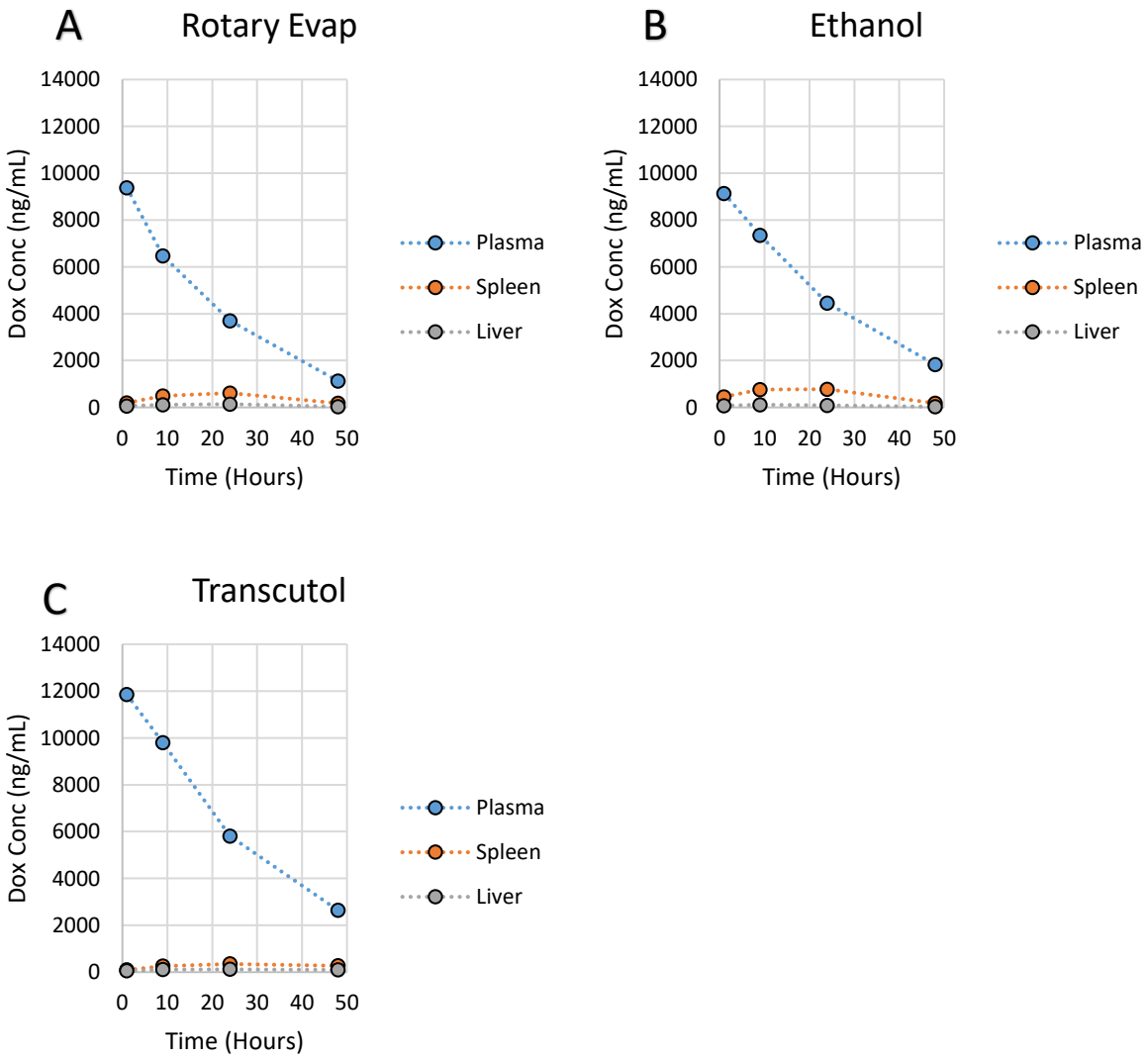

Figure 5.5: Combined concentration – time curve of each tissue in rats injected with liposomes produced via A) Rotary evaporator, B) Microfluidics with ethanol and C) Microfluidics with Transcutol. Results represent mean ± SD, n=3 of independent samples, except for 48 h time point where results represent mean ± SD, n=6 of independent samples.

5.4 Discussion

The aim of this chapter was to characterise the *in vitro* release and *in vivo* clearance of doxorubicin from liposomes produced by different manufacturing methods, thin film hydration and microfluidic

manufacturing to consider the impact of manufacturing on the liposomal attributes given that it has been shown that small differences in manufacturing processes can have a major impact of liposomal attributes (118). Liposomes are complex delivery systems with heterogeneous structures of varying physicochemical characteristics and qualities. The extent of similarity is therefore important when comparing new formulations with any reference products (120). Previous research has demonstrated how it is possible to tailor liposome critical quality attributes by varying the manufacturing parameters (i.e. FRR and TFR (16)); however, it is also important to understand how these small changes can alter the performance of these liposome both *in vitro* and *in vivo*. Since the development of the first liposomal drug delivery system, Doxil®/Caelyx, many generic products have been developed, for example, Myocet, which is the unPEGylated version of Doxil®/Caelyx. Although both of these formulations contain the same compound and are of similar characteristics, they show different biodistribution profiles (121).

Therefore, liposomes with similar CQAs were produced using different manufacturing techniques to determine whether the method affected the resultant liposome release profiles. Liposomes were also produced using microfluidics using two different organic phases (one in ethanol and one in Transcutol) to identify whether the solvent has any effect on the resultant liposome properties.

5.4.1. Liposomes prepared via different methods have similar *in vitro* release profiles

The results from the *in vitro* release study using the USP-4 apparatus (Figure 5.1) showed no difference in release profile between the 3 formulations, with all 3 showing prolonged and comparable release when compared to free doxorubicin, thereby demonstrating that both manufacturing processes, as well as the solvent used as the organic phase, have no effect on *in vitro* release of doxorubicin. These results are supported by results previously published that have shown that particle size has no effect on the release of doxorubicin (16).

There are a number of factors that can affect the *in vitro* release of liposomal formulations, these include (i) membrane composition (and proportion of components in the lipid membrane), (ii) the size distribution of the liposome sample, (iii) the lamellarity, (iv) the nature of the drug and physical state of the drug within the liposome and (v) the release mechanism of the drug (122, 123).

The membrane composition is a key factor in determining the release of drug from liposomes. Both the choice of the phospholipid (and its transition temperature) and the helper lipid/cholesterol content selected for the liposomal membrane, in part, determine the release kinetics of the liposomes. Phosphatidylcholine lipids are usually selected as the main/helper lipids in the liposomal formulation as they are non-toxic and biodegradable in nature. The helper lipid acts as the main structural lipid in the lipid bilayer. As these lipids form the major component of the lipid membrane,

it is crucial to understand the properties of the helper lipids that will be implemented. One of the key factors that can determine the membrane permeability and stability is the transition temperature of these helper lipids. The transition temperature refers to the temperature at which the lipids undergo a change in physical state from an ordered gel phase to a more disordered liquid crystalline phase (71). The transition temperature is determined by the hydrocarbon tail length and the degree of saturation. Cholesterol is another important component of the liposome membrane, as it acts to stabilise the lipid bilayer and reduce its permeability. Therefore playing a key role in drug retention and release. High cholesterol content has been shown to decrease membrane fluidity and increase the rigidity of the membrane, with the inclusion of 50 mol% showing increased stability and reduced permeability (124).

However, even when liposomal formulations are mapped , small changes in manufacturing processes can impact release characteristics. To investigate this, Yuan et al., optimised the USP-4 method and demonstrated how it was able to distinguish between not only different liposomal formulations but also different generic versions of the same liposomal doxorubicin product (118). In their studies, they demonstrated that the USP-4 could discriminate between liposomes composed of POPC when compared with liposomes composed of HSPC. The results showed that liposomes composed of POPC had a more rapid and complete release of doxorubicin compared with HSPC. This is thought to be due to the nature of these lipids as POPC has a lower transition temperature than HPSC; therefore, when heated at 45°C, these lipids would be in a more fluid phase, allowing for diffusion of doxorubicin across the membrane. Whereas HSPC requires heating above 55°C to be in a more fluid phase, and therefore, the membrane would not be as permeable to doxorubicin. These studies (118) also indicated that the USP-4 assay developed could be used to compare DOX release from generic DOX formulations to the innovator product Doxil®.

The lamellarity and polydispersity of the liposomes may be another factor affecting *in vitro* drug release. When liposomes are produced using thin-film hydration, downstream processing is required to reduce particle size and polydispersity. When the thin film is hydrated, this can result in the formation of large multilamellar vesicles, and through downstream size reduction, e.g. extrusion and sonication, these larger particles are broken down to produce small unilamellar vesicles. Yuan et al. were also able to demonstrate how the USP-4 apparatus was able to determine different release profiles of liposomes produced via different methods (homogenisation vs extrusion), with liposomes produced via homogenisation showing faster release (118). This was thought to be due to differences in the polydispersity of the liposome samples. Release profiles of liposomal paclitaxel showed that liposomes with higher lamellarity released the drug more slowly, and this is due to the presence of several lamellae inside the liposomes that prevent and delay the release of paclitaxel from the interior

membrane (125). Although the liposomes studied in this chapter are all similar in size, the internal structure of the liposomes was not determined. This could be achieved using cryo-TEM or SAXS analysis to determine whether the manufacturing parameters can affect liposome lamellarity and, indeed the choice of solvent may affect lamellarity, as shown by Webb et al. (60) where the use of ethanol in the production of liposomes produced SUVs, whereas the use of IPA resulted in liposomes with 2 bilayers.

All the liposomes within this chapter have the same lipid concentration and the same ratio of lipids in each. Therefore, membrane composition would not be a determining factor in the release of doxorubicin from these liposomes. However, it may be important to consider how the manufacturing conditions may affect the lipid properties. The liposomes produced via thin film hydration required heating during the manufacturing process. Thin film hydration is classed as a top-down approach in which the lipids need to be heated when rehydrated, as the lipid film needs to be broken down and reformed during this process in order to form a bilayer structure. Whereas microfluidics is a bottom-up process where the liposomes are formed from individual monomers therefore, the phase transition temperature is not a factor during membrane formation (78). This breaking down and reformation under high temperatures could potentially have an impact on the structure, packing and composition of the membrane, which may lead to alterations in the release profile of these liposomes. The mechanism by which extrusion breaks down multilamellar vesicles into unilamellar vesicles is not well understood. It has been observed that the particle size of liposome post-extrusion is larger than the pore size of the extrusion membrane, indicating that liposome shape is being altered when passing through the pore, specifically when small pore sizes are used (< 200 nm) (126). In order to determine whether the extrusion and sonication process was affecting lipid composition, HPLC-ELSD could be used to determine the concentration of each component. Cryo-TEM could also be used to determine the morphology of the resultant liposomes (127).

5.4.2 *In vitro* release does not map to *in vivo* drug biodistribution

Whilst the *in vitro* release data for doxorubicin from liposomes (Figure 5.1) suggest that the release of doxorubicin was not significantly different for the liposomes prepared by different manufacturing methods and using different solvents, the results from the *in vivo* biodistribution study suggest that solvent may have an important role in the manufacturing and structure of the liposomal membrane (Figure 5.5). It may be important to note that, similar to many PK studies looking at liposomal doxorubicin, it is not possible to conclude whether the doxorubicin detected in each sample is encapsulated or free drug. During the preparation process, any residual loaded liposome still present in the sample may be destroyed, resulting in the release of the encapsulated doxorubicin (128).

The higher concentrations of doxorubicin in the plasma (Figure 5.2) and reduced accumulation in the liver (Figure 5.3) and spleen (Figure 5.4) may be indicative of a structural difference in liposomes produced from Transcutol compared with the ethanol and the rotary evaporator. The choice of solvent can affect the packing and conformation of the lipid acyl chains with solvents that favour interactions with the lipid tails, promoting lipid ordering and membrane stability, while solvents that disrupt lipid tail interactions can result in membrane fluidisation and phase separation. Therefore, solvents that promote lipid fluidisation may enhance drug release by increasing the mobility of lipids, thereby facilitating drug diffusion across the liposome membrane. Weber et al. (129) demonstrated that alkanols, such as ethanol, interact with the head group of the phospholipid with their hydrocarbon chains being aligned in between the phospholipid acyl chains. It was also shown how the hydrocarbon chain length could affect the transition temperature of the phospholipid with shorter chain ($C < 3$), decreasing the transition temperature and those with hydrocarbon chain > 10, resulting in increased transition temperature. However, these effects were only observed at very high concentrations of solvent (1 M). Forbes et al. demonstrated that after 12 wash cycles, the levels of residual solvent were below 0.3% (78), therefore, there is not expected to be high concentrations of solvent within these samples after two purification cycles via TFF; any residual solvent that had not been removed could influence the packing and permeability of the resultant liposomes. Maeki et al. investigated the effect of ethanol exposure on the lipid bilayer structure and found that upon contact with ethanol for 0.8 s, the structure of the liposomes changed from unilamellar to multilamellar (130). These results demonstrate the importance of complete solvent removal for stable lipid bilayer formation. The Transcutol liposomes were produced at a much slower TFR than the ethanol formulations (5 mL/min vs 10 mL/min) and, therefore, would've been in contact with the solvent for a longer period of time. These liposomes were also produced at 60°C and were left to cool to room temperature prior to TFF purification therefore being exposed to high concentrations of solvent for a longer time period. Both factors may have caused disruption and reorganisation of the lipid membrane to multilamellar vesicles, which would also account for the slower release if there were increased lipid bilayer barriers preventing the release of the encapsulated doxorubicin.

Solvent has been shown to have an impact on liposome formation, with the rate of change in polarity having a significant effect on liposome particle size. Particle size, in turn, also has an impact on liposome biodistribution, with liposomes in the range of 100-150 nm favouring cell uptake and liposomes between 50-100 nm being able to avoid detection by the immune system (131). However, to address this, all liposomes produced were of similar size of between 99 – 123 nm, and it has been shown that PEGylated liposomes within the size range of 80 – 250 nm are less sensitive to the effect of size compared to non-PEGylated liposomes (132). The increase in size of the liposomes post-loading

(Figure 5.1) is thought to be due to the way in which doxorubicin loads and complexes with the sulfate ions in the aqueous core of the liposomes. Doxorubicin has been shown to form rod-like structures across the diameter of the liposomes which can result in a slight change in morphology and subsequently the PDI of the sample (133).

However, it has also been suggested that drug release from liposomes may be controlled by size. Nagayasu et al (134) produced HEPC:Cholesterol:DCP liposomes of 50 nm and 100 nm encapsulating daunorubicin and showed that the larger liposomes showed no drug release over 240 minutes compared to the 50 nm liposomes which showed a gradual release with 40% drug release at 240 minutes. Although the liposomes here do not have as large a difference in particle size, the 20 nm difference between the ethanol and Transcutol samples may result in a slightly slower release of doxorubicin across the 48 h time points.

Higher concentrations of doxorubicin in the plasma of rats treated with liposomes produced from Transcutol may be due to increased stability of liposomes leading to slower drug release or may be associated with reduced cellular uptake of these liposomes (135). Transcutol is often used in the cosmetic and pharmaceutical industries as a permeability enhancer. It is a very attractive penetration enhancer due to its non-toxic and biocompatibility with the skin. Transcutol is a hygroscopic compound that can adsorb water from the skin. Then by maximising their thermodynamic activity due to changes in solubility, can improve skin penetration of certain drugs (84). When used in dermal delivery, Transcutol helps to enhance solubility in the skin whilst being able to penetration into the skin where, in certain circumstances, it can form a depot (136). This would, therefore, demonstrate the ability of Transcutol to retain the encapsulated compound for prolonged periods of time, resulting in slower release.

5.5 Conclusion

From these studies, it was demonstrated that there is not always a correlation between *in vitro* and *in vivo* data. It was shown that it is possible to produce liposomes of similar physicochemical characteristics using traditional thin-film hydration and more modern manufacturing using microfluidics. The effect of the manufacturing technique on the release profiles of the resultant liposomes was therefore investigated. *In vitro* studies showed that the manufacturing technique had no effect on the release profiles of the liposomes. However, *in vivo* biodistribution studies demonstrated that solvent may play a role in determining the biodistribution profile of the liposomes. These results demonstrate that even when liposomes are produced with the same physicochemical characteristics using different methods, it is important to test these products both *in vitro* and *in vivo*

as small changes in the manufacturing process (such as using a different solvent during microfluidics), may have significant effects on the bioequivalence of the final drug product.

Chapter 6 – *In Vitro* and *In Vivo* Correlation of mRNA Encapsulating Lipid Nanoparticles

6.1 Chapter Declaration

This work was done in collaboration with Burcu Binici and Muattaz Hussain.

Sarah Lindsay, Muattaz Hussain, Burcu Binici, Yvonne Perrie

The named researchers below contributed to this chapter as follows:

Sarah Lindsay: Formal analysis, *In Vitro* expression, viability and uptake studies, writing of the manuscript

Muattaz Hussain: Formal analysis, *In Vivo* immunisation study

Burcu Binici: Formal analysis, *In Vivo* expression (IVIS) study

Yvonne Perrie: Conceptualisation, Supervision and Writing – Review & Editing

6.2 Introduction

Having established microfluidic manufacturing of liposomes, the same methods were applied to the manufacturing of lipid nanoparticles. Lipid nanoparticles (LNPs) can be considered as having their design and formulation foundations derived from liposomes. Liposomes are well recognised for their lipid bilayer and aqueous core. In contrast, in their basic form, LNPs are protective lipid shells wrapped around cargo intended for cellular uptake and processing. Most commonly, their cargo is nucleic acid, and this is incorporated through electrostatic interactions with ionisable lipids in the lipid structure of the LNPs (137).

Cationic lipids were first employed for the encapsulation of nucleic acids, as they were shown to effectively encapsulate nucleic acids due to their permanent positive charge and enhanced the immune response (26). However, although these cationic particles were effective at promoting cellular uptake and gene delivery, they were also shown to be toxic due to their interactions with cell membranes and their ability to mediate uncontrolled activation of pro-apoptotic and pro-inflammatory pathways (138, 139). Therefore, an alternative lipid was required that did not produce these toxic side effects, and therefore, cationic ionisable lipids were developed. To address this, a series of ionisable lipids were developed (140, 141). These ionisable lipids have a pKa 6-7, meaning that at acidic pH, they have a positive charge, and as the pH increases towards physiological pH (pH 7), they become nearly neutral in charge. This change in charge helps to facilitate endosomal escape and release of the nucleic acid payload without causing toxic side effects, as observed when there was a permanent positive charge on the lipids. DODMA was the first ionisable lipid developed for nucleic acid delivery and its chemical structure has evolved and led to the development of the ionisable lipid, D-Lin-MC3-DMA which was used in the Onpattro formulation (139).

The concept of mRNA therapeutics has been suggested since the discovery of mRNA in 1961 but has only recently gained attention as obstacles such as mRNA instability, inefficient *in vivo* delivery, and the stimulation of undesirable inflammatory responses have been overcome (142). To address the issues with nucleic acid delivery, LNP delivery systems were first developed for the delivery of siRNA, with the first approved LNP drug, Onpattro, being approved by the FDA in 2018 for the treatment of hereditary transthyretin amyloidosis (143). Onpattro is a lipid nanoparticle-based short-interfering RNA (siRNA) drug that acts by inhibiting synthesis of the transthyretin protein in the liver and is composed of the ionisable lipid DLin-MC3-DMA, the helper lipid DSPC, cholesterol and the PEG-lipid DMG-PEG2000 (50:10:38.5:1.5 molar ratio respectively) (143). The success of Onpattro allowed for continued research, and the COVID-19 pandemic highlighted the use of, specifically, mRNA-LNPs as a highly effective vaccine delivery system, which is demonstrated by the 2 approved mRNA vaccines against SARS-CoV-2, Comirnaty® and Spikevax™ (139).

Messenger RNA (mRNA) has shown great therapeutic potential in a range of applications, such as vaccines and cancer immunotherapies. In order to have a therapeutic effect, the mRNA molecules need to be delivered to the target cell and be taken up and transcribed to produce sufficient proteins of interest (144). mRNA is readily degraded by nucleases, is rapidly cleared from the circulation and can induce immunostimulatory effects (145). Therefore, a delivery strategy is required that protects the mRNA from degradation, prevents interception and clearance by the MPS, and allows the mRNA formulation to reach the target tissue and be internalised into the target cells (144).

LNP-mRNA vaccines represent a new and emerging platform technology in vaccine development. The speed and efficiency of this vaccine delivery platform has been exemplified by the COVID-19 pandemic and the speed at which these new vaccines appeared in the clinic (146). The performance of LNPs for mRNA delivery is dependent on their potency, *in vivo* distribution and targeting, ability to induce an immune response and their inherent adjuvanticity (147).

Cellular uptake of these LNPs is a multi-step process that is mediated by both the size of the LNP and the interaction between the LNP and biological fluids, more specifically, biomolecules such as immunoglobulins and lipoproteins (146). LNPs can be internalised by a number of methods, including micropinocytosis and clathrin-mediated endocytosis, with the endocytic pathway being dependent on the nanoparticle properties and the type of cells (144). After entering the cells, the LNPs enter the endosome, where the ionisable lipid becomes protonated due to the lower, acidic pH in the endosomal compartment. This positive charge on the ionisable lipid then allows for interaction with the negatively charged phospholipids within the endosome, thereby facilitating endosomal escape and release of the mRNA payload into the cytosol, where it is translated (139).

The first approved mRNA vaccines were the Pfizer/BioNTech (Comirnaty®) and Moderna (Spikevax) vaccines, which were approved by the MHRA in December 2020 (148). The Pfizer/BioNTech vaccine is composed of the ionisable lipid, ALC-0315, DSPC, Cholesterol and the novel PEGylated lipid, ALC-0159 at a molar ratio of 46.3:9.4:42.7:1.6 respectively (137). Whereas the Moderna formulation is composed of the ionisable lipid, SM-102, DSPC, Cholesterol and DMG-PEG2000 at a molar ratio of 50:10:38.5:1.5, respectively (137).

Aim and Objective:

The aim of these studies was to characterise and identify correlations of both *in vitro* expression, viability, and uptake with *in vivo* expression and biodistribution. Here four LNP formulations containing the ionisable lipids, SM-102, ALC-0315, DLin-MC3-DMA (MC3) and C12-200 (Figure 6.1) will be compared for *in vitro* and *in vivo* potency. To achieve this, the objectives were:

- Produce and characterise 4 different LNP formulations using microfluidics.
- Investigate the *in vitro* expression profiles using 3 cell lines.
- Compare the *in vitro* and *in vivo* expression profiles to determine any correlations.

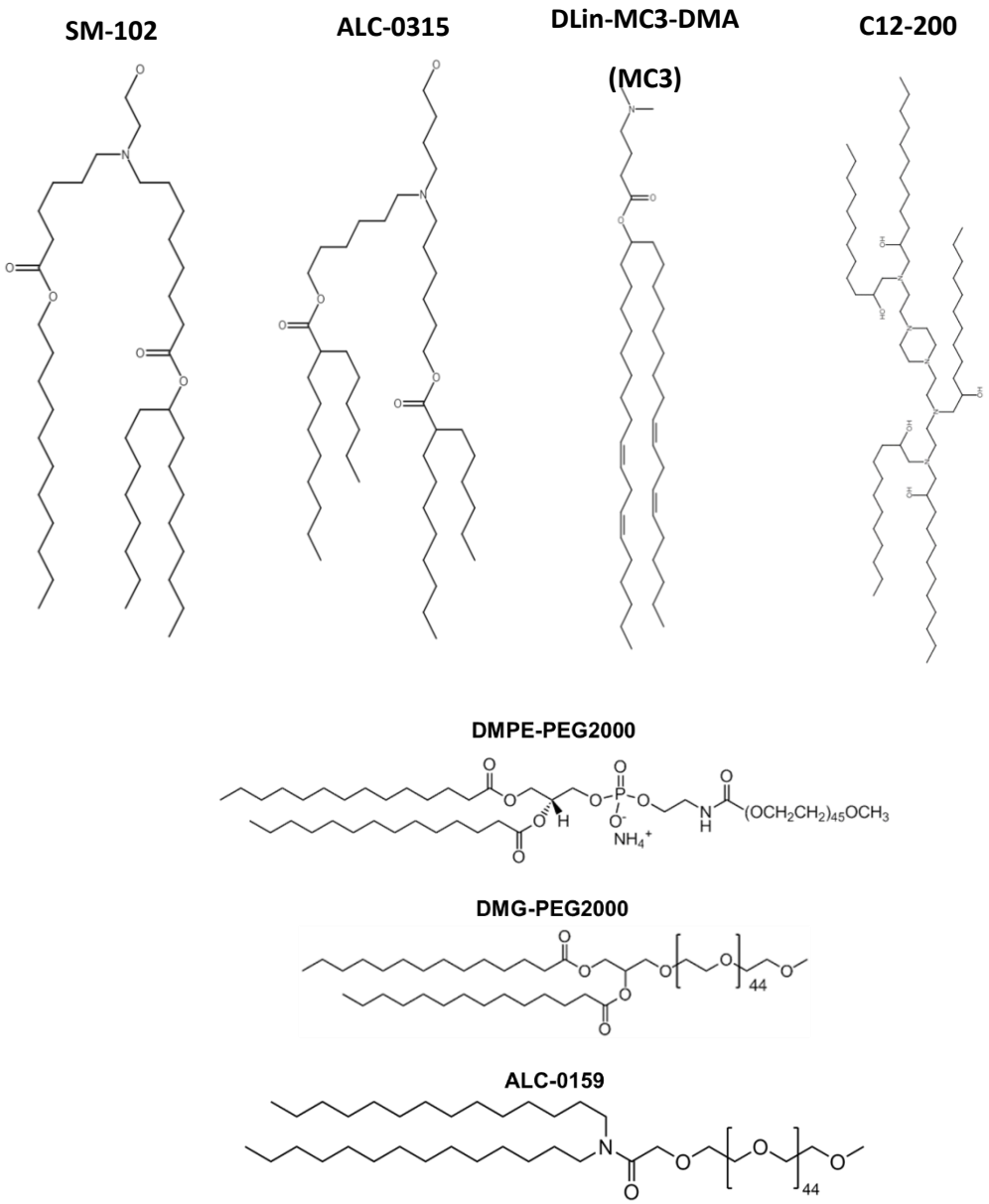

Figure 6.1:Chemical structures of the ionisable lipids (SM-102, ALC-0315, MC3 and C12-200) and the PEGylated lipids (DMPE-PEG2000, DMG-PEG2000 and ALC-0159). The ionisable lipid structures were created using Reaxys. The structures of DMPE-PEG2000 and DMG-PEG2000 were taken from Avanti Polar Lipids and the structure of ALC-0159 was taken from Croda Pharma.

6.3 Materials and Methods

6.3.1. Materials

The ionisable lipid Heptadecan-9-yl 8-((2-hydroxyethyl)[6-oxo-6-(undecyloxy)hexyl]amino)octanoate (SM-102), 4-hydroxybutyl)azanediyl]di(hexane-6,1-diyl) bis(2-hexyldecanoate (ALC-0315), (6Z,9Z,28Z,31Z)-Heptatriaconta-6,9,28,31-tetraen-19-yl 4-(dimethylamino)butanoate (D-Lin-MC3-

DMA) and 1,1'-[[2-[4-[2-[[2-[*bis*(2-hydroxydodecyl)amino]ethyl](2-hydroxydodecyl)amino]ethyl]-1-piperazinyl]ethyl]imino]*bis*-2-dodecanol (C12-200) was purchased from Broadpharm (San Diego, CA, USA). 1,2-dimyristoylrac-glycero-3-methoxypolyethylene glycol-2000 (DMG-PEG2000) were purchased from Avanti Polar Lipids (Alabaster, AL, USA). 1,2-distearoyl-sn-glycero-3-phosphocholine (DSPC) was obtained from Lipoid (Ludwigshafen, Germany). Cholesterol (Chol), citric acid, sodium citrate tribasic dehydrate, and polyadenylic acid (PolyA) were acquired from Merck Life Science (Hertfordshire, UK). Phosphate-buffered saline tablets (PBS pH 7.4) were acquired from Oxoid Ltd. (Basingstoke, UK). Tris (hydroxymethyl) aminomethane (TRIS-base), Amicone Spin column® 100K, ethanol (EtOH), Sodium acetate and sodium chloride were obtained from Fisher Scientific (Loughborough, UK). One-Glo luciferase Assay system and D-Luciferin+K (VivoGlo Luciferin) were purchased from Promega Ltd. (Chilworth, UK). Messenger RNA (EZ Cap Firefly Luciferase mRNA, R1018-APE) and messenger RNA (EZ Cap OVA mRNA, R1028-APE) were obtained from Stratech Scientific (St Thomas' Place, Cambridgeshire, UK). Dulbecoo's Modified Eagle's Medium (DMEM), Minimal Essential Medium (MEM), fetal bovine serum (FBS), sodium pyruvate, and penicillin/streptomycin were acquired from Gibco technologies. RPMI 1640 Medium was acquired from Corning (Flintshire, UK). All solvents and other chemicals were of analytical grade, and milliQ-water was provided by an in-house system.

6.3.2. Formulation of Lipid nanoparticles (LNPs)

Four LNPs formulations (Table 6.1) were prepared using NanoAssemblr Ignite from Precision NanoSystem Inc (Vancouver, BC, Canada) using a toroidal microfluidic chip. Lipid stocks were prepared individually in ethanol. Lipid nanoparticles (LNPs) were composed of DSPC: Chol:SM-102/DLin-MC3:DMG-PEG2000 at molar ratio of 10:38.5:50:1.5% respectively, DSPC: Chol:ALC-0315:ALC-0159 with a molar ratio of 9.4:42.7:46.3:1.6% and DSPC:Chol:C12-200:DMPE-PEG2000 at molar ratio of 16:46.5:35:2.5% respectively in ethanol. All formulations were prepared at a final mRNA concentration of 70 µg/mL. Citrate buffer (SM-102, ALC-0315 and MC3) or sodium acetate pH 4 50 mM (C12-200) was used as an aqueous buffer that contains the firefly luciferase (Fluc-mRNA) or OVA mRNA at an N/P ratio of 8 (Table 6.1). The flow rate ratio (aqueous to solvent) of 3:1 and total flow rate of 15 mL/min were selected based on previous results (Chapter 2), demonstrating that production of liposomes at 3:1 produced small, homogenous nanoparticle dispersion of below 100 nm. PolyA was used as a surrogate for the mRNA in cellular uptake studies, and the fluorescent marker dye DilC was

added to the organic phase to prepare DilC labelled LNPs. A concentration of 1% of the total molarity of the lipid mixture were used for the fluorescent dyes.

Table 6.1: Four different LNP formulations were selected and included the formulations used in the Pfizer/BioNTech, Moderna and Onpattro formulations which are all approved for clincal use. C12-200 was also selected for comparison. All formulations were composed of the same phospholipid (DSPC) and sterol (cholesterol) with the ionisable lipid and PEG lipid varied between the formulations. All formulations were formulated at an N/P ratio of 8 and purified in 10 mM Tris/300 mM sucrose buffer.

	C12-200	Pfizer/BioNTech	Moderna	Onpattro
Phospholipid	DSPC			
Sterol	Cholesterol			
Ionisable Lipid	C12-200	ALC-0315	SM102	DLin-MC3-DMA
PEG Lipid	DMPE-PEG2000	ALC-0159	DMG-PEG2000	
Molar Ratio (PL:Sterol:IL:PEG)	16:46.5:35:2.5	9.4:42.7:46.3:1.6	10:38.5:50:1.5	
Wt/wt ratio	16.4:23.3:51.6:8.7	11.7:26.1:56:6.2	12.7:24:57.2:6.1	13.5:25.4:54.7:6.4
mRNA Buffer	50 mM Sodium Acetate, 100 mM Sodium Chloride (pH 5.5)	50 mM Citrate Buffer (pH 4)		
Lipid:mRNA Ratio (w/w)	5.4	17.9	16.8	15
N/P Molar	8			
External Buffer	10 mM Tris/ 300 mM Sucrose			

6.3.3 Removal of Ethanol Content and Buffer Exchange with Centrifugal Filter Unit

Following the preparation of the LNPs, they were purified by a spin column centrifugal filter unit to remove ethanol content and increase pH to physiological conditions through buffer exchange. The LNPs were diluted 1:40 times in 10 mM Tris/300 mM Sucrose and then centrifuged at 2,000 g at 20°C until the desired volume of the LNPs is recovered.

6.3.4 LNP Characterisation: Particle Size, Polydispersity and Zeta Potential

Particle size (Z-average diameter), polydispersity index (PDI) and zeta potential (ZP) were measured by dynamic light scattering (DLS) using a Zetasizer Nano ZS (Malvern Panalytical Ltd., Worcestershire, UK) equipped with a 633 nm laser and a detection angle of 173◦. LNPs were diluted in filtered (0.22 µm) 10 mM Tris to 0.1 mg/mL LNP concentration. The same dilution was used for zeta potential measurements. The dispersant (Tris) refractive index (RI) and viscosity values were 1.34 and 1.0037 cP, respectively, whereas the material absorbance and RI were 0.001 and 1.45 respectively. Zetasizer Software v.7.11 (Malvern Panalytical Ltd., Worcestershire, UK) was used for the acquisition of data. All measurements were undertaken in triplicate with the attenuation value between 7 and 8.

6.3.5 Quantification of Nucleic Acid Loading: Poly(A) and mRNA

The encapsulation efficiency of PolyA/Fluc mRNA was determined using Ribogreen Assay according to the manufacturer's instructions. Briefly, 50 µL of samples were added to the 96-well black plates in the presence or absence of 0.1 w/v% Triton X-100, referring to the total mRNA and unencapsulated mRNA, respectively. The plate was incubated at 37 °C for 15 minutes followed by the addition of Ribogreen fluorescent dye. To the Triton (+) wells, Ribogreen dye was added at a concentration of 1:200 and to the Triton (-) 1:500. The fluorescence intensity was quantified using GloMax® Discover Microplate Reader at excitation and emission wavelength of 480 nm/520 nm respectively. The encapsulation efficiency (%) was calculated according to the standard curve of Triton (+) and Triton (-) using Equation 6.1.

Equation 6.1: Equation used to calculate the mRNA encapsulation efficiency

$$\textbf{mRNA encapsulation } \% = \frac{\boldsymbol{Encapsulated\ mRNA - Unencapsulated\ mRNA}}{\boldsymbol{Encapsulated\ mRNA}} \times \mathbf{100}\ \%$$

6.3.6 Cell Culture

HEK293 cells were maintained in MEM media, HeLa cells were maintained in DMEM media and THP-1 cells were maintained in RPMI 1649 media all supplemented with 10 % fetal bovine serum (FBS), 1% L-glutamine, 1% penicillin/streptomycin, 1% sodium pyruvate and 2.5 µg/mL amphotericin B. Cells were incubated at 37°C in a 5% CO_2 atmosphere.

6.3.7 *In vitro* assays

Cytotoxicity and uptake assays for PolyA loaded LNPs/1% mole DilC18 were carried out using the HEK293, HeLa and THP-1 cell lines. Briefly, 100 µL cells (80% confluence) were seeded into 96 well plates at 1.5 x 10^4 cell/ well for HEK293, 1 x 10^4 cell/ well for HeLa and 4 x 10^4 cell/ well for THP-1 cells and incubated for 48h at 37°C, 5% CO_2. THP-1 cells were differentiated prior to seeding with 0.2 µM phorbol 12-myristate 13-acetate (PMA). Then, cells were treated with 100 µL of LNPs at a concentration of 0.25 to 2 µg/mL for 24 or 48 h, followed by incubation with 1X alamarBlue reagent (alamarBlue™ cell viability reagent, ThermoFisher) for 4 h or treatment with 2% TritonX in PBS for 10 min. Cell viability was quantified by measuring the fluorescence of the plate at 570 nm and 595 nm. While cell uptake for LNPs was quantified by measuring fluorescence intensity using GloMax® Discover

Microplate Reader. A linear calibration curve up to 500 ng/mL was obtained (R2 ≥ 0.998) for LNPs. mRNA expression in cells assessment, an *in vitro* FLuc mRNA expression was carried out 100 µL cells (80% confluence) were seeded into 96 well plates at 1.5 x 10^4 cell/ well for HEK293, 1 x 10^4 cell/ well for HeLa and 4 x 10^4 cell/ well for THP-1 cells and incubate for 48h at 37°C, 5% CO2. Cells were treated with LNPs at a concentration of 0.25 to 2 µg/mL for 24 or 48 h, followed by adding 100 µL of One-Glo Luciferase assay system (Promega). Bioluminescence was quantified by measuring total luminescence for the total range of wavelength.

6.3.8 *In vivo* Gene Expression studies

mRNA-loaded LNPs were used for the biodistribution *in vivo* tracking. Groups of five (6–9 week old) female BALB/c mice were housed under conventional conditions (22 °C, 55 % humidity, 12 h day/night cycle) in their experimental cage and were given a standard diet ad libitum. Mice were injected 50 µL (100 µg/mL mRNA) intramuscularly in both quadricep muscles. Mice imaging was carried out using an IVIS Spectrum (Perkin Elmer) using Living Image software for data capture and analysis. The mRNA expression was detected using the bioluminescence at the emission wavelength firefly luciferase (560 nm). A medium binning and f/stop of 2 was used and acquisition time was determined for each image with auto-exposure settings. Mice were anaesthetized for imaging using 3% Isoflurane. Anaesthesia was maintained during imaging at 1% Isoflurane. Images were taken after administration of formulations at Time 0, 6, 24 and 48 h post injection. The total flux (p/s) was calculated at the injection site (region of interest) for bioluminescence. The average total flux was calculated and expressed as mean ± SEM.

6.3.9 Immunization studies

Groups of three (6-9weeks old) female BALB/c mice were immunized intramuscularly on days 0 and 28 in their right thighs (50 µL) with (5 µg/dose) mRNA encoding for ovalbumin (OVA) formulated in SM-102- LNPs or free mRNA encoding for ovalbumin (OVA). Two further mice were used as a control. Sera from individual mice were collected on days 0 prior to immunisation, four weeks after the first vaccination (day 27) and two weeks after the second vaccination (day 42).

6.3.10 Specific IgG isotype responses

Blood samples collected over the course of the study were used to assess the efficacy of formulations on serum-specific IgG isotype (Total IgG, IgG1 and IgG2a), and antibody titres could be determined. Briefly, a 96 well micro-titre plate (Greiner Bio-One GmbH, Frickenhausen, Germany) was coated with 100 µL (1 µg/mL PBS pH 9.0) of albumin from chicken egg white (OVA) (Merck Life Science, Hertfordshire, UK) overnight at 4ºC. The plates were then washed three times with wash buffer (PBS pH 7.4/0.05% v/v Tween-20). The plates were blocked by adding 150 µL of Marvel® solution (4% w/v

in PBS pH 7.4) to the appropriate wells of the plate, and the plate was incubated for 1 hour at 37ºC. The plate was washed three times in wash buffer, and then 100 µL of the relevant serum sample, serially diluted in PBS buffer (1:800 or higher depending on the experiment), was added to the appropriate wells of the plate. The plate was incubated as before for 1 hour, washed three times in wash buffer, and 100 µL/well of horseradish peroxidase (HRP) conjugated goat anti-mouse Total IgG, IgG1 or IgG2a used of 1:2500, 1:20000 or 1:5000 respectively dilution /PBS pH 7.4 /10 % v/v FCS were added to the appropriate wells of the plate. The plate was incubated for 1 hour as before, washed three times with wash buffer, and 100 µL/well of TMB substrate (Fisher Scientific, Loughborough, UK) were added. The reaction was stopped after 20 minutes by the addition 50 µL/well of 10% aqueous sulphuric acid. The absorbance of the wells was measured at 450 nm using a Microplate Manager® Device (Bio-Rad Laboratories, Inc, California. USA) and the mean endpoint ± standard deviation (SD) for each group was determined.

6.3.11 Ethics Statement

Animal experiments and experimental procedures were carried out in accordance with UK Home Office regulations and the University of Strathclyde Animal Welfare and Ethical Review Board regulations under project license number PPL PP1650440. BALB/c mice were bred and maintained in the Biological Procedures Unit at the University of Strathclyde, Glasgow, and experimental design and reporting adhered to the ARRIVE guidelines.

6.3.12 Statistical Analysis

Results are represented as the mean ± SD of at least n = 3 independent batches. ANOVA tests were used to assess statistical significance, with a Tukey's post ad hoc test (p-value of less than 0.05).

6.4 Results

6.4.1 Production and Characterisation of mRNA-LNPs

The production of LNPs is very similar to liposomes. However, the mRNA payload is added to the aqueous phase prior to microfluidic production, compared to liposomes produced previously that were loaded with drug after microfluidic production. In this way, the negatively charged nucleic acid can electrostatically interact with the ionisable lipid due to the acid pH of the aqueous buffer. LNPs were prepared encapsulating Fluc mRNA for the *in vitro* cell expression and viability, and *in vivo* expression and encapsulating PolyA for *in vitro* cell uptake studies. All formulations were prepared at an N/P of eight, assuming SM-102, ALC-0315, and MC3 have 1 positive headgroup, and C12-200 has 5, encapsulating a final mRNA/PolyA concentration of 70 µg/mL. Samples prepared for *in vivo* studies were then concentrated to a final mRNA concentration of 0.14 mg/mL. Studies were carried out to

determine whether this dilution affected the physicochemical properties as well as the *in vitro* and *in vivo* profiles.

The final lipid CQAs in Table 6.2 show that all LNPs could effectively entrap mRNA with encapsulation efficiency > 85% in LNPs with a diameter < 100 nm and a low polydispersity index (PDI) (< 0.1) and near neutral zeta potential.

Table 6.2: LNP physicochemical characteristics produced at a FRR 3:1 and TFR 15 mL/min using microfluidics. Results represent n=4 independent batches.

LNP	Size (nm)	PDI	Zeta Potential (mV)	%EE
SM102	97 ± 7.0	0.07 ± 0.02	9.3 ± 3.5	94 ± 1.8
ALC-0135	85 ± 6.4	0.09 ± 0.02	-2.2 ± 3.3	85 ± 4.5
MC3	93 ± 3.0	0.05 ± 0.02	6.9 ± 2.2	92 ± 1.2
C12-200	73 ± 2.3	0.08 ± 0.03	-3.7 ± 3.6	98 ± 1.6

6.4.2 SM102 Cell Expression, Viability and Uptake Optimisation

Initially, to establish cell expression, viability, and uptake studies, LNPs using SM-102 as the ionisable lipid were investigated. These were manufactured using protocols previously established in this thesis and in line with other published work (25). Three cell lines were selected: HEK293, HeLa and THP-1 cells, which were differentiated into macrophages prior to the addition of the sample. These cell lines were selected as they are readily available and can be easily expanded (149). Cells were treated with 0.25 to 2 µg/mL of mRNA-LNPs, as characterised in Table 6.2. Cells were then incubated for 24, 48 and 72 h to determine the optimal incubation time for LNP expression, viability, and uptake (Figure 6.2).

The results from the cell expression study showed that both the HEK293 (Figure 6.2A) and HeLa (Figure 6.2B) had higher expression than the THP-1 (Figure 6.2C) cell lines, with expression decreasing across the 3 time points. HEK293 cells showed significantly higher levels of expression after a 48-h incubation period ($P<0.05$), with a dose-dependent increase in expression observed when the mRNA concentration increased from 0.25 to 1 µg/mL mRNA (Figure 6.2A). HeLa cells showed overall significantly ($p<0.05$) higher levels of expression at 24 h with expression levels decreasing as the incubation period increased (Figure 6.2B). A dose-dependent increase in expression was observed as

the mRNA concentration increased from 0.25 to 2 μg/mL mRNA with no advantage in increasing the incubation period. In general, there was no significant difference in the expression across all 3 time points for the THP-1 cells, and overall expression was low in this cell line.

Cell viability studies were carried out to determine whether the differences in cell expression were due to a decrease in cell viability with increasing incubation time. The results showed HEK293 cells had no notable difference in cell viability across all mRNA concentrations with a slight decrease in viability with increasing incubation period (Figure 6.2D). HeLa cells showed no notable differences in cell viability across all 3 time points and mRNA concentrations demonstrating that the LNPs were not having any toxic effects on these cells (Figure 6.2E). THP-1 cells had decreased viability with increasing mRNA concentration, and the longer the cells were incubated with the mRNA-LNPs, the lower the cell viability ($p<0.05$) (Figure 6.2F). This decrease in viability may account for the decrease in cell expression with increasing mRNA concentration and incubation time.

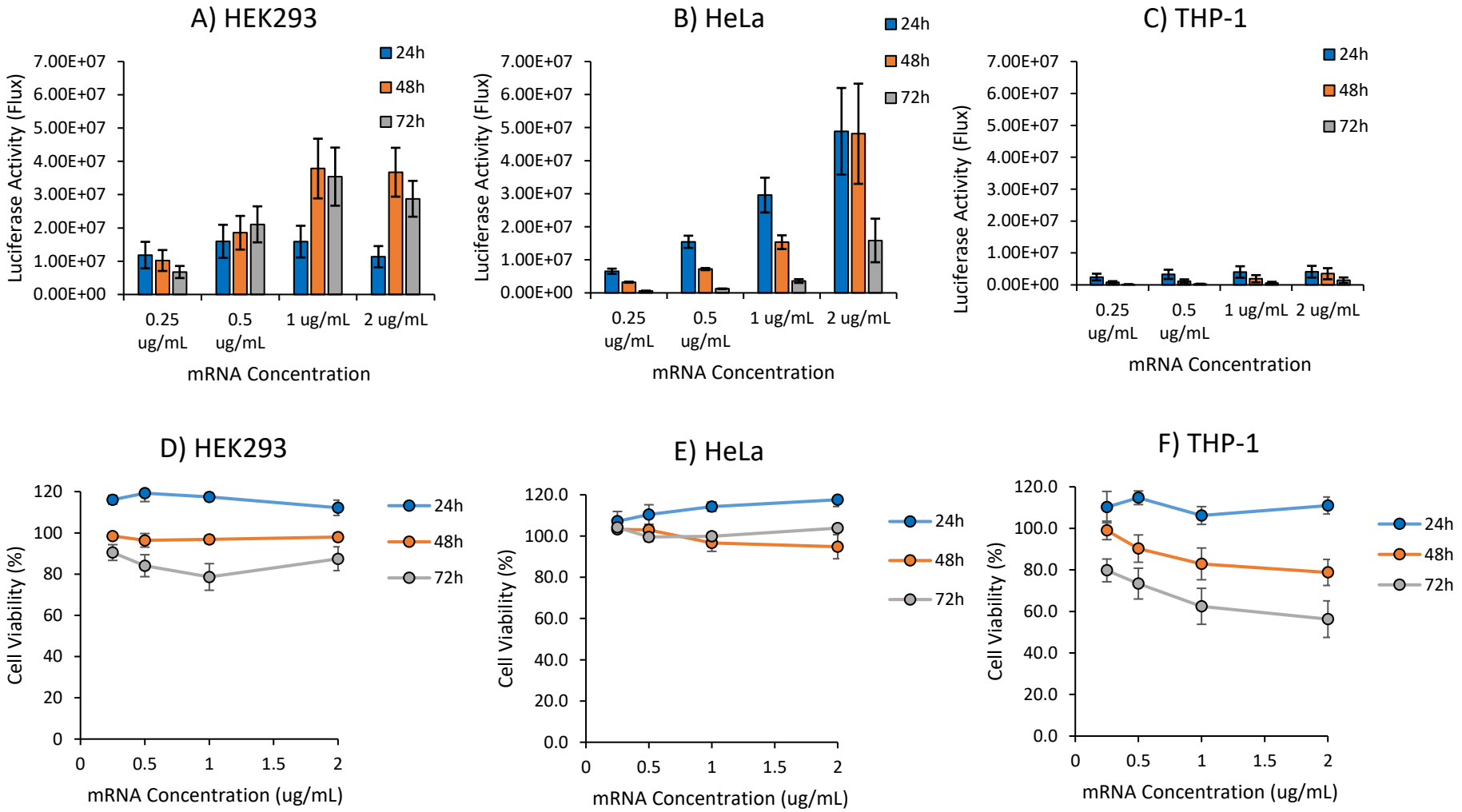

Figure 6.2: SM102 cell expression in A) HEK293, B) HeLa and C) THP-1 cells and cell viability in D) HEK293, E) HeLa, and F) THP-1 cells treated with 0.25. 0.5, 1 and 2 µg/mL mRNA and incubated for 24, 48 and 72 hours. Results represent mean ± SEM, n=3 independent batches of LNPs

To further investigate this, cell uptake studies were performed over a 48 h time period to determine whether the differences in cell expression were due to varying levels of cell uptake of the LNPs. To achieve this, LNPs were tagged with a fluorescent dye, DilC as previously used in Chapter 4. LNPs, containing DilC were added to cells at the same mRNA concentrations as was used for cell expression and viability. At each time point, the cells were then lysed with 10% TritonX-100, and the fluorescence was measured. All cell lines showed increased cell uptake at 48 h compared with 24 h; however, in the HeLa (Figure 6.3B) and THP-1 (Figure 6.3C) and cell lines, this did not correspond with increased cell expression. Therefore, from these results, it was concluded that the optimal incubation period was cell-line dependent. We therefore selected 48 h for the HEK293 (Figure 6.3A) cell line and 24 h incubation for both HeLa (Figure 6.3B) and THP-1 (Figure 6.3C) cell lines for all future experiments.

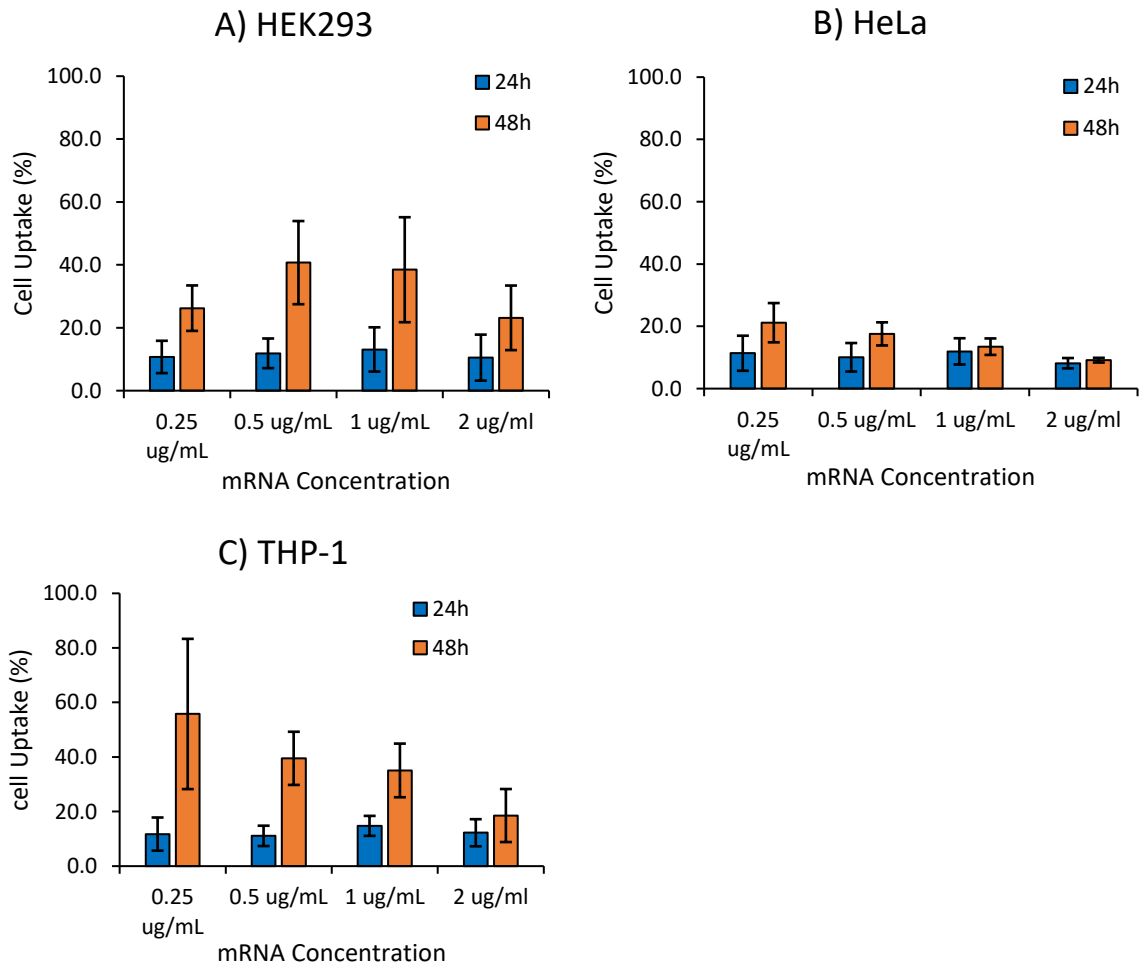

Figure 6.3: SM-102 cell uptake in A) HEK293, B) HeLa and C) THP-1 cells lines incubated with 0.25, 0.5, 1 and 2 µg/mL mRNA. Results represent mean ± SEM, n=3 independent batches

6.4.3 *In vitro* cell expression and uptake of mRNA-LNPs

Once the optimal *in vitro* parameters were identified, this protocol was used to investigate 4 LNP formulations (Table 6.1). Cells were again treated with LNPs at an mRNA concentration of 0.25 to 2 µg/mL and incubated for the selected time period as established by the SM-102 optimisation studies.

The results for the cell expression studies showed that the THP-1 cells had an overall lower concentration than the other 2 cell lines. However, a dose-response was observed for all 4 LNP formulations (Figure 6.4C). Cell expression studies showed that across all three cell lines tested, SM-102 showed the highest levels of expression, followed by ALC-0315. HEK293 cells (Figure 6.4A) showed overall higher levels of expression for all 4 formulations tested with a dose response curve for SM-102, ALC-0315 and MC3. However, there was no dose response trend observed for C12-200 in either the HEK293 (Figure 6.4A) or HeLa (Figure 6.4B) cell lines. This may potentially be due to the cellular uptake mechanism used for each formulation.. Cell viability data indicated that all four formulations showed high cell viability, indicating no toxic effects from any of the formulations across all the mRNA concentrations tested. There was a slight decrease in viability observed at the highest concentrations of SM-102 and C12-200 in the THP-1 (Figure 6.4F) and HeLa (Figure 6.4E) cells; however, this was no more than 20%.

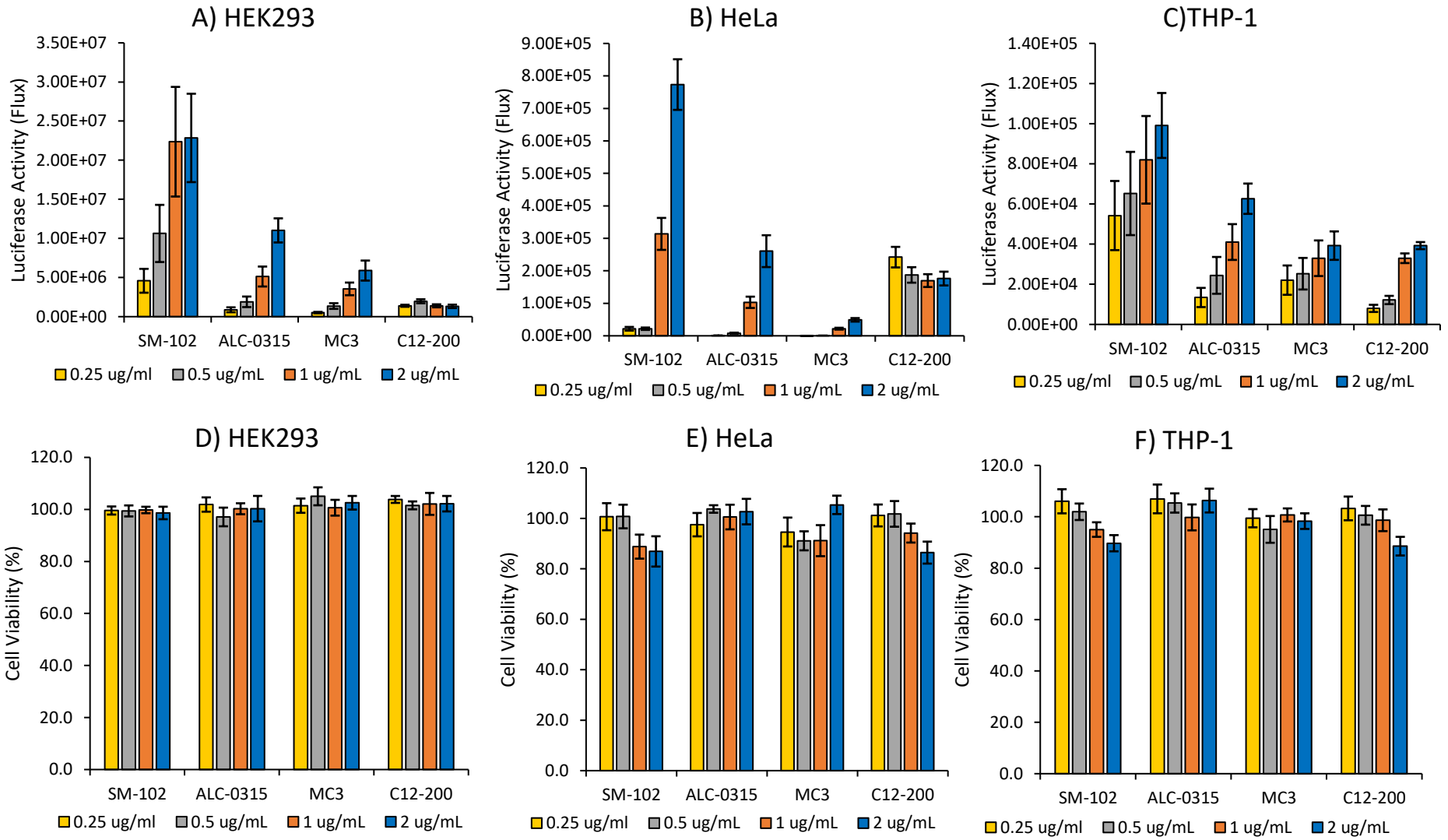

Figure 6.4: Cell expression for SM-102, ALC-0315, MC3 and C12-200 in A) HEK293, B) HeLa and C) THP-1 cells and cell viability in D) HEK293, E) HeLa, and F) THP-1 cells treated with 0.25, 0.5, 1 and 2 µg/mL mRNA.. Results represent mean ± SEM, n=3 independent batches

In order to determine whether high levels of expression were correlated with high LNP internalisation, cellular uptake studies were carried out (Figure 6.5). The results from these experiments show the highest uptake in the HEK293 cell for all four formulations, which may contribute to the higher levels of expression in this cell line. In general, higher % levels of uptake were achieved at lower mRNA concentrations. When the lipid concentration was calculated there was increased lipid concentration at higher mRNA concentration, specifically in the HEK293 cells, however this was not always correlated with increased uptake. This would suggest that cells have a limit of the amount of lipid they are capable of internalising.

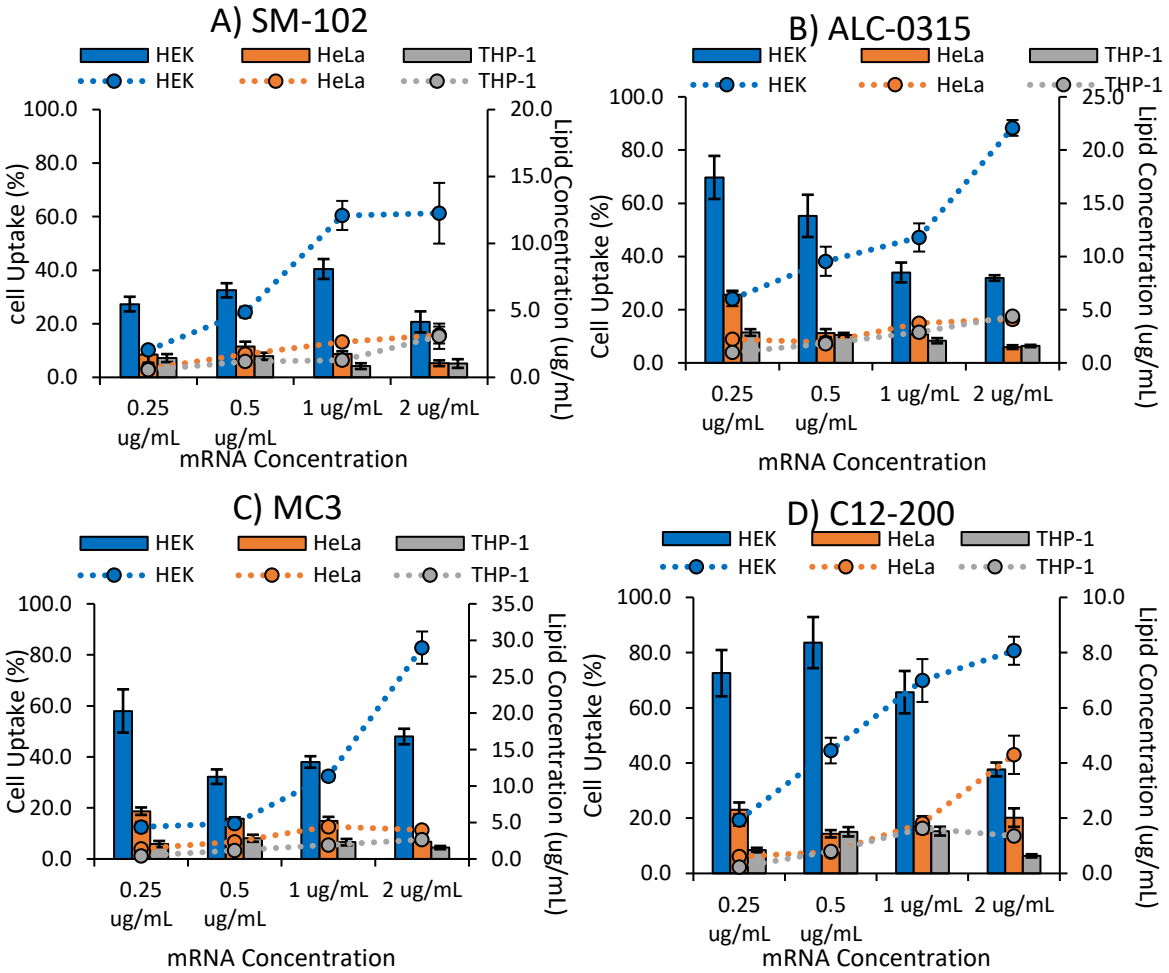

Figure 6.5: Cell uptake and calculated lipid concentration of A) SM-102, B) ALC-0315, C) MC3 and D) C12-200 in THP-1, HeLa and HEK293 cells lines incubated with 0.25, 0.5, 1 and 2 µg/mL mRNA. Results represent mean ± SEM, n=3 independent batches

6.4.4 GFP Cell Expression

The 4 LNP formulations were then prepared encapsulating GFP-mRNA. These were then incubated in all 3 cell lines for either 24 (HeLa and THP-1 cell lines) or 48 h (HEK293 cells), and images were taken for each formulation at the same concentration and using the same light settings on the microscope. The results in Figure 6.6 align with the cell expression data in Figure 6.4 and confirm that SM102 has the highest levels of cell expression, followed by ALC, DLin and C12-200. When comparing between the cell lines, HEK293 and THP-1 cells showed the clearest cell expression with minimal background fluorescence. HeLa cells show overall good fluorescence; however, the expression in individual cells was not as clear as the other 2 cell lines.

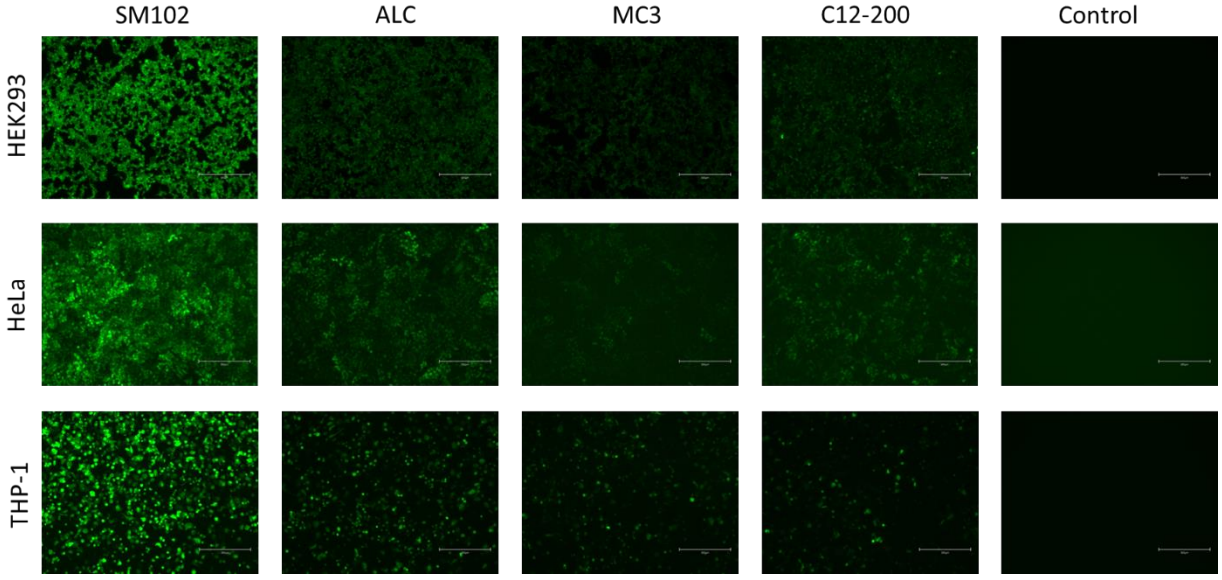

Figure 6.6:Cell images of HEK293, HeLa and THP-1 cells treated with 2 µg/mL GFP-mRNA.

6.4.5 *In vivo* Fluc-mRNA expression

Having identified the biodistribution and drug release of doxorubicin liposomes as a measure of efficacy (Chapter 5), it was also important to consider the efficacy of the 4 LNP formulations. The *in vivo* expression of mRNA-LNPs was tested using BALB/c mice. The mice were intramuscularly injected 5 µg per dose in both hind legs. The LNPs were evaluated for the *in vivo* expression profile (Figure 6.7). The presence of expressed luciferase was noted mainly at the injection site (Figure 6.7A) and the liver (Figure 6.7B). At 6h, LNPs prepared with ALC-0315 and SM-102 had similar level expression at the injection site (Figure 6.7A) and were significantly higher than both MC3 and C12-200 ($P < 0.05$). Both had 5 fold higher expression than C12-200 and MC3, which had almost the same level of expression. The expression was lowest at 48 h, and there was no significant difference in expression between the 4 LNP formulations. ALC-0315 had significantly higher expression in the liver compared with the other four LNPs ($P<0.05$) followed by SM-102 with 5-fold less expression at 6 h. However, the expression in

the liver among SM-102, MC3 and C12-200 was non-significant compared to the ALC-0315. After 6h, the expression level was not significantly different between the four formulations (P>0.05).

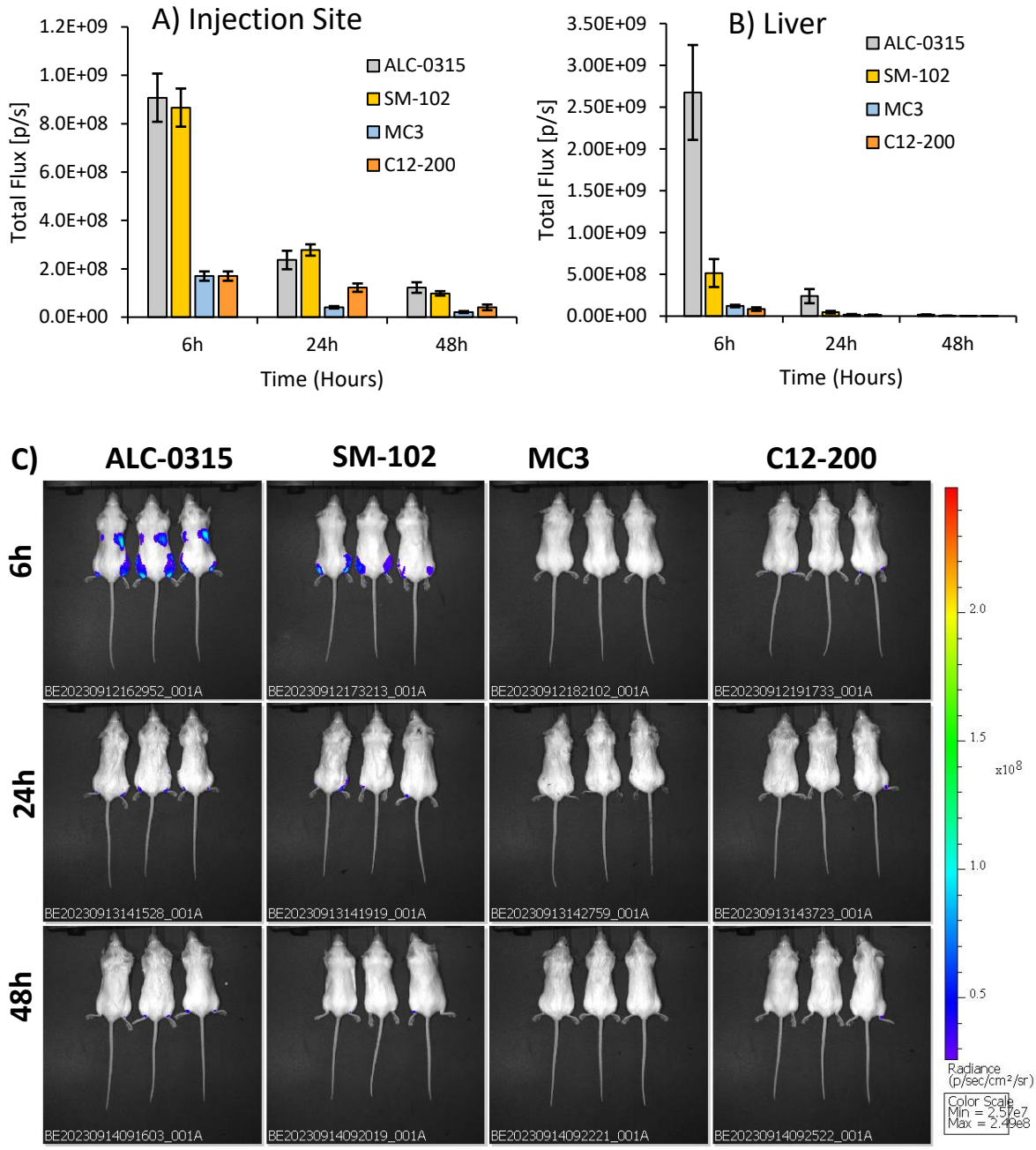

Figure 6.7: Luciferase expression after Fluc-mRNA LNP intramuscular injection in female BALB/c mice. The injected mRNA dose was 5 µg mRNA encapsulated in LNPs. A) Bioluminescence signal per injection site at 6, 24 and 48 h, B) Bioluminescence signal per liver at 6, 24 and 48 h and C) Representative bioluminescence IVIS images at selected time point after mRNA-LNP injection. Data are expressed by the mean ± SEM (a total of 6 mice per group split over 2 independent studies.

6.4.5 Immunisation Study

The application of LNPs as vaccines means that it is not just important to determine the expression and biodistribution of the formulation but also to assess the ability of each formulation to produce an immune response. To study the vaccine efficacy of the mRNA-LNPs, BALB/c mice were immunised with 5 µg of OVA mRNA encapsulated in the 4 different LNPs. Mice were dosed via intramuscular injection with a prime (day 0) and boosters (day 28). Mice were tail bled for serum collecting on day 0, 27 days after the first injection and two weeks after the second injection (day 42), and the antibody endpoint titres were detected by ELISA (Figure 6.8). The results demonstrate that all formulations mounted a stronger total IgG and IgG2a responses at day 42 compared with IgG1. SM-102 showed to have the highest response for total IgG, followed by DLin and then ALC. Whereas DLin showed to have the highest response for IgG2a followed by ALC. Moreover, from the IgG2a/IgG1 ratio, all formulations demonstrated to have IgG2a/IgG1 ratio > 1. confirming that all formulated LNPs can stimulate a strong Th1 response (Figure 6.8D).

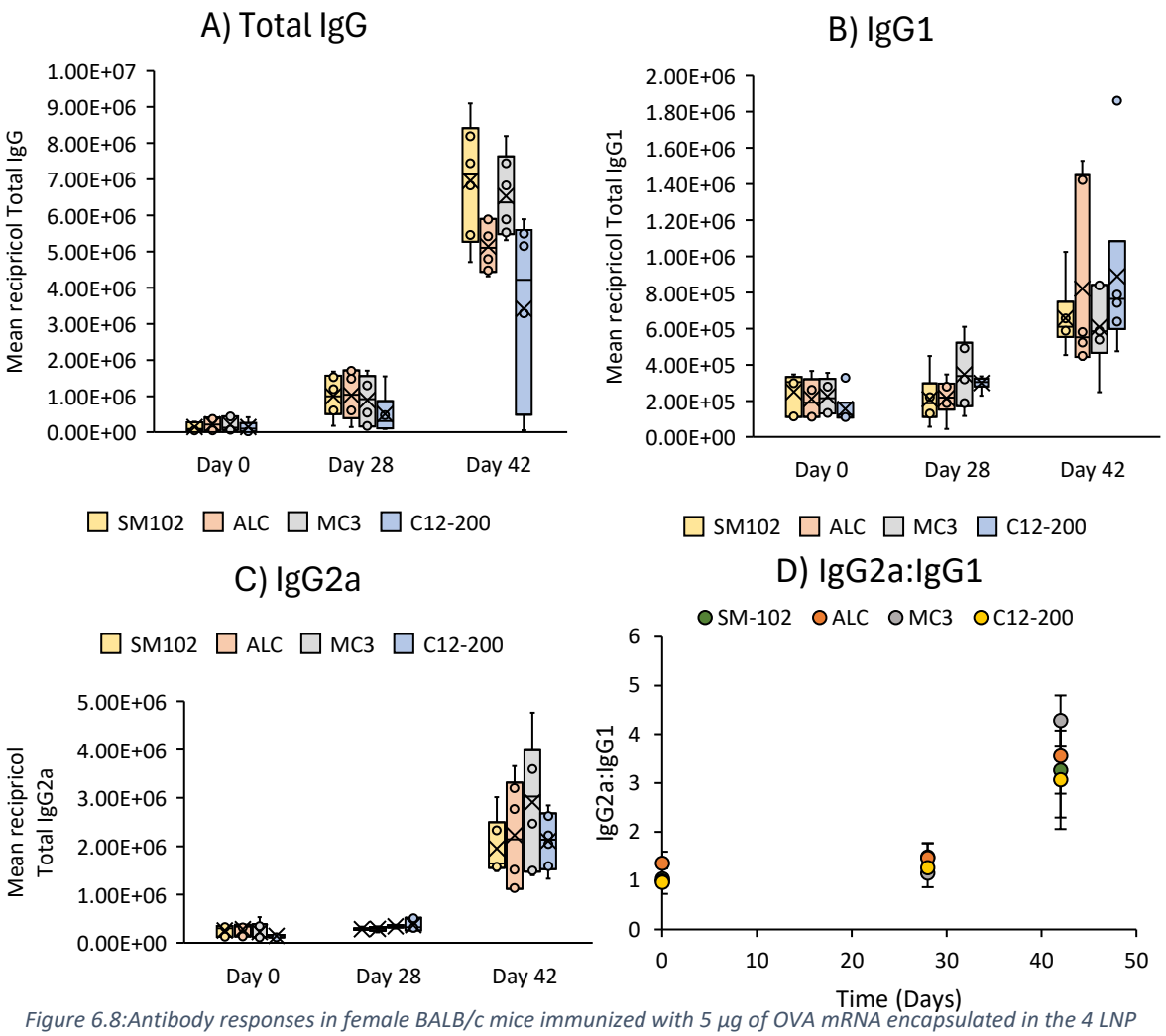

Figure 6.8:Antibody responses in female BALB/c mice immunized with 5 µg of OVA mRNA encapsulated in the 4 LNP formulations on days 0 and 28. Serums were collected prior to the first dose, and after the first and second doses via tail bleeding. A) Total anti-OVA IgG endpoint titres elicited by OVA mRNA LNPs, B) Anti-OVA protein directed IgG1, C) Anti-OVA IgG2a endpoint titres elicited by OVA mRNA LNPs and D) IgG2a:IgG1 ratio.

6.5 Discussion

The discovery of liposomes for the delivery of small molecule compounds created the building blocks for the further development of novel lipids for the delivery of nucleic acids. Together with the development of novel scalable manufacturing techniques, such as microfluidics, has allowed the development of novel nanoparticle delivery systems to be translated from bench to bedside. The performance of mRNA-LNPs is dependent on their *in vivo* biodistribution, ability to trigger an immune response and their inherent adjuvanticity (147). The uptake and delivery of mRNA-LNPs is a complex, multi-step process relying on the ability of the LNP to attach to the target cell surface, enter the cell, and release the mRNA in the endosome allowing for ribosomal protein expression (146). During this process, some of the mRNA payload is lost at each stage making it very difficult to accurately predict the efficacy of the LNP-mRNA formulation *in vitro* (150).

Four different LNP formulations (SM-102, ALC-0315, MC3 and C12-200) were selected for determination of *in vitro* and *in vivo* correlations. All formulations were produced using microfluidics and showed similar characteristics (particle size < 100 nm, PDI < 0.1, and encapsulation > 80%). Cell culture models represent an important pre-clinical assessment of LNP delivery and efficacy *in vitro* (151). The *in vitro* studies were carried out in immortalised (HEK293 and HeLa) and immune cells (THP-1) to allow for initial assessment of mRNA-LNP cell viability and transfection potency. These cell lines were selected as they are most commonly used for vaccine testing and development (152-154). Cell expression studies showed the same trend for all four formulations in all 3 cell lines (Figure 6.4 A, B & C). The HEK293 cells showed the highest levels of expression for all four formulations, with SM-102 showing the highest expression, followed by ALC-0315, MC3 and C12-200. The HEK293 cells were also shown to require the longest incubation time to achieve optimal expression, requiring 48-hour incubation, compared with the HeLa and THP-1 cells that only required 24-hour incubation (Figure 6.2 A, B & C). It was also shown that increased incubation time did not correlate with increased expression (Figure 6.2), and no notable *in vitro* toxicity was observed for any formulation in all 3 cell lines (Figure 6.4 D, E & F). Based on these results, HeLa cells would be the best cells for *in vitro* screening due to the short incubation period required for high cell expression.

Cellular uptake of LNPs is a complex process and can be dependent on the binding of endogenous proteins to the LNPs, which can then direct them to different organs. Apolipoprotein E (ApoE) has been shown to favourably bind to neutral LNPs and direct them to hepatocytes through receptor-mediated endocytosis by low-density lipoprotein receptor (LDL-R) (146, 147). Cell lines that are derived from the liver and kidneys naturally produce ApoE, which may explain why the HEK293 cells displayed the highest levels of expression. HeLa cells do not naturally produce ApoE; however, they express ApoE receptors (155). THP-1 cells, once differentiated, have been shown to express ApoE.

However, the expression pattern is heterogeneous, with approximately 5% of the cells overexpressing ApoE, which subsequently results in apoptosis of the cells (156). Endogenous ApoE is present in the FBS supplemented in the media. However, the concentration of ApoE is unknown, which may lead to varying concentrations of ApoE within the media, resulting in differences in the uptake and subsequent expression of the LNPs (146). The major mechanism for the internalisation of LNPs is mediated through a clathrin-mediated pathway due to the structural similarities between LNPs and chylomicrons (lipoprotein particles composed of phospholipids, triglycerides, cholesterol and protein). However, C12-200 has been reported to undergo cell uptake via an ApoE-independent, micropinocytosis pathway (157). Love et al. investigated the mechanism by which C12-200 is internalised, specifically using HeLa cells (158). In this study, C12-200 particles encapsulating siRNA were incubated in the presence of labelled cargoes that are known to enter cells by different endocytic pathways. The results suggested that C12-200 was internalised via a macropinocytosis mechanism due to the presence of membrane ruffling and actin rearrangement observed in the cells. The most important pathway for mRNA LNP cellular uptake is endocytosis, which has been demonstrated to be dependent on the LNP CQAs, including the charge on the LNP surfaces. Neutral LNPs have shown an increased preference for cellular uptake compared with highly positive or negatively charged LNPs due to electrostatic repulsion in the presence of phospholipids and proteoglycans in the cell membrane (159, 160).

One of the key factors for efficient protein expression is the endosomal escape ability, which is determined by the pKa values and chemical structures of the ionisable lipid (142). As cone-shaped ionisable lipids with a small head group and broader tail are incompatible with cylindrical lipids in the lipid bilayer of the endosome, resulting in destabilisation of the endosomal membrane and mRNA release into the cytosol for subsequent translation. The degree of ionisation of the ionisable lipid may explain the higher expression levels observed from SM-102, as this has the highest pKa and is therefore more ionised at intraluminal pH (161). Despite the low expression level for C12-200, results showed that C12-200 had a dose-dependent expression in the THP-1 cells. C12-200 LNPs have demonstrated potency in inducing robust T-cell proliferation and cytokine expression in THP-1 cells (162). Although the studies cited primarily focus on animal models and other cell types, the findings suggest that C12-200 LNPs could be a promising tool for enhancing THP-1 cell responses. The ability of LNPs to deliver mRNA and induce immune responses, as well as their potential in gene editing, underscores their versatility and potential in immunotherapy and vaccine development. Further research is needed to directly assess the effects of C12-200 LNPs on THP-1 cells and to optimize their formulation for specific therapeutic applications. The uptake profile for all formulations across the cell line was revealed to have the same observations.

The lower transfection rate of THP-1 cells with LNPs can be attributed to several factors, including the activation state of immune cells, the charge of ionizable lipids at physiological pH, the lipid composition of LNPs, the need for cell-specific transfection methods and the transient nature of mRNA expression (144, 163, 164).

The next step was to examine the four formulations *in vivo* to determine whether there was any correlation in expression with the *in vitro* results. All LNP formulations were manufactured, encapsulating flu mRNA encoding the luciferase protein for IVIS mRNA expression studies and with mRNA encoding OVA albumin protein for the immune stimulation study. The results showed high levels of mRNA expression 6 hours post-injection for all formulations (Figure 6.7), with SM-102 and ALC-0315 showing higher levels of expression than MC3 and C12-200. When analysing the injection site, there was no significant difference in expression between SM-102 and ALC-0315. However, ALC-

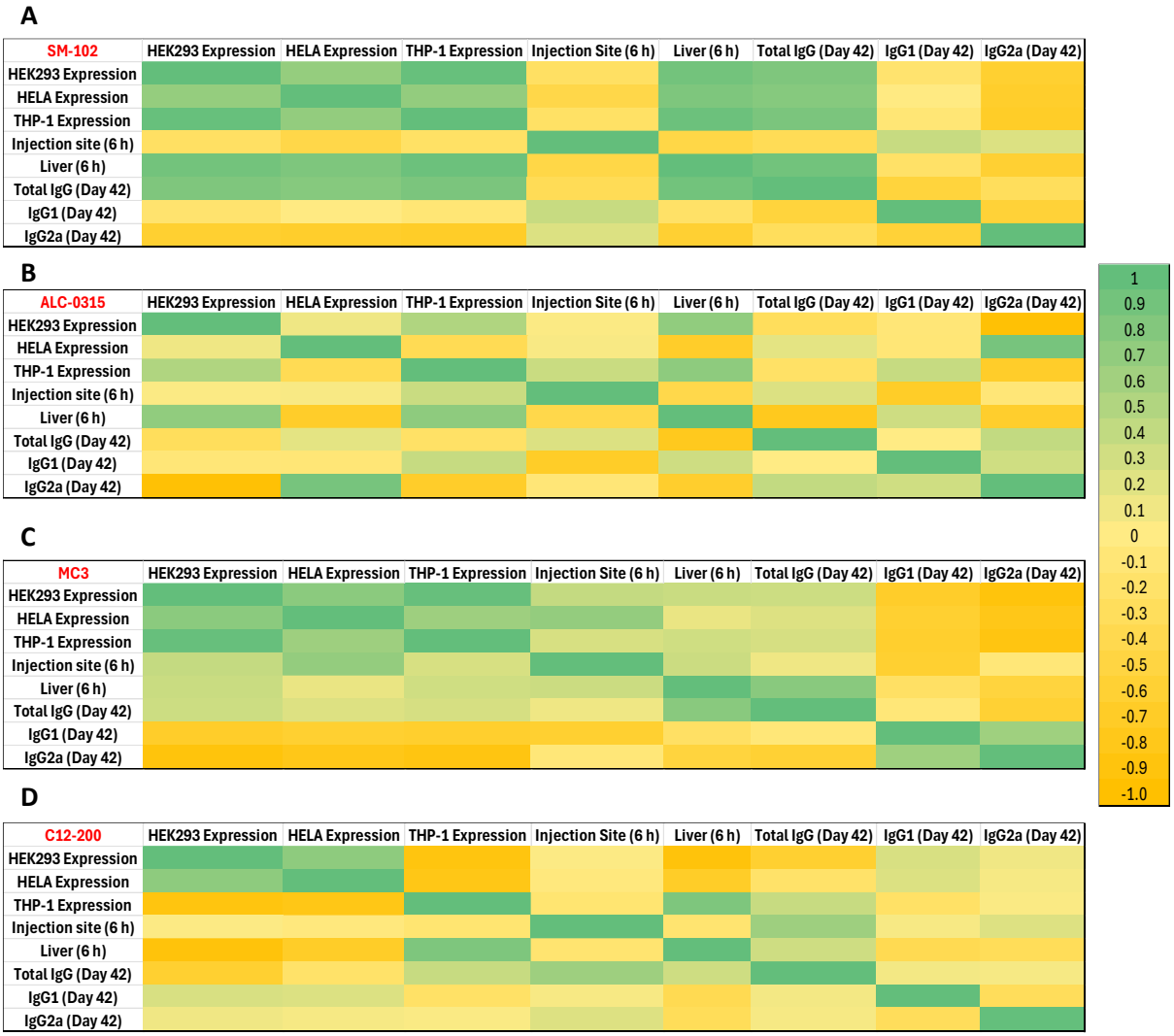

Figure 6.9:Heat maps generated for the correlation between in vitro cell studies and in vivo studies for A) SM102, B) ALC-0315, C) MC3 and D) C12-200. All cell expression values were taken for cells treated with 2 µg/mL mRNA. The IVIS results for the injection site and liver fluorescence were taken from the measurements at 6 h and the immunisation data was taken from the 42-day time point.

0315 showed significantly higher expression in the liver compared with SM-102, MC3 and C12-200. A study on rats showed that in intramuscular administration of ALC LNPs with labelled cholesterol, the highest accumulation for transfection was in the liver, with 18% of the transfection (29). These differences in expression were less obvious in the immunisation study, suggesting that high protein expression levels do not always translate to a high immune response. The use of high doses in the mice may mean that the response is at its maximum therefore any differences in immune response would be difficult to determine. Studying a range of lower response may allow for more discrimination between formulations.

Heat maps were generated to determine whether there was any correlation between *in vitro* and *in vivo* expression levels (Figure 6.9). In this, the expression in all three cell lines treated with 2 µg/mL mRNA was compared with the *in vivo* injection site and liver expression after 6 h post-injection and with the ELISA data on day 42 post-injection. These data points were selected as they gave the highest expression levels. The results from these demonstrate a strong correlation for SM-102 (Figure 6.9A) both *in vitro* when comparing across the cell lines but also with the expression in the liver and the total IgG *in vivo*. MC3 also showed a strong trend *in vitro* across the cell lines and this was positively correlated with both expression at the injection site and in the liver and the total IgG (Figure 6.9C). ALC-0315 (Figure 6.9B) and C12-200 (Figure 6.9D) did not show any strong correlation between *in vitro* and *in vivo* expression. This may be due to the mRNA doses used. In this study SM-102 and ALC-0315 were administered at the same dose whereas when administered in human vaccines the SM-102 dose is 3-fold higher than that of ALC-0315.

Collectively, these results suggest that *in vitro* Fluc expression does not correlate well with *in vivo* Fluc expression and that this *in vivo* Fluc expression does not correlate with vaccine efficacy. These differences in expression may be due the challenges of simulating all the factors that affect LNPs *in vivo*, such as, systemic and local immune cells and unwanted delivery to clearance organs (150). The development of tissue culture techniques has been crucial for biological research, however, although tissue culture aims to mimic *in vivo* conditions, the lack of tissue architecture and heterogenous populations of cells often negates innate tissue functions (165). The genotypes and phenotypes of these cultured cells also differ from those *in vivo* due to exposure to foreign serum and static flow (150). In order to overcome these issues, it is suggested to use primary cell lines, rather than immortalised cell lines. Whitehead et al. compared the *in vitro* and *in vivo* silencing of siRNA lipidoid in both immortalised and primary hepatocytes and demonstrated increased correlation when primary hepatocytes were used (166). The disadvantage of using primary cell lines is that the inherent expression profile only lasts for 1-2 days post-isolation and the culturing of these cells technical, time consuming and expensive (166)Therefore, when analysing only a small number of compounds, readily

available immortalised cell lines are more efficient. A recent study carried out by Binici et al demonstrated the different responses to mRNA-LNP vaccines in male and female mice (167). The results demonstrated that both male and female mice had similar levels of protein expression; however, the IgG response was significantly different suggesting that it is the immune response against the proteins (and LNPs) that drives IgG response.

6.6 Conclusions

In this chapter, the previously developed microfluidic manufacturing processes were applied to LNPs rather than liposomes and four different LNPs were produced and tested *in vitro* and *in vivo*. Initially, *in vitro* protocols were established with one LNP formulation and then applied to all 4 LNPs. *In vitro*, generally SM102 LNPs were shown to be the most effective. *In vivo* for protein expression, both SM102 and ALC-0315 gave the highest expression but this did not translate to notable differences across the 4 LNPs in terms of vaccine potency. Based on these findings it would suggest that there is not a strong correlation between *in vitro* and *in vivo* studies and that current screen tools for LNPs need to be improved to ensure effective down-selection of lead mRNA-LNP formulations in preclinical studies.

Chapter 7 - Final Conclusions

7.1 Introduction

The main aim of this thesis was to investigate the impact of both manufacturing and formulation parameters in determining the *in vitro* and *in vivo* efficacy of nanoparticles, specifically liposomes and LNPs. From their discovery by Bangham et al in 1965, the development of nanoparticles has accelerated in recent years, from the application of liposomes for more targeted therapy of small molecule compounds, to the development of more specialised lipids for the delivery of nucleic acids.

Liposomes were one of the first developed lipid drug delivery systems and were the earliest nanomedicine delivery platform to make it from concept to clinic (168). The first approved liposomal delivery systems approved for clinical use was liposomal doxorubicin also known as Doxil®/Caelyx. The encapsulation of doxorubicin increased the therapeutic potential due to reduced off target side effects and increased delivery to the target tissue. However, in 2011 there was a shortage of Doxil® resulting in hundreds of patients being unable to receive treatment (169). The main limitation of the clinical development of these delivery systems is the manufacturing and production of the liposomes at GMP scale. Conventional manufacturing techniques often rely on batch manufacturing that frequently require downstream processing in order to produce liposomes small enough and homogenous in nature. These techniques, including thin film hydration and extrusion, can be very time consuming and expensive, therefore improved production techniques that allow for high throughput and efficient production of nanoparticles is required. Microfluidics is a relatively new, and novel technique for the manufacturing of various types of nanoparticles. Microfluidics offers the ability to produce small heterogenous nanoparticles in a single step and to tailor the characteristics of these formulations for their intended target and biological application.

7.1 Identification of the microfluidic interactions critical for liposome formation and characterisation

Initial experiments carried out in this thesis aimed to determine the critical parameters for liposomes production and subsequent remote loading with the model compound, acridine orange. This would then provide the critical parameters required for liposome formation and loading efficiency. In agreement with previous research, FRR was found to be one of the main parameters affecting liposomal characteristics in terms of size and PDI, however this was not found to affect the loading capability of the liposomal formulation. Altering the loading conditions (such as the incubation time and the drug:lipid ratio were also found to have minimal impact on the liposome characteristics and subsequent encapsulation. Based on these results it was important to not only determine how these various parameters can affect liposome characteristics individually, but also how these parameters may interact to determine final liposome characteristics.

The ability to simulate the final liposomes characteristics would provide a major advantage to the further development of tailored liposome delivery systems. Therefore, a DOE approach was used in order to analyse these complex interactions and to give a broader and more detailed overview of the liposome formation design space. There have been extensive studies that have used a DOE approach for the determination of microfluidic parameters on liposome characteristic, however, not many have covered all the aspects of liposome formation with the majority focussing on the impact of FRR, and TFR and only within a small range. Here we have covered not only the production parameters (FRR, TFR, and production temperature), but also the formulation parameters (lipid composition, initial lipid concentration, solvent and aqueous buffer). Machine learning was used to help analyse and simulate the interactions between factors and their effect on result liposomes size and polydispersity. This studied demonstrated the versatility of microfluidics in being able to produce liposomes of various sizes and compositions. The complex interactions between both production and formulation parameters were highlighted demonstrating the complex interplay of various factors in determining the final liposome characteristics. The development of a predictive model for liposome formation would be of great advantage to the future development of specialised, targeted therapies.

7.2 Factors affecting the remote loading of small molecule compounds into liposomes.

The efficient and stable encapsulation of the active compound is critical for nanoparticle efficacy. In the case of doxorubicin, a high dose is required for effective therapy (approx., 50 mg/m^2). When working with liposomes (and LNPs) the aqueous volumes are very low which can limit the encapsulation potential of these formulations and it is often very hard to achieve high encapsulation through passive methods. Therefore, the development of active loading was critical for the high encapsulation required for effective therapeutic targeting and delivery. In order for these therapies to be effective they need to be present in the circulation long enough to be able to target the desired tissues and avoid detection and removal by cells of the immune system. The introduction of new manufacturing techniques, such as microfluidics, has increased in recent years with the first approved microfluidic formulation being produced using microfluidics (Onpattro) in 2018 to the use in the rapid production of the Pfizer/BioNTech and Moderna vaccines as part of the COVID-19 pandemic. However, with the introduction of new techniques it is important to determine how the manufacturing conditions will affect resultant nanoparticle properties and whether these techniques can be used in place of previous, more traditional methods, such as thin film hydration. In chapter 4 the effect of altering microfluidic parameters was investigated for the effect on liposome characteristics and encapsulation of small molecule compounds. The remote loading process is not limited to the encapsulation of doxorubicin but can be used for the encapsulation of a weak, amphiphilic molecules. Therefore doxorubicin, as well as daunorubicin, vincristine and ciprofloxacin were selected for

investigation to better understand whether the same effects were seen when compounds of similar properties were encapsulated within liposomes. The results from these studies showed that liposome characteristics, specifically particle size, had a significant effect on the loading potential of these liposomes and that these effects were compound dependent.

7.3 Effect of microfluidic production on *in vitro* and *in vivo* release

For lipid formulations to progress from bench to bedside, *in vitro* and *in vivo* characterisation is vital for understanding the release profiles, biodistribution and therapeutic efficacy of each formulation. When introducing new manufacturing procedures, it is important to make sure that the formulations show the same profile across the different techniques and devices. Thin film hydration is the most commonly used technique for industrial scale production; therefore, it was selected as our control for mapping the microfluidic formulations. Based on the results from both the DOE (Chapter 3) and the encapsulation data (Chapter 4) two formulations were selected for further *in vitro* and *in vivo* characterisation, one using ethanol and the other using Transcutol for the microfluidic production of liposomes. The aim of this study was to determine the effect of solvent and production technique on the release and biodistribution of doxorubicin encapsulated in liposomes. The results from this study showed no significant differences *in vitro* however the *in vivo* biodistribution revealed a difference in the biodistribution of the liposomes produced using microfluidics with no differences observed between the traditional thin film hydration method and the more commonly used microfluidic production using ethanol. These results show that the newer microfluidic manufacturing process is capable of producing liposomes of similar characteristics to the older methods whilst reducing the number of processing steps required to generate the same samples. The difference between the ethanol and Transcutol samples highlight the importance of pre-clinical validation as changing even just one variable may not show significant differences in the physicochemical characteristics of the samples the *in vitro* and *in vivo* release profiles may be affected.

Determination of *in vitro* and *in vivo* efficacy is particularly important for the evaluation and assessment of potency. mRNA-LNPs represent the newest development in vaccine delivery and have allowed the rapid production and clinical application of lipid delivery systems as part of the fight against COVID-19. The four selected ionisable lipid formulations selected for evaluation in this thesis are all well characterised and have been used in clinically approved LNP formulations. The data from both *in vitro* and *in vivo* studies showed very little correlation with samples showing low *in vitro* expression having high immune responses. In general, *in vitro* studies are carried out prior to *in vivo* and are used for screening formulations in order to find the most efficient and highest expressing. However, it has been shown that formulations that show low expression *in vitro* can have high expression *in vivo*, with high immune responses, as detected by ELISA. In this way, there is high

potential for formulations that would otherwise show high *in vivo* efficacy to be disregarded due to their low expression *in vitro*. It is therefore important to develop new methods that would then allow for comparison between *in vitro* and *in vivo* formulations so as to more efficiently screen for new formulations.

7.4 Final Conclusion and Future Work

Microfluidics has been demonstrated to be an efficient and scalable manufacturing technique allowing for increased production and screening of new novel drug formulations. The overall aim of this thesis was to explore the impact of microfluidic manufacturing on resultant nanoparticle characteristics and subsequent *in vitro* and *in vivo* profiles. Within this thesis, both liposomes and LNPs were produced, and the effect of microfluidic production was assessed. Using liposomes as our model for assessing microfluidic parameters it was shown that it is very difficult to accurately simulate the impact of microfluidic production on final liposome properties, highlighting the complex interactions occurring between both the manufacturing technique and the formulation. In order to investigate whether a programme could be created that would be able to accurately simulate the final liposome properties screening of a larger library of lipid compositions and buffers would need to be tested, which is not feasible for a research lab environment, also complex analytical software and analysis would need to be carried out in order to full analyse the complete data set. While the analysis of both *in vitro* and *in vivo* efficacy is used for the determination of potency, the results do not always correlate and can, in some cases, prevent the future development of therapeutics. Higher correlation can be achieved by the use of primary cells from the same target tissues however the advantages of using such systems needs to be weighed against the cost and time required for establishing such cell lines.

Based on the findings of this thesis future work would focus on the further development of liposomes for small molecule drug delivery and could investigate the effect of production on the encapsulation of bilayer loaded compounds. Further studies using Transcutol could be carried out, such as using cryo-TEM or SAXS analysis, to determine the effect of this solvent on the structure of liposomes. Investigation into different *in vitro* models that better simulate the *in vivo* environments could be undertaken, such as the use of cell free assays.

Chapter 8 - Appendix

8.1 Statistical methodology for data analysis

8.1.1 DoE

The study design involved setting up an I-optimal DoE (A) with 135 experimental runs including control runs to check the reproducibility of the process and measurements. The DoE has a possibility to estimate several third-order interaction terms and fourth order interaction term.

Additionally, 18 validation runs were created to check how well the model simulates the PSD and PDI on new combinations of factor settings which were not used in the first DoE.

8.1.2 Statistical modeling

As the current dataset was obtained via I-Optimal DoE, the multiple linear regression models as well as regularized linear regression models (such as Elastic Net and Lasso) were considered. The primary linear regression model had very good performance on the training set and high error on the validation set of experiments, the phenomenon known in statistical data analysis as overfitting. To overcome the overfitting, regularized linear models were employed. Application of regularized models allows to avoid overfitting and perform model selection at the same time, as the least relevant model terms would be set to zero. The resulting simulation error of regularized regression using Elastic Net was higher compared to the original multiple linear regression model, however, the simulation error was comparable for training and validation set, which justifies its use from the simulation perspective. Additional modeling efforts have included machine learning methods, such as Random Forests and XGBoost but their performance in terms of simulation error was not better compared to the Elastic Net models.

8.1.3 Visualization of modeling results

Due to complexity of DoE and the final selected models involving higher order interactions which were relevant for simulation, contour plots were constructed for ease of interpretation. A typical contour plot would display the average response surface in terms of continuous factors TFR and FRR for different combinations of categorical factors solvent, buffer, lipid and discretized lipid concentrations and temperatures. Contour plots allow to visualize and put emphasis on the complex interactions, however the model uncertainty (i.e. average simulation error) is not taken into account. In addition, the measured data points from training set and validation set were added to the contour plots to demonstrate how the final selected model fits measurements from both sets of results.

8.2 Supplementary information: Statistical methodology

8.2.1 Data preparation

The main dataset (referred to as training dataset) consists of 135 DOE runs. Additionally, 18 validation runs were generated to check how well the model simlates the PSD and PDI on new observations which were not used in the model.

As the main dataset was created according to the DoE, the construction of simulator matrix X had to include not only main effects of the seven considered factors (TFR, FRR, Temperature, Lipid Concentration, Lipid, Solvent, Buffer), but also their interactions. The original design had a possibility to estimate several third-order interaction terms and fourth-order interaction term, but after collecting the data it became clear that more complex model may be needed with additional higher order interaction terms. Since these additional higher order interaction terms are highly correlated with the model terms in original DoE, model selection was necessary. The classical approaches for multiple linear regression such as stepwise procedure was not able to suggest a good predictive model which would perform well both on training set and on the validation data.

The continuous DoE factors TFR, FRR, Temperature and Lipid Concentration were normalized to the range [-1; 1] by equation $X_{norm} = 2 * (X - (X_{min} + X_{max})/2)/(X_{max} - X_{min})$. The Lipids were encoded as 1 in case of Lipid A and -1 in case of Lipid B, the Buffers were encoded as 1 for PBS and -1 for Ammonium Sulfate. For solvents, the set of three "dummy" 0-1 variables were constructed: Solvent EtOH = 1 if EtOH was used, and 0 otherwise, Solvent IPA=1 if IPA was used and 0 otherwise, Solvent MeOH = 1 if MeOH was used and 0 otherwise.

The factors in the validation data were also normalized using the same ranges as the training set to avoid potential bias due to normalization. This normalization to [-1;1] scale allows for less correlation between main effects and quadratic terms and at the same time give equal weight to all model terms. Subsequently, no additional normalization is required during modeling.

Final set of normalized predictors (matrix X) contained main effects of all experimental factors, quadratic effects of TFR, FRR and actual Lipid concentration, the interactions included up to the 4th order of these factors. In this way terms like quadratic TFR effect, quadratic FRR effect with the combination of any other two factors would be considered and even result in higher order effects. For instance, $TFR^2 * TFR$ would be third order term for TFR included in the model.

The responses, PSD and PDI were also transformed prior to analysis due to the fact that PSD can only be positive and PDI can be only between (0 and 1): log(PSD) was used for the former and logit(PDI)=log(PDI/(1-PDI)) for the latter response.

The construction of model matrix is also a part of R script provided for reproducibility purpose

8.3 Modelling by regularised linear models

8.3.1 Method description

The family of regularized linear models consists of Ridge regression, LASSO (least absolute shrinkage and selection operator) and the generalization Elastic Net (B). These methods essentially are linear regression models, which on one hand can work with multiple model terms which are highly correlated (primary goal of Ridge regression) and on the other hand they can perform selection of model terms most relevant for simulation by shrinking the least important model terms to zero. Unlike multiple linear regression models, which are based on ordinary least squares estimates and do not have any specific parameters which should be selected, the regularized linear models have additional parameters, such as amount of shrinkage, λ in case of ridge regression and LASSO and extra parameter α for Elastic Net, which would allow to determine the balance between model selection (LASSO) and inclusion of correlated terms (Ridge regression).

As the dataset was generated using DOE, in order not to destroy the structure leave-one-out cross validation scheme was used.

The modeling was performed in R4.0.3 using the packages caret_6.0-86 and glmnet_4.0-2.

8.3.2 Cross validation results

8.3.2.1 PSD model

Figure 8.1 shows the results for selection of the regularization λ and mixing parameters α, for modelling of PSD, suggesting that Lasso models have the lowest RMSE (α=1), which allows to make a parsimonious model. The optimal regularization parameter, λ, was chosen to be 0.01568802.

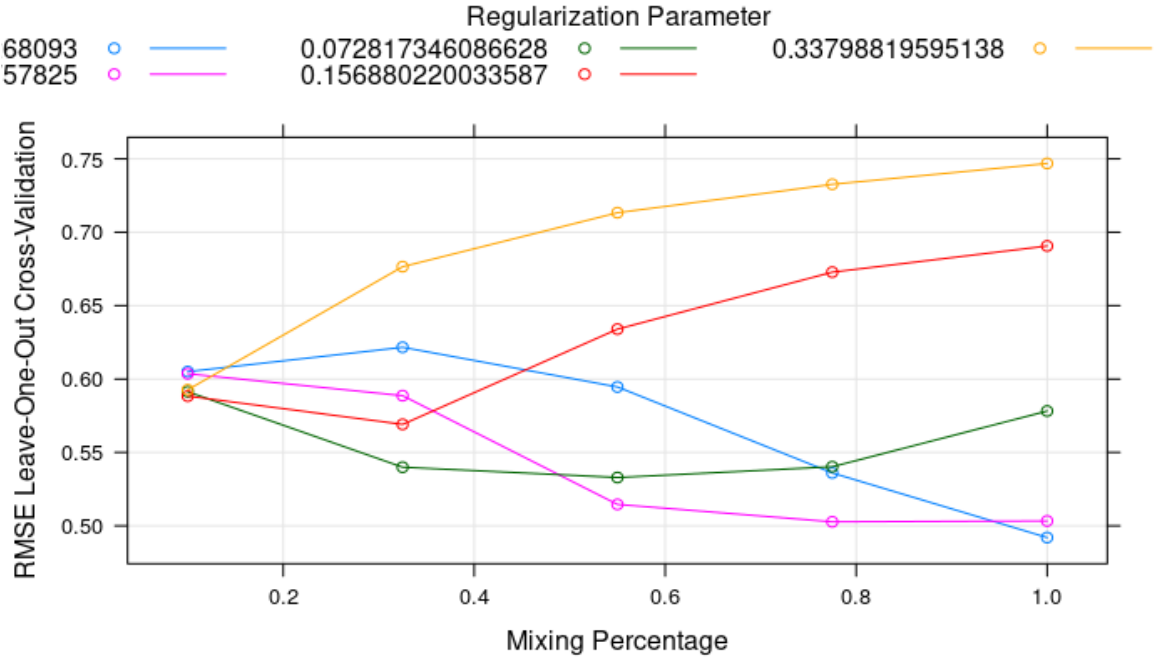

Figure 8.1: Results of cross validation for shrinkage and mixing parameters selection for log(PSD).

The final model for log(PSD) of 50 terms, which are shown in the supplementary HTML document.

Figure 8.2 shows the results of simulations against the observed PSD D50 for both training and validation datasets, demonstrating comparable simulation error.

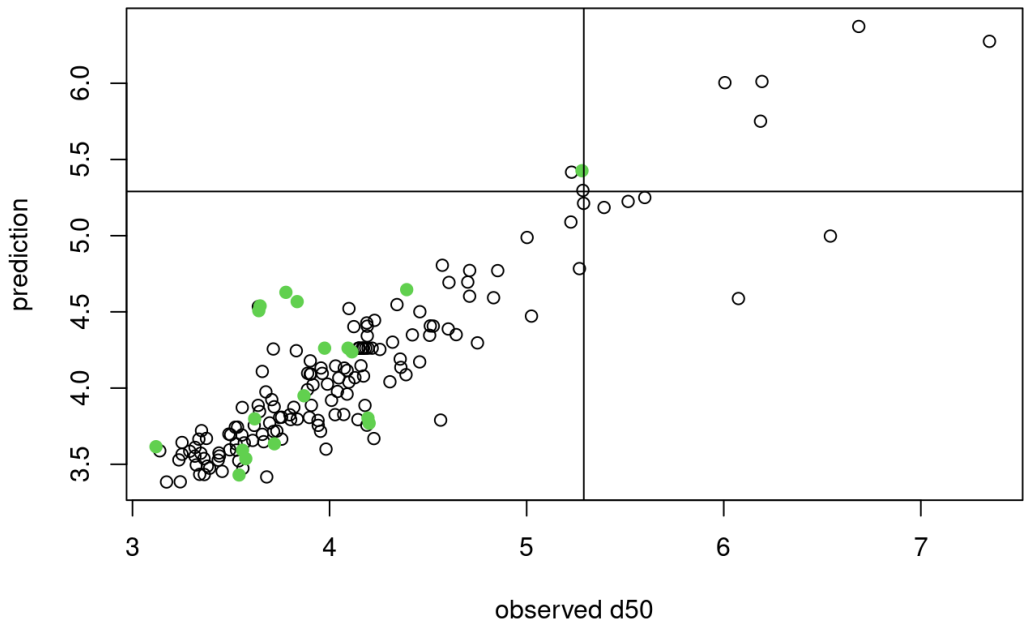

Figure 8.2: Simulations of the final model for PSD d50 (on log scale) versus observed: green solid dots are results for validation set, black circles are results for training set.

8.3.2.2 PDI model

Figure 8.3 shows the results for selection of the regularization λ and mixing parameters α, for modelling of PDI, and unlike for PSD, here suggesting that models closer to Ridge Regression have the lowest RMSE (α=0.1). The model is also more complex compared to the model of PSD and consists of 273 terms. In the end, we have also used LASSO model, to sacrifice a part of simulation error towards the parsimony of the model. For LASSO the optimal shrinkage value λ was set to 0.05226027. The

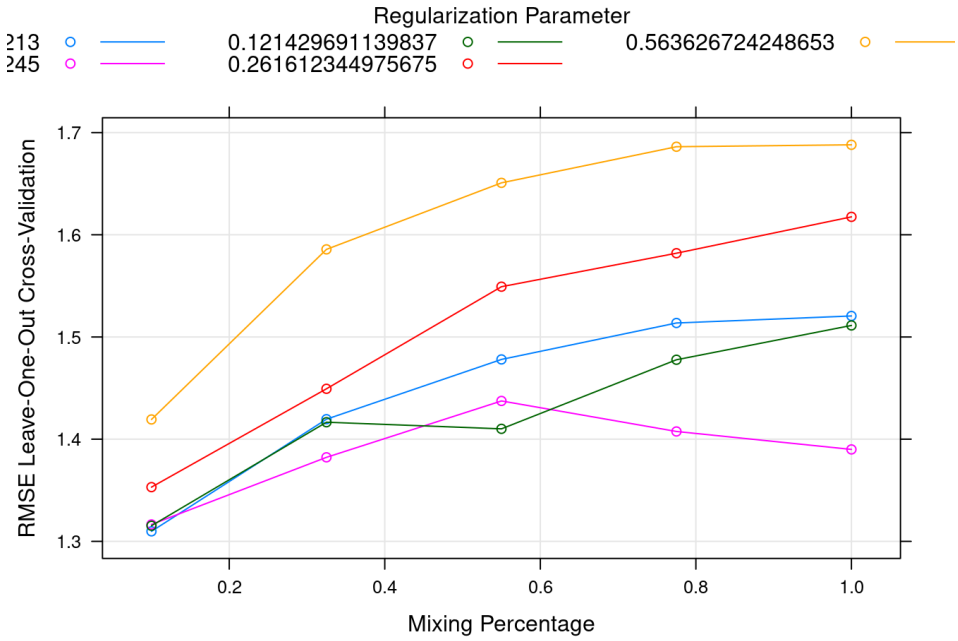

Figure 8.3: Results of cross validation for shrinkage and mixing parameters selection for logit(PDI).

model selection by LASSO resulted in 51 model terms, out of which 14 terms were common with the selected model of PSD.

Figure 8.4 shows the results of simulations against the observed PDI for both training and validation datasets, demonstrating comparable simulation error.

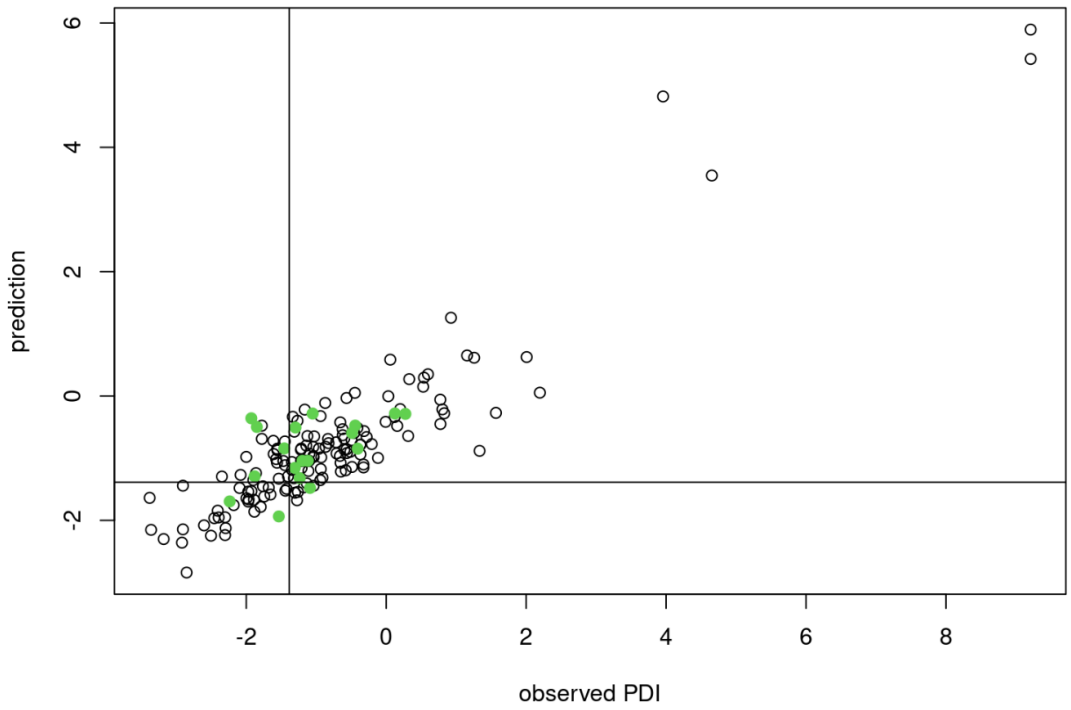

Figure 8.4: Simulations of the LASSO model for PDI (on logit scale) versus observed: green solid dots are results for validation set, black circles are results for training set.

8.4 Comparison of regularised linear regression models to the machine learning methods

In order to attempt finding a better predictive model which would do better than regularized linear regression on both training and validation data, a comparative study has been conducted involving several machine learning methods, such as random forests, XGboost, MARS, PLS and QRF. Here we briefly summarize the methods.

Random forest (C) is a non-parametric predictive modeling approach where a set of regression tree is constructed based on bootstrapping the data. In general, it does not require specification of complex higher order interactions in predictor matrix X, like in linear models, as the regression trees handle complex interactions while modeling the data.

XGboost (D) is a scalable end-to-end tree boosting system which is used widely by data scientists to achieve state-of-the-art results on many machine learning challenges. It is an implementation of

gradient boosted decision trees designed for speed and performance in form of software library that you can download and install on your machine, then access from a variety of interfaces.

Like neural networks and partial least squares, MARS (E) uses surrogate features instead of the original predictors. However, whereas PLS and neural networks are based on linear combinations of the predictors, MARS creates two contrasted versions of a predictor to enter the model. Also, the surrogate features in MARS are usually a function of only one or two predictors at a time. For MARS models that can include two or more terms at a time, we have observed occasional instabilities in the model simulations where a few sample simulations are wildly inaccurate (perhaps an order of magnitude off of the true value). This problem has not been observed with additive MARS models.

PLS is a commonly applied method in chemometrics which tries to find optimal predictive model by maximizing covariance between predictors and response. It requires setting of the number of components that should be used for prediction, which should be selected by cross validation. When the number of components gets to its maximum (here, to the number of experiments in the dataset), the solution corresponds to the ridge regression.

Quantile Random Forest (F) also called Quantile Regression Forests, give a non-parametric and accurate way of estimating conditional quantiles for high-dimensional predictor variables.

Table 8.1 shows the results of the comparative study for PSD. The LASSO models have very reasonable performance both on training and test set and involvement of more sophisticated machine learning methods did not improve the performance considerably. We can see that XGboost outperforms the rest on the training set, but its performance on the test set was comparable to the LASSO one. Therefore, to work with models which are easier to interpret, we concluded that LASSO would be the optimal choice.

Table 8.1: Comparative study results for different predictive models - PSD.

ModelName	RMSE.train	RMSE.test	Rsq.train	Rsq.test
lassoTuned	0.363	0.309	0.799	0.693
elasticNetTuned	0.361	0.326	0.801	0.659
rfTuned	0.207	0.297	0.936	0.643
xgbTuned	0.007	0.281	1.000	0.628
gbmTuned	0.310	0.297	0.839	0.578
marsTuned	0.401	0.404	0.707	0.437
ridgeTuned	0.385	0.392	0.842	0.259
plsTuned	0.393	0.414	0.719	0.192
qrfTuned	0.701	0.448	0.221	0.044

Below Table 8.2 shows results of the comparative study for PDI.

Table 8.2: Comparative study results for different predictive models - PDI

ModelName	RMSE.train	RMSE.test	Rsq.train	Rsq.test
lassoTuned_PDI	0.190	0.778	0.988	0.189
elasticNetTuned_PDI	0.377	0.654	0.960	0.171
plsTuned_PDI	0.442	0.705	0.931	0.165
ridgeTuned_PDI	0.667	0.664	0.899	0.112
xgbTuned_PDI	0.012	0.829	1.000	0.108
rfTuned_PDI	0.791	0.867	0.881	0.018
qrfTuned_PDI	1.649	0.679	0.119	0.010
marsTuned_PDI	1.531	1.188	0.166	0.006
gbmTuned_PDI	0.620	1.072	0.883	0.000

8.5 Size and PDI SOP Optimization

Before beginning the Design of Experiments project it was important to determine the sensitivity of the Malvern Zetasizer to different concentrations of liposomes. To do this, DSPC:Chol:PEG2000 liposomes were produced from a 40 mg/mL stock solution in ethanol at FRR 3:1 and TFR 10 mL/min with a final lipid concentration of 10 mg/mL. These liposomes then underwent TFF purification before being diluted in filtered PBS to the desired concentrations for sizing. The parameters for the sizing protocol are shown in section 2.3. The results show that at lower concentrations (<0.2 mg/mL) there is an increase in variation of both size and PDI which is corrected when the sample is left to stabilise and remeasured (Figure 8.5).

A

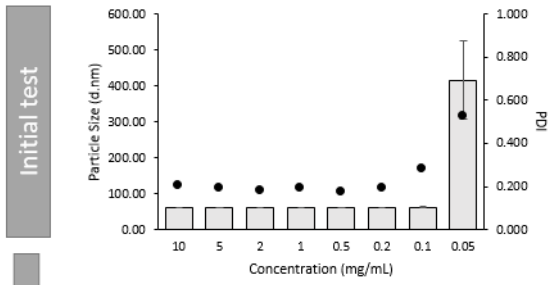

Liposome concentration (mg/mL)	Size (d.nm)	PDI	Derived Count Rate	Attenuation
10	60.61	0.203	298157.23	5
5	60.83	0.191	179646.33	5
2	61.51	0.179	86337.167	6
1	60.58	0.189	42202.7	6
0.5	61.05	0.175	20382.533	7
0.2	61.16	0.192	7605.4333	8
0.1	62.72	0.279	3218.3	8
0.05	415.57	0.522	401.66667	11

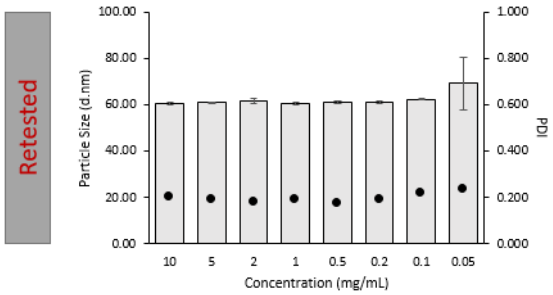

Liposome concentration (mg/mL)	Size (d.nm)	PDI	Derived Count Rate	Attenuation
10	60.61	0.203	298157.2	5
5	60.83	0.191	179646.3	5
2	61.51	0.179	86337.17	6
1	60.58	0.189	42202.7	6
0.5	61.05	0.175	20382.53	7
0.2	61.16	0.192	7605.433	8
0.1	62.22	0.219	4217.867	8
0.05	69.23	0.232	1818.1	10

B

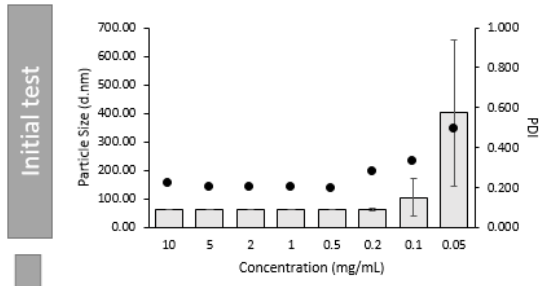

Liposome concentration (mg/mL)	Size (d.nm)	PDI	Derived Count Rate	Attenuation
10	63.11	0.218	290323.7	5
5	62.48	0.198	175091.63	5
2	62.72	0.204	83357.5	6
1	62.63	0.201	43827.1	6
0.5	63.03	0.197	18738.633	7
0.2	63.63	0.279	1608.7667	11
0.1	105.78	0.328	929.26667	8
0.05	401.37	0.493	194.03333	11

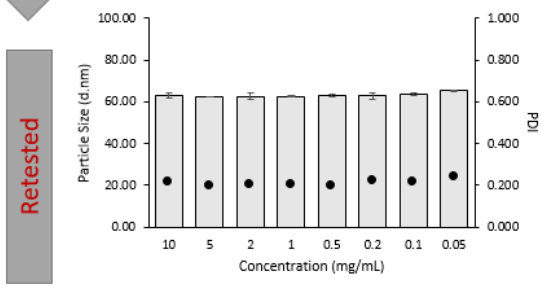

Liposome concentration (mg/mL)	Size (d.nm)	PDI	Derived Count Rate	Attenuation
10	63.11	0.218	290323.7	5
5	62.48	0.198	175091.6	5
2	62.72	0.204	83357.5	6
1	62.63	0.201	43827.1	6
0.5	63.03	0.197	18738.63	7
0.2	62.83	0.221	5590.20	8
0.1	63.51	0.215	4371.467	8
0.05	65.28	0.240	2205.4	9

Figure 8.5: Sensitivity of Malvern Zetasizer. DSPC:Chol:DSPE-PEG2000 liposomes were measured at varying concentrations for size, PDI, Derived count rate and attenuation. A) Shows one batch of liposomes measure at concentrations from 0.05-10 mg/mL, B) shows a second batch of liposomes measured at concentrations from 0.05-10 mg/mL. Demonstrates that the zetasizer is sensitive and accurate at concentrations > 0.2 mg/mL. Each figure represents n=1.

References

1. Sercombe L, Veerati T, Moheimani F, Wu SY, Sood AK, Hua S. Advances and Challenges of Liposome Assisted Drug Delivery. Front Pharmacol. 2015;6:286.
2. Fan Y, Zhang Q. Development of liposomal formulations: From concept to clinical investigations. Asian Journal of Pharmaceutical Sciences. 2013;8(2):81-7.
3. Bangham AD, Standish MM, Watkins JC. Diffusion of univalent ions across the lamellae of swollen phospholipids. Journal of Molecular Biology. 1965;13(1):238-IN27.
4. Gregoriadis G. Drug entrapment in liposomes. FEBS Letters. 1973;36(3):292-6.
5. Bulbake U, Doppalapudi S, Kommineni N, Khan W. Liposomal Formulations in Clinical Use: An Updated Review. Pharmaceutics. 2017;9(2).
6. Liu G, Hou S, Tong P, Li J. Liposomes: Preparation, Characteristics, and Application Strategies in Analytical Chemistry. Critical Reviews in Analytical Chemistry. 2020:1-21.
7. Akbarzadeh A, Rezaei-Sadabady R, Davaran S, Joo SW, Zarghami N, Hanifehpour Y, et al. Liposome: classification, preparation, and applications. Nanoscale Res Lett. 2013;8(1):102.
8. Elhissi A, Phoenix D, Ahmed W, Jackson MJ. Chapter 15 - Some approaches to large-scale manufacturing of liposomes. Emerging Nanotechnologies for Manufacturing (Second Edition). Boston: William Andrew Publishing; 2015. p. 402-17.
9. Sawant RR, Torchilin VP. Challenges in development of targeted liposomal therapeutics. Aaps j. 2012;14(2):303-15.
10. Hood RR, Vreeland WN, DeVoe DL. Microfluidic remote loading for rapid single-step liposomal drug preparation. Lab Chip. 2014;14(17):3359-67.
11. Shah S, Dhawan V, Holm R, Nagarsenker MS, Perrie Y. Liposomes: Advancements and innovation in the manufacturing process. Advanced Drug Delivery Reviews. 2020.
12. Al-Jamal WT, Kostarelos K. Liposomes: From a Clinically Established Drug Delivery System to a Nanoparticle Platform for Theranostic Nanomedicine. Accounts of Chemical Research. 2011;44(10):1094-104.
13. Tian B, Al-Jamal WT, Al-Jamal KT, Kostarelos K. Doxorubicin-loaded lipid-quantum dot hybrids: Surface topography and release properties. International Journal of Pharmaceutics. 2011;416(2):443-7.
14. Sur S, Fries AC, Kinzler KW, Zhou S, Vogelstein B. Remote loading of preencapsulated drugs into stealth liposomes. Proc Natl Acad Sci U S A. 2014;111(6):2283-8.
15. Allen TM, Cullis PR. Liposomal drug delivery systems: From concept to clinical applications. Advanced Drug Delivery Reviews. 2013;65(1):36-48.
16. Roces CB, Port EC, Daskalakis NN, Watts JA, Aylott JW, Halbert GW, et al. Rapid scale-up and production of active-loaded PEGylated liposomes. International journal of pharmaceutics. 2020;586:119566.
17. Li Q, Li X, Zhao C. Strategies to Obtain Encapsulation and Controlled Release of Small Hydrophilic Molecules. Frontiers in Bioengineering and Biotechnology. 2020;8.
18. Schwendener RA, Schott H. Liposome Formulations of Hydrophobic Drugs. In: Weissig V, editor. Liposomes: Methods and Protocols, Volume 1: Pharmaceutical Nanocarriers. Totowa, NJ: Humana Press; 2010. p. 129-38.
19. Webb C, Forbes N, Roces CB, Anderluzzi G, Lou G, Abraham S, et al. Using microfluidics for scalable manufacturing of nanomedicines from bench to GMP: A case study using protein-loaded liposomes. International Journal of Pharmaceutics. 2020;582:119266.
20. Gabizon A, Shmeeda H, Barenholz Y. Pharmacokinetics of Pegylated Liposomal Doxorubicin. Clinical Pharmacokinetics. 2003;42(5):419-36.
21. Gabizon A, Papahadjopoulos D. Liposome formulations with prolonged circulation time in blood and enhanced uptake by tumors. Proceedings of the National Academy of Sciences. 1988;85(18):6949-53.

22. Nagayasu A, Uchiyama K, Kiwada H. The size of liposomes: a factor which affects their targeting efficiency to tumors and therapeutic activity of liposomal antitumor drugs. Advanced Drug Delivery Reviews. 1999;40(1):75-87.
23. Peravali R, Brock R, Bright E, Mills P, Petty D, Alberts J. Enhancing the Enhanced Recovery Program in Colorectal Surgery - Use of Extended-Release Epidural Morphine (DepoDur®). Ann Coloproctol. 2014;30(4):186-91.
24. Malik O, Kaye AD, Kaye A, Belani K, Urman RD. Emerging roles of liposomal bupivacaine in anesthesia practice. J Anaesthesiol Clin Pharmacol. 2017;33(2):151-6.
25. Roces CB, Lou G, Jain N, Abraham S, Thomas A, Halbert GW, et al. Manufacturing Considerations for the Development of Lipid Nanoparticles Using Microfluidics. Pharmaceutics. 2020;12(11).
26. Aldosari BN, Alfagih IM, Almurshedi AS. Lipid Nanoparticles as Delivery Systems for RNA-Based Vaccines. Pharmaceutics. 2021;13(2).
27. Swetha K, Kotla NG, Tunki L, Jayaraj A, Bhargava SK, Hu H, et al. Recent Advances in the Lipid Nanoparticle-Mediated Delivery of mRNA Vaccines. Vaccines (Basel). 2023;11(3).
28. Eygeris Y, Gupta M, Kim J, Sahay G. Chemistry of Lipid Nanoparticles for RNA Delivery. Accounts of Chemical Research. 2022;55(1):2-12.
29. Suzuki Y, Ishihara H. Difference in the lipid nanoparticle technology employed in three approved siRNA (Patisiran) and mRNA (COVID-19 vaccine) drugs. Drug Metab Pharmacokinet. 2021;41:100424.
30. Kowalski PS, Rudra A, Miao L, Anderson DG. Delivering the Messenger: Advances in Technologies for Therapeutic mRNA Delivery. Mol Ther. 2019;27(4):710-28.
31. Maugeri M, Nawaz M, Papadimitriou A, Angerfors A, Camponeschi A, Na M, et al. Linkage between endosomal escape of LNP-mRNA and loading into EVs for transport to other cells. Nature Communications. 2019;10(1):4333.
32. Reichmuth AM, Oberli MA, Jaklenec A, Langer R, Blankschtein D. mRNA vaccine delivery using lipid nanoparticles. Ther Deliv. 2016;7(5):319-34.
33. Shah VM, Nguyen DX, Patel P, Cote B, Al-Fatease A, Pham Y, et al. Liposomes produced by microfluidics and extrusion: A comparison for scale-up purposes. Nanomedicine: Nanotechnology, Biology and Medicine. 2019;18:146-56.
34. Perrie Y, Kastner E, Khadke S, Roces CB, Stone P. Manufacturing Methods for Liposome Adjuvants. In: Fox CB, editor. Vaccine Adjuvants: Methods and Protocols. New York, NY: Springer New York; 2017. p. 127-44.
35. Yu B, Lee RJ, Lee LJ. Microfluidic methods for production of liposomes. Methods Enzymol. 2009;465:129-41.
36. Liu P, Chen G, Zhang J. A Review of Liposomes as a Drug Delivery System: Current Status of Approved Products, Regulatory Environments, and Future Perspectives. Molecules. 2022;27(4).
37. Has C, Sunthar P. A comprehensive review on recent preparation techniques of liposomes. Journal of Liposome Research. 2020;30(4):336-65.
38. van Swaay D, deMello A. Microfluidic methods for forming liposomes. Lab on a Chip. 2013;13(5):752-67.
39. Lee C-Y, Chang C-L, Wang Y-N, Fu L-M. Microfluidic Mixing: A Review. International Journal of Molecular Sciences. 2011;12(5):3263-87.
40. Maeki M, Uno S, Niwa A, Okada Y, Tokeshi M. Microfluidic technologies and devices for lipid nanoparticle-based RNA delivery. Journal of Controlled Release. 2022;344:80-96.
41. Carugo D, Bottaro E, Owen J, Stride E, Nastruzzi C. Liposome production by microfluidics: potential and limiting factors. Scientific Reports. 2016;6(1):25876.
42. Song Y, Hormes J, Kumar CSSR. Microfluidic Synthesis of Nanomaterials. Small. 2008;4(6):698-711.
43. Bayareh M, Ashani MN, Usefian A. Active and passive micromixers: A comprehensive review. Chemical Engineering and Processing - Process Intensification. 2020;147:107771.

44. Afzal A, Kim K-Y. Three-objective optimization of a staggered herringbone micromixer. Sensors and Actuators B: Chemical. 2014;192:350-60.
45. Saravanakumar SM, Cicek PV. Microfluidic Mixing: A Physics-Oriented Review. Micromachines (Basel). 2023;14(10).
46. Duncombe TA, Tentori AM, Herr AE. Microfluidics: reframing biological enquiry. Nat Rev Mol Cell Biol. 2015;16(9):554-67.
47. Niculescu AG, Mihaiescu DE, Grumezescu AM. A Review of Microfluidic Experimental Designs for Nanoparticle Synthesis. Int J Mol Sci. 2022;23(15).
48. Damiati S, Kompella UB, Damiati SA, Kodzius R. Microfluidic Devices for Drug Delivery Systems and Drug Screening. Genes (Basel). 2018;9(2).
49. Williams MS, Longmuir KJ, Yager P. A practical guide to the staggered herringbone mixer. Lab Chip. 2008;8(7):1121-9.
50. Lou G, Anderluzzi G, Woods S, Roberts CW, Perrie Y. A novel microfluidic-based approach to formulate size-tuneable large unilamellar cationic liposomes: Formulation, cellular uptake and biodistribution investigations. European Journal of Pharmaceutics and Biopharmaceutics. 2019;143:51-60.
51. Aggarwal P, Hall JB, McLeland CB, Dobrovolskaia MA, McNeil SE. Nanoparticle interaction with plasma proteins as it relates to particle biodistribution, biocompatibility and therapeutic efficacy. Adv Drug Deliv Rev. 2009;61(6):428-37.
52. Rafiyath SM, Rasul M, Lee B, Wei G, Lamba G, Liu D. Comparison of safety and toxicity of liposomal doxorubicin vs. conventional anthracyclines: a meta-analysis. Exp Hematol Oncol. 2012;1(1):10.
53. Ni C, Fang J, Qian H, Xu Q, Shen F. Liposomal doxorubicin-related palmar-plantar erythrodysesthesia (hand-foot syndrome): a case report. J Int Med Res. 2020;48(12):300060520974854.
54. Aloss K, Hamar P. Recent Preclinical and Clinical Progress in Liposomal Doxorubicin. Pharmaceutics. 2023;15(3).
55. Pereira S, Ma G, Na L, Hudoklin S, Kreft ME, Kostevsek N, et al. Encapsulation of doxorubicin prodrug in heat-triggered liposomes overcomes off-target activation for advanced prostate cancer therapy. Acta Biomaterialia. 2022;140:530-46.
56. Mantripragada S. A lipid based depot (DepoFoam® technology) for sustained release drug delivery. Progress in Lipid Research. 2002;41(5):392-406.
57. Hald Albertsen C, Kulkarni JA, Witzigmann D, Lind M, Petersson K, Simonsen JB. The role of lipid components in lipid nanoparticles for vaccines and gene therapy. Adv Drug Deliv Rev. 2022;188:114416.
58. Patel P, Ibrahim NM, Cheng K. The Importance of Apparent pKa in the Development of Nanoparticles Encapsulating siRNA and mRNA. Trends Pharmacol Sci. 2021;42(6):448-60.
59. Han X, Zhang H, Butowska K, Swingle KL, Alameh M-G, Weissman D, et al. An ionizable lipid toolbox for RNA delivery. Nature Communications. 2021;12(1):7233.
60. Webb C, Khadke S, Schmidt ST, Roces CB, Forbes N, Berrie G, et al. The Impact of Solvent Selection: Strategies to Guide the Manufacturing of Liposomes Using Microfluidics. Pharmaceutics. 2019;11(12).
61. López RR, G. Font de Rubinat P, Sánchez L-M, Tsering T, Alazzam A, Bergeron K-F, et al. The effect of different organic solvents in liposome properties produced in a periodic disturbance mixer: Transcutol®, a potential organic solvent replacement. Colloids and Surfaces B: Biointerfaces. 2021;198:111447.
62. Clerc S, Barenholz Y. A Quantitative Model for Using Acridine Orange as a Transmembrane pH Gradient Probe. Analytical Biochemistry. 1998;259(1):104-11.
63. Pasarin D, Ghizdareanu AI, Enascuta CE, Matei CB, Bilbie C, Paraschiv-Palada L, et al. Coating Materials to Increase the Stability of Liposomes. Polymers (Basel). 2023;15(3).

64. Kastner E, Kaur R, Lowry D, Moghaddam B, Wilkinson A, Perrie Y. High-throughput manufacturing of size-tuned liposomes by a new microfluidics method using enhanced statistical tools for characterization. International Journal of Pharmaceutics. 2014;477(1):361-8.
65. Kastner E, Verma V, Lowry D, Perrie Y. Microfluidic-controlled manufacture of liposomes for the solubilisation of a poorly water soluble drug. International Journal of Pharmaceutics. 2015;485(1):122-30.
66. Dong Y-D, Tchung E, Nowell C, Kaga S, Leong N, Mehta D, et al. Microfluidic preparation of drug-loaded PEGylated liposomes, and the impact of liposome size on tumour retention and penetration. Journal of Liposome Research. 2019;29(1):1-9.
67. Hood RR, DeVoe DL. High-Throughput Continuous Flow Production of Nanoscale Liposomes by Microfluidic Vertical Flow Focusing. Small. 2015;11(43):5790-9.
68. Jahn A, Vreeland WN, DeVoe DL, Locascio LE, Gaitan M. Microfluidic Directed Formation of Liposomes of Controlled Size. Langmuir. 2007;23(11):6289-93.
69. Jose J, Kanniyappan H, Muthuvijayan V. A novel, rapid and cost-effective method for separating drug-loaded liposomes prepared from egg yolk phospholipids. Process Biochemistry. 2022;115:80-91.
70. Nambiar NR, Gaur S, Ramachandran G, Pandey RS, M S, Nath LR, et al. Remote loading in liposome: a review of current strategies and recent developments. Journal of Liposome Research.1-13.
71. Pande S. Liposomes for drug delivery: review of vesicular composition, factors affecting drug release and drug loading in liposomes. Artificial Cells, Nanomedicine, and Biotechnology. 2023;51(1):428-40.
72. Alavi M, Karimi N, Safaei M. Application of Various Types of Liposomes in Drug Delivery Systems. Adv Pharm Bull. 2017;7(1):3-9.
73. Desai D, Guerrero YA, Balachandran V, Morton A, Lyon L, Larkin B, et al. Towards a microfluidics platform for the continuous manufacture of organic and inorganic nanoparticles. Nanomedicine: Nanotechnology, Biology and Medicine. 2021;35:102402.
74. Tomeh MA, Zhao X. Recent Advances in Microfluidics for the Preparation of Drug and Gene Delivery Systems. Molecular Pharmaceutics. 2020;17(12):4421-34.
75. Shepherd SJ, Issadore D, Mitchell MJ. Microfluidic formulation of nanoparticles for biomedical applications. Biomaterials. 2021;274:120826.
76. Jahn A, Vreeland WN, Gaitan M, Locascio LE. Controlled Vesicle Self-Assembly in Microfluidic Channels with Hydrodynamic Focusing. Journal of the American Chemical Society. 2004;126(9):2674-5.
77. Sedighi M, Sieber S, Rahimi F, Shahbazi M-A, Rezayan AH, Huwyler J, et al. Rapid optimization of liposome characteristics using a combined microfluidics and design-of-experiment approach. Drug Delivery and Translational Research. 2019;9(1):404-13.
78. Forbes N, Hussain MT, Briuglia ML, Edwards DP, Horst JHt, Szita N, et al. Rapid and scale-independent microfluidic manufacture of liposomes entrapping protein incorporating in-line purification and at-line size monitoring. International Journal of Pharmaceutics. 2019;556:68-81.
79. Papahadjopoulos D, Allen TM, Gabizon A, Mayhew E, Matthay K, Huang SK, et al. Sterically stabilized liposomes: improvements in pharmacokinetics and antitumor therapeutic efficacy. Proceedings of the National Academy of Sciences. 1991;88(24):11460.
80. Allen TM, Hansen C, Martin F, Redemann C, Yau-Young A. Liposomes containing synthetic lipid derivatives of poly(ethylene glycol) show prolonged circulation half-lives in vivo. Biochimica et Biophysica Acta (BBA) - Biomembranes. 1991;1066(1):29-36.
81. Joshi S, Hussain MT, Roces CB, Anderluzzi G, Kastner E, Salmaso S, et al. Microfluidics based manufacture of liposomes simultaneously entrapping hydrophilic and lipophilic drugs. International Journal of Pharmaceutics. 2016;514(1):160-8.

82. Shen Z, Fisher A, Liu WK, Li Y. 1 - PEGylated “stealth” nanoparticles and liposomes. In: Parambath A, editor. Engineering of Biomaterials for Drug Delivery Systems: Woodhead Publishing; 2018. p. 1-26.
83. Garbuzenko O, Barenholz Y, Priev A. Effect of grafted PEG on liposome size and on compressibility and packing of lipid bilayer. Chemistry and Physics of Lipids. 2005;135(2):117-29.
84. Javadzadeh Y, Adibkia K, Hamishekar H. Transcutol® (Diethylene Glycol Monoethyl Ether): A Potential Penetration Enhancer. In: Dragicevic N, Maibach HI, editors. Percutaneous Penetration Enhancers Chemical Methods in Penetration Enhancement: Modification of the Stratum Corneum. Berlin, Heidelberg: Springer Berlin Heidelberg; 2015. p. 195-205.
85. Sullivan DW, Gad SC, Julien M. A review of the nonclinical safety of Transcutol®, a highly purified form of diethylene glycol monoethyl ether (DEGEE) used as a pharmaceutical excipient. Food and Chemical Toxicology. 2014;72:40-50.
86. Lee CY, Tsai T, Peng PC, Chen CT. Fabrication of Doxorubicin-Loaded Lipid-Based Nanocarriers by Microfluidic Rapid Mixing. Biomedicines. 2022;10(6).
87. Thorn CF, Oshiro C, Marsh S, Hernandez-Boussard T, McLeod H, Klein TE, et al. Doxorubicin pathways: pharmacodynamics and adverse effects. Pharmacogenet Genomics. 2011;21(7):440-6.
88. Danta CC, Sahu AN. Chapter 16 - Naturally occurring anticancer drugs. In: Acharya PC, Kurosu M, editors. Medicinal Chemistry of Chemotherapeutic Agents: Academic Press; 2023. p. 539-88.
89. Rawat PS, Jaiswal A, Khurana A, Bhatti JS, Navik U. Doxorubicin-induced cardiotoxicity: An update on the molecular mechanism and novel therapeutic strategies for effective management. Biomedicine & Pharmacotherapy. 2021;139:111708.
90. Abraham SA, Waterhouse DN, Mayer LD, Cullis PR, Madden TD, Bally MB. The Liposomal Formulation of Doxorubicin. Methods in Enzymology. 391: Academic Press; 2005. p. 71-97.
91. Anselmo AC, Mitragotri S. An overview of clinical and commercial impact of drug delivery systems. Journal of Controlled Release. 2014;190:15-28.
92. Zucker D, Marcus D, Barenholz Y, Goldblum A. Liposome drugs' loading efficiency: A working model based on loading conditions and drug's physicochemical properties. Journal of Controlled Release. 2009;139(1):73-80.
93. Pourmadadi M, Ghaemi A, Shamsabadipour A, Rajabzadeh-Khosroshahi M, Shaghaghi M, Rahdar A, et al. Nanoparticles loaded with Daunorubicin as an advanced tool for cancer therapy. European Journal of Medicinal Chemistry. 2023;258:115547.
94. Fassas A, Anagnostopoulos A. The use of liposomal daunorubicin (DaunoXome) in acute myeloid leukemia. Leukemia & Lymphoma. 2005;46(6):795-802.
95. Embree L, Gelmon K, Tolcher A, Hudon N, Heggie J, Dedhar C, et al. Pharmacokinetic behavior of vincristine sulfate following administration of vincristine sulfate liposome injection. Cancer Chemotherapy and Pharmacology. 1998;41(5):347-52.
96. Zhang Y, Wong CYJ, Gholizadeh H, Aluigi A, Tiboni M, Casettari L, et al. Microfluidics assembly of inhalable liposomal ciprofloxacin characterised by an innovative in vitro pulmonary model. International Journal of Pharmaceutics. 2023;635:122667.
97. Cipolla D, Blanchard J, Gonda I. Development of Liposomal Ciprofloxacin to Treat Lung Infections. Pharmaceutics. 2016;8(1).
98. Noble CO, Guo Z, Hayes ME, Marks JD, Park JW, Benz CC, et al. Characterization of highly stable liposomal and immunoliposomal formulations of vincristine and vinblastine. Cancer Chemother Pharmacol. 2009;64(4):741-51.
99. Fenske DB, Wong KF, Maurer E, Maurer N, Leenhouts JM, Boman N, et al. Ionophore-mediated uptake of ciprofloxacin and vincristine into large unilamellar vesicles exhibiting transmembrane ion gradients. Biochim Biophys Acta. 1998;1414(1-2):188-204.
100. Yanar F, Mosayyebi A, Nastruzzi C, Carugo D, Zhang X. Continuous-Flow Production of Liposomes with a Millireactor under Varying Fluidic Conditions. Pharmaceutics. 2020;12(11).

101. Maurer N, Wong KF, Hope MJ, Cullis PR. Anomalous solubility behavior of the antibiotic ciprofloxacin encapsulated in liposomes: a 1H-NMR study. Biochimica et Biophysica Acta (BBA) - Biomembranes. 1998;1374(1):9-20.
102. Shrestha B, Pokhrel AR, Darsandhari S, Parajuli P, Sohng JK, Pandey RP. Engineering Streptomyces peucetius for Doxorubicin and Daunorubicin Biosynthesis. In: Arora D, Sharma C, Jaglan S, Lichtfouse E, editors. Pharmaceuticals from Microbes: The Bioengineering Perspective. Cham: Springer International Publishing; 2019. p. 191-209.
103. Ruiz A, Ma G, Seitsonen J, Pereira SGT, Ruokolainen J, Al-Jamal WT. Encapsulated doxorubicin crystals influence lysolipid temperature-sensitive liposomes release and therapeutic efficacy in vitro and in vivo. Journal of Controlled Release. 2020;328:665-78.
104. Fritze A, Hens F, Kimpfler A, Schubert R, Peschka-Süss R. Remote loading of doxorubicin into liposomes driven by a transmembrane phosphate gradient. Biochimica et Biophysica Acta (BBA) - Biomembranes. 2006;1758(10):1633-40.
105. Yamada Y. Dimerization of Doxorubicin Causes Its Precipitation. ACS Omega. 2020;5(51):33235-41.
106. Lasic DD, Frederik PM, Stuart MC, Barenholz Y, McIntosh TJ. Gelation of liposome interior. A novel method for drug encapsulation. FEBS Lett. 1992;312(2-3):255-8.
107. Li T, Cipolla D, Rades T, Boyd BJ. Drug nanocrystallisation within liposomes. Journal of Controlled Release. 2018;288:96-110.
108. Yamamoto E, Hosogi N, Takechi-Haraya Y, Izutsu K-i, Uchiyama N, Goda Y. Folded, undulating, and fibrous doxorubicin sulfate crystals in liposomes. Nanomedicine: Nanotechnology, Biology and Medicine. 2023;47:102631.
109. Wei X, Cohen R, Barenholz Y. Insights into composition/structure/function relationships of Doxil® gained from "high-sensitivity" differential scanning calorimetry. European Journal of Pharmaceutics and Biopharmaceutics. 2016;104:260-70.
110. Wang Y, Grainger DW. Regulatory Considerations Specific to Liposome Drug Development as Complex Drug Products. Frontiers in Drug Delivery. 2022;2.
111. Fonseca MJ, van Winden ECA, Crommelin DJA. Doxorubicin induces aggregation of small negatively charged liposomes. European Journal of Pharmaceutics and Biopharmaceutics. 1997;43(1):9-17.
112. Wei X, Shamrakov D, Nudelman S, Peretz-Damari S, Nativ-Roth E, Regev O, et al. Cardinal Role of Intraliposome Doxorubicin-Sulfate Nanorod Crystal in Doxil Properties and Performance. ACS Omega. 2018;3(3):2508-17.
113. Brgles M, Jurašin D, Sikirić MD, Frkanec R, Tomašić J. Entrapment of Ovalbumin into Liposomes—Factors Affecting Entrapment Efficiency, Liposome Size, and Zeta Potential. Journal of Liposome Research. 2008;18(3):235-48.
114. Hwang SY, Kim HK, Choo J, Seong GH, Hien TBD, Lee EK. Effects of operating parameters on the efficiency of liposomal encapsulation of enzymes. Colloids and Surfaces B: Biointerfaces. 2012;94:296-303.
115. Zhigaltsev IV, Maurer N, Akhong Q-F, Leone R, Leng E, Wang J, et al. Liposome-encapsulated vincristine, vinblastine and vinorelbine: A comparative study of drug loading and retention. Journal of Controlled Release. 2005;104(1):103-11.
116. Sheikholeslami B, Lam NW, Dua K, Haghi M. Exploring the impact of physicochemical properties of liposomal formulations on their in vivo fate. Life Sciences. 2022;300:120574.
117. Kaźmierczak Z, Szostak-Paluch K, Przybyło M, Langner M, Witkiewicz W, Jędruchniewicz N, et al. Endocytosis in cellular uptake of drug delivery vectors: Molecular aspects in drug development. Bioorganic & Medicinal Chemistry. 2020;28(18):115556.
118. Yuan W, Kuai R, Dai Z, Yuan Y, Zheng N, Jiang W, et al. Development of a Flow-Through USP-4 Apparatus Drug Release Assay to Evaluate Doxorubicin Liposomes. The AAPS Journal. 2017;19(1):150-60.

119. Devrim B, Bozkır A. Chapter 7 - Nanocarriers and Their Potential Application as Antimicrobial Drug Delivery. In: Ficai A, Grumezescu AM, editors. Nanostructures for Antimicrobial Therapy: Elsevier; 2017. p. 169-202.
120. Mühlebach S. Regulatory challenges of nanomedicines and their follow-on versions: A generic or similar approach? Advanced Drug Delivery Reviews. 2018;131:122-31.
121. Waterhouse DN, Tardi PG, Mayer LD, Bally MB. A Comparison of Liposomal Formulations of Doxorubicin with Drug Administered in Free Form. Drug Safety. 2001;24(12):903-20.
122. Cipolla D, Wu H, Eastman S, Redelmeier T, Gonda I, Chan HK. Development and Characterization of an In Vitro Release Assay for Liposomal Ciprofloxacin for Inhalation. Journal of Pharmaceutical Sciences. 2014;103(1):314-27.
123. Shibata H, Izutsu K-i, Yomota C, Okuda H, Goda Y. Investigation of factors affecting in vitro doxorubicin release from PEGylated liposomal doxorubicin for the development of in vitro release testing conditions. Drug Development and Industrial Pharmacy. 2015;41(8):1376-86.
124. Nsairat H, Khater D, Sayed U, Odeh F, Al Bawab A, Alshaer W. Liposomes: structure, composition, types, and clinical applications. Heliyon. 2022;8(5):e09394.
125. Matsuura-Sawada Y, Maeki M, Uno S, Wada K, Tokeshi M. Controlling lamellarity and physicochemical properties of liposomes prepared using a microfluidic device. Biomaterials Science. 2023;11(7):2419-26.
126. Doskocz J, Dałek P, Przybyło M, Trzebicka B, Foryś A, Kobyliukh A, et al. The Elucidation of the Molecular Mechanism of the Extrusion Process. Materials (Basel). 2021;14(15).
127. Nordström R, Zhu L, Härmark J, Levi-Kalisman Y, Koren E, Barenholz Y, et al. Quantitative Cryo-TEM Reveals New Structural Details of Doxil-Like PEGylated Liposomal Doxorubicin Formulation. Pharmaceutics. 2021;13(1).
128. Wang H, Zheng M, Gao J, Wang J, Zhang Q, Fawcett JP, et al. Uptake and release profiles of PEGylated liposomal doxorubicin nanoparticles: A comprehensive picture based on separate determination of encapsulated and total drug concentrations in tissues of tumor-bearing mice. Talanta. 2020;208:120358.
129. Weber FJ, de Bont JAM. Adaptation mechanisms of microorganisms to the toxic effects of organic solvents on membranes. Biochimica et Biophysica Acta (BBA) - Reviews on Biomembranes. 1996;1286(3):225-45.
130. Maeki M, Kimura N, Okada Y, Shimizu K, Shibata K, Miyazaki Y, et al. Understanding the effects of ethanol on the liposome bilayer structure using microfluidic-based time-resolved small-angle X-ray scattering and molecular dynamics simulations. Nanoscale Adv. 2024;6(8):2166-76.
131. Lombardo D, Kiselev MA. Methods of Liposomes Preparation: Formation and Control Factors of Versatile Nanocarriers for Biomedical and Nanomedicine Application. Pharmaceutics. 2022;14(3).
132. Drummond DC, Noble CO, Hayes ME, Park JW, Kirpotin DB. Pharmacokinetics and in vivo drug release rates in liposomal nanocarrier development. Journal of Pharmaceutical Sciences. 2008;97(11):4696-740.
133. Ibrahim M, Abuwatfa WH, Awad NS, Sabouni R, Husseini GA. Encapsulation, Release, and Cytotoxicity of Doxorubicin Loaded in Liposomes, Micelles, and Metal-Organic Frameworks: A Review. Pharmaceutics. 2022;14(2):254.
134. Nagayasu A, Shimooka T, Kiwada H. Effect of Vesicle Size on in Vivo Release of Daunorubicin from Hydrogenated Egg Phosphatidylcholine-Based Liposomes into Blood Circulation. Biological & Pharmaceutical Bulletin. 1995;18(7):1020-3.
135. Merino M, Zalba S, Garrido MJ. Immunoliposomes in clinical oncology: State of the art and future perspectives. Journal of Controlled Release. 2018;275:162-76.
136. Osborne DW. Diethylene glycol monoethyl ether: an emerging solvent in topical dermatology products. Journal of Cosmetic Dermatology. 2011;10(4):324-9.
137. Mashima R, Takada S. Lipid Nanoparticles: A Novel Gene Delivery Technique for Clinical Application. Curr Issues Mol Biol. 2022;44(10):5013-27.

138. Lee Y, Jeong M, Park J, Jung H, Lee H. Immunogenicity of lipid nanoparticles and its impact on the efficacy of mRNA vaccines and therapeutics. Experimental & Molecular Medicine. 2023;55(10):2085-96.
139. Sharma P, Hoorn D, Aitha A, Breier D, Peer D. The immunostimulatory nature of mRNA lipid nanoparticles. Advanced Drug Delivery Reviews. 2024;205:115175.
140. Bailey AL, Cullis PR. Modulation of Membrane Fusion by Asymmetric Transbilayer Distributions of Amino Lipids. Biochemistry. 1994;33(42):12573-80.
141. Kulkarni JA, Cullis PR, van der Meel R. Lipid Nanoparticles Enabling Gene Therapies: From Concepts to Clinical Utility. Nucleic Acid Therapeutics. 2018;28(3):146-57.
142. Zhang L, More KR, Ojha A, Jackson CB, Quinlan BD, Li H, et al. Effect of mRNA-LNP components of two globally-marketed COVID-19 vaccines on efficacy and stability. npj Vaccines. 2023;8(1):156.
143. Akinc A, Maier MA, Manoharan M, Fitzgerald K, Jayaraman M, Barros S, et al. The Onpattro story and the clinical translation of nanomedicines containing nucleic acid-based drugs. Nature Nanotechnology. 2019;14(12):1084-7.
144. Hou X, Zaks T, Langer R, Dong Y. Lipid nanoparticles for mRNA delivery. Nature Reviews Materials. 2021;6(12):1078-94.
145. Witzigmann D, Kulkarni JA, Leung J, Chen S, Cullis PR, van der Meel R. Lipid nanoparticle technology for therapeutic gene regulation in the liver. Adv Drug Deliv Rev. 2020;159:344-63.
146. Patel N, Davis Z, Hofmann C, Vlasak J, Loughney JW, DePhillips P, et al. Development and Characterization of an In Vitro Cell-Based Assay to Predict Potency of mRNA–LNP-Based Vaccines. Vaccines. 2023;11(7):1224.
147. Carrasco MJ, Alishetty S, Alameh MG, Said H, Wright L, Paige M, et al. Ionization and structural properties of mRNA lipid nanoparticles influence expression in intramuscular and intravascular administration. Commun Biol. 2021;4(1):956.
148. Milane L, Amiji M. Clinical approval of nanotechnology-based SARS-CoV-2 mRNA vaccines: impact on translational nanomedicine. Drug Deliv Transl Res. 2021;11(4):1309-15.
149. Tan E, Chin CSH, Lim ZFS, Ng SK. HEK293 Cell Line as a Platform to Produce Recombinant Proteins and Viral Vectors. Front Bioeng Biotechnol. 2021;9:796991.
150. Paunovska K, Sago CD, Monaco CM, Hudson WH, Castro MG, Rudoltz TG, et al. A Direct Comparison of in Vitro and in Vivo Nucleic Acid Delivery Mediated by Hundreds of Nanoparticles Reveals a Weak Correlation. Nano Letters. 2018;18(3):2148-57.
151. Sayers EJ, Peel SE, Schantz A, England RM, Beano M, Bates SM, et al. Endocytic Profiling of Cancer Cell Models Reveals Critical Factors Influencing LNP-Mediated mRNA Delivery and Protein Expression. Molecular Therapy. 2019;27(11):1950-62.
152. Tatalick LM, Gerard CJ, Takeya R, Price DN, Thorne BA, Wyatt LM, et al. Safety characterization of HeLa-based cell substrates used in the manufacture of a recombinant adeno-associated virus-HIV vaccine. Vaccine. 2005;23(20):2628-38.
153. Le Ru A, Jacob D, Transfiguracion J, Ansorge S, Henry O, Kamen AA. Scalable production of influenza virus in HEK-293 cells for efficient vaccine manufacturing. Vaccine. 2010;28(21):3661-71.
154. Feather LAJ, Nadella V, Kastner E, Perrie Y, Hilton AC, Devitt A. Development of a rapid in vitro pre-screen for distinguishing effective liposome-adjuvant delivery systems. Sci Rep. 2022;12(1):12448.
155. Akinc A, Querbes W, De S, Qin J, Frank-Kamenetsky M, Jayaprakash KN, et al. Targeted Delivery of RNAi Therapeutics With Endogenous and Exogenous Ligand-Based Mechanisms. Molecular Therapy. 2010;18(7):1357-64.
156. Tedla N, Glaros EN, Brunk UT, Jessup W, Garner B. Heterogeneous expression of apolipoprotein-E by human macrophages. Immunology. 2004;113(3):338-47.
157. Semple SC, Leone R, Barbosa CJ, Tam YK, Lin PJC. Lipid Nanoparticle Delivery Systems to Enable mRNA-Based Therapeutics. Pharmaceutics. 2022;14(2):398.
158. Love KT, Mahon KP, Levins CG, Whitehead KA, Querbes W, Dorkin JR, et al. Lipid-like materials for low-dose, in vivo gene silencing. Proc Natl Acad Sci U S A. 2010;107(5):1864-9.

159. Salatin S, Maleki Dizaj S, Yari Khosroushahi A. Effect of the surface modification, size, and shape on cellular uptake of nanoparticles. Cell Biology International. 2015;39(8):881-90.
160. Oh N, Park JH. Endocytosis and exocytosis of nanoparticles in mammalian cells. Int J Nanomedicine. 2014;9 Suppl 1(Suppl 1):51-63.
161. Escalona-Rayo O, Zeng Y, Knol RA, Kock TJF, Aschmann D, Slütter B, et al. In vitro and in vivo evaluation of clinically-approved ionizable cationic lipids shows divergent results between mRNA transfection and vaccine efficacy. Biomedicine & Pharmacotherapy. 2023;165:115065.
162. Zeng Y, Escalona-Rayo O, Knol R, Kros A, Slütter B. Lipid nanoparticle-based mRNA candidates elicit potent T cell responses. Biomater Sci. 2023;11(3):964-74.
163. Prazeres PHDM, Ferreira H, Costa PAC, da Silva W, Alves MT, Padilla M, et al. Delivery of Plasmid DNA by Ionizable Lipid Nanoparticles to Induce CAR Expression in T Cells. International Journal of Nanomedicine. 2023;18(null):5891-904.
164. Moradian H, Roch T, Lendlein A, Gossen M. mRNA Transfection-Induced Activation of Primary Human Monocytes and Macrophages: Dependence on Carrier System and Nucleotide Modification. Scientific Reports. 2020;10(1):4181.
165. Pan C, Kumar C, Bohl S, Klingmueller U, Mann M. Comparative proteomic phenotyping of cell lines and primary cells to assess preservation of cell type-specific functions. Mol Cell Proteomics. 2009;8(3):443-50.
166. Whitehead KA, Matthews J, Chang PH, Niroui F, Dorkin JR, Severgnini M, et al. In Vitro–In Vivo Translation of Lipid Nanoparticles for Hepatocellular siRNA Delivery. ACS Nano. 2012;6(8):6922-9.
167. Binici B, Rattray Z, Schroeder A, Perrie Y. The Role of Biological Sex in Pre-Clinical (Mouse) mRNA Vaccine Studies. Vaccines (Basel). 2024;12(3).
168. Tenchov R, Bird R, Curtze AE, Zhou Q. Lipid Nanoparticles–From Liposomes to mRNA Vaccine Delivery, a Landscape of Research Diversity and Advancement. ACS Nano. 2021;15(11):16982-7015.
169. Barlas S. FDA strategies to prevent and respond to drug shortages: finding a better way to predict and prevent company closures. P t. 2013;38(5):261-3.